

UCLA

UCLA Electronic Theses and Dissertations

Title

Explorations in Cobalt Promoted Cyclocarbonylation, Intramolecular Cyclization of Vinyl Ethers, and Formation of Metal-Carbene Complexes with mRNA 5'-Cap Analogs

Permalink

<https://escholarship.org/uc/item/7079q231>

Author

Ferber, Carl

Publication Date

2022

Peer reviewed|Thesis/dissertation

UNIVERSITY OF CALIFORNIA

Los Angeles

Explorations in Cobalt Promoted Cyclocarbonylation,
Intramolecular Cyclization of Vinyl Ethers, and
Formation of Metal-Carbene Complexes with
mRNA 5'-Cap Analogs

A dissertation submitted in partial satisfaction of the
requirements for the degree Doctor of Philosophy
in Chemistry

by

Carl John Ferber

2022

© Copyright by

Carl John Ferber

2022

ABSTRACT OF THE DISSERTATION

Explorations in Cobalt Promoted Cyclocarbonylation, Intramolecular Cyclization of Vinyl Ethers, and Formation of Metal-Carbene Complexes with mRNA 5'-Cap Analogs

by

Carl John Ferber

Doctor of Philosophy in Chemistry

University of California, Los Angeles, 2022

Professor Craig A. Merlic, Chair

Chapter one describes a [2+2+1+1] reaction for the synthesis of quinones from alkynes. Cobalt octacarbonyl, in a mechanism reminiscent of the Pauson-Khand reaction, combines two equivalents of an alkyne with two equivalents of carbon monoxide via a series of insertions and reductive eliminations, to form a quinone. In theory, this reaction provides rapid access to complicated quinone structures. Unfortunately, a competing [2+2+2] reaction which is catalyzed by cobalt to give benzene derivatives out competes the desired reaction, and high yields were never achieved.

Chapter two details the investigation of three different intramolecular cyclization reactions which endeavor to take advantage of the unique reactivity of vinyl ethers. Using complex vinyl ether substrates synthesized by methods previously described by our group, these reactions should provide easy access to relatively complex fused ring systems. The chapter primarily

focuses on the [2+2] cycloaddition of vinyl ethers with both ketenes and ketene iminium ions, which yield cyclobutanone products. Also described is the investigation into the nucleophilic attack of epoxides by vinyl ethers. Although perfectly sound from a mechanistic perspective, as born out by intermolecular examples, the challenge of performing these intramolecular reactions remains the incompatibility of vinyl ethers with certain necessary reaction conditions.

Chapter three describes the synthesis of a metal carbene complex using gold and an analog of the 5'-cap of mRNA; the first such example to be synthesized via in situ generation of a carbene at the C8 position of guanosine. The only previous example was generated via an oxidative addition with platinum under extreme conditions. In our example we use extremely mild conditions which suggest the possibility of forming such a complex with mRNA oligonucleotides, and perhaps even *in vivo*. Such reactivity of mRNA is unprecedented and could lead to interesting pharmaceutical possibilities.

The dissertation of Carl John Ferber is approved:

Alexander Michael Spakoyny

Yves F. Rubin

Caius Gabriel Radu

Craig A. Merlic, Chair

University of California, Los Angeles

2022

TABLE OF CONTENTS

ABSTRACT OF DISSERTATION.....	ii
COMMITTEE PAGE.....	iv
TABLE OF CONTENTS.....	v
LIST OF SCHEMES.....	vii
LIST OF FIGURES.....	ix
LIST OF TABLES.....	x
ABBREVIATIONS.....	xii
ACKNOWLEDGMENTS.....	xvi
CURICULUM VITAE.....	xvii
CHAPTER ONE: Cobalt Promoted Cyclocarbonylation of Alkynes.....	1
1.1 Background.....	2
1.2 Introduction.....	9
1.3 Efforts Towards a Practical Synthesis of Quinones via a [2+2+1+1] Cycloaddition of Alkynes and Dicobalt Octacarbonyl.....	10
1.4 Conclusion.....	16
1.5 Experimental Section.....	16
1.6 ¹ H and ¹³ C NMR Data.....	20
1.7 References.....	54
CHAPTER TWO: Intramolecular Cyclization Reactions of Vinylic Ethers.....	56
2.1 Background.....	57
2.2 Introduction.....	64
2.3 Intramolecular [2+2] Cyclization of Vinyl Ethers and Ketene Iminium Ions.....	64

2.4 Intramolecular [2+2] Cyclization of Vinyl Ethers and Ketenes.....	66
2.5 Lewis Acid Promoted Cyclization of Vinyl Ethers with Epoxides.....	71
2.6 Conclusion.....	74
2.7 Experimental Section.....	74
2.8 ¹ H and ¹³ C NMR Data.....	84
2.9 References.....	143
CHAPTER THREE: Synthesis of a Gold-Carbene Complex with a mRNA 5'-Cap Analog....	146
3.1 Introduction.....	147
3.2 Background.....	149
3.3 Synthesis of 5'-Cap Analogs and Silver NHC Complexes.....	152
3.4 Synthesis of a Gold-NHC Complex with a 5-Cap Analog.....	155
3.5 Conclusion and Future Studies.....	157
3.6 Experimental Section.....	158
3.7 ¹ H and ¹³ C NMR Data.....	162
3.8 References.....	176

LIST OF SCHEMES

CHAPTER ONE

<i>Scheme 1.1</i> Chemical Equation of the Reppe Reaction and Intermediate.....	2
<i>Scheme 1.2</i> Reaction of 2-butyne with Chlorodicarbonyl Rhodium Dimer.....	2
<i>Scheme 1.3</i> Benzoquinones from the Photoreaction of Alkynes and Fe(CO) ₅	3
<i>Scheme 1.4</i> Mechanism of Quinone Synthesis via Metallacyclopent-3-ene-2,5-dione.....	5
<i>Scheme 1.5</i> More Effective Maleocobalt Complexes.....	5
<i>Scheme 1.6</i> Synthesis of Trisquinones.....	7
<i>Scheme 1.7</i> Discovery of Cobalt Promoted [2+2+1+1] Cycloaddition.....	9
<i>Scheme 1.8</i> Reaction Products and Proposed Mechanism.....	12
<i>Scheme 1.9</i> Reductive and Oxidative Workups.....	15

CHAPTER TWO

<i>Scheme 2.1</i> [2+2] Cycloaddition of Cyclopentadiene and Diphenyl Ketene.....	57
<i>Scheme 2.2</i> Formation of Ketene Iminium with Triflic Anhydride and Cyclization.....	60
<i>Scheme 2.3</i> Regioselectivity of Trans Alkenes.....	63
<i>Scheme 2.4</i> Copper Promoted Coupling of Vinyl Boronates and Alcohols.....	64
<i>Scheme 2.5</i> Initial Ketene Iminium Experiments.....	65
<i>Scheme 2.6</i> Synthesis of Authentic Product Samples.....	66
<i>Scheme 2.7</i> Reaction of Ethyl Vinyl Ether and Triflic Anhydride.....	66
<i>Scheme 2.8</i> Replication of Matsuo's Results.....	67
<i>Scheme 2.9</i> Thionyl Chloride Decomposes Vinyl Ethers.....	67
<i>Scheme 2.10</i> Failed Alternative Access to Acid Chlorides.....	67
<i>Scheme 2.11</i> Acid Bromide Synthesis.....	68

<i>Scheme 2.12</i> Triphenylphosphine Dibromide Decomposes Vinyl Ether.....	68
<i>Scheme 2.13</i> Investigation of Intermolecular Model.....	69
<i>Scheme 2.14</i> Synthesis of Intramolecular Substrate Ester.....	70
<i>Scheme 2.15</i> Attempted Intramolecular Cyclization.....	71
<i>Scheme 2.16</i> Precedent for Nucleophilic Vinyl Ether.....	72
<i>Scheme 2.17</i> Synthesis of Coupling Partners for Intramolecular Substrate.....	72

CHAPTER THREE:

<i>Scheme 3.1</i> Proposed General Scheme.....	149
<i>Scheme 3.2</i> Transmetalation of Silver NHC Complexes.....	150
<i>Scheme 3.3</i> NHC-Metal Complexes with Methylated Caffeine.....	150
<i>Scheme 3.4</i> Purported Silver Complex with 7,9-Dimethylguanine.....	150
<i>Scheme 3.5</i> Direct Formation of Gold-NHC Complexes.....	151
<i>Scheme 3.6</i> Direct Formation of Gold-NHC Complex with Methylated Caffeine.....	151
<i>Scheme 3.7</i> Modification of Guanosine.....	153
<i>Scheme 3.8</i> Reaction of 7-Methylguanosine with Ag ₂ O.....	154
<i>Scheme 3.9</i> Methylation of Guanosine Monophosphate and Reaction with Ag ₂ O.....	155
<i>Scheme 3.10</i> Synthesis of Gold-NHC Complex with Guanosine.....	156

LIST OF FIGURES

CHAPTER ONE

Figure 1.1 Nanaomycin A.....5

CHAPTER TWO

Figure 2.1 *Cis* Vs *Trans* Olefin Transition States.....58

Figure 2.2 Transition State of Intramolecular [2+2] Reaction with 1,2-Substituted
Olefins.....63

Figure 2.3 Potential Reaction Pathways of Vinyl Ether Cyclization with Epoxides.....71

CHAPTER THREE

Figure 3.1 Structure of the 5'-Cap.....147

Figure 3.2 Role of the 5'-Cap.....148

Figure 3.3 5'-Cap Bound to eLF4E.....148

LIST OF TABLES

CHAPTER ONE

<i>Table 1.1</i> Disubstituted Benzoquinones from the Photoreaction of Primary Alkynes and Fe(CO) ₅	3
<i>Table 1.2</i> Synthesis of Naphthoquinones.....	4
<i>Table 1.3</i> Alkyl Benzoquinone Products (% Yield, Isomeric Ratio, Favored Isomer Shown).....	6
<i>Table 1.4</i> Trifluoroacetate Substituted Cobalt Complex Reaction.....	6
<i>Table 1.5</i> Synthesis of Functionalized Hydroquinones via Ruthenium Catalyzed Carbonylation.....	7
<i>Table 1.6</i> Rhodium Catalyzed Cyclocarbonylative Coupling of Alkynes.....	8
<i>Table 1.7</i> Initial Reaction Optimization.....	11
<i>Table 1.8</i> Optimization of Conditions.....	13
<i>Table 1.9</i> Activator Screen.....	14
<i>Table 1.10</i> Additional Substrates Examined.....	15

CHAPTER TWO

<i>Table 2.1</i> Zinc Catalyzed Cycloaddition of Ketene and Vinyl Ethers.....	59
<i>Table 2.2</i> Cyclization of Ethyl Vinyl Ether and Ketenes.....	59
<i>Table 2.3</i> Intramolecular [2+2] Cycloaddition of Ketenes and Ketene Iminiums.....	61
<i>Table 2.4</i> Intermolecular Reaction Optimization.....	66
<i>Table 2.5</i> Acid Chloride Synthesis using Pivaloyl Chloride.....	68
<i>Table 2.6</i> Optimization of Intermolecular Model.....	70
<i>Table 2.7</i> Hydrolysis of Ester Solvent Screen.....	71

Table 2.8 Synthesis of Epoxide Cyclization Substrate.....73

Table 2.9 Attempted Cyclization with Epoxide.....73

CHAPTER THREE

Table 3.1 Attempted Replication of Youngs Patent.....152

Table 3.2 Failed Methylation of Guanosine Monophosphate.....154

Table 3.3 Conditions for Gold Complex Formation.....156

ABBREVIATIONS

°C	degrees Celsius
δ	delta
Δ	heat
¹ H NMR	proton NMR
7-MeG	7-methylguanosine
¹³ C NMR	Carbon thirteen NMR
Ac	acetyl
AcOH	acetic acid
Allyl	allylic
Aq.	aqueous
C ₂ H ₂	ethyne
C ₆ H ₆	benzene
C ₆ D ₆	deutero-benzene
CDCl ₃	deutero-chloroform
Ce(IV)	Cerium four
CH ₃ CN	acetonitrile
CHCl ₃	chloroform
Co ₂ (CO) ₈	dicobalt octacarbonyl
(COCl) ₂	phosgene
Conv.	conversion
D ₂ O	deuterium oxide
DCM	dichloromethane

DFT	density functional theory
DMAP	dimethylaminopyridine
DMF	N,N-dimethylformamide
DMF-d7	heptadeutero-N,N-dimethylformamide
DMSO	dimethylsulfoxide
DMSO-d6	hexadeuterodimethylsulfoxide
DNA	deoxyribose nucleic acid
EDTA	ethylenediaminetetraacetic acid
Et	ethyl
Et ₂ O	diethyl ether
EtOAc	ethyl acetate
EtOH	ethanol
Equiv.	equivalents
G	gram
H	proton
h	hours
H ₂	hydrogen
H ₂ O	water
HBpin	pinacol borane
Hex	hexyl
hν	light
Hz	hertz
IMes	1,3-Bis(2,4,6-trimethylphenyl)-1,3-dihydro-2H-imidazol-2-ylidene

<i>i</i> Pr	isopropyl
<i>i</i> -Pr ₂ NEt	N,N-diisopropylethylamine
<i>i</i> -PrOH	isopropanol
KOH	potassium hydroxide
LDA	lithium diisopropylamide
M	molar
[M]	concentration
m ⁷ Gppp	7-methylguanosine triphosphate
MALDI	matrix-assisted laser desorption/ionization
mCPBA	meta-chloroperoxybenzoic acid
Me	methyl
MeCN	acetonitrile
MeI	iodomethane
MgSO ₄	magnesium sulfate
MHz	megahertz
MicroED	microcrystal electron diffraction
Min.	minutes
mL	milliliters
mRNA	messenger ribonucleic acid
Na ₂ S	sodium sulfide
Na ₂ S ₂ O ₃	sodium thiosulfide
NaOD	sodium deuterohydroxide
NaOH	sodium hydroxide

Naph	naphthyl
n-Bu	n-butyl
NHC	N-heterocyclic carbene
NMO	N-methylmorpholine N-oxide
NMR	nuclear magnetic resonance
NR	no reaction
Ph	phenyl
Piv	pivalyl
Pr	propyl
RNA	ribonucleic acid
rt	room temperature
SiMe ₃	trimethyl silyl
SOCl ₂	thionyl chloride
Solv.	solvent
TBAI	tetrabutylammonium iodide
TBS	tert-butyl-dimethylsilyl
TBSCl	tert-butyl-dimethylsilyl chloride
<i>t</i> -Bu	tert-butyl
TeCA	1,1,2,2-tetrachloroethane
Tf ₂ O	triflic anhydride
TMS	trimethylsilyl
Tol.	toluene

ACKNOWLEDGMENTS

Firstly, I would like to thank my research advisor, Craig Merlic, for everything he has done for me over the course of graduate school. Thank you for everything you have taught me about chemistry, teaching, and research, and for continuing to believe in me over the last six years, even when the chemistry wasn't going the way we had hoped. Secondly, thank you to my fellow graduate student Chih-Te Zee for his work acquiring x-ray crystal structures of the metal complexes in chapter three, and my undergraduate mentee Maziar Montazer for his help synthesizing compound **2-19**. I would also like to thank the other members of my committee, Alexander Spakoyny, Yves Rubin, and Caius Radu, for taking the time to advise me on my research and read this dissertation.

Thank you to all the other members of the Merlic research group for your continuous friendship and support, and especially Robert Tobolowsky and Brett Cory for all the wisdom and guidance you provided in my early years of graduate school, and Paul Balzer for proofreading this thesis. Lastly, thank you to my family, Jennifer, Jeff, and Grace; and my fiancé Adrian, for all of their love and support, especially through the times I was struggling. I would not have made it here without you.

CIRICULUM VITAE

Education

University of California, Los Angeles

- PhD, Chemistry *Expected December 2022*

University of California, Los Angeles

- Masters of Science, Chemistry *March 2018*

University of San Diego

- Bachelor of Arts, Biochemistry, Magna Cum Laude, Honors Program, GPA: 3.78 *May 2016*

Academic Awards/Honors

- American Chemical Society Division of Organic Chemistry Summer Undergraduate Research Fellowship recipient (\$5000)
- Alice B. Hayes Research Fellowship recipient
- Beckman Research Fellowship recipient (declined by recipient)
- USD Department of Chemistry and Biochemistry Organic Chemistry Student of the Year

Publications

- Moore, C. M.; Medina, C. R.; Cannamela, P. C.; McIntosh, M. L.; Ferber, C. J.; Roering, A. J.; Clark, T. B.; "Facile Formation of β -Hydroxyboronate Esters by a Cu-Catalyzed Diboration/Matteson Homologation Sequence" *Org. Lett.* **2014**, *16* (23), 6056-6059.

- Marcum, J. M.; McGarry, K. A.; Ferber, C. J.; Clark, T. B.; “Synthesis of Biaryl Ethers by the Copper-Catalyzed Chan-Evans-Lam Etherification from Benzylic Amine Boronate Esters” *J. Org. Chem.* **2016**, *81*(17), 7963-7969.
- Meyer, G. F.; Nistler, M. A.; Samoshin, A. V.; McManus, B. D.; Thane, T. A.; Ferber, C. J.; O’Neil, G. W.; Clark, T. B.; “ β -Silyloxy Allylboronate Esters through an Aldehyde Borylation/Homologation Sequence” *Tetrahedron Lett.* **2020**, *61* (28), 152082.
- Merlic, C. A.; Ferber, C. J.; Schroder, I.; “Lesson Learned – Lithium Aluminum Hydride Fires” *Published ASAP ACS Chem. Health Saf.* doi.org/10.1021/acs.chas.2c00035

Presentations

- “Conversion of Aldehydes to β -Hydroxyboronate Esters by Diboration/Homologation Sequences” The American Chemical Society 250th National Meeting, Boston, MA, August 2015.
- “Conversion of Aldehydes to β -Hydroxyboronate Esters by Diboration/Homologation Sequences” ACS DOC SURF Symposium, Newark, NJ, August 2015.
- “Synthesis of Biaryl Ethers from Benzylic Amine Boronate Esters by the Copper-Catalyzed Chan-Evans-Lam Etherification” The American Chemical Society 251st National Meeting, San Diego, CA, March 2016.

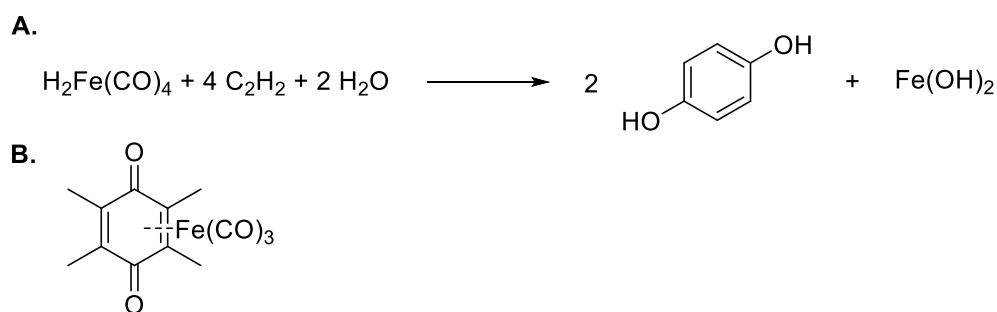
Chapter 1
Cobalt Promoted Cyclocarbonylation of Alkynes

1.1 Background

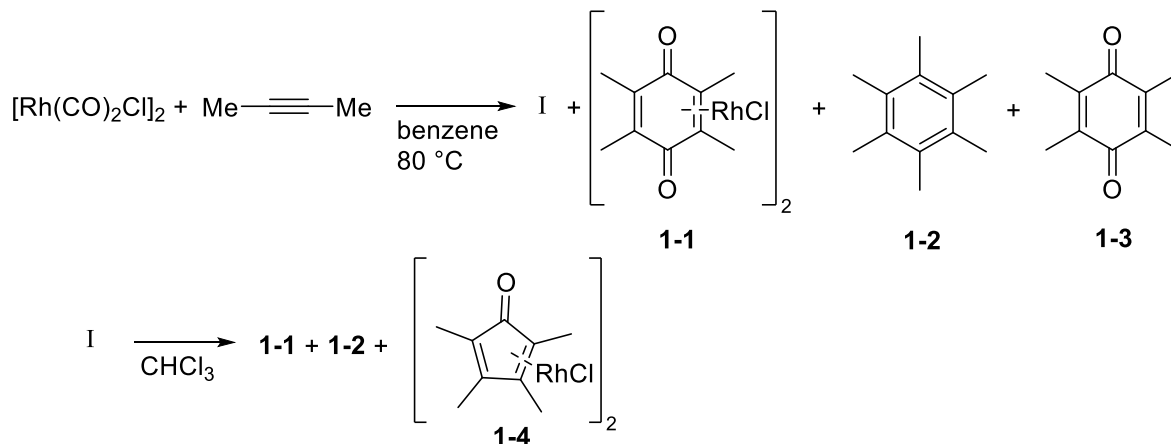
Quinones have long been studied for their wide-ranging biological activities.¹ They act in beneficial roles as vitamins, antioxidants, antibacterial agents and anticancer drugs; but they have also been shown to be acutely toxic, carcinogenic and even toxic towards the immune system. These negative effects are generally due to their photoreactivity, including the presence of quinones in the atmosphere as pollutants. Thanks to this relevance in a wide range of scientific studies, new synthetic methods to access a variety of quinone structures continues to be of interest. This chapter will specifically focus on methods of quinone synthesis using stoichiometric transition metal complexes and catalysts.

The first report of a metal carbonyl complex reacting with an alkyne to form a hydroquinone is the Reppe reaction, in which iron tetracarbonyl dihydride and acetylene react in water to give

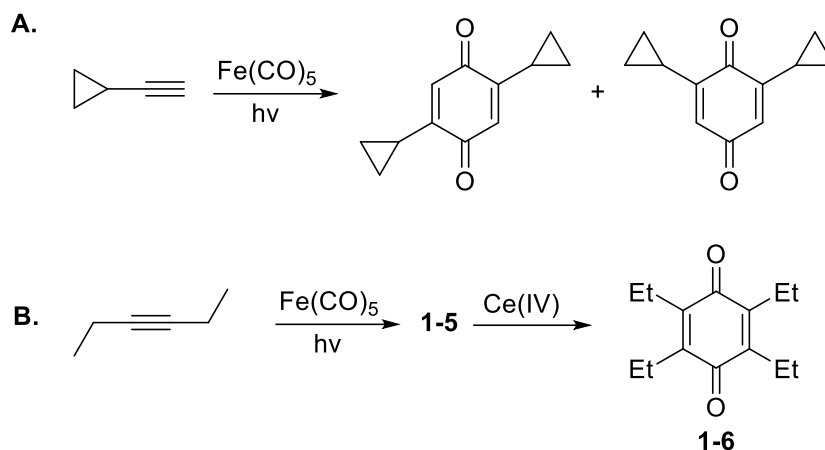
Scheme 1.1 Chemical Equation of the Reppe Reaction and Intermediate



Scheme 1.2 Reaction of 2-butyne with Chlorodicarbonyl Rhodium Dimer

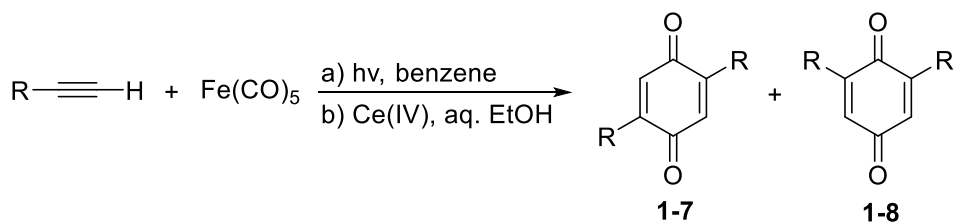


Scheme 1.3 Benzoquinones from the Photoreaction of Alkynes and Fe(CO)₅.



hydroquinone (Scheme 1.1A).² Following this report, Wender and co-workers further elucidated the metal complexes involved in this reaction, including the discovery that prior to reduction, the product exists as a quinone coordinated to iron (Scheme 1.1B).³ Several years later, Kang and co-workers described the reaction of rhodium carbonyl chloride and dimethyl acetylene, which gave a mixture of several products; most interestingly duroquinone **1-3** and the duroquinone rhodium complex **1-1** (Scheme 1.2).⁴ Inspired by results they obtained in experiments with vinyl cyclopropanes, Victor and co-workers observed that irradiation of cyclopropylacetylene with iron pentacarbonyl gave a mixture of quinone isomers (Scheme 1.3A).⁵

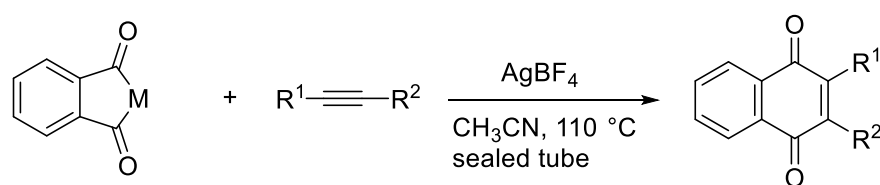
Table 1.1 Disubstituted Benzoquinones from the Photoreaction of Primary Alkynes and Fe(CO)₅.



<i>Entry</i>	<i>R</i>	<i>% Yield 1</i>	<i>% Yield 2</i>
1	-(CH ₂) ₅ CH ₃	28	22
2	-(CH ₂) ₃ Cl	11	9
3	-(CH ₂) ₈ CO ₂ CH ₃	22	16
4	-C ₆ H ₅	22	9
5	-C ₆ H ₄ CH ₃	18	9
6	-C ₆ H ₄ Cl	17	10

3-Hexyne also led to the quinone product, although treatment of an unknown intermediate **1-5**, likely an iron-quinone complex, with Ce(IV) was required to liberate the product **1-6** (Scheme 1.3b). While searching for methodology for the synthesis of disubstituted benzoquinone derivatives, the group of Kazuhiro Maruyama undertook a more thorough examination of this reaction with more common primary alkynes, and found the yields to be lacking (Table 1.1).⁶ They concluded that internal alkynes are much more suited to this reaction than primary alkynes.

Table 1.2 Synthesis of Naphthoquinones.



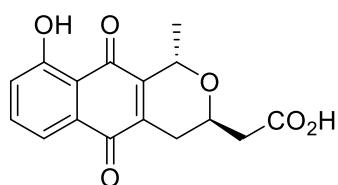
1-9 M = Co(PPh₃)₂Cl
1-10 M = Fe(CO)₄

<i>Entry</i>	<i>R¹</i>	<i>R²</i>	<i>% Yield from 1-9</i>	<i>% Yield from 2-10</i>
1	Me	Me	73	99
2	Et	Et	90	95
3	Ph	Ph	68	88
4	Ph	Me	78	100
5	<i>n</i> -Bu	H	65	95
6	Ph	H	57	94
7	<i>t</i> -Bu	Me	72	37
8	Et	Allyl	80	75
9	EtO-	Et	89	Low
10	<i>n</i> -Bu	SiMe ₃	68	22
11	Ph	-(CH ₂) ₂ OH	27	81
12	Me	CO ₂ Et	0	74
13	Et	Ac		68

The first truly general syntheses of quinone compounds using alkynes and transition metal complexes were developed by the group of Lanny Liebeskind at Florida State University. Wender and co-workers reported dicobalt octacarbonyl complexes with alkynes in the 1950's, and more recently Michael Jung's group had developed a Diels Alder reaction between benzoquinone and substituted benzocyclobutene-1,2-diones.⁷ Combining these precedents with

the knowledge of some intermediates isolated by Kang, Liebeskind and co-workers developed the reaction shown in Table 1.2, reacting both iron and cobalt metalla-2-indane-1,3-diones with alkynes to form a variety of substituted naphthoquinones.^{8,9} The basic mechanism of this reaction is shown in Scheme 1.4. They were also able to make use of this reaction to affect an intramolecular ring closure in the racemic total synthesis of Nanaomycin A (Figure 1.1), completing the synthesis in nine steps and an overall yield of 6.8 percent.¹⁰ In a follow-up study,

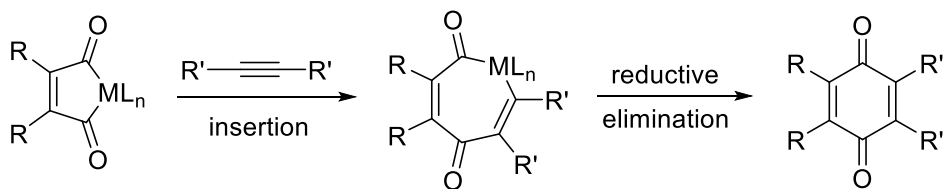
Figure 1.1 Nanaomycin A.



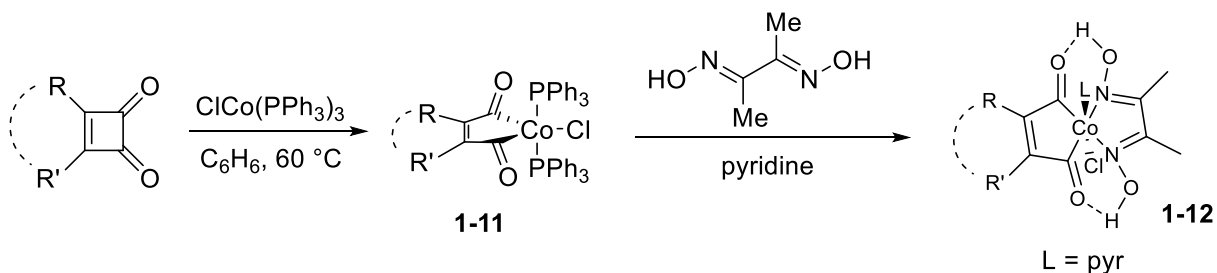
Liebeskind and co-workers were able to greatly expand the substrate scope of the reaction to include alkyl cyclobutendiones.¹¹ Once the maleoylcobalt complexes **1-11** have undergone ligand exchange to the dimethylglyoxime complexes **1-12** (Scheme 1.5), they are able

to react with a wide variety of alkynes without AgBF₄ to give the substituted benzoquinone products shown in Table 1.3. Most notable of these results is the clear trend toward electronically controlled regioselectivity when both an asymmetric cyclobutadiene and alkyne are used (**1-13h-l**). Further tuning of the dimethylglyoxime complex and addition of a different Lewis acid

Scheme 1.4 Mechanism of Quinone Synthesis via Metallacyclopent-3-ene-2,5-dione.



Scheme 1.5 More Effective Maleocobalt Complexes.



provided excellent regioselectivity with asymmetric alkynes, especially those bearing an electron withdrawing group (Table 1.4).¹²

Table 1.3 Alkyl Benzoquinone Products (% Yield, Isomeric Ratio, Favored Isomer Shown).

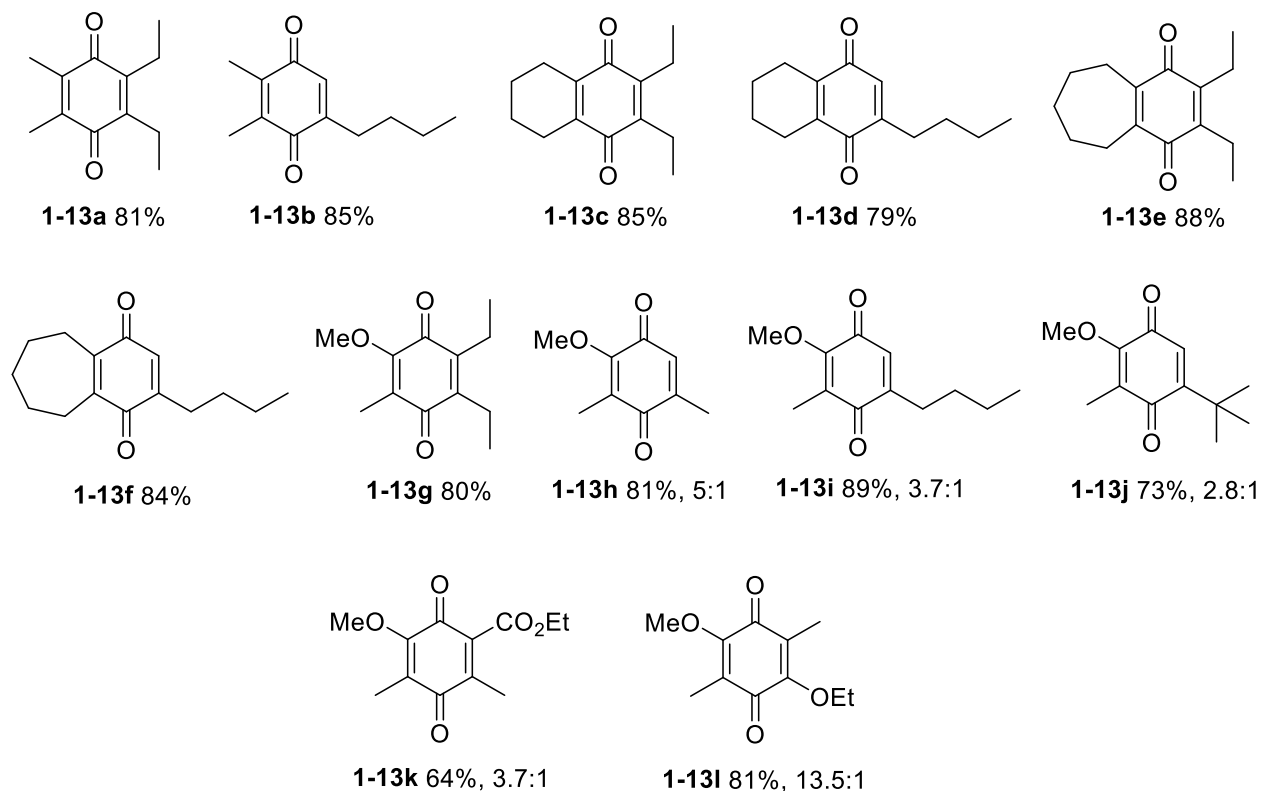
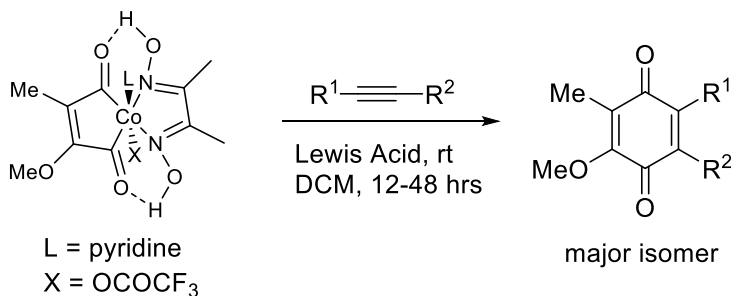
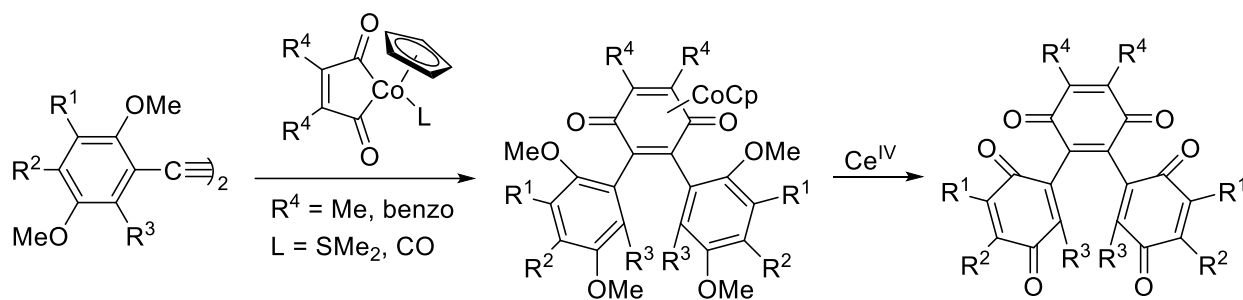


Table 1.4 Trifluoroacetate Substituted Cobalt Complex Reaction.



Entry	R ¹	R ²	Lewis Acid	% Yield	Isomeric Ratio
1	<i>n</i> -Bu	H	SnCl ₄	71	10:1
2	<i>n</i> -Bu	H	Zn(SO ₃ CF ₃) ₂	74	12:1
3	Me	CO ₂ Et	SnCl ₄	76	18:1
4	Me	CO ₂ Et	Zn(SO ₃ CF ₃) ₂	79	21:1
5	<i>t</i> -BuMe ₂ SiOCH ₂ -	Me	SnCl ₄	55	20:1
6	<i>t</i> -BuMe ₂ SiOCH ₂ -	H	SnCl ₄	57	10:1

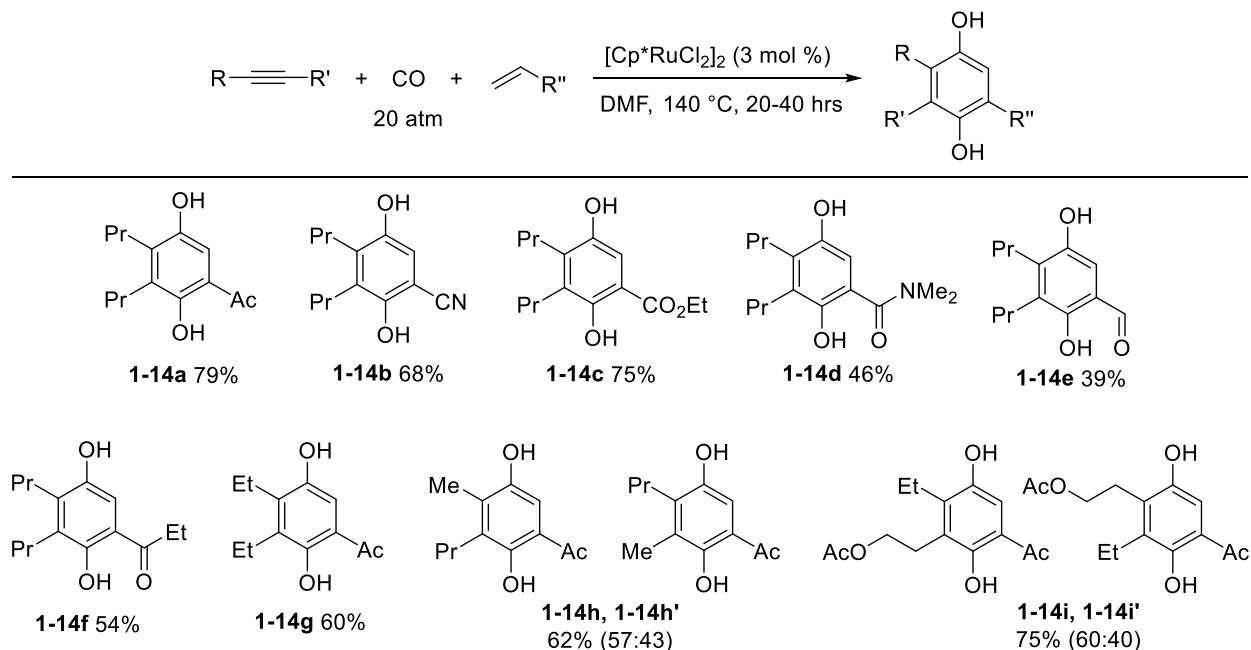
Scheme 1.6 Synthesis of Trisquinones.



This methodology was also leveraged for the synthesis of trisquinones in high yield, a traditionally challenging structural motif of great interest for their biological activity (Scheme 1.6).¹³

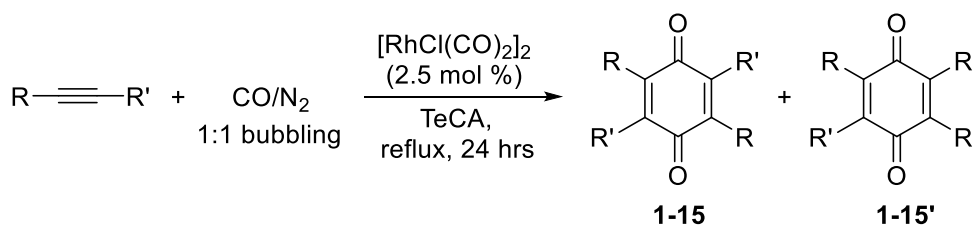
While the work of Liebeskind represented a huge step forward in the use of metals to synthesize benzoquinone derivatives, the stoichiometric metal required posed a major limitation on the practicality of the reaction. Taking inspiration from the well-studied Pauson-Khand reaction, Mitsudo and co-workers developed a set of conditions for the general reaction of alkynes with electron deficient alkenes and carbon monoxide to yield hydroquinone products

Table 1.5 Synthesis of Functionalized Hydroquinones via Ruthenium Catalyzed Carbonylation.



catalyzed by ruthenium (Table 1.5).¹⁴ The hydroquinone results from tautomerization of the initial 2-cyclohexene-1,4-dione product. Comparing these results to earlier [2+2+1+1] reactions

Table 1.6 Rhodium Catalyzed Cyclocarbonylative Coupling of Alkynes.



Entry	R	R'	% Yield	1-15 : 1-15'
1	C ₂ H ₅	C ₂ H ₅	87	
2	<i>n</i> -C ₄ H ₉	<i>n</i> -C ₄ H ₉	96	
3	<i>n</i> -C ₅ H ₁₁	CH ₃	28	48:52
4	PhCH ₂	<i>n</i> -C ₅ H ₁₁	35	53:47
5	<i>p</i> -ClC ₆ H ₄ CH ₂	<i>n</i> -C ₅ H ₁₁	40	51:49
6	Ph	CH ₃	89	80:20
7	Ph	C ₂ H ₅	85	84:16
8	Ph	<i>n</i> -C ₄ H ₉	65	51:49
9	Ph	<i>n</i> -C ₅ H ₁₁	59	46:54
10	<i>p</i> -CH ₃ C ₆ H ₄	<i>n</i> -C ₅ H ₁₁	87	52:48
11	<i>p</i> -CH ₃ OC ₆ H ₄	<i>n</i> -C ₆ H ₁₃	80	50:50
12	<i>p</i> -CH ₃ OC ₆ H ₄	<i>n</i> -C ₅ H ₁₁	86	47:53
13	<i>p</i> -CH ₃ OC ₆ H ₄	NC(CH ₂) ₃	53	49:51
14		<i>n</i> -C ₅ H ₁₁	50	52:48
15	<i>p</i> -ClC ₆ H ₄	<i>n</i> -C ₅ H ₁₁	40	59:41
16		<i>n</i> -C ₅ H ₁₁	45	59:41
17		<i>n</i> -C ₅ H ₁₁	31	75:25
18		<i>n</i> -C ₅ H ₁₁	26	61:39

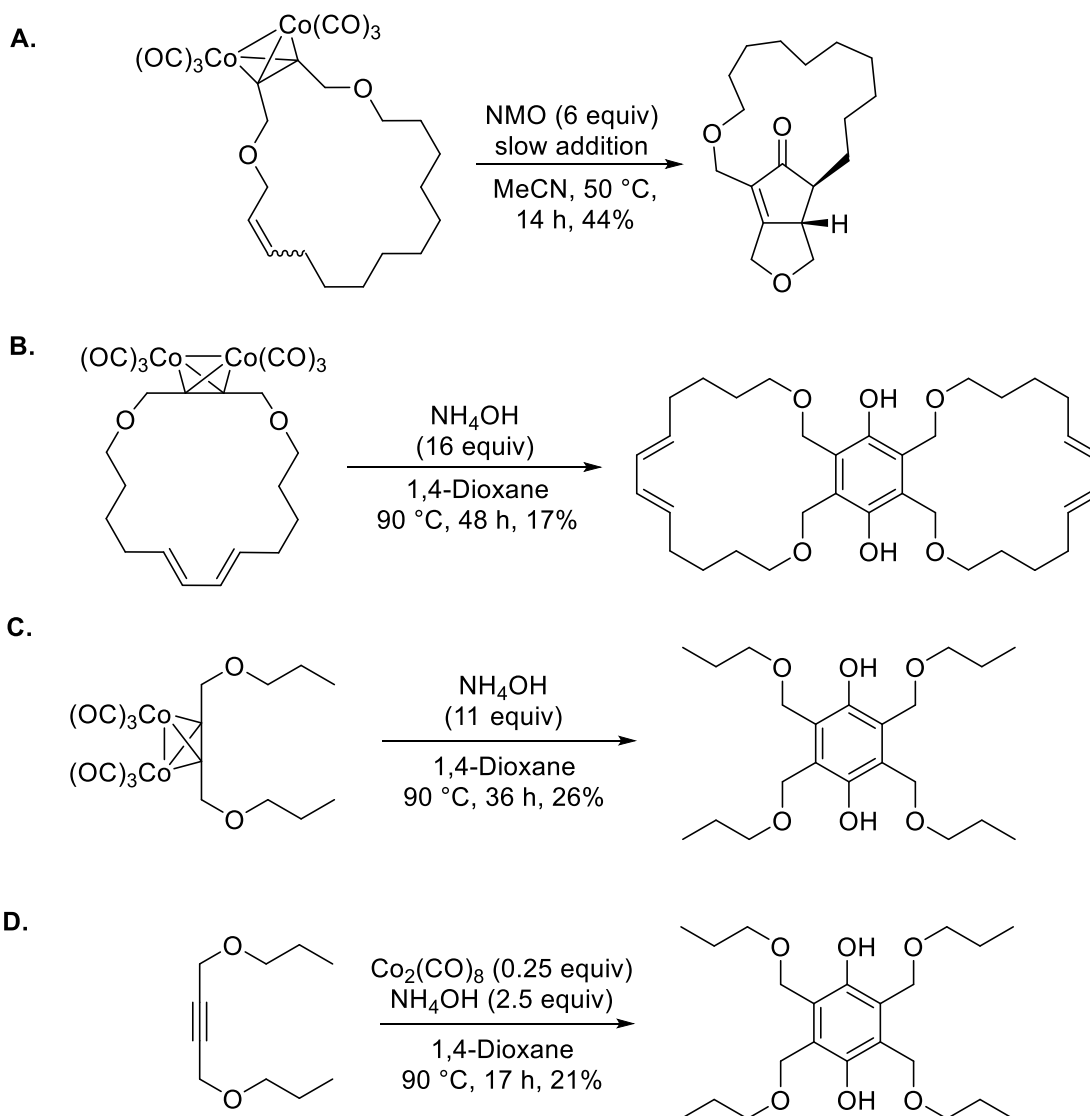
involving two alkynes and two molecules of carbon monoxide such as that of Kang and Maruyama discussed earlier, the high pressure of carbon monoxide appears to be vital to the success of the reaction. By switching to a rhodium catalyst, Huang and Hua were able to successfully perform the [2+2+1+1] cyclocarbonylative coupling between two alkynes in good to

excellent yield, resulting in the benzoquinone product directly, rather than the hydroquinone (Table 1.6).^{8,6,15} Unfortunately, this reaction only showed a moderate regioselectivity of 4:1 in the best example.

1.2 Introduction

The Hua reaction for the cyclocarbonylative homocoupling of alkynes is the current state of the art for synthesis of quinones from alkynes. There are, however, two major drawbacks to the method. Firstly, the high cost of rhodium metal, roughly nine times the price of gold, and second,

Scheme 1.7 Discovery of Cobalt Promoted [2+2+1+1] Cycloaddition.



the requirement for use of highly toxic carbon monoxide gas. We hoped to develop a method which overcomes both of these shortcomings.

A previous member of the group made a serendipitous discovery while developing the transannular Pauson-Khand reaction shown in Scheme 1.7A, using cobalt complexes of alkynes to promote the reaction.¹⁶ It was found that the complex formed between dicobalt octacarbonyl and an alkyne would undergo a [2+2+1+1] cycloaddition to form the hydroquinone product under the correct conditions and with addition of the ammonium hydroxide as an additive (Scheme 1.7A-B). Ammonium hydroxide is known to accelerate the rate of the Pauson-Khand reaction by promoting the decomplexation of carbon monoxide.¹⁷ Surprisingly, similar results were also achieved using uncomplexed alkyne and dicobalt octacarbonyl (Scheme 1.7D). The remainder of this chapter will describe efforts to optimize this [2+2+1+1] reaction for the practical synthesis of quinones and hydroquinones.

1.3 Efforts Towards a Practical Synthesis of Quinones via a [2+2+1+1] Cycloaddition of Alkynes and Dicobalt Octacarbonyl

Optimization of the reaction began using 1,4-dimethoxy-2-butyne **1-16** as the substrate (Table 1.7). Repetition of the previously reported conditions gave not the expected hydroquinone, but the oxidized quinone form **1-17** in 22% yield, with low conversion of **1-16** (entry 1). The crude NMR of this reaction clearly shows two products and the starting material with only trace impurities. Increasing the temperature of the reaction to 120 °C gave an entirely different product, a hexa-substituted benzene ring **1-18**, in 75% yield (entry 2). Lowering the temperature to 70 °C greatly reduced conversion of the starting material, giving only a 6 % yield of **1-18** and trace quantities of **1-17** (entry 4). Increasing the molar equivalents of the $\text{Co}_2(\text{CO})_8$ complex gave **1-17** in 16.6% yield and a 50% yield of **1-18**, with almost total consumption of substrate

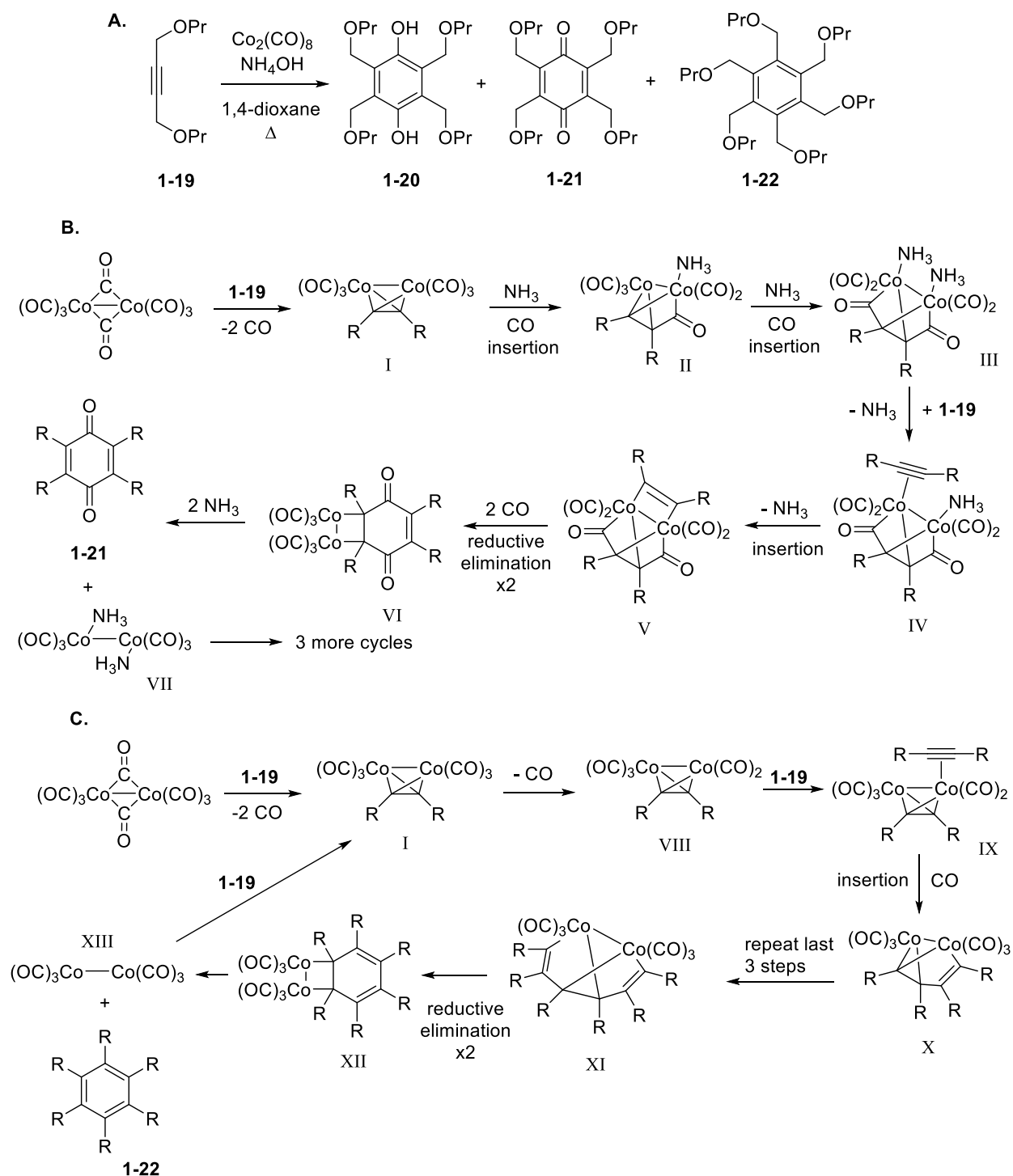
(entry 3). In previous preliminary results addition of carbon monoxide gas was shown to have no positive effect of the outcome of the reaction. At this point the workup was modified from the original report to better remove cobalt by adding a wash with ethylenediaminetetraacetic acid to complex and extract into an aqueous layer the cobalt which could not be removed by physical filtration. The model substrate was also changed to the propyl compound **1-19** for ease of handling due to the increased molecular weight of the substrate (Scheme 1.8A).

Table 1.7 Initial Reaction Optimization.

<i>Entry</i>	<i>Temperature (°C)</i>	<i>Co₂(CO)₈ equiv.</i>	<i>1-17 % yield</i>	<i>1-18 % yield</i>
1	90	0.25	22	-
2	120	0.25	0	75
3	90	0.5	16.6	50
4	70	0.5	trace	(6)

Switching substrates to **1-19** led to a mixture of the hydroquinone and quinone products **1-20** and **1-21**, as well as the substituted benzene product **1-22**. Presumably, **1-20** is generated via the reduction of **1-21**. The proposed mechanism for the formation of quinone **1-21** is shown in Scheme 1.8B. Dicobalt octacarbonyl complexes to the alkyne **1-19** to form complex I, which then undergoes two rounds of carbon monoxide insertion promoted by aqueous ammonia to give complex III. The cobalt then forms a π -complex with another equivalent of **1-19**, followed by a migratory insertion leading to complex V. Two rounds of reductive elimination leads to VI, which can then release quinone **1-21**. This process is not technically catalytic, but the cobalt complex should, in theory, react multiple times until the carbon monoxide is consumed. The catalytic cycle for the formation of substituted benzene **1-22** is shown in Scheme 1.8C. Dicobalt

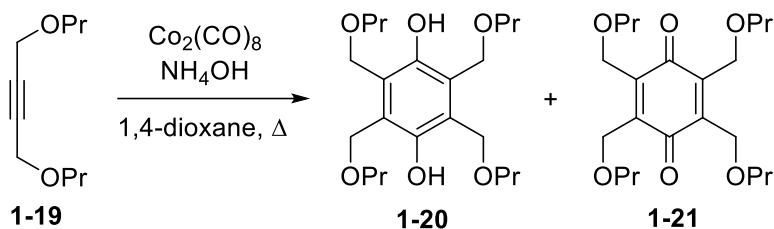
Scheme 1.8 Reaction Products and Proposed Mechanisms



octacarbonyl and **1-19** again form complex I, which then exchanges a carbon monoxide ligand for a π -complex with **1-19** (IX). The alkyne then inserts to give complex X. This process then

repeats to give XI, which can then undergo two rounds of reductive elimination to give complex XII. Release of the product **1-22** then restarts the cycle.

Table 1.8 Optimization of Conditions



<i>Entry</i>	<i>Time (h)</i>	<i>Co₂(CO)₈ equiv.</i>	<i>NH₄OH equiv.</i>	<i>[M]</i>	<i>Combined Yield (%)^a</i>
1	16	0.25	2.5	0.5	27
2	16	0.25	2.5	0.25	(25)
3	16	0.35	2.5	0.5	(16)
4	16	0.5	2.5	0.5	(26)19
5	16	0.5	2.5	0.25	22
6	16	0.75	2.5	0.5	(28)
7	16	1.0	2.5	0.5	(20)
8	16	0.5	1.5	0.5	23
9	16	0.5	3.5	0.5	(22)
10	48	0.25	2.5	0.25	(37)

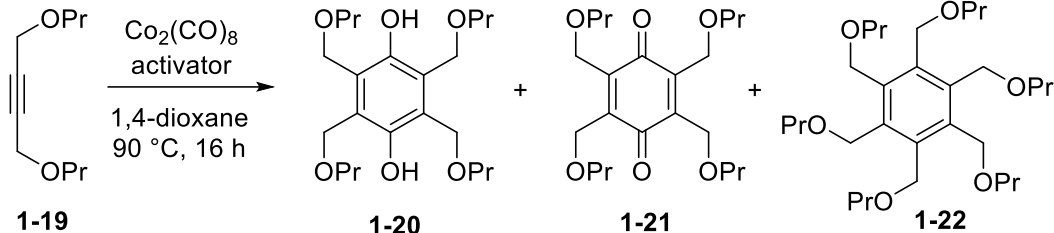
(a) numbers in parenthesis are nmr standard yield.

A range of reaction conditions were examined with ammonium hydroxide as an activator (Table 1.8). It is known that the acidity of the glass of the reaction flask can affect the yield of Pauson-Khand reactions.¹⁸ Believing our reaction to follow a similar mechanism, we pre-treated the pressure tube in a bath of concentrated potassium hydroxide in isopropyl alcohol. This resulted in an increased ratio of **1-20** to **1-22**, so this method was used for all subsequent reactions (entry 1). Concentration did not have an effect on the result of the reaction (entries 1-2). Varying the molar equivalents of the cobalt complex had no significant effect, positive or negative, on the yield of the reaction (entries 3-7). Varying the equivalents of ammonium hydroxide had a small negative effect on the yield (entries 8-9). A significantly increased reaction time did have a small, but meaningful, positive effect on yield due to increased

conversion (entry 10). Yields in parenthesis were obtained by internal ^1H NMR standard in all tables.

Convinced that simply altering the conditions would not lead to a practical yield, we screened several alternative activators (Table 1.9).¹⁹ Out of the six activators screened, *n*-butylamine was the only reagent that led to yields comparable to ammonium hydroxide. No additional activator led to the [2+2+2] reaction pathway, indicating that the activator serves to promote the [2+2+1+1] pathway over the thermodynamically preferred pathway.

Table 1.9 Activator Screen



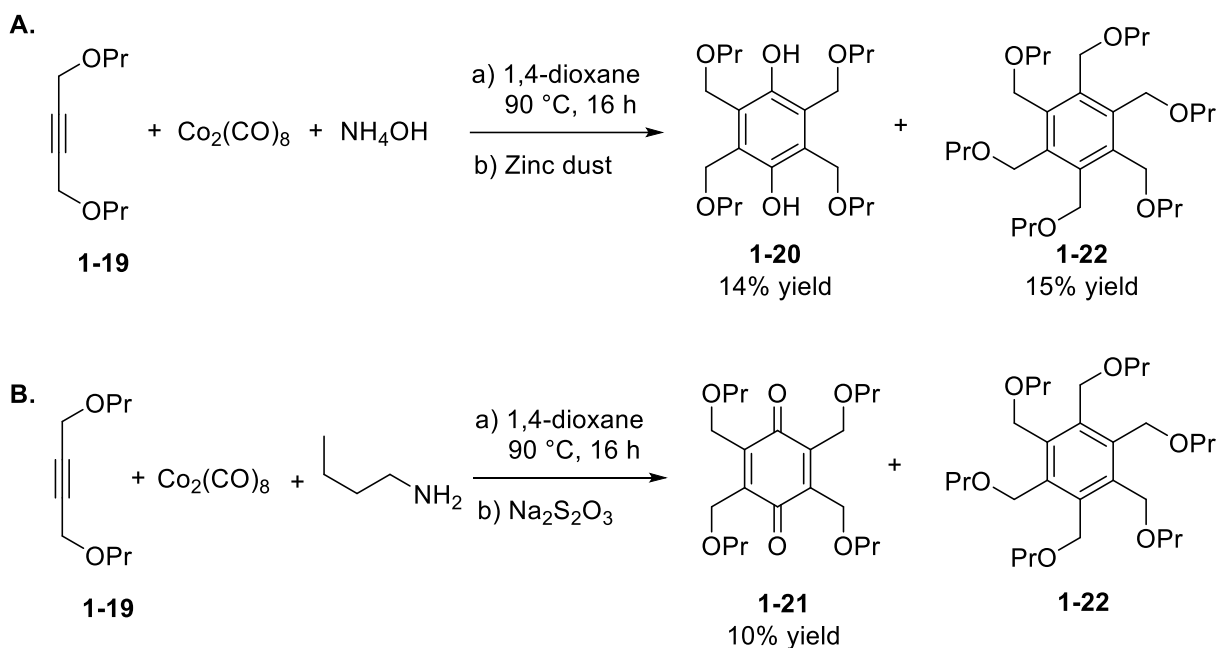
The reaction scheme shows diene **1-19** reacting with $\text{Co}_2(\text{CO})_8$ and an activator in 1,4-dioxane at 90 °C for 16 h. The products are **1-20** (a hydroquinone derivative), **1-21** (a quinone derivative), and **1-22** (a dihydroquinone derivative).

<i>Entry</i>	<i>Activator</i>	<i>Product</i>	<i>Yield (%)^a</i>
1	NHMe_2	NR	-
2	BnMe_3NOH	1-21/1-22	(1.7)/(34)
3	Pyridine	1-22	(13)
4	<i>n</i> -butylamine	1-20 + 1-21/1-22	15.5(32)/19
5	Pyrrolidine	1-21/1-22	(10.5)/(24)
6	Dimethyl Sulfoxide	NR	-
7	none	NR	-

(a) numbers in parenthesis are nmr standard yield.

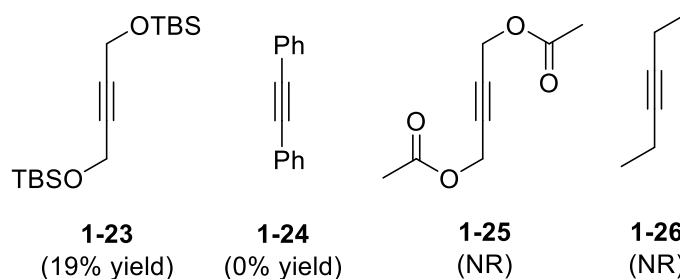
A series of experiments were also performed attempting to find a reductive or oxidative workup which would yield only hydroquinone or only quinone product. Ceric ammonium nitrate and sodium borohydride were both examined, but failed to give a single quinone derived product. Zinc dust provided exclusively the reduced hydroquinone form, and sodium thiosulfate the oxidized quinone, but both resulted in reduced yields (Scheme 1.9).

Scheme 1.9 Reductive and Oxidative Workups.



Having seen no significant improvement in yield with any alteration of the conditions or reagents, a handful of alternative substrates were examined (Table 1.10). The *t*-butyldimethylsilyl ether protected diol **1-23** gave a yield of the quinone product comparable to that of **1-19**. Diphenyl acetylene (**1-24**) was consumed under reaction conditions, but led to undesired side products. The diacetate **1-25** and 3-hexyne (**1-26**) were both unreactive, with most of the starting material recovered.

Table 1.10 Additional Substrates Examined



1.4 Conclusion

At this time we stopped pursuing the optimization of this reaction. As discussed above, significant effort to find a proper set of conditions has yielded only a very small amount of progress, and alternate substrates also appear to have no positive effect on the results. The requirement for the reaction to be run in a pressure tube also prevents practical safe scale-up, at least in an academic lab setting. Ultimately, the [2+2+2] reaction out competes the desired [2+2+1+1] pathway, despite our best efforts, and prevents the quinone product from being obtained in high yields.

1.5 Experimental Section

General Information

Unless otherwise specified, reactions were run under nitrogen using dry solvents. DCM was distilled over CaH₂. Dioxane was used as purchased from Fisher Scientific. All chemicals were used as purchased from commercial sources. NMR data was obtained using a Bruker ARX-400 instrument and calibrated to the solvent signal (CDCl₃ : δ = 7.26 ppm for ¹H NMR, δ = 77.2 ppm for ¹³C NMR). Data for ¹H NMR spectra are reported as follows: chemical shift (δ ppm), multiplicity, coupling constant (Hz), then integration. Data for ¹³C NMR spectra are reported in terms of chemical shift. The following abbreviations are used for the multiplicities: s = singlet, t = triplet, sex. = sextet. Flash column chromatography was performed using 40-63 mesh silica gel.

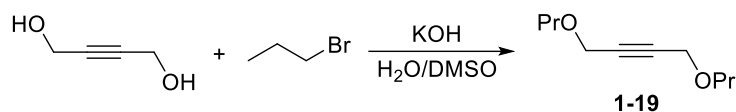
Experimental Procedures

Table 1.7 Representative Procedure (Entry 1)

To a glass pressure tube was added dioxane (2 mL), **1-16** (0.114 g), and cobalt octacarbonyl (0.085 g), then while stirring added ammonium hydroxide (4 M in H₂O, 0.625 mL), flushed with

nitrogen gas and capped. The reaction was heated at 90 °C for 16 hours. After cooling to room temperature, the dark green solution was diluted with EtOAc, filtered through celite, and concentrated *in vacuo* to an orange oil. The crude product was purified by flash column chromatography (silica gel, 65:35 hexanes/EtOAc) to give pure **1-17** (32 mg, 22% yield) as a pale-yellow oil. ¹H NMR (400 MHz, CDCl₃): δ 4.43 (s, 8 H), δ 3.38 (s, 12 H).

Synthesis of 1,4-Dipropoxy-2-butyne (**1-19**)



A round bottom flask under nitrogen atmosphere was charged with 1,4-dihydroxy-2-butyne (1.08 g) and DMSO (20 mL). KOH (1.75 g) dissolved in H₂O (5 mL) was added and stirred for 30 minutes. The reaction immediately changed from a light orange to a dark orange brown color upon addition. The reaction was cooled to 0 °C and bromopropane (2.5 mL) was added dropwise. After 10 minutes the reaction was heated at 70 °C for 24 hours. The reaction was then cooled to 0 °C and 35 mL of H₂O was added. The solution was then extracted 3x with Et₂O, and the combined organic layer was washed 3x with H₂O, dried with anhydrous MgSO₄, filtered, and concentrated *in vacuo* to a pale-yellow oil. The crude product was purified via flash column chromatography (silica gel, 95:5 hexanes/EtOAc) to give **1-19** as a colorless oil (1.22 g, 57% yield). ¹H NMR (400 MHz, CDCl₃): δ 4.18 (s, 4 H), δ 3.46 (t, *J* = 6.7, 4 H), δ 1.61 (sex, *J* = 7.4, 4 H), δ 0.93 (t, *J* = 7.4, 6 H). ¹³C NMR (100 MHz, CDCl₃): δ 10.5, 22.8, 58.3, 71.9, 82.3.

Tables 1.8 and 1.9 Representative Procedure (Table 1.8, Entry 8)

A pressure tube which was pretreated in a potassium hydroxide and isopropanol base bath was charged with cobalt octacarbonyl (0.171 g), evacuated, and backfilled with nitrogen gas. Dioxane (4 mL), **1-19** (0.17 g), and ammonium hydroxide (4 M in H₂O, 0.375 mL) were added.

The tube was sealed and heated at 90 °C for 16 hours. After cooling to room temperature, the reaction was diluted with Et₂O and filtered through filter paper to remove precipitate. The filtrate was washed once with aqueous EDTA, dried over anhydrous MgSO₄, filtered, and concentrated *in vacuo* to an orange oil. The crude product was purified via flash column chromatography (silica gel, 93:7 hexanes/EtOAc) to yield **1-20** as a white solid (22 mg, 11% yield) and **1-21** as a yellow oil (23 mg, 12% yield). **1-20** ¹H NMR (400 MHz, CDCl₃): δ 8.11 (s, 2 H), δ 4.71 (s, 8 H), δ 3.45 (t, *J* = 6.7, 8 H), δ 1.61 (sex., *J* = 6.8, 8 H), δ 0.91 (t, *J* = 7.4, 12 H). **1-21** ¹H NMR (400 MHz, CDCl₃): δ 4.48 (s, 8 H), δ 3.45 (t, *J* = 6.7, 8 H), δ 1.57 (sex., *J* = 6.8, 8 H), δ 0.89 (t, *J* = 7.4, 12 H).

Reductive Workup with Zn (Scheme 1.9A)

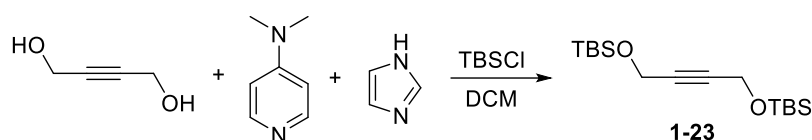
A pressure tube which was treated in a base bath was charged with cobalt octacarbonyl (0.171 g), evacuated, and backfilled with nitrogen gas. Dioxane (4 mL), **1-19** (0.17 g), and ammonium hydroxide (4M in H₂O, 0.625 mL) were added. The tube was sealed and heated at 90 °C for 16 hours. After cooling to room temperature, the reaction was diluted with Et₂O and filtered through filter paper to remove precipitate. The filtrate was washed once with aqueous EDTA, dried over anhydrous MgSO₄, filtered, and concentrated *in vacuo* to an orange oil. The crude product was dissolved in 2 mL of AcOH and Zn dust (100 mg) was added. After sonication for five minutes the Zinc dust was removed via filtration and the solution was concentrated *in vacuo*, giving **1-20** in 14% yield by NMR mesitylene internal standard, **1-19** in 14% yield by NMR mesitylene internal standard, and **1-22** in 15% yield by NMR internal standard.

Oxidative Workup with Na₂S₂O₃ (Scheme 1.9B)

A pressure tube which was treated in a base bath was charged with cobalt octacarbonyl (0.171 g), evacuated, and backfilled with nitrogen gas. Dioxane (4 mL), **1-19** (0.17 g), and butylamine

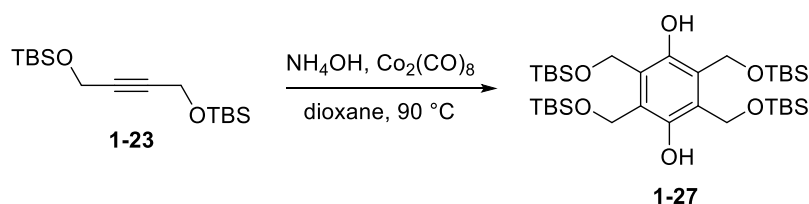
(0.24 mL) were added. The tube was sealed and heated at 90 °C for 16 hours. After cooling to room temperature, Na₂S₂O₃ was added (0.32 g), followed by water until all solid was dissolved. After the reaction was stirred vigorously for 30 minutes, Et₂O was added and the organic layer isolated. The organic solution was washed with aqueous EDTA, dried over anhydrous MgSO₄, filtered, and concentrated *in vacuo*. **1-21** was obtained in 10% yield by NMR mesitylene internal standard.

Synthesis of 1,4-bis(tert-butyldimethylsilyloxy)-2-butyne (**1-23**)



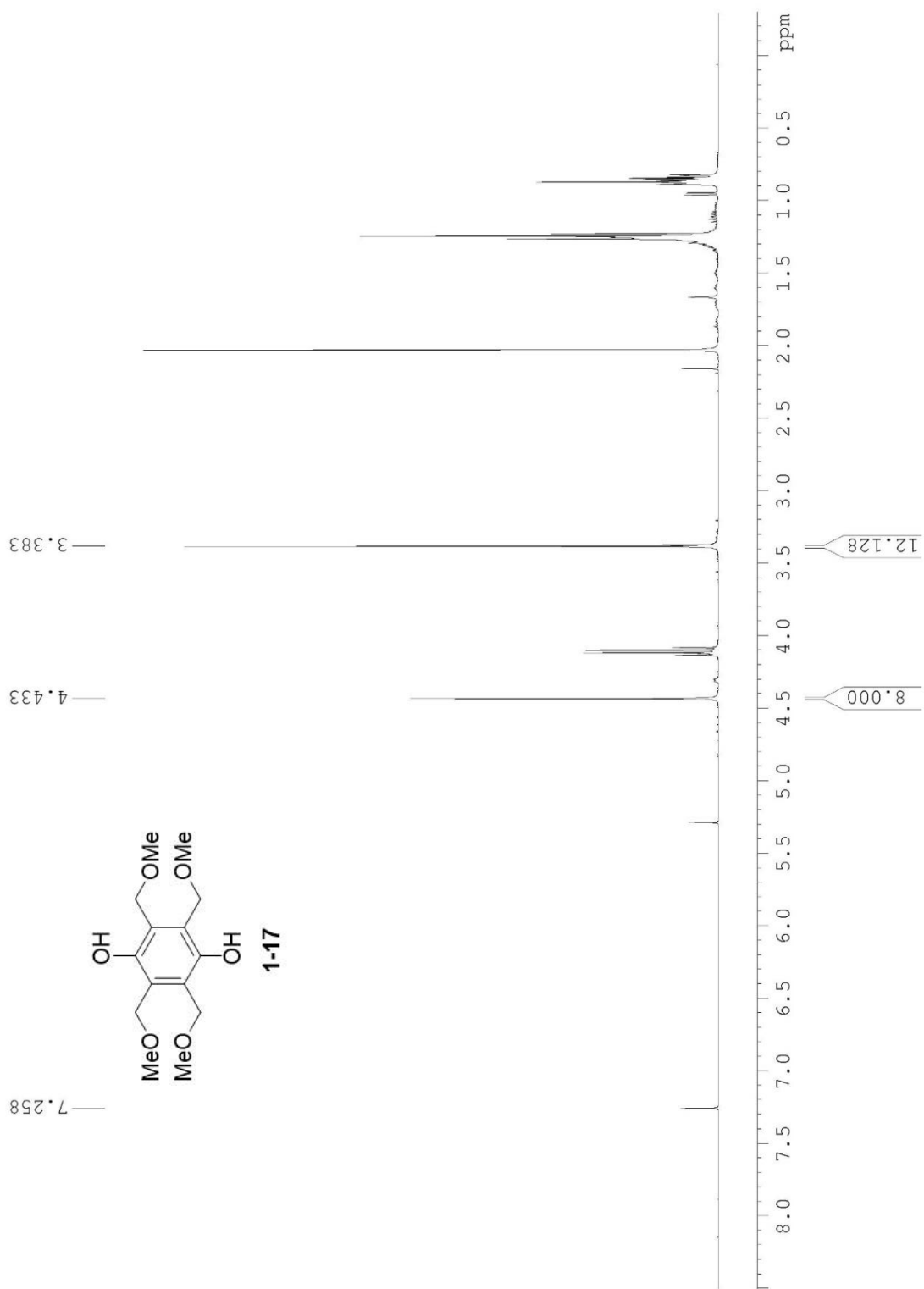
Anhydrous DCM (80 mL) was added to a flame dried round bottom flask under nitrogen atmosphere. 1,4-dihydroxy-2-butyne (1.00 g, 11.6 mmol) was added and stirred vigorously, followed by DMAP (0.14 g) and imidazole (1.9 g), giving a semi-transparent yellow suspension. Tert-butyldimethylsilyl chloride (4.2 g) was added, immediately turning the reaction opaque white. After 1 hour 10% aqueous potassium carbonate (40 mL) was added, and the aqueous layer was isolated and extracted with Et₂O (3x 40 mL). The combined organic layers were washed with brine, dried over anhydrous MgSO₄, filtered, and concentrated *in vacuo* to give an orange yellow oil. The crude product was purified via flash column chromatography (98:2 hexanes/EtOAc) to give **1-23** as a colorless oil (3.47 g, 95% yield). ¹H NMR (400 MHz, CDCl₃): δ 4.34 (s, 4 H), δ 0.90 (s, 18 H), δ 0.11 (s, 12 H).

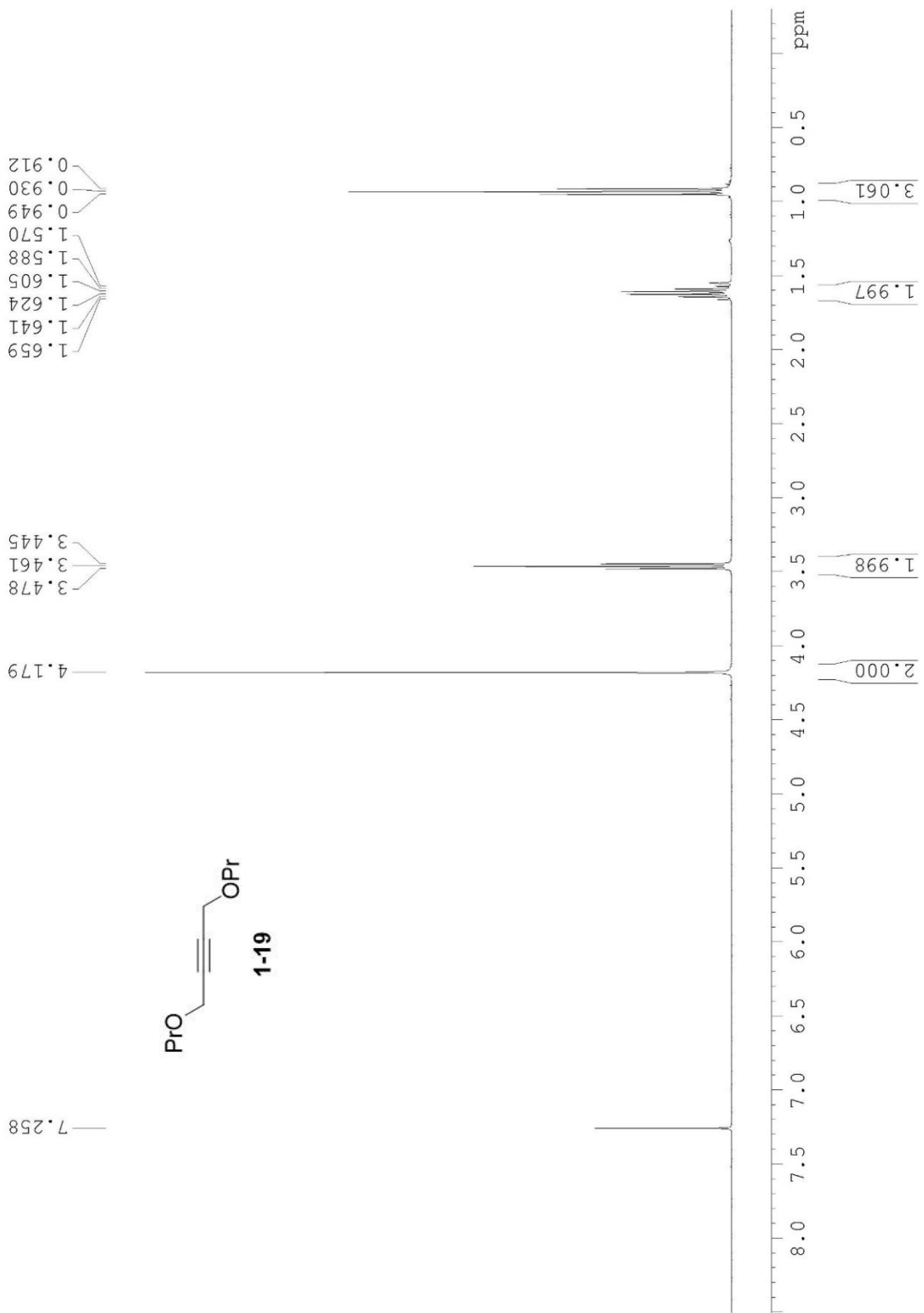
Synthesis of **1-27**

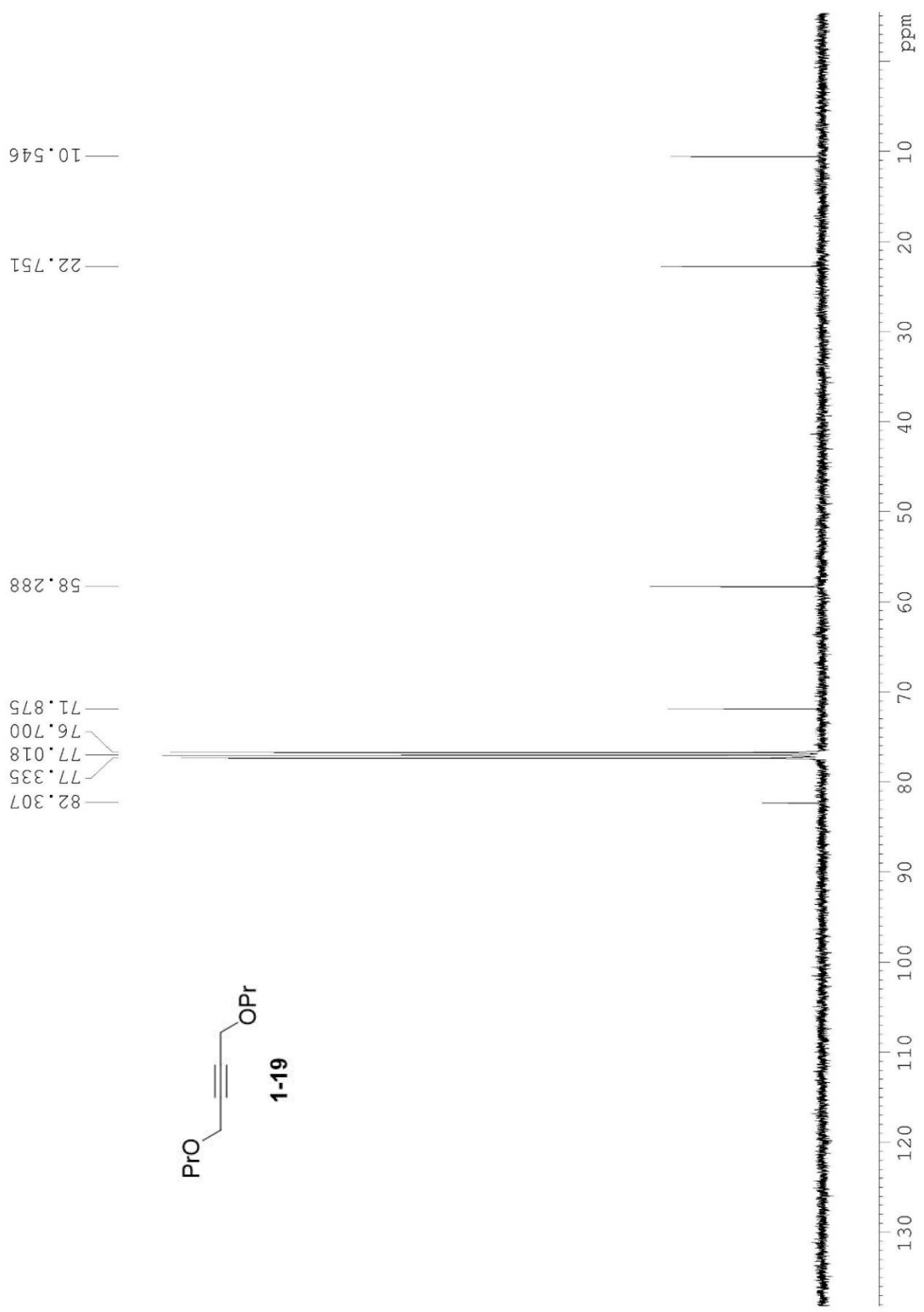


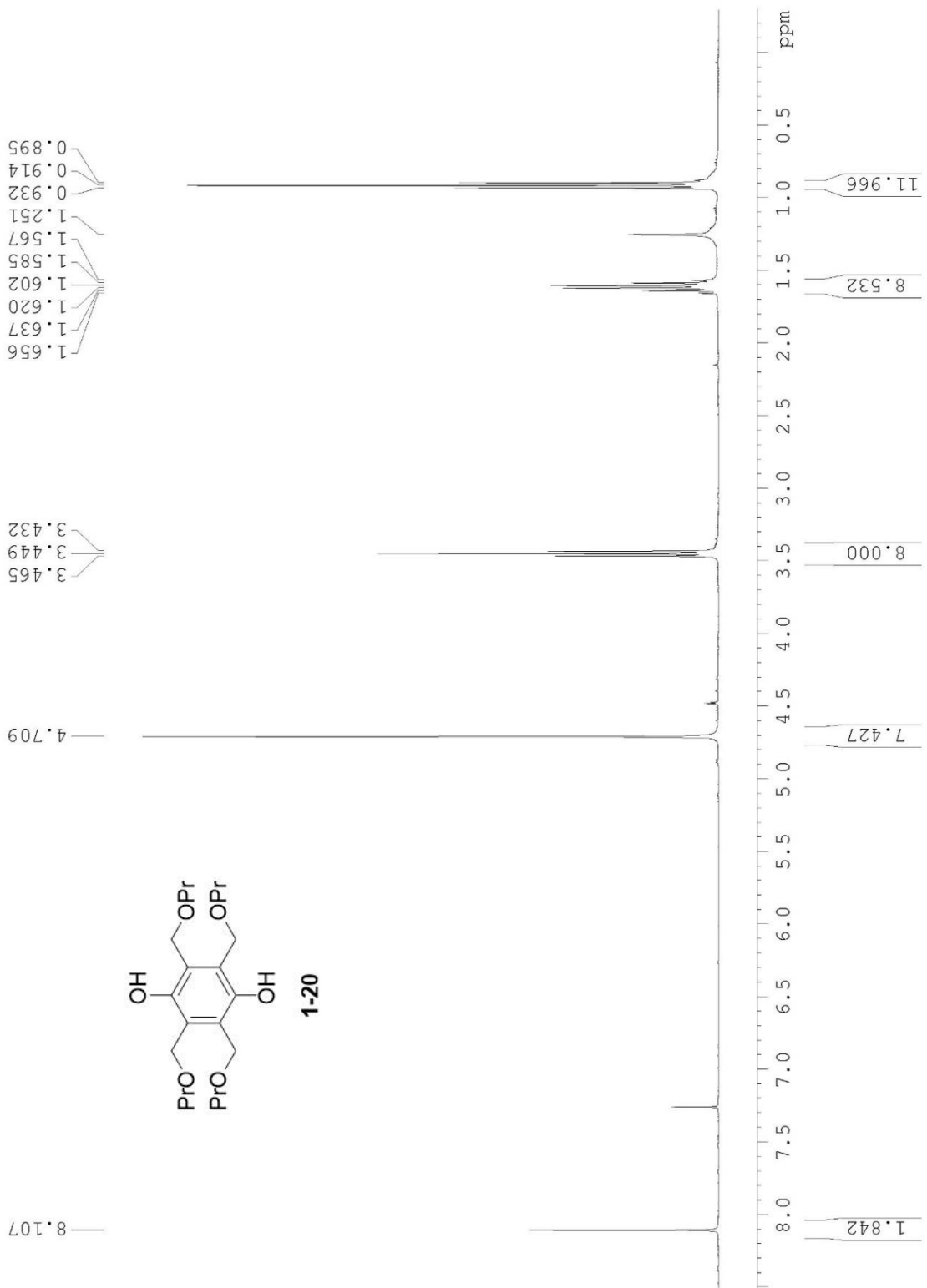
A pressure tube which was pretreated in a NaOH isopropanol base bath was charged with cobalt octacarbonyl (0.171 g), evacuated, and backfilled with nitrogen gas. Dioxane (4 mL), **1-23** (0.315 g), and ammonium hydroxide (4M in H₂O, 0.625 mL) were added. The tube was sealed and heated at 90 °C for 16 hours. After cooling to room temperature, the reaction was diluted with EtOAc and filtered through silica to remove precipitate. The filtrate was concentrated *in vacuo*, diluted with Et₂O washed once with aqueous Na₂S, then with H₂O. The aqueous layer was then back extracted with Et₂O, and the combined organic layers were dried over anhydrous MgSO₄, filtered, and concentrated *in vacuo* to an orange brown solid. The crude product was purified via flash column chromatography (97.5:2.5 hexanes/Et₂O) to give **1-27** (67 mg, 19% yield). ¹H NMR (400 MHz, CDCl₃): δ 8.40 (s, 2 H), δ 4.90 (s, 8 H), δ 0.89 (s, 36 H), δ (s, 24 H). ¹³C NMR (100 MHz, CDCl₃): δ 124.1, 59.3, 25.9, 18.2, -5.4.

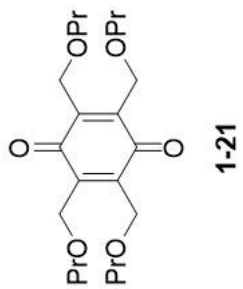
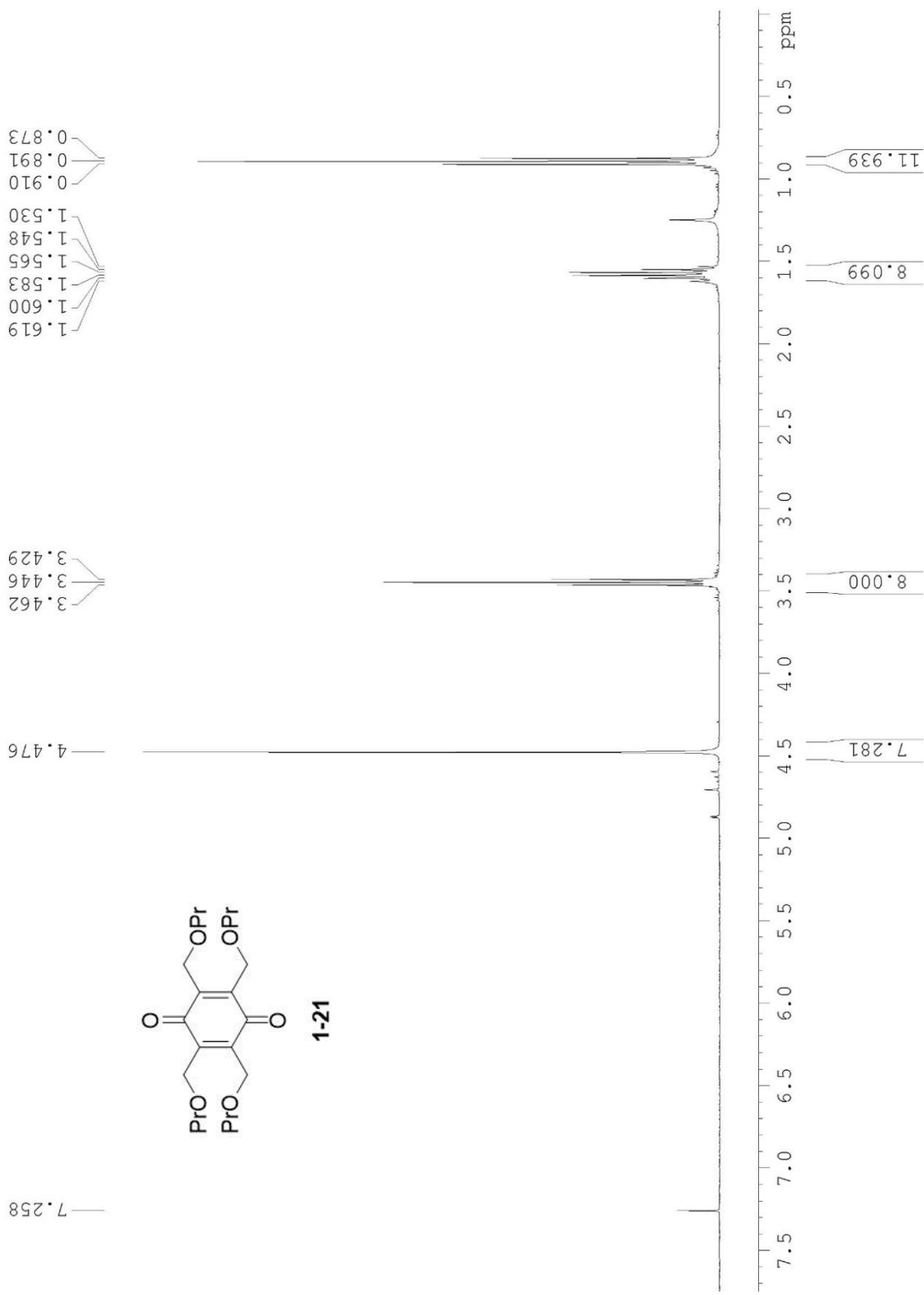
1.6 ¹H and ¹³C NMR Data

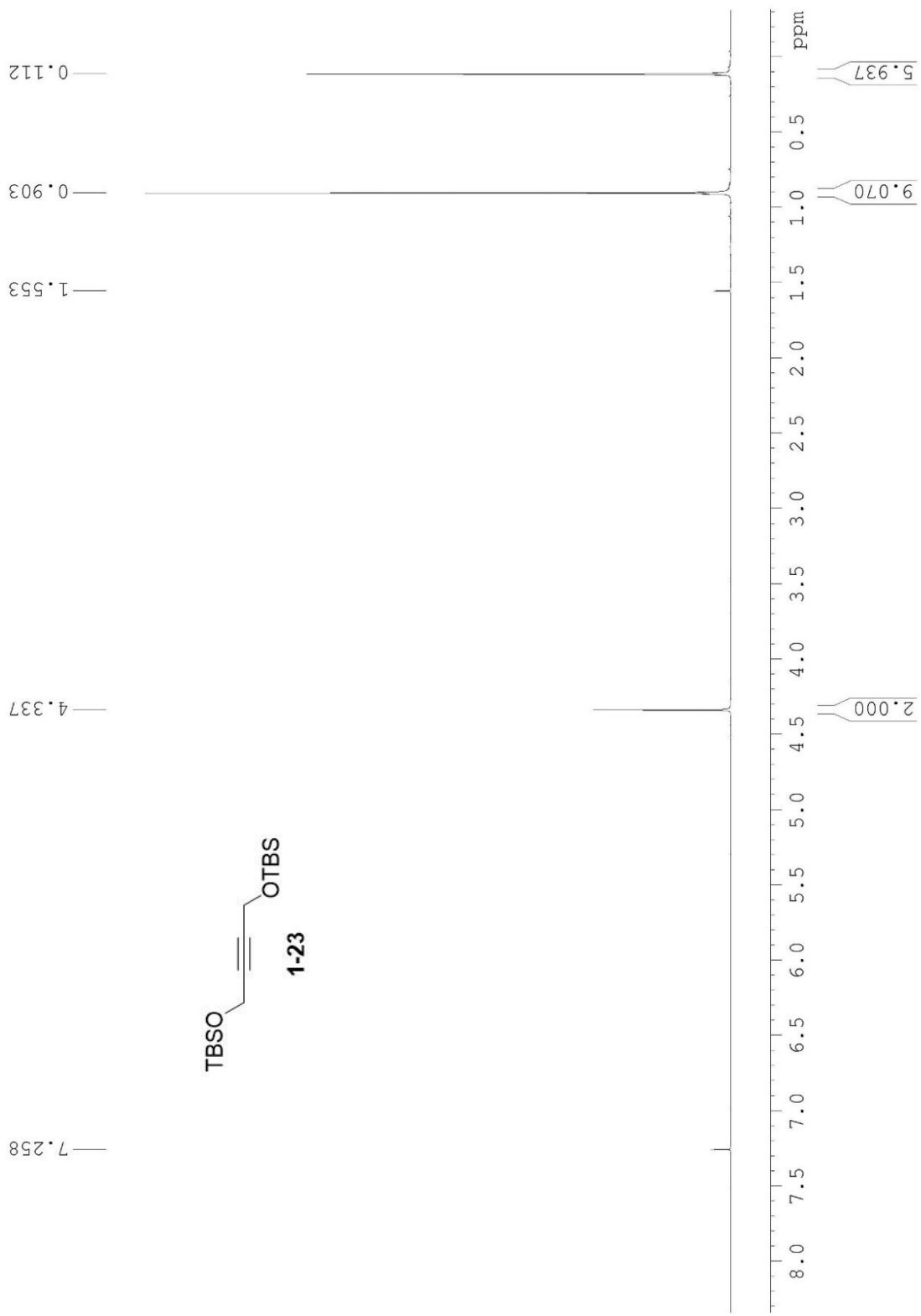


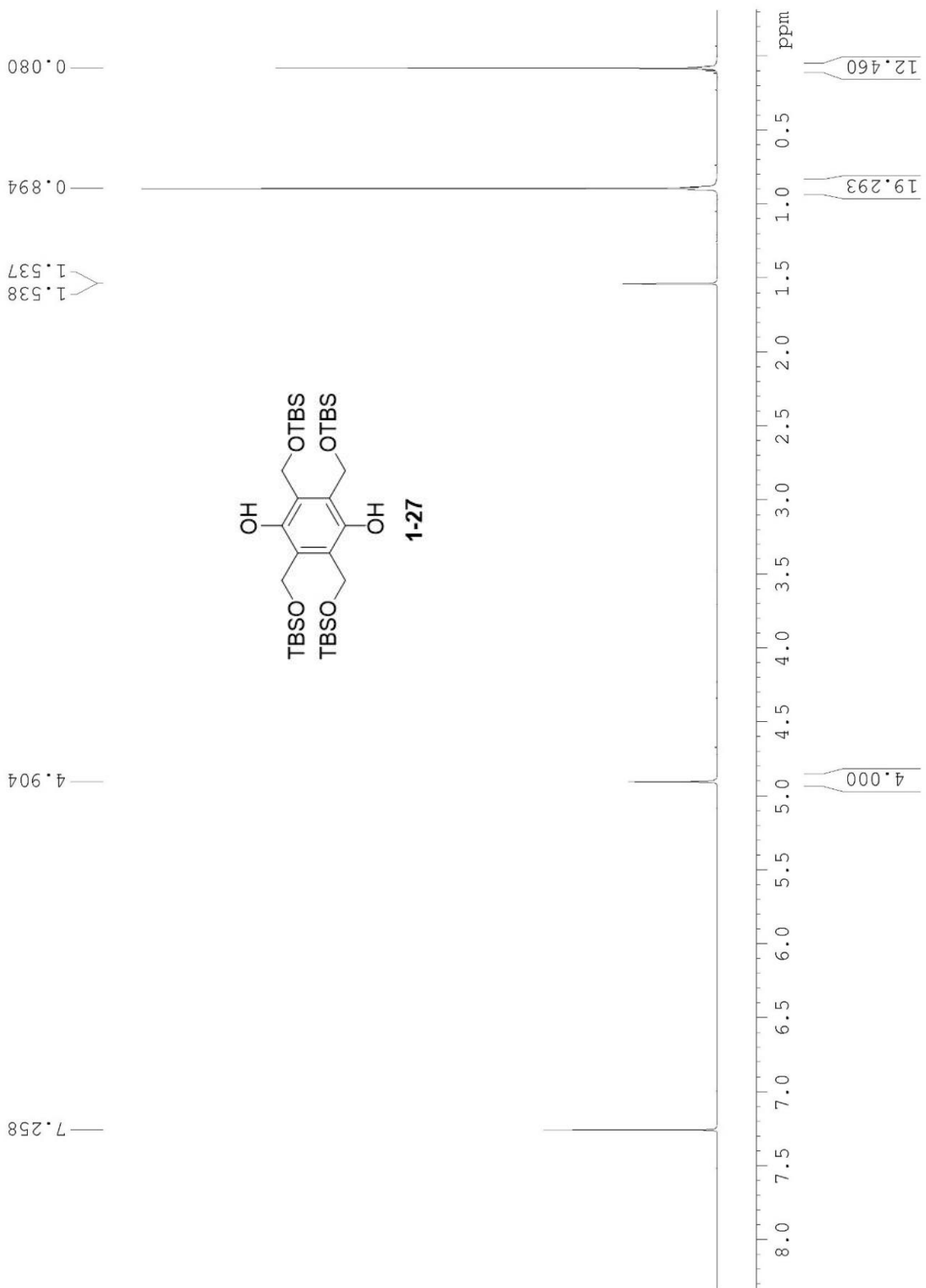












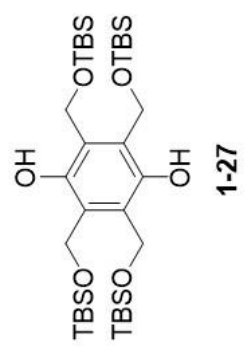
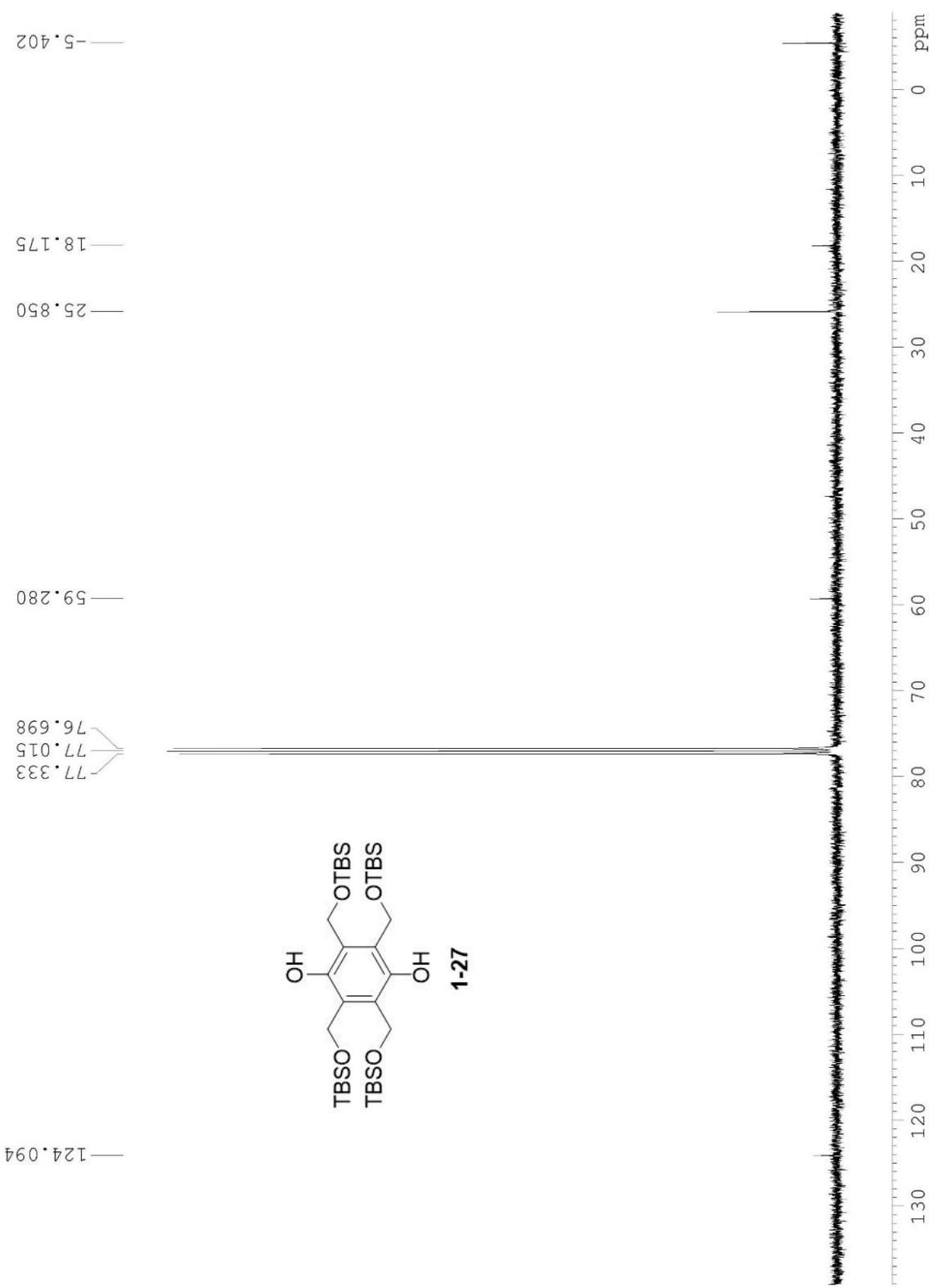


Table 1.7, Entry 2

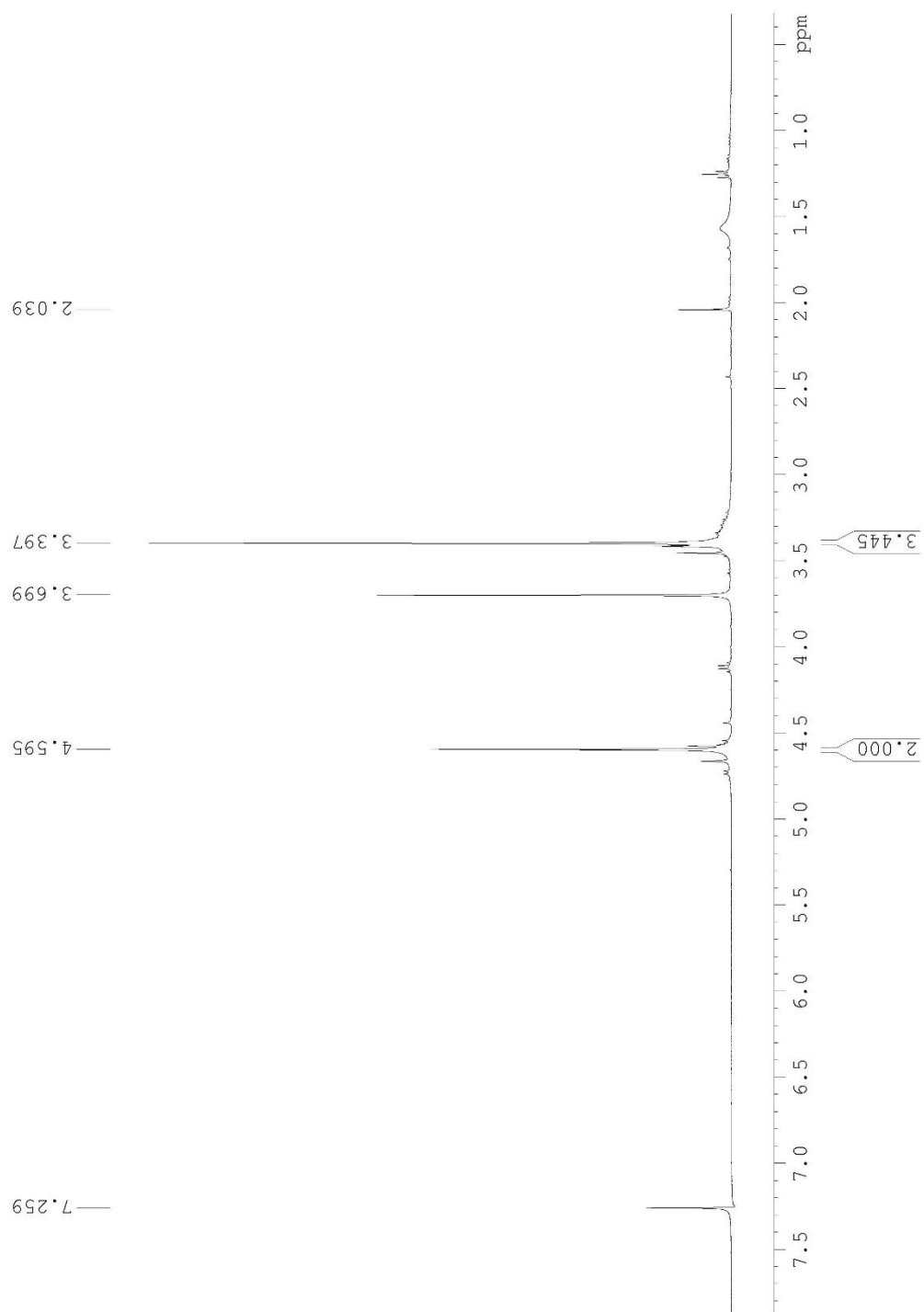


Table 1.7, Entry 3a

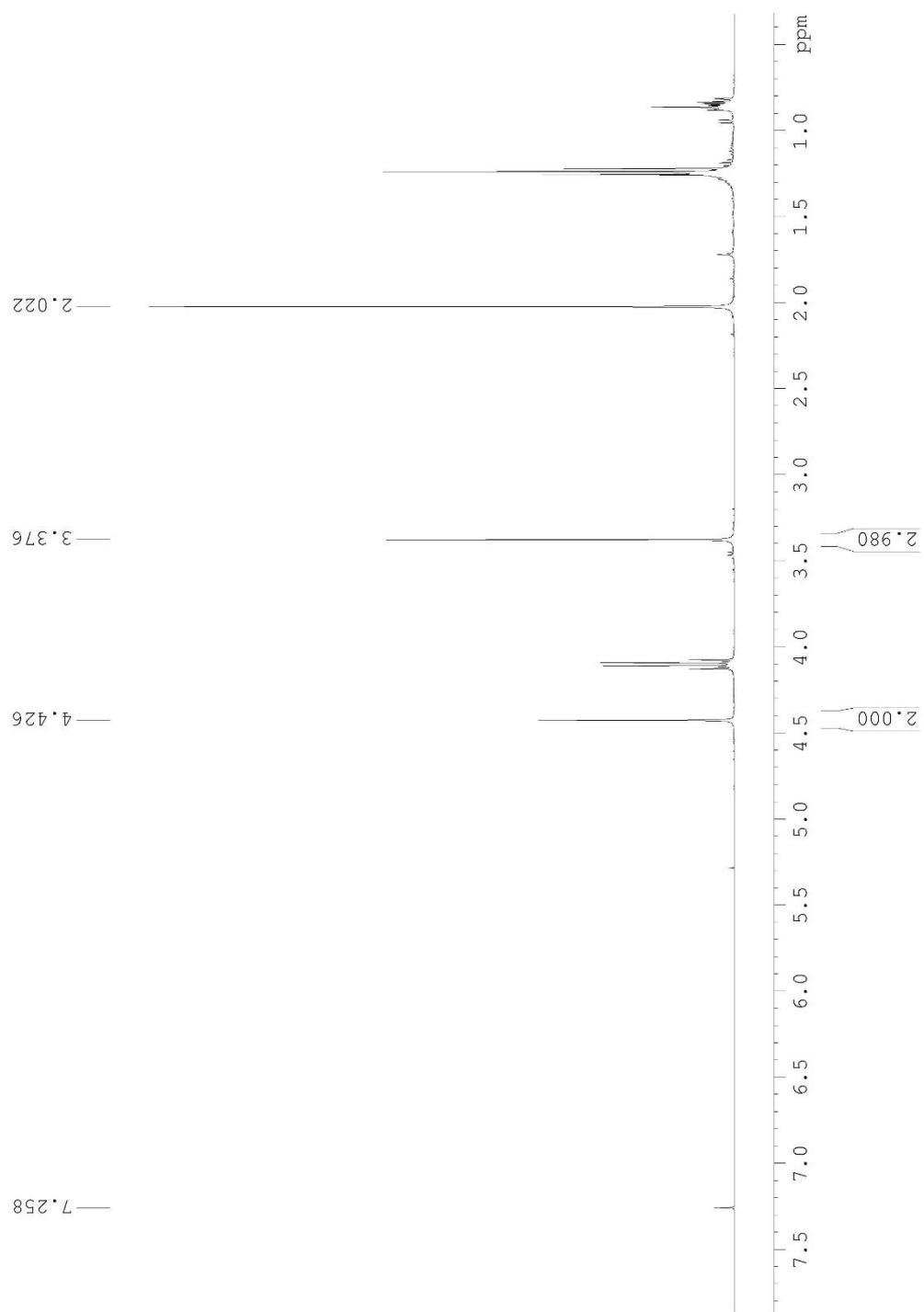


Table 1.7, Entry 3b

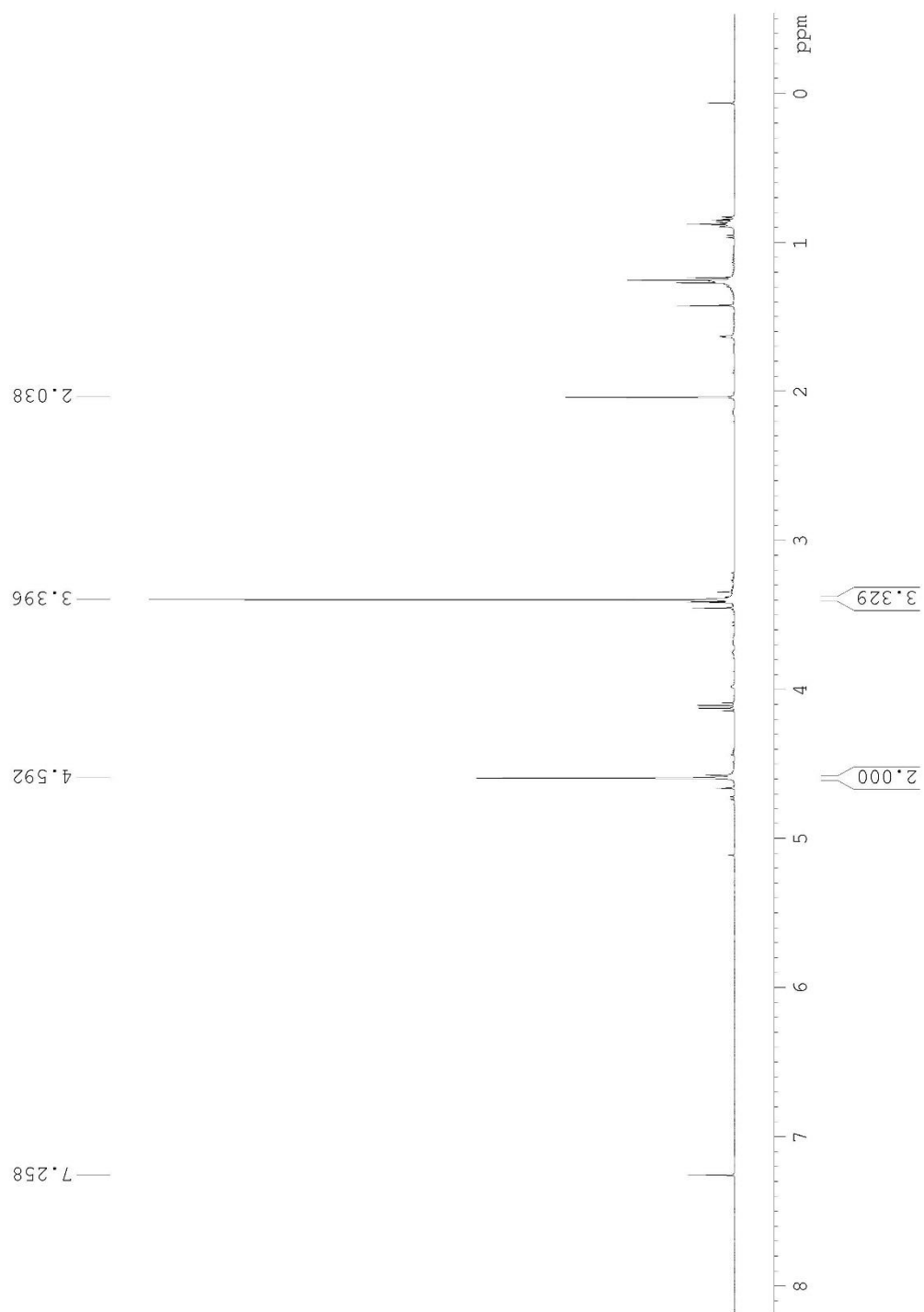


Table 1.8, Entry 1a

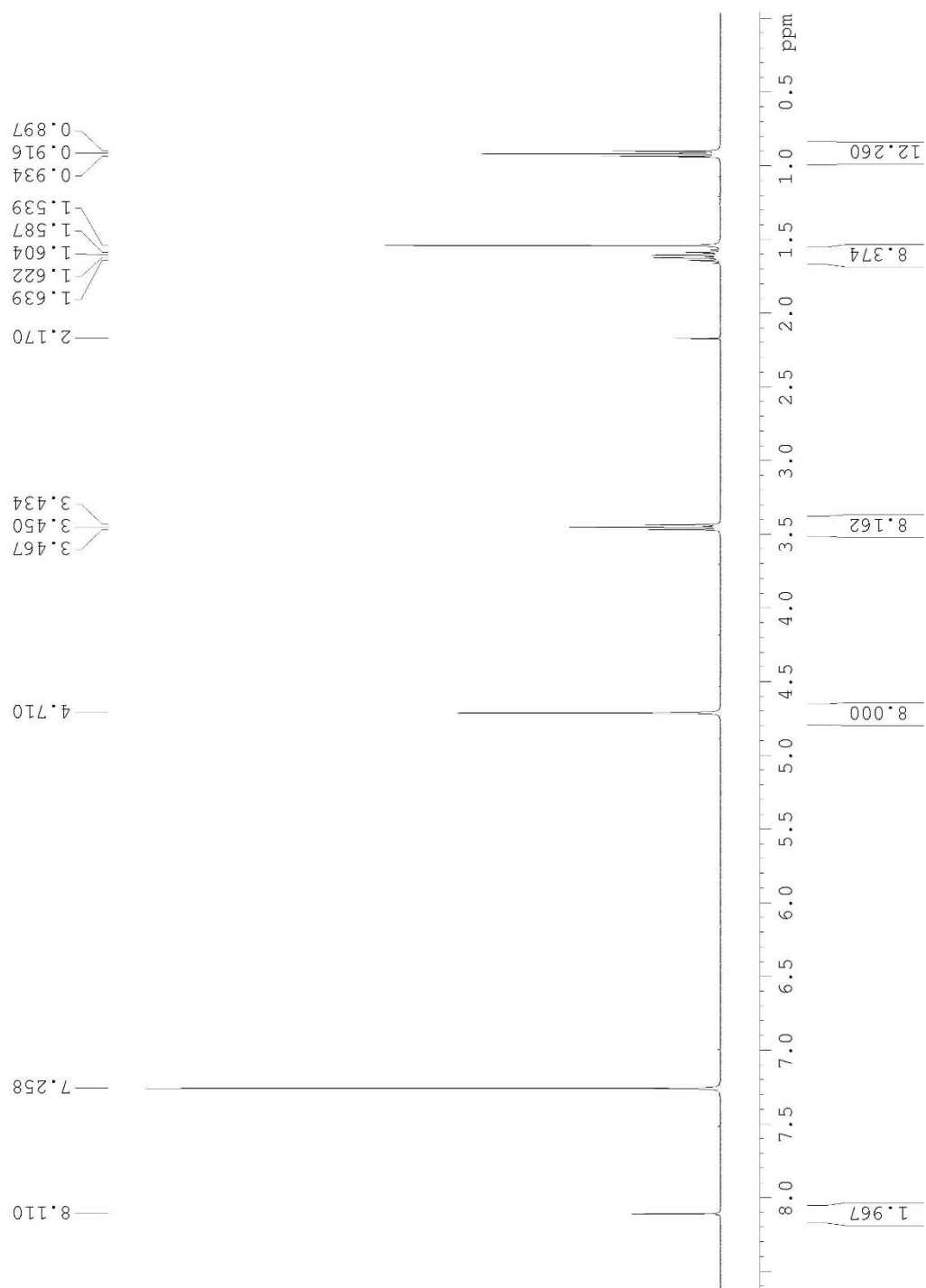


Table 1.8, Entry 1b

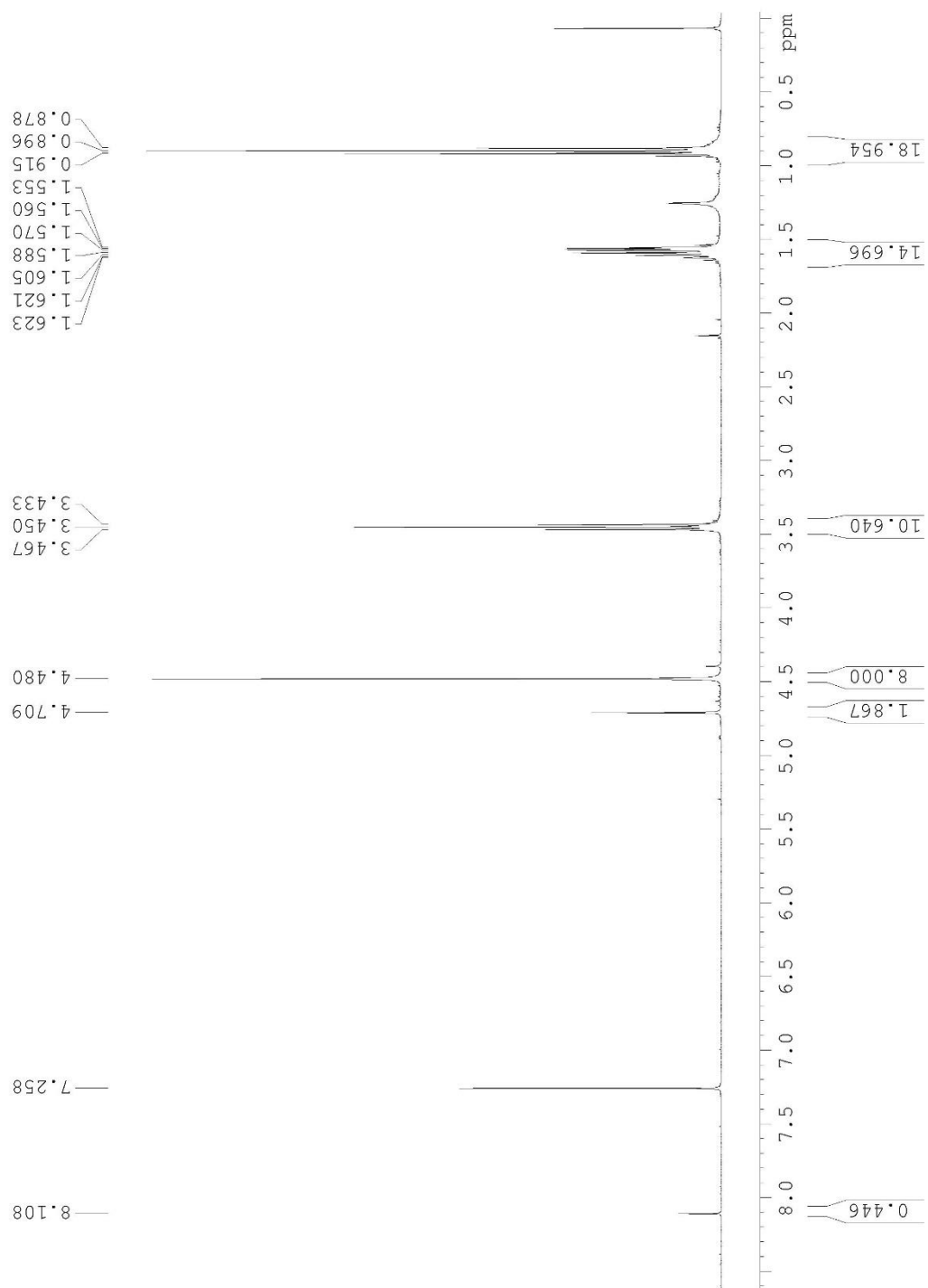


Table 1.8, Entry 2

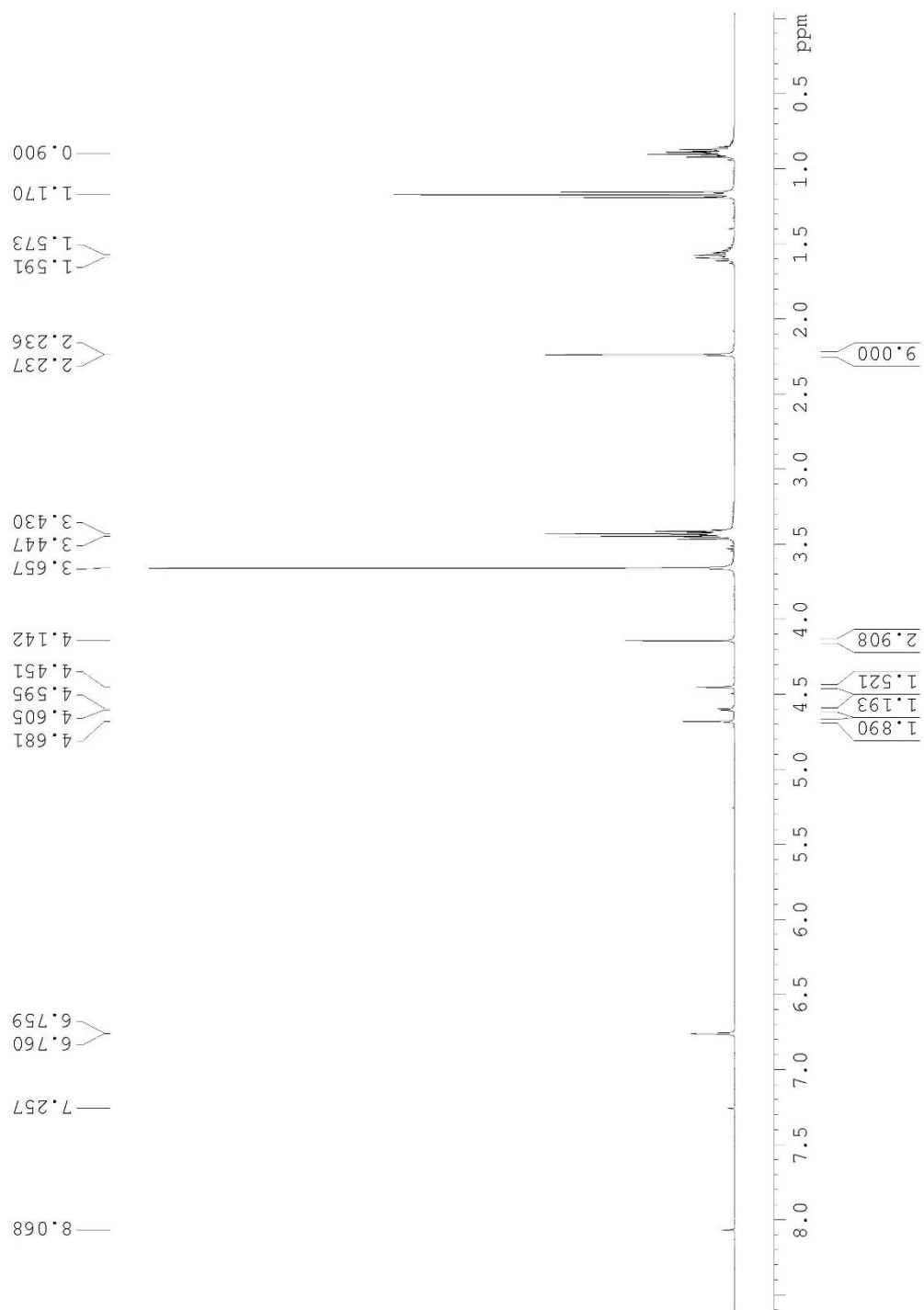


Table 1.8, Entry 3

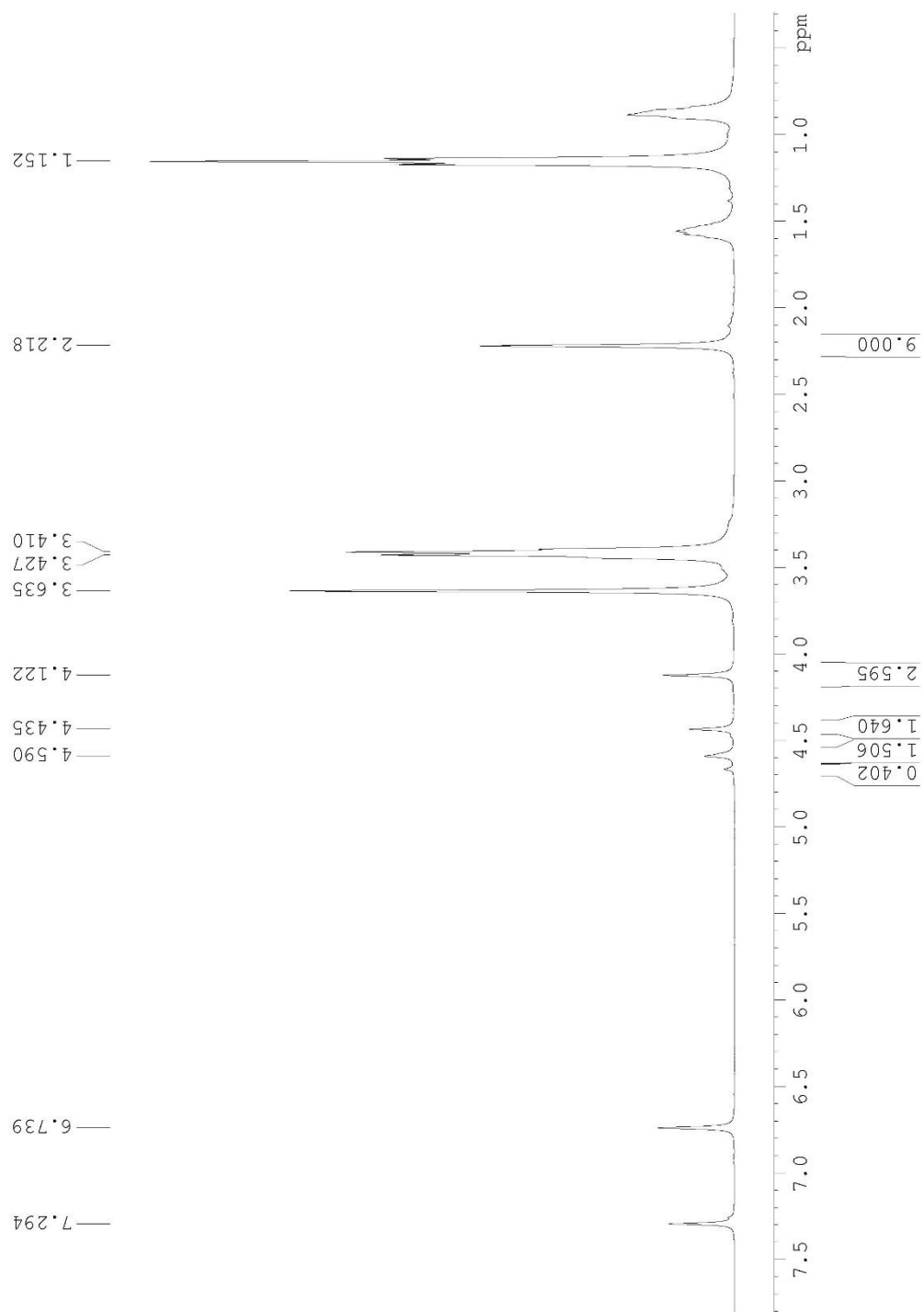


Table 1.8, Entry 4

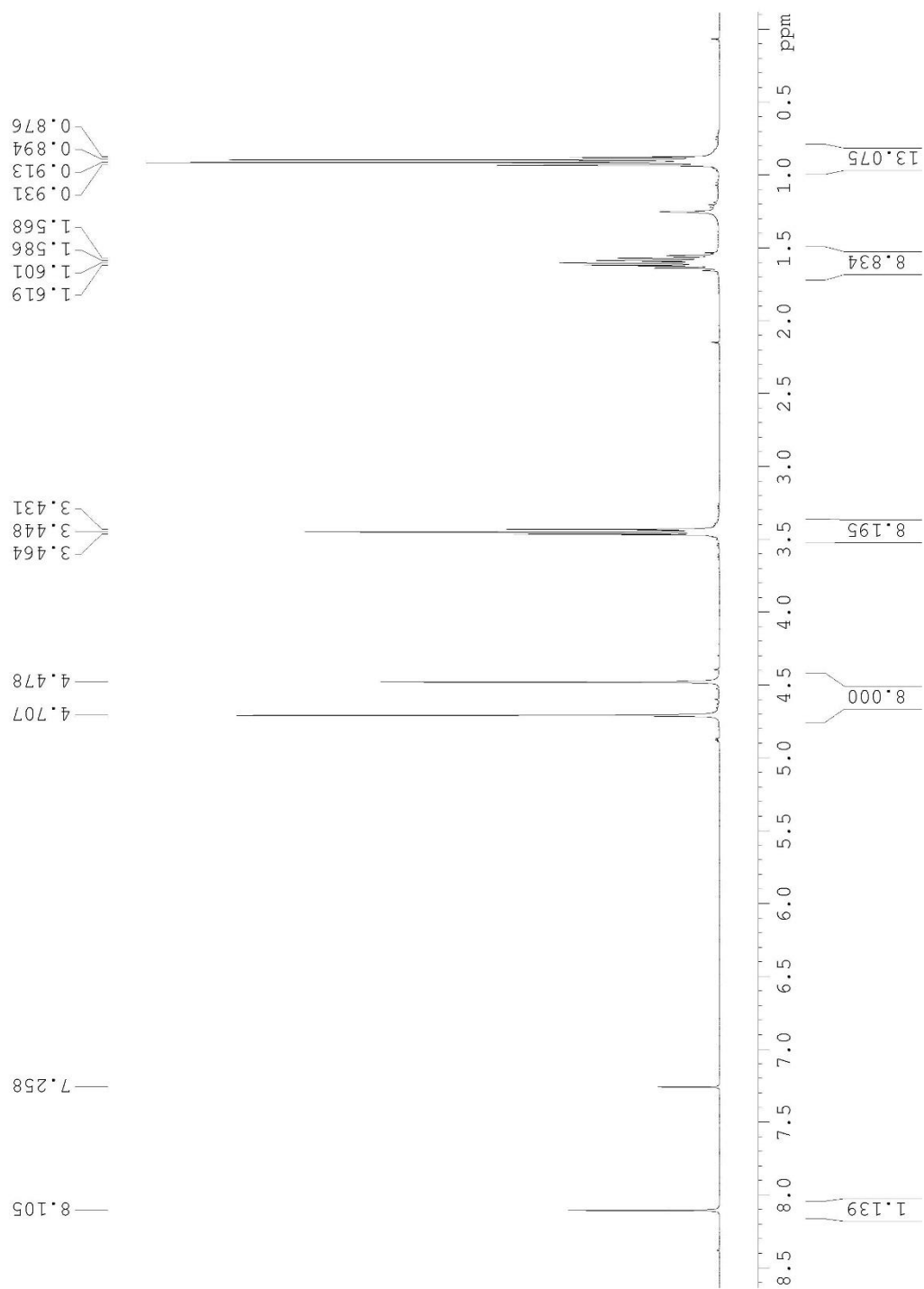


Table 1.8, Entry 5

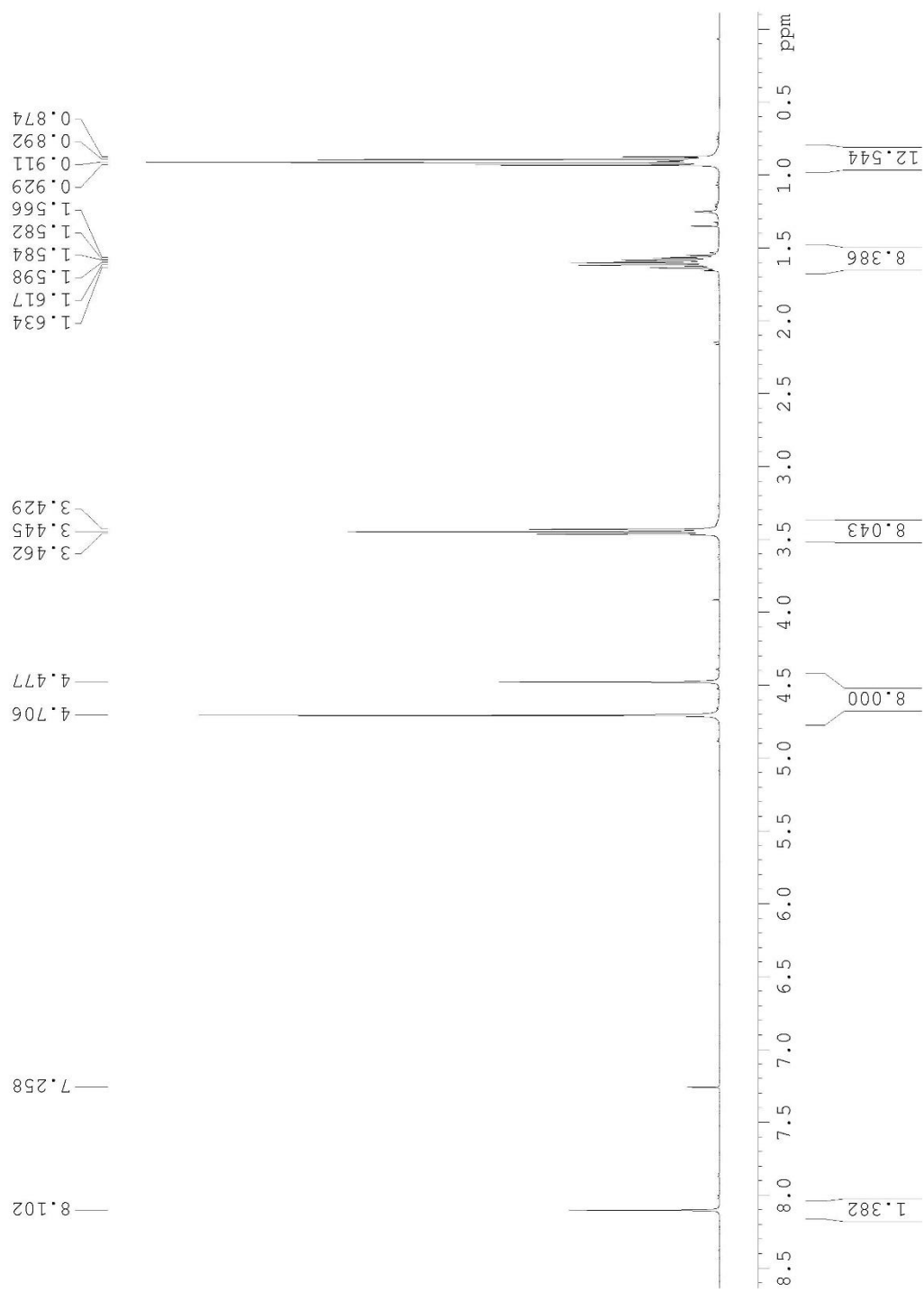


Table 1.8, Entry 6

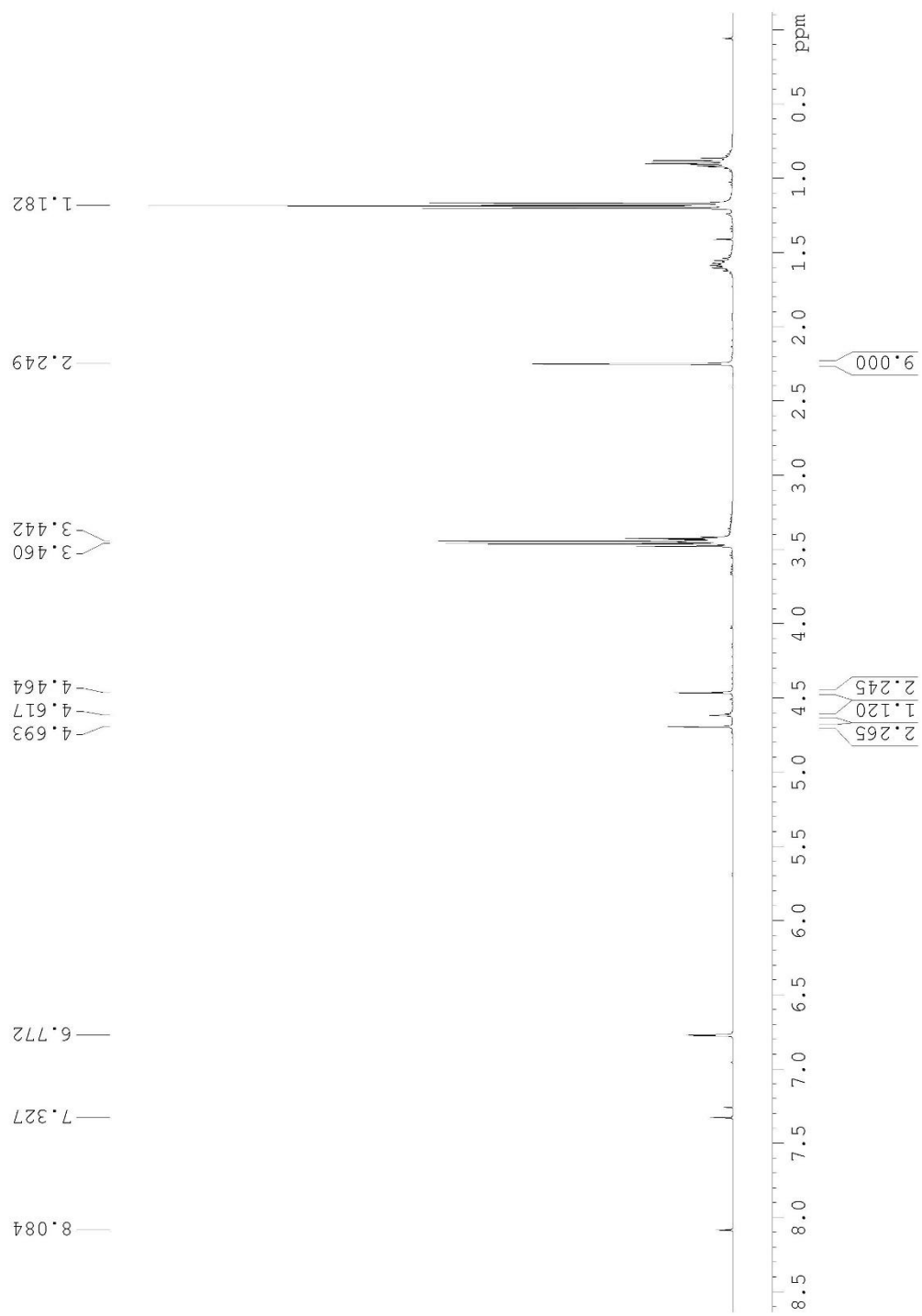


Table 1.8, Entry 7

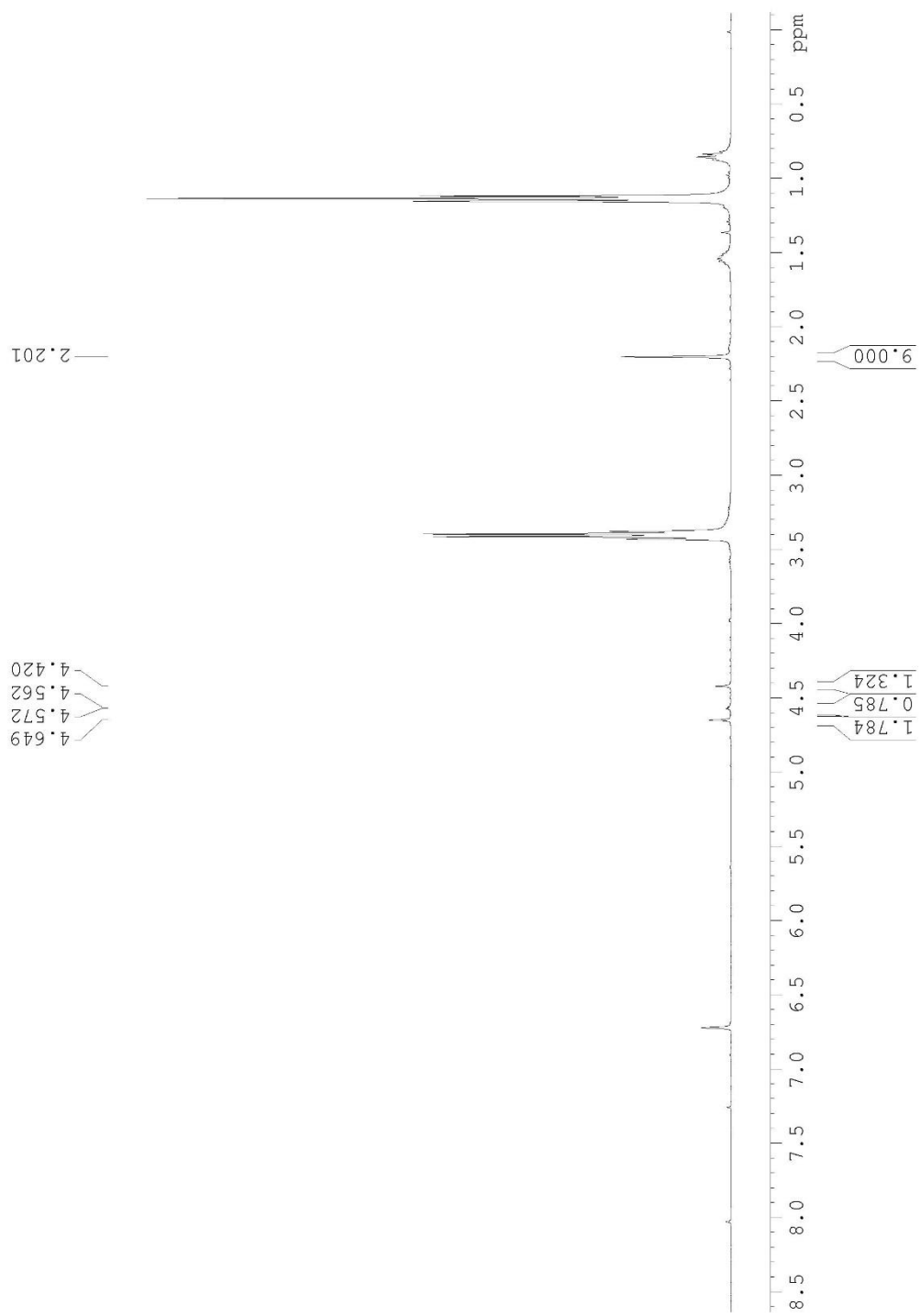


Table 1.8, Entry 9

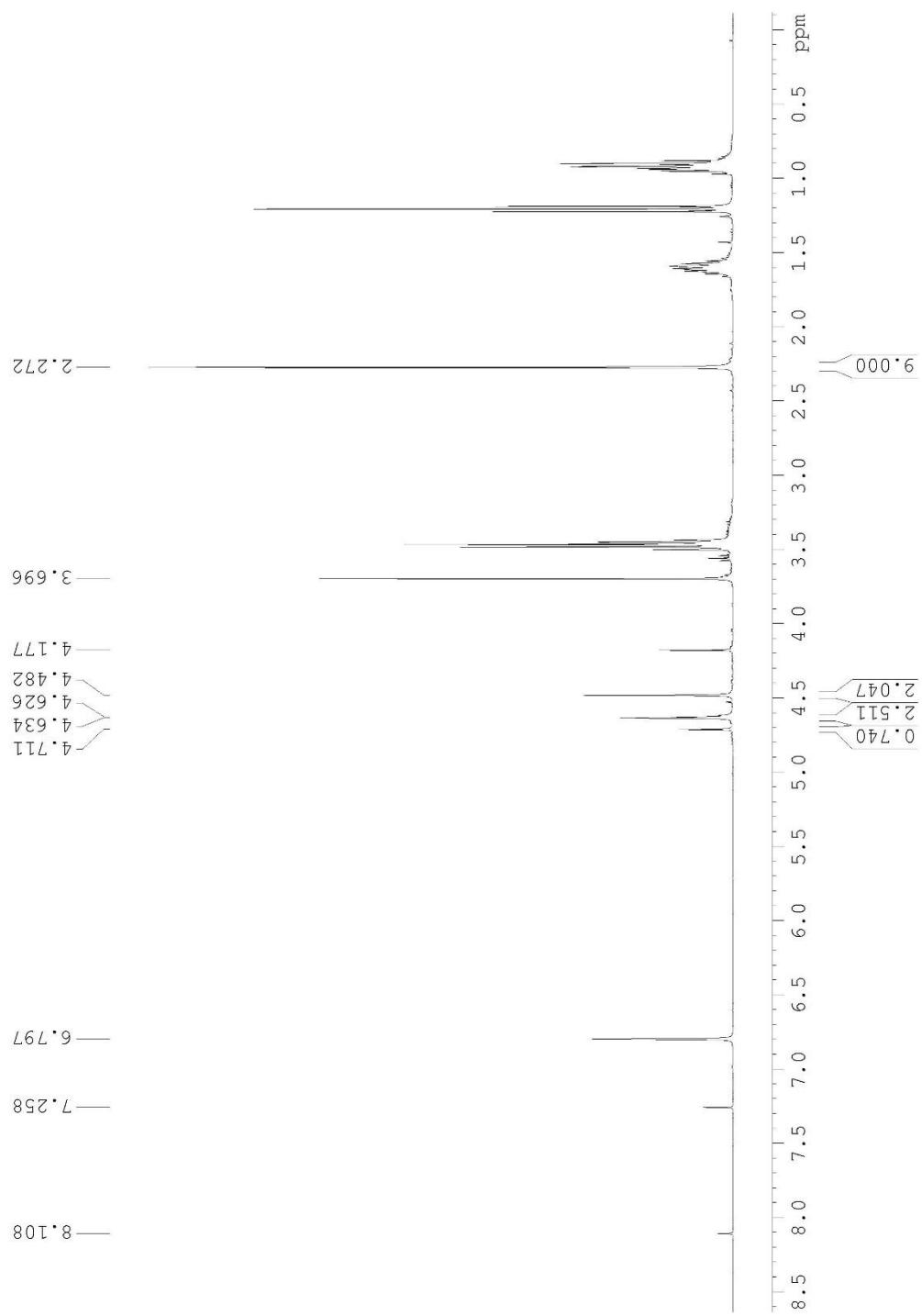


Table 1.8, Entry 10

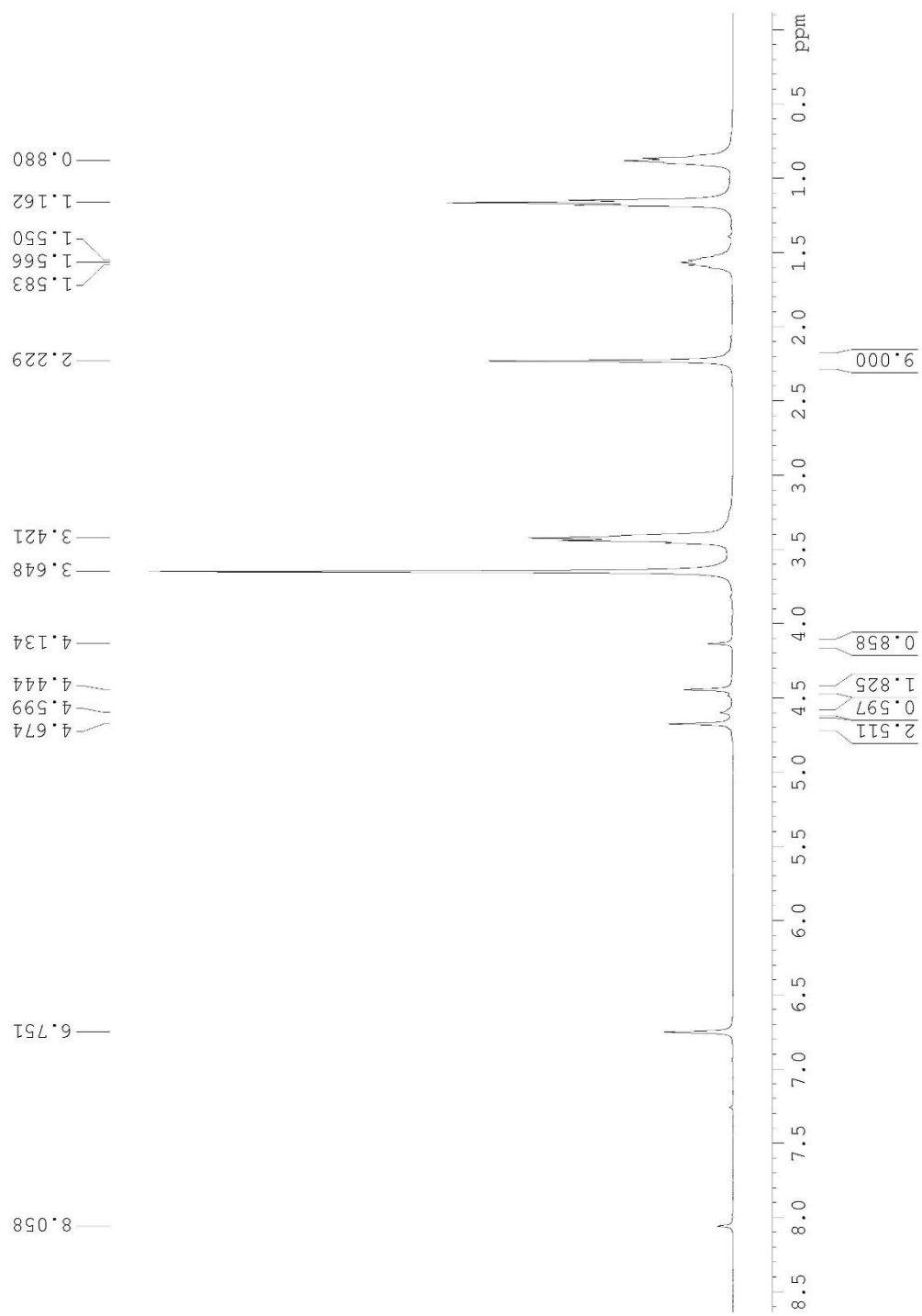


Table 1.9, Entry 1

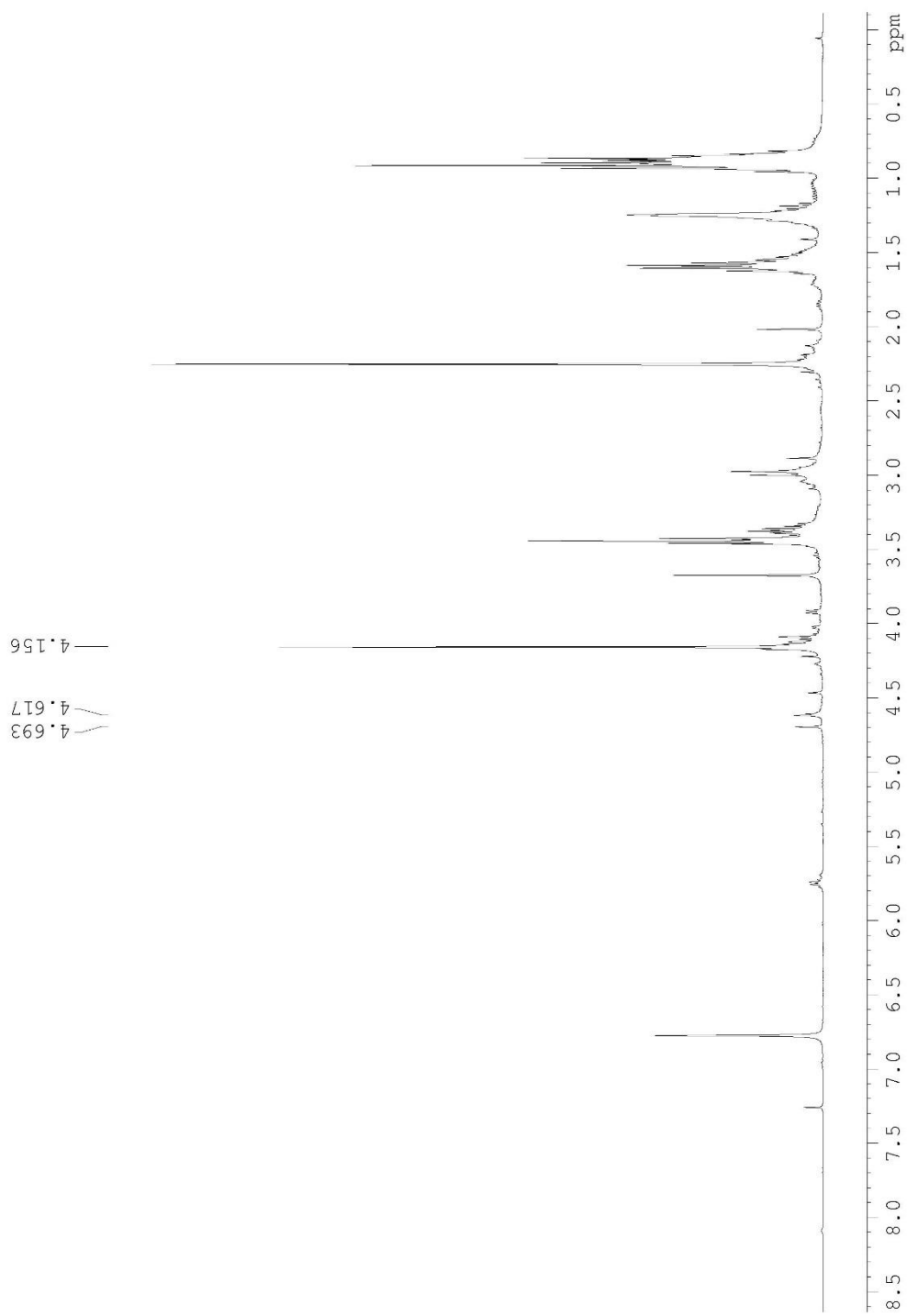


Table 1.9, Entry 2

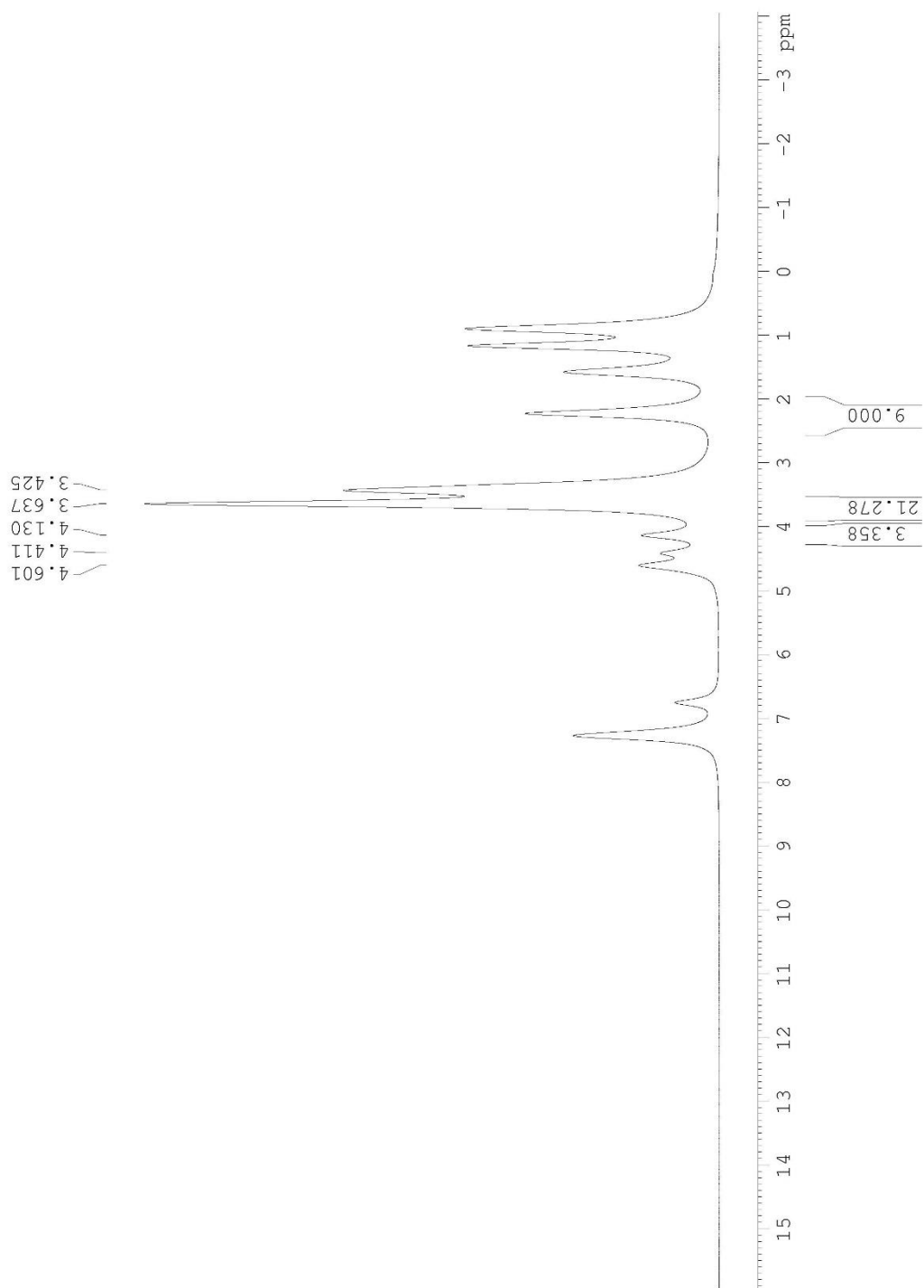


Table 1.9, Entry 3

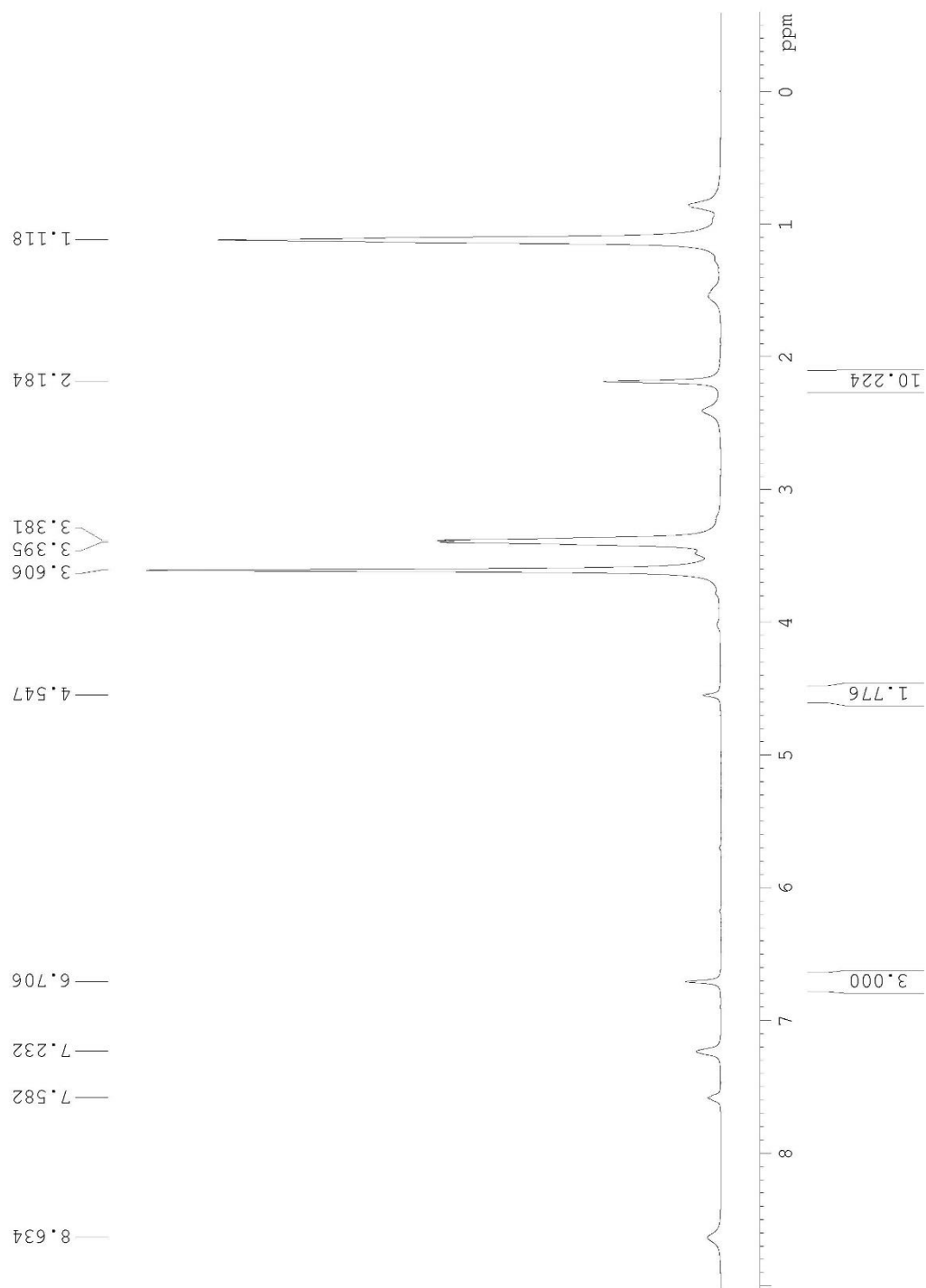


Table 1.9, Entry 4a

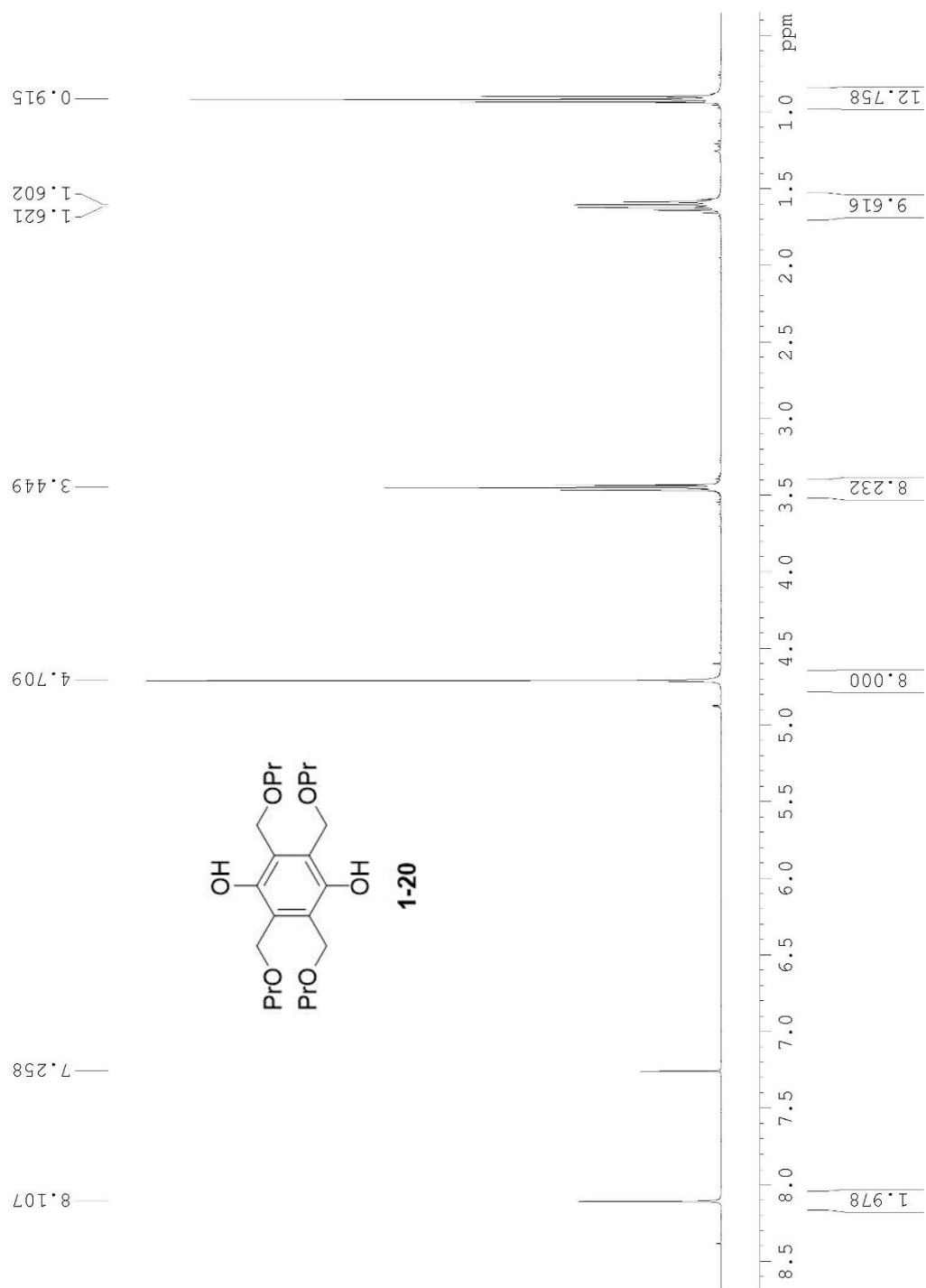


Table 1.9, Entry 4b

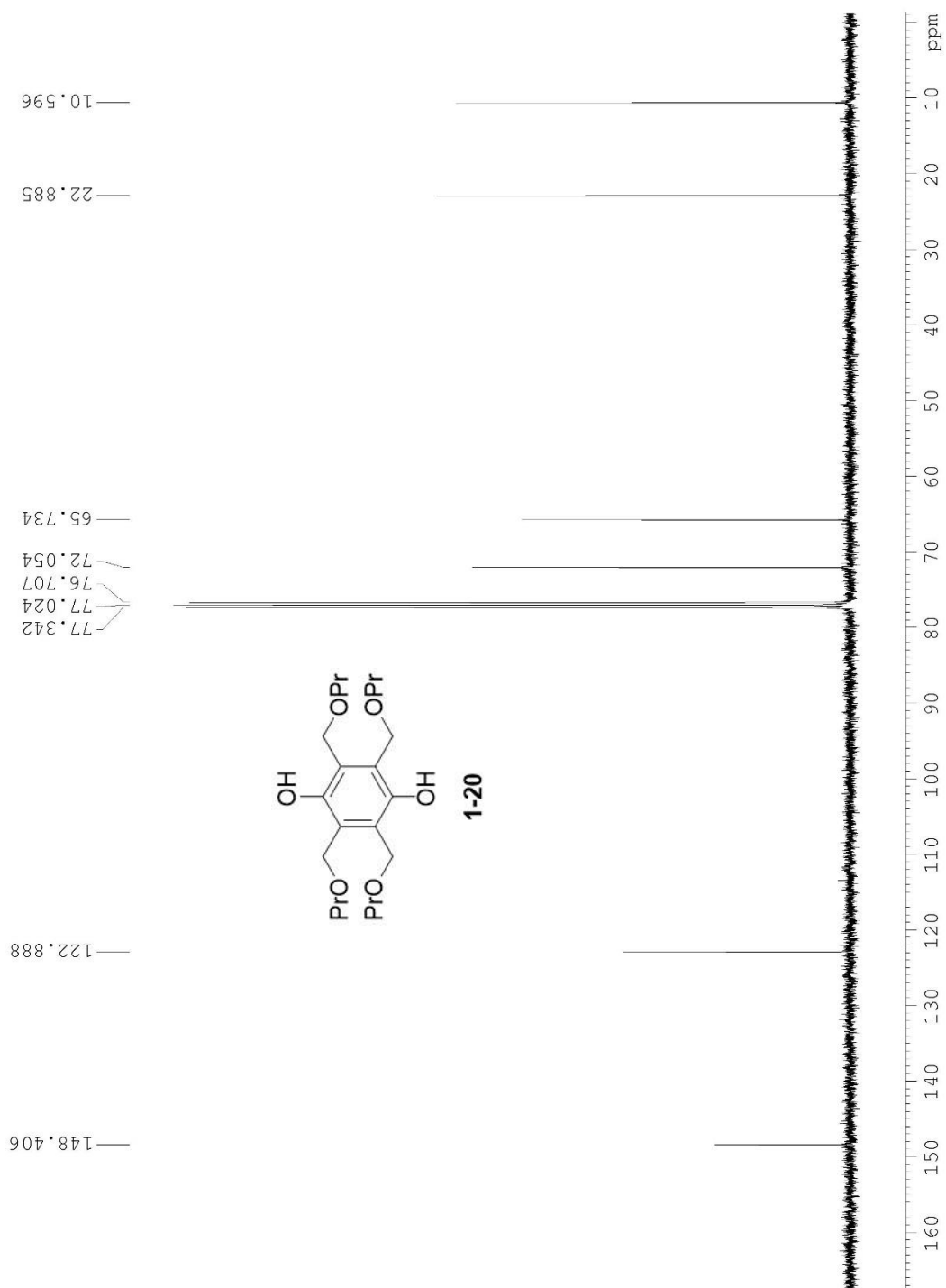


Table 1.9, Entry 4c

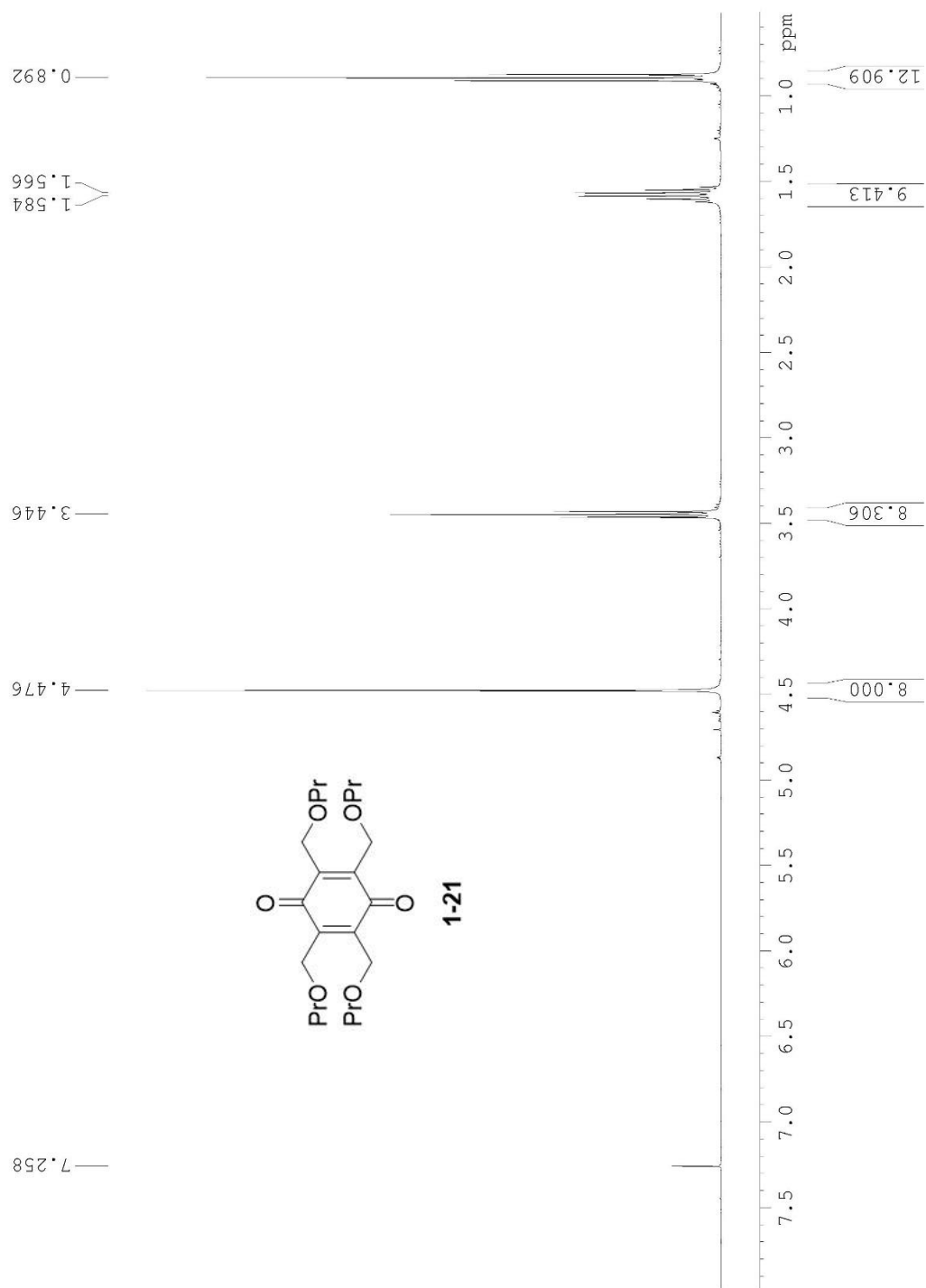


Table 1.9, Entry 4d

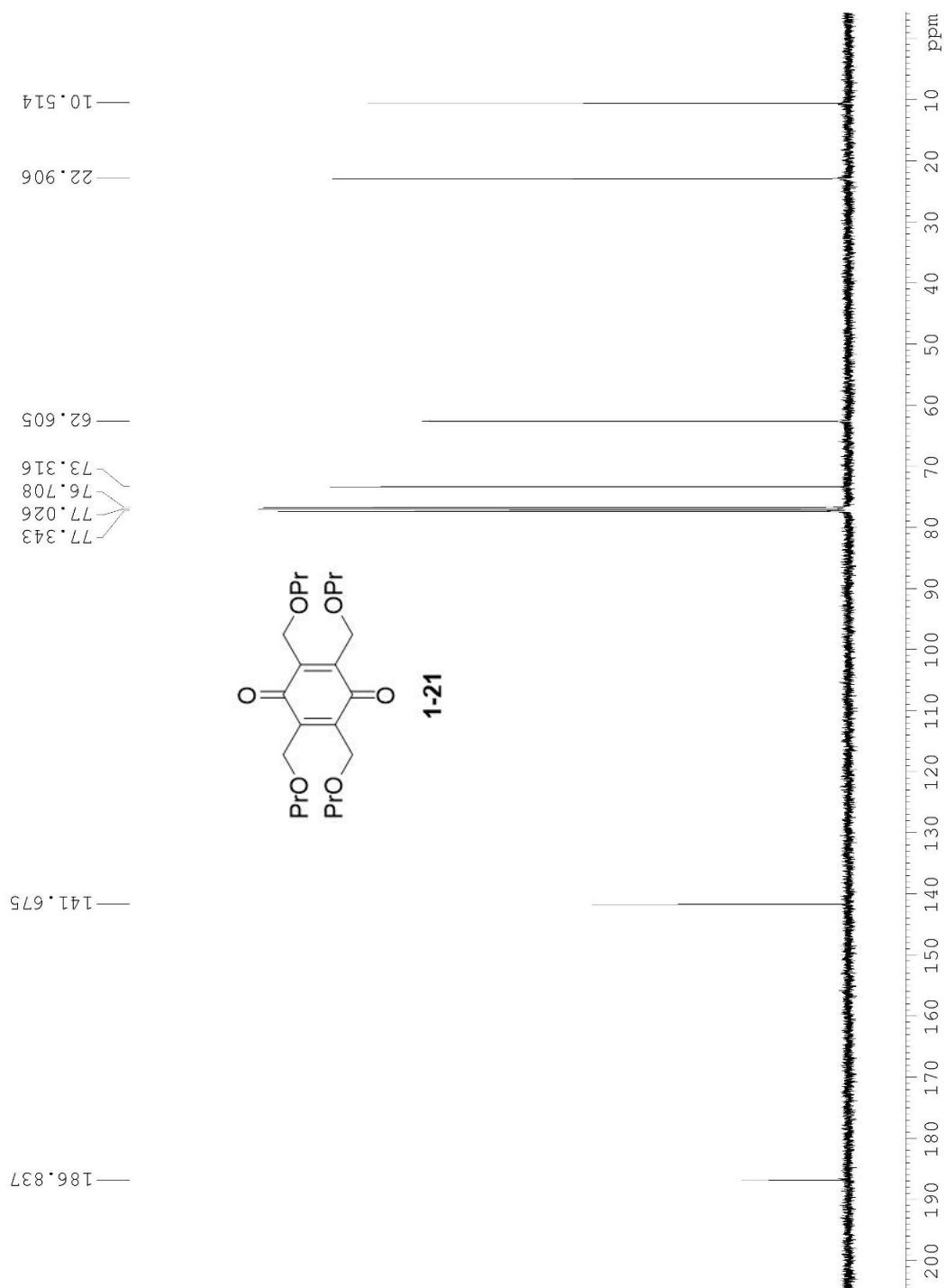


Table 1.9, Entry 4e

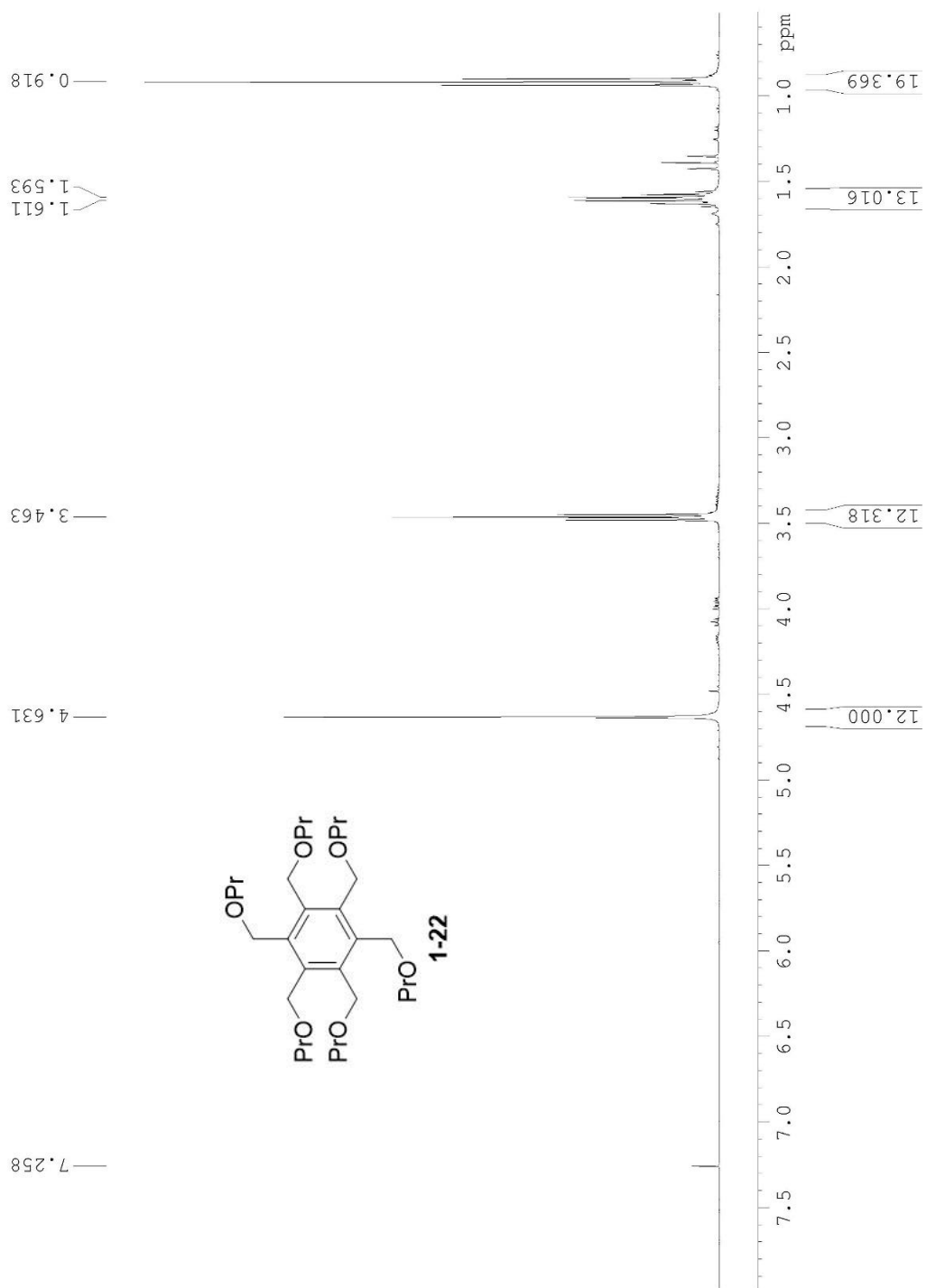


Table 1.9, Entry 4f

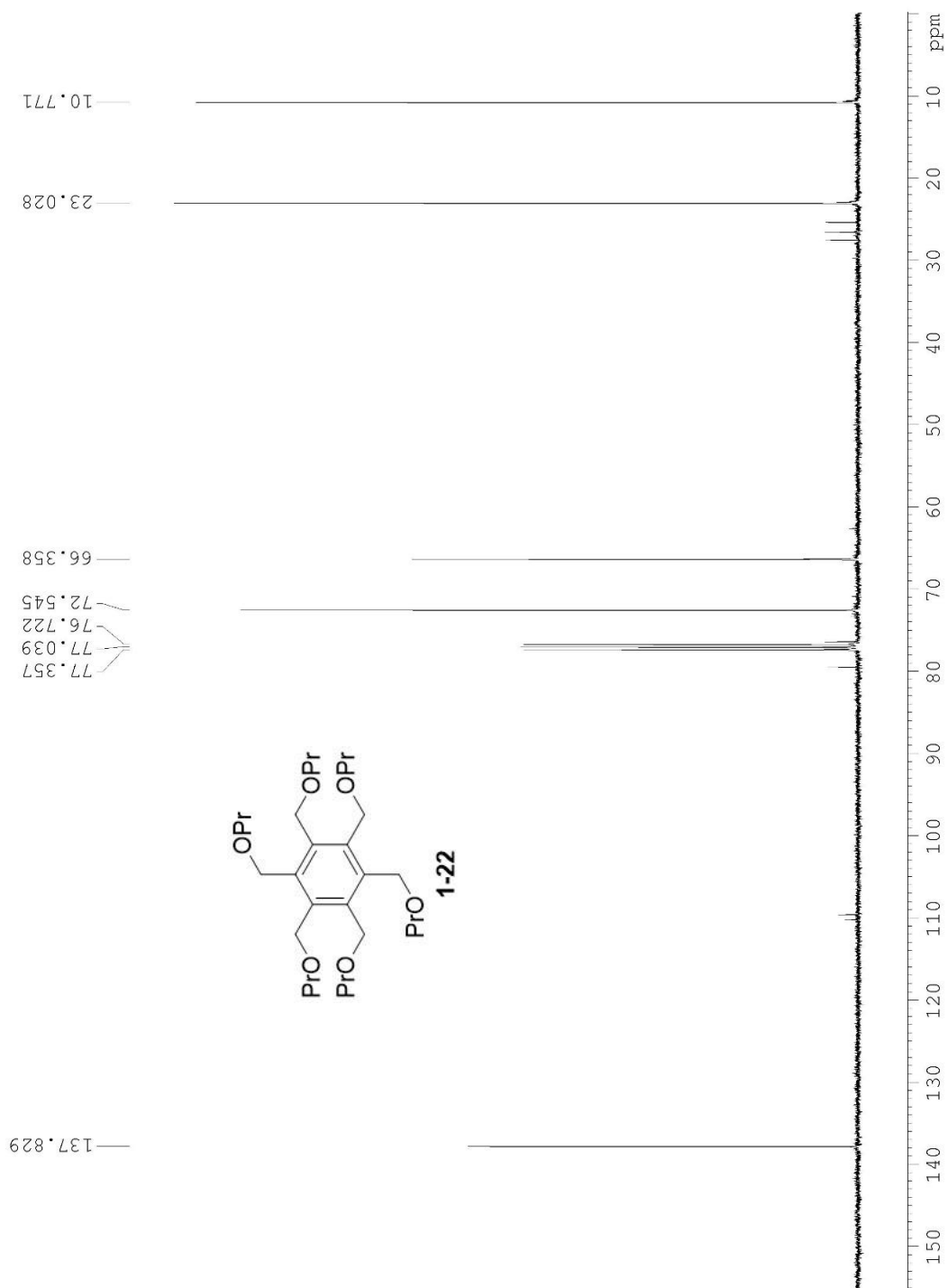
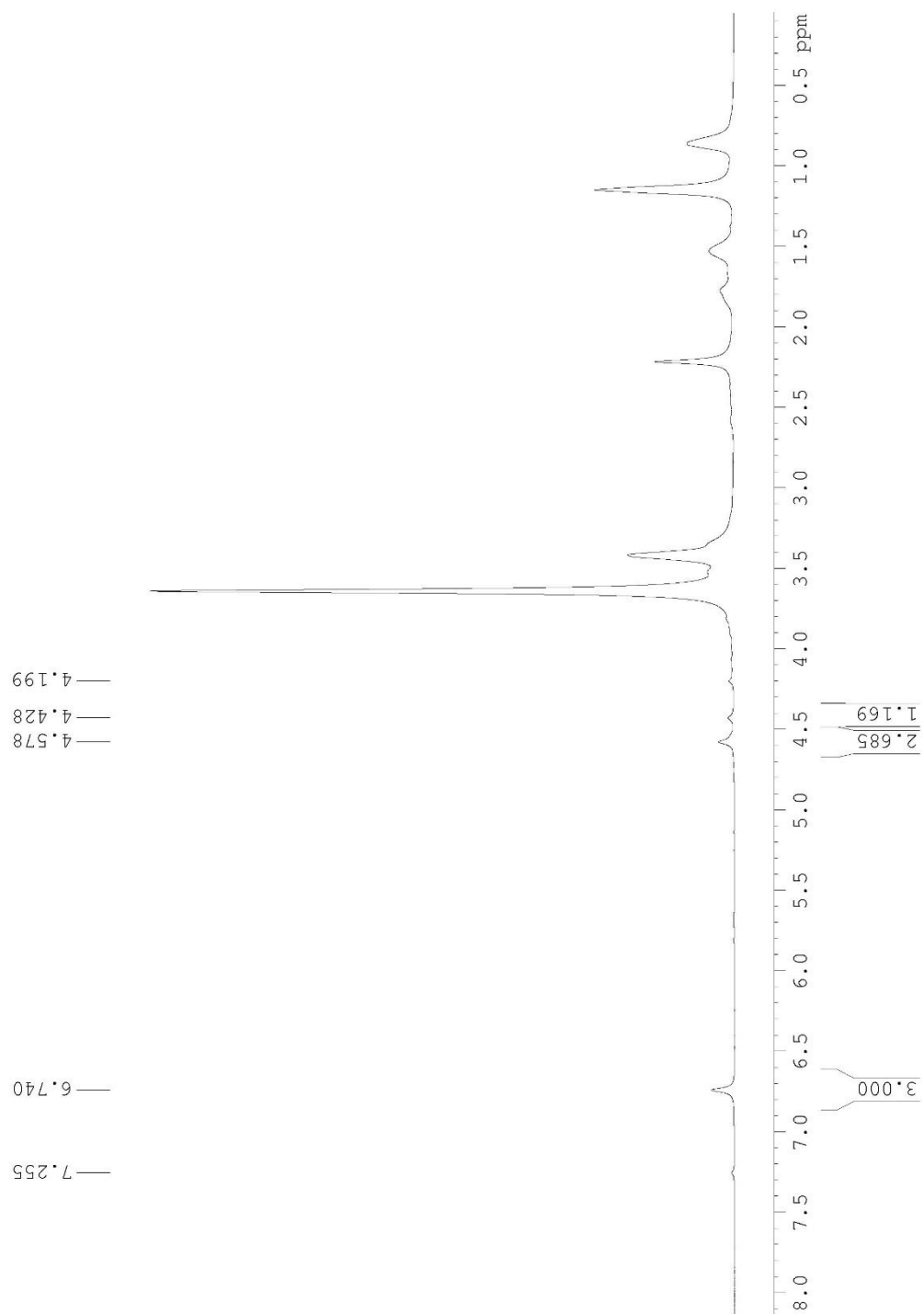
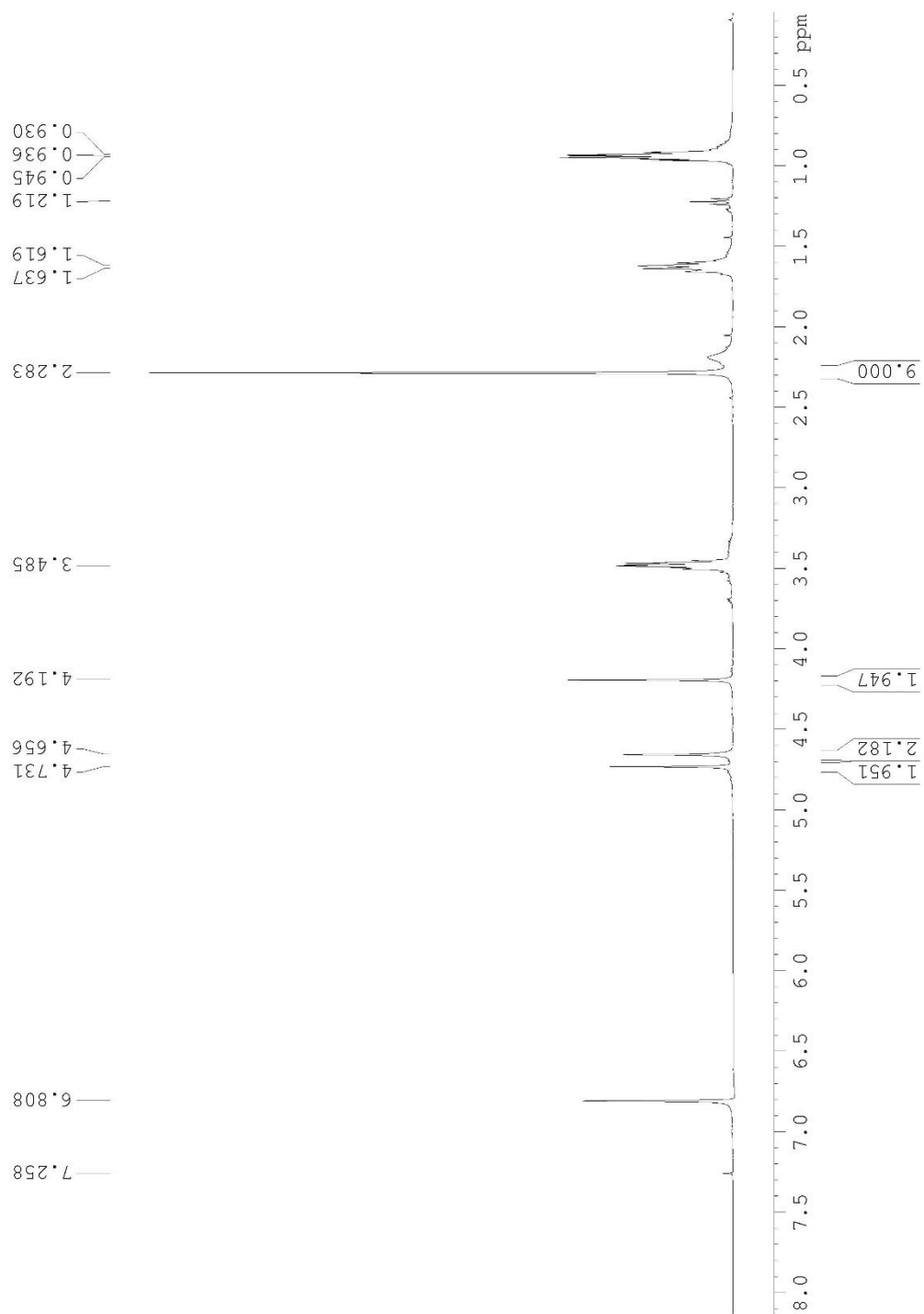


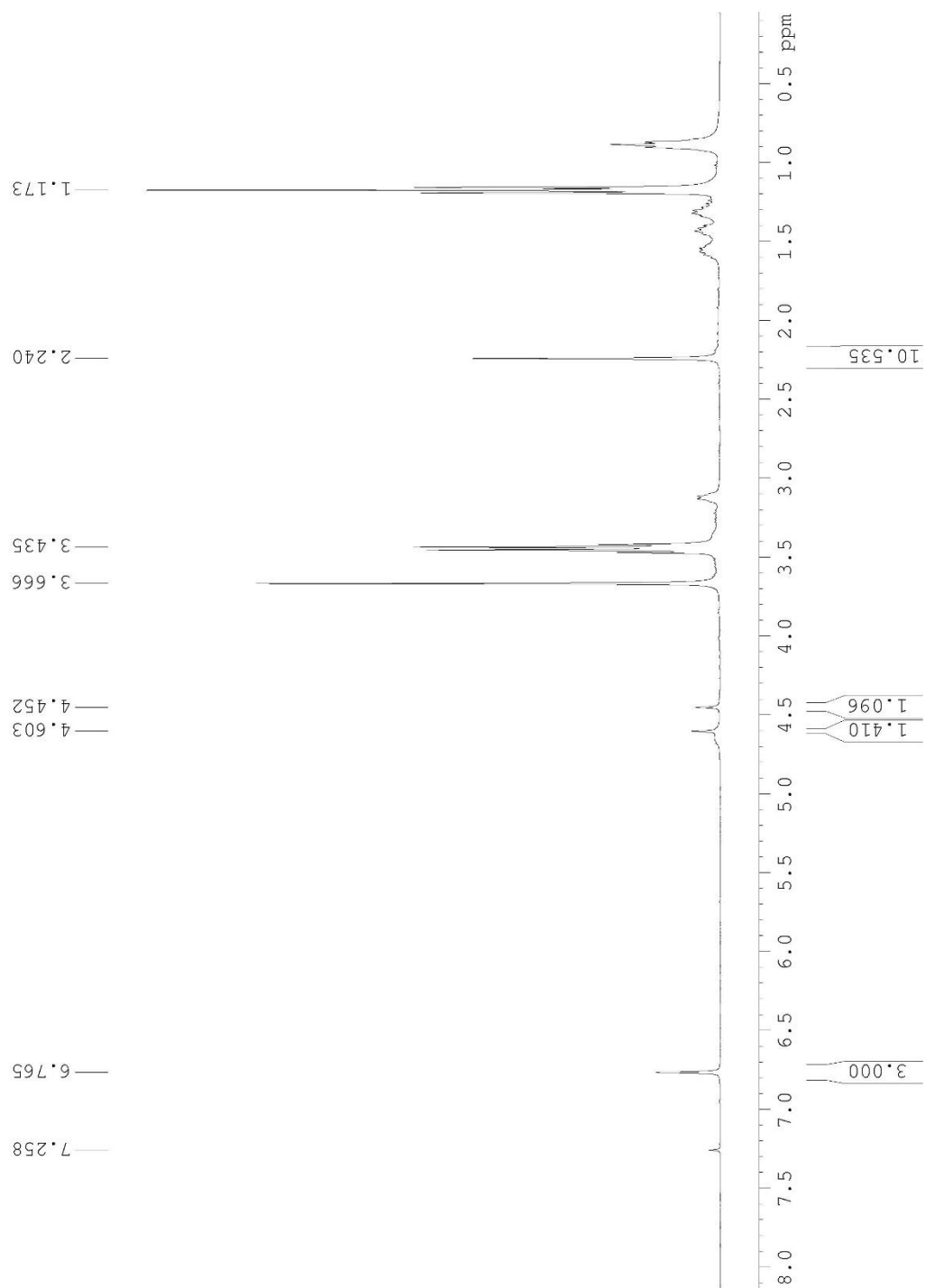
Table 1.9, Entry 5



Zn Workup



Na₂S₂O₃ Workup



1.7 References

1. (a) Martinez, M. J. A.; Benito, P. B. *Studies in Natural Products Chemistry* **2005**, *30*, 303-366.
(b) El-Najjar, N.; Gali-Muhtasib, H.; Ketola, R. A.; Vuorela, P.; Urtti, A.; Vuorela, H. *Phytochem. Rev.* **2011**, *10*, 353-370. (c) Bolton, J. L.; Dunlap, T. *Chem. Res. Toxicol.* **2017**, *30*, 13-37. (d) Bernardo, P. H.; Chai, C. L. L.; Guen, M. L.; Smith, G. D.; Waring, P. *Bioorg. Med. Chem. Lett.* **2007**, *17*, 82-85. (e) Kondracki, M.-L.; Guyot, M. *Tetrahedron* **1989**, *45*, 1995-2004.
2. Reppe, V. W.; Vetter, H. *Justus Liebigs Ann. Chem.* **1953**, *582*, 133-161.
3. (a) Sternberg, H. W.; Friedel, R. A.; Markby, R.; Wender, I. *J. Am. Chem. Soc.* **1956**, *78*, 3621-3624. (b) Sternberg, H. W.; Markby, R.; Wender, I. *J. Am. Chem. Soc.* **1958**, *80*, 1009-1010.
4. Kang, J. W.; McVey, S.; Maitlis P. M. *Can. J. Chem.* **1968**, *46*, 3189-3196.
5. Victor, R.; Ben-Shoshan, R.; Sarel, S. *Tet. Lett.* **1973**, *43*, 4211-4214.
6. Maruyama, K.; Shio, T.; Yamamoto, Y. *Bull. Chem. Soc. Jpn.* **1979**, *52*, 1877-1878.
7. (a) Greenfield, H.; Sternberg, H. W.; Friedel, R. A.; Wotiz, J. H.; Markby, R.; Wender, I. *J. Am. Chem. Soc.* **1956**, *78*, 120-124. (b) Sternberg, H. W.; Shukys, J. G.; Donne, C. D.; Markby, R.; Friedel, R. A.; Wender, I. *J. Am. Chem. Soc.* **1959**, *81*, 2339-2342. (c) Jung, M. E.; Lowe, J. *A. J. Org. Chem.* **1977**, *42*, 2371-2373.
8. Kang, J. W.; McVey, S.; Maitlis, P. M. *Can. J. Chem.* **1968**, *46*, 3189-3196.
9. (a) Liebeskind, L. S.; Baysdon, S. L.; South, M. S. *J. Organometal. Chem.* **1980**, *202*, C73-C76. (b) Miller, R. D.; Yannoni, C. S. *J. Am. Chem. Soc.* **1980**, *102*, 7397-7398.
10. South, M. S.; Liebeskind, L. S. *J. Am. Chem. Soc.* **1984**, *106*, 4181-4185.
11. Liebeskind, L. S.; Leeds, J. P.; Baysdon, S. L.; Iyer, S. *J. Am. Chem. Soc.* **1984**, *106*, 6451-6453.

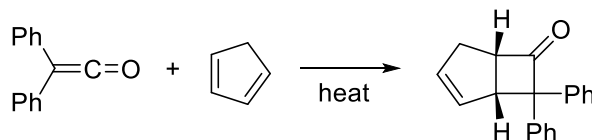
12. Iyer, S.; Liebeskind, L. S. *J. Am. Chem. Soc.* **1987**, *109*, 2759-2770.
13. Yin, J.; Liebeskind, L. S. *J. Org. Chem.* **1998**, *63*, 5726-5727.
14. (a) Suzuki, N.; Kondo, T.; Mitsudo, T. *Organometallics* **1998**, *17*, 766-769. (b) Fukuyama, T.; Yamaura, R.; Higashibeppu, Y.; Okamura, T.; Ryu, I.; Kondo, T.; Mitsudo, T. *Org. Lett.* **2005**, *7*, 5781-5783.
15. Huang, Q.; Hua, R. *Chem. Eur. J.* **2007**, *13*, 8333-8337.
16. Karabiyikoglu, S.; Boon, B. A.; Merlic, C. A. *J. Org. Chem.* **2017**, *82*, 7732-7744.
17. (a) Sugihara, T.; Yamada, M.; Ban, H.; Yamaguchi, M.; Kaneko, C. *Angew. Chem. Int. Ed. Engl.* **1997**, *36*, 2801-2804. (b) Sugihara, T.; Ban, H.; Yamaguchi, M. *J. Organomet. Chem.* **1998**, *554*, 163-166.
18. Krafft, M. E.; Bonaga, L. V. R.; Hirose, C. *Tetrahedron Lett.*, **1999**, *40*, 9171-917.
19. (a) Tang, Y.; Deng, L.; Zhang, Y.; Dong, G.; Chen, J.; Yang, Z. *Org. Lett.*, **2005**, *7*, 593-595. (b) Chung, Y. K.; Lee, B. Y.; Jeong, N.; Hudecek, M.; Pauson, P. L. *Organometallics*, **1993**, *12*, 220-223. (c) Sugihara, T.; Yamada, M.; Ban, H.; Yamaguchi, M.; Kaneko, C. *Angew. Chem. Int. Ed. Engl.*, **1997**, *36*, 2801-2804.

Chapter 2
Intramolecular Cyclization Reactions of Vinylic Ethers

2.1 Background

The [2+2] cycloaddition of ketenes with alkenes was first discovered by Staudinger and co-workers in 1906.¹ This included the reaction of cyclopentadiene, shown in scheme 2.1, which was originally expected to undergo a Diels-Alder reaction. The regioselectivity of this reaction was determined simultaneously several years later by both Lewis and Smith.² Over the last 100 years an enormous amount of research has been conducted on this reaction. This mini review will focus on work which directly influenced the experiments which are the main focus of this chapter; for more detailed relevant reviews, see the writings of Brady, Snider, Hyatt, and Reynolds.³

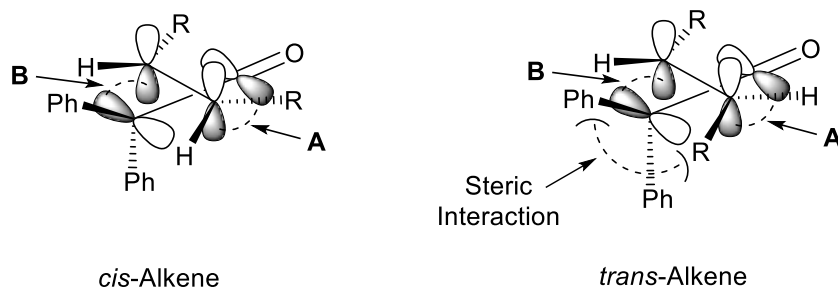
Scheme 2.1 [2+2] Cycloaddition of Cyclopentadiene and Diphenyl Ketene



Vinyl ethers have been known to form cyclobutanones with ketenes since the early Staudinger reports. However, it was Huisgen and co-workers who demonstrated that when using propenyl propyl ether, the *cis* isomer of vinyl ethers reacts at a rate at least two orders of magnitude faster than the *trans* isomer.⁴ This turns out to be a general trend for all alkenes, including simple alkyl-substituted double bonds. This fits into the mechanism of Staudinger's cycloaddition which was debated for decades, with evidence presented to support both stepwise and concerted mechanisms. Loss of stereochemistry with *trans* alkenes and kinetic isotope effects imply a stepwise mechanism; while retention of *cis* alkene stereochemistry, a lack of solvent effect, and adherence to Woodward-Hoffman rules suggest a concerted mode with a single transition state. As is the case with so many reaction mechanisms, the reality lies somewhere in the middle, and is dependent on the substrates. Neil Issacs provides a good summary of evidence and an explanation of the mechanism.⁵ The transition state takes on an orthogonal orientation, with the

ketene adding antarafacially and the alkene reacting suprafacially (Figure 2.1). The suprafacial reaction of the alkene leads to conservation of the alkene stereochemistry. *Trans* olefins react slower due to steric interactions between one of the alkene substituents with one on the ketene, whereas *cis* olefins are able to avoid this steric conflict. The mechanism can be best described as semi-concerted, with bond **A** in the transition state being more fully formed than bond **B**, which has some diradical character. More steric hinderance between the olefin and ketene leads to a less concerted mechanism. It's also worth noting that because little solvent effect was observed, it is likely that polarity of the substrates has little effect on the mechanism, although it does influence regiochemistry.

Figure 2.1 *Cis* Vs *Trans* Olefin Transition States



The first attempt at general conditions for the cyclization of vinyl ethers with ketenes was reported by Aben and Sheeren (Table 2.1).⁶ They used zinc chloride as a catalyst, which presumably acts as a Lewis acid to activate the ketene. Unfortunately, yields were poor unless a more electron rich ethoxyketene was used. Much more recently, Matsuo and co-workers developed a much more general set of conditions using modern chemical techniques which gave generally good yields across the board (Table 2.2).⁷ Bulky aromatic R groups on the ketene strongly favored *trans* relative stereochemistry (entry 10-18), while bulky alkyl groups do not (entry 1-9). While the *trans* product is more thermodynamically stable, there is little differentiation in the steric environments of positions 1 or 2 for the ether group. This implies that an aromatic group promotes a more stepwise reaction mechanism where rotation may occur

about the axis of the vinyl ether olefin.

Table 2.1 Zinc Catalyzed Cycloaddition of Ketene and Vinyl Ethers

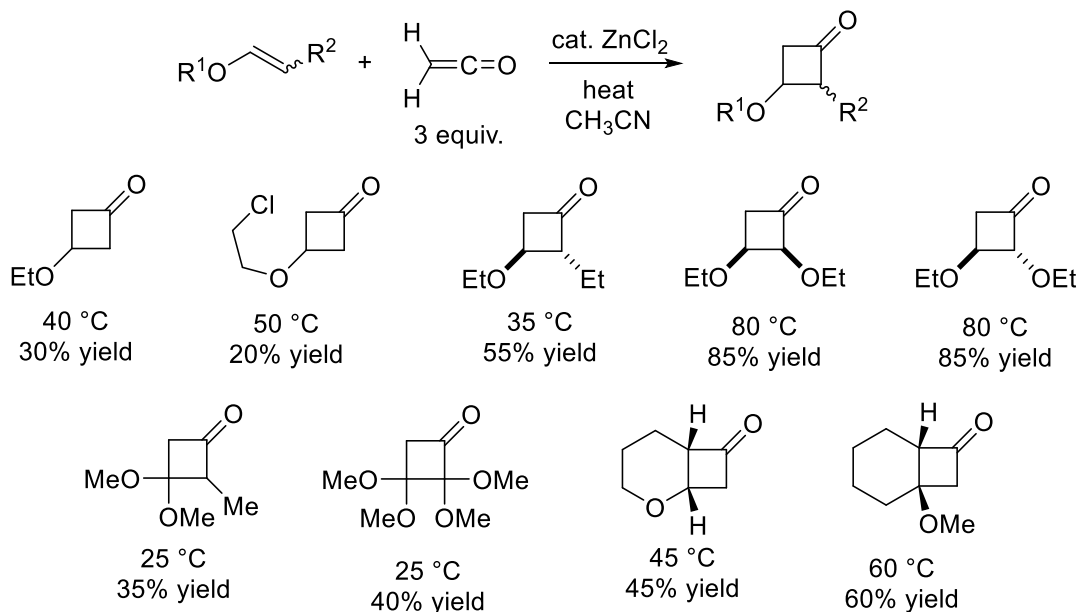
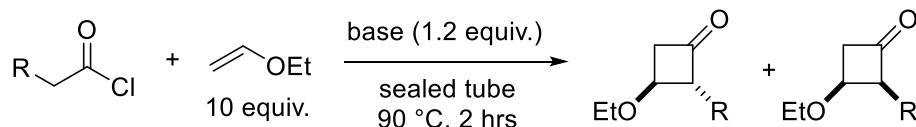


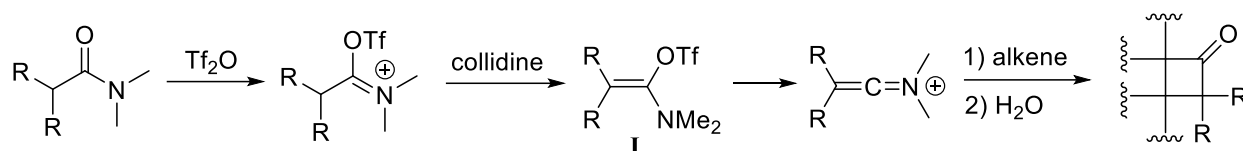
Table 2.2 Cyclization of Ethyl Vinyl Ether and Ketenes



Entry	R	Base	% Yield	Cis/Trans
1	H	<i>i</i> -Pr ₂ NEt	37	-
2	Me	<i>i</i> -Pr ₂ NEt	77	53:47
3	Et	<i>i</i> -Pr ₂ NEt	78	16:84
4	Pr	<i>i</i> -Pr ₂ NEt	71	27:73
5	<i>n</i> -Bu	<i>i</i> -Pr ₂ NEt	76	30:70
6	Hex	<i>i</i> -Pr ₂ NEt	77	58:42
7	<i>i</i> -Bu	<i>i</i> -Pr ₂ NEt	77	24:76
8	<i>i</i> -Pr	<i>i</i> -Pr ₂ NEt	50	31:69
9	<i>t</i> -Bu	Et ₃ N	74	54:46
10	Ph	2,6-lutidine	75	11:89
11	<i>p</i> -MeOC ₆ H ₄	2,6-lutidine	74	14:86
12	<i>p</i> -MeC ₆ H ₄	2,6-lutidine	56	11:89
13	<i>o</i> -MeC ₆ H ₄	2,6-lutidine	74	6:94
14	<i>p</i> -ClC ₆ H ₄	2,6-lutidine	56	12:88
15	1-Naph	2,6-lutidine	83	7:93
16	2-Naph	2,6-lutidine	64	6:94
17	2-Thienyl	2,6-lutidine	62	7:93
18	3-Thienyl	2,6-lutidine	70	7:93

In the 1980's the group of Leon Ghosez thoroughly developed the [2+2] cyclization of olefins with ketene iminium ions. They also invented a method of forming ketene iminium ions from amides, allowing for exceptionally stable substrates; which was previously a barrier to the practical use of ketene iminiums (Scheme 2.2).⁸ After the amide attacks triflic anhydride, deprotonation leads to intermediate **I**. This can then collapse to form the ketene iminium, which undergoes cyclization with the olefin. Hydrolysis yields the cyclobutanone product. Ding and Fang performed DFT calculations on this reaction, and found that it follows a more stepwise mechanism than the ketene reaction which inspired it.⁹

Scheme 2.2 Formation of Ketene Iminium with Triflic Anhydride and Cyclization



To the best of our knowledge, the first intramolecular [2+2] cycloaddition of a ketene and an olefin was reported in 1965 by J. J. Beereboom, although he appears to have misinterpreted his results.¹⁰ Baldwin and Page demonstrated that even in an unconstrained intramolecular system, the cyclobutanone is in fact obtained via the [2+2] mechanism.¹¹ The groups of Ghosez and Snider collaborated on a thorough investigation of intramolecular [2+2] reactions with olefins which served as the primary inspiration for the work described later in this chapter.¹² Ghosez and co-workers investigated ketenes and ketene iminium ions, while Snider and co-workers focused on alkoxyketenes (Table 2.3). Between the two reports a wide variety of fused ring systems were synthesized, with the main limitation being the focus on primary alkenes. However, a particularly interesting result can be seen in entries 23 and 24 of Table 2.3, showing that a *cis* alkene failed to cyclize with a ketene, while successfully reacting with ketene iminium to form the fused cyclobutanone. This is because the transition state of the concerted ketene mechanism

would force the cis alkene into a sterically untenable orientation, while the stepwise mechanism of the ketene iminium allows for more flexibility.

Table 2.3 Intramolecular [2+2] Cycloaddition of Ketenes and Ketene Iminium Ions

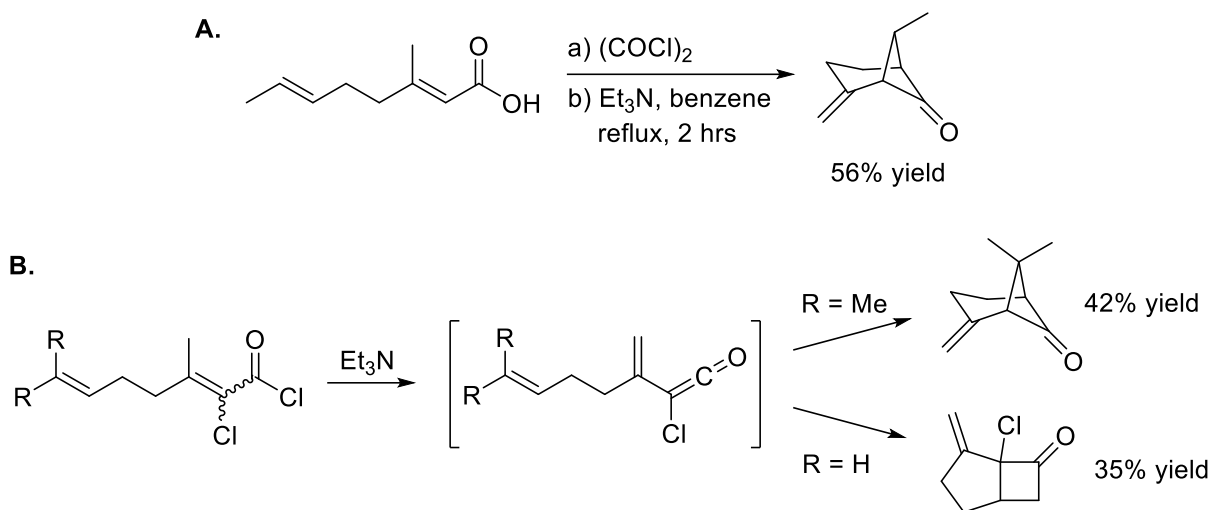
<i>Entry</i>	<i>Substrate</i>	<i>Product</i>	<i>% Yield</i>
1			3
2			75
3			80
4			83
5			84
6			3
7			87
8			65
9			89
10			71
11			78
12			72

13			30
14			55
15			72
16			62
17			73
18			58
19			63
20			16
21			79
22			70
23			0
24			47, 9
25			52
26			30

In a follow up paper, Snider demonstrated that intramolecular cyclization of a trans alkene with a ketene follows inverse regioselectivity to that of primary and 1,1 substituted alkenes,

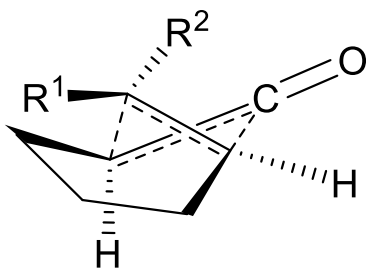
yielding not a fused, but rather a bridged bicyclic product (Scheme 2.3 A).¹³ They found this trend to be consistent; the regioselectivity is governed by the substitution of the alkene (Scheme 2.3 B, Table 2.3 entries 25-26). The proposed transition state for intramolecular cyclization with

Scheme 2.3 Regioselectivity of Trans Alkenes



ketene and a 1,2 substituted alkene is shown in Figure 2.2. When comparing the steric environments of R¹ and R², it becomes clear why a *trans*-alkene is able to react and *cis*-alkene is not. The intramolecular nature of the reaction forces the alkene to attack from the more hindered side, leading to strong steric interactions at R¹ in the case of a *cis*-alkene. Several other groups have applied this chemistry and updated it's use with more modern techniques, but the chemistry of Ghosez and Snider is yet to be expanded.¹⁴

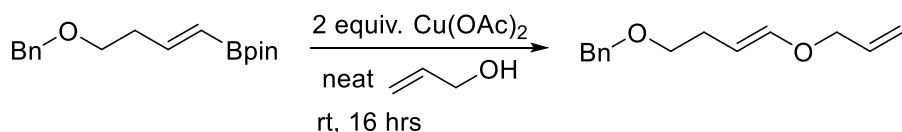
Figure 2.2 Transition State of Intramolecular [2+2] Reaction with 1,2-Substituted Olefins



2.2 Introduction

Our group previously developed a copper promoted coupling of vinyl boronates and alcohols to synthesize vinyl ethers (Scheme 2.4).¹⁵ This methodology allows access to compounds with complex functionality on the vinyl side of the vinyl ether, not previously accessible via other established methods of vinyl ether synthesis such as Lewis acid catalyzed transesterification.¹⁶ Further development has shown that pi-ligands on copper greatly improve the results of this reaction, and updates to the conditions now allow for use of stoichiometric equivalents of the alcohol coupling partner.¹⁷ This chapter focuses on our efforts to enact intramolecular cyclization reactions between vinyl ethers synthesized using this method and a variety of electrophilic functional groups. These reactions should provide rapid access to heterocyclic structures of significant complexity.

Scheme 2.4 Copper Promoted Coupling of Vinyl Boronates and Alcohols



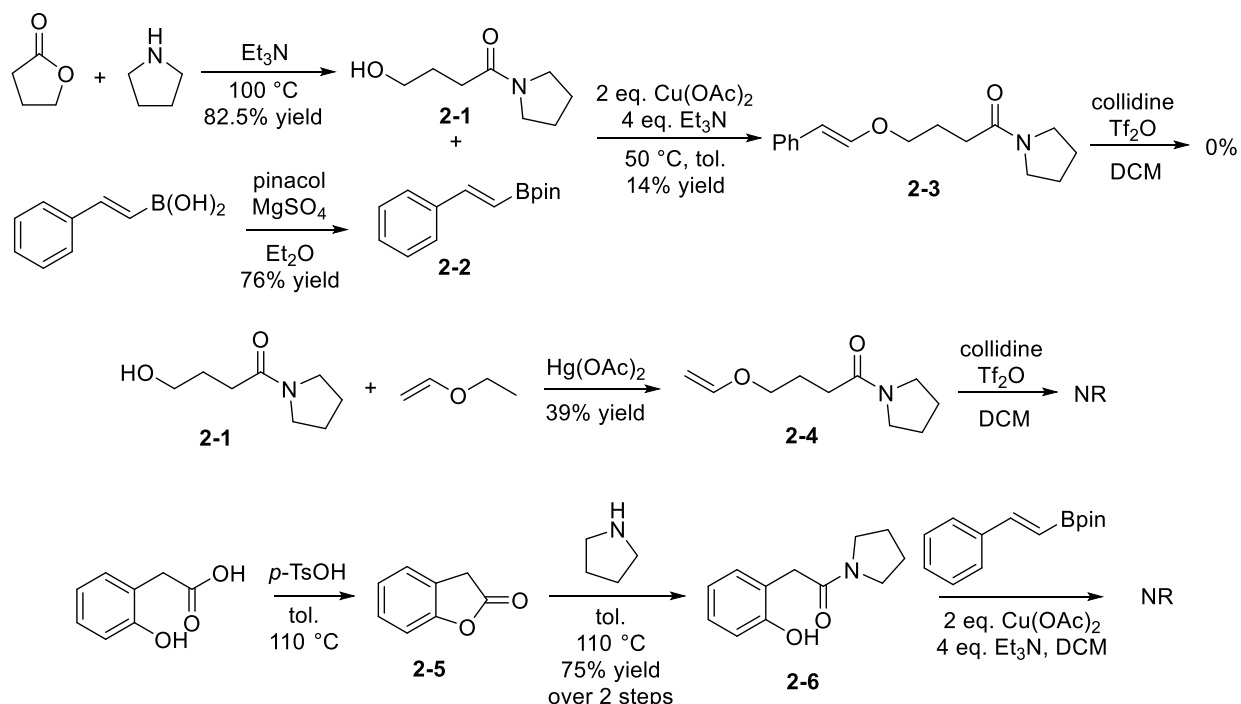
2.3 Intramolecular [2+2] Cyclization of Vinyl Ethers and Ketene Iminium Ions

The intramolecular cyclization of vinyl ethers with ketene iminium ions was investigated first because of the inherent stability of amides, the simplest and most practical precursor to a ketene iminium. Vinyl ethers are, in our experience, quite reactive, especially under acidic conditions. Therefore, we foresaw the greatest challenge of this project to be the generation of two highly reactive functional groups in the same molecule. Concerns over the acidity of a carboxylic acid with respect to the vinyl ether led us to investigate ketene iminium ion cyclization first.

Our copper coupling chemistry for the synthesis of vinyl ethers turned out to be very challenging with amides located on the alcohol coupling partners (Scheme 2.5). Two different

substrates were synthesized, compound **2-3** using copper coupling and **2-4** using an old mercury catalyzed method,¹⁶ but neither of these cyclized when submitted to the conditions developed by Ghosez and coworkers to generate the ketene iminium ion. The copper coupling of **2-6** was unsuccessful.

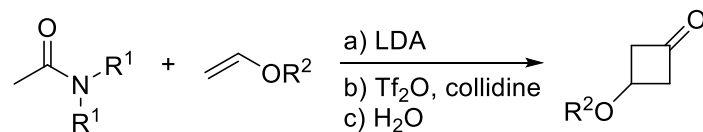
Scheme 2.5 Initial Ketene Iminium Experiments



An intermolecular analogue of the reaction was examined in hopes of finding viable reaction conditions before improving the synthesis of the substrates (Table 2.4). Lithium diisopropyl amine was added in order to further activate the amide for ketene iminium ion generation via an amide enolate. The reaction temperature was altered, as well as the equivalents of the vinyl ether. The substrates were also modified to increase molecular weight for ease of handling. Authentic samples of the products were synthesized via ketene and the increased molecular weight of the butyl ether led to a much higher yield thanks to easier isolation and purification (Scheme 2.6). We then discovered the reason the reaction employing amides and vinyl ethers failed. It was found that ethyl vinyl ether, when combined with triflic anhydride, rapidly forms ethanol triflate, as shown in Scheme 2.7. This reaction occurs extremely fast, and precludes any chance of a

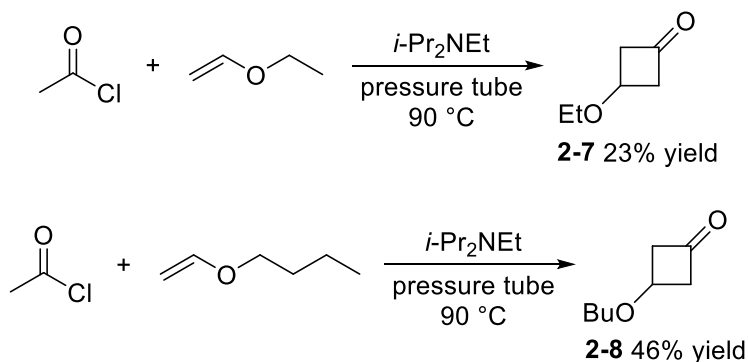
vinyl ether surviving the conditions required for the intramolecular cyclization to occur from amide based substrates.

Table 2.4 Intermolecular Reaction Optimization

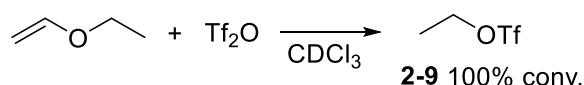


Entry	R ¹	R ²	Temp. After Tf ₂ O (°C)	Equiv. Vinyl Ether
1	Me	Et	20	1
2	Me	Bu	20	1
3	Pyrrolidine	Bu	20	1
4	Pyrrolidine	Bu	20	4
5	Pyrrolidine	Bu	55	1
6	Pyrrolidine	Bu	70	1

Scheme 2.6 Synthesis of Authentic Product Samples



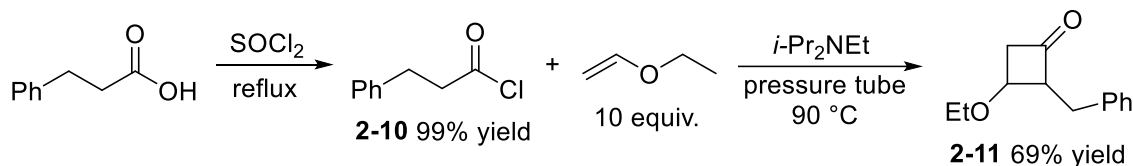
Scheme 2.7 Reaction of Ethyl Vinyl Ether and Triflic Anhydride



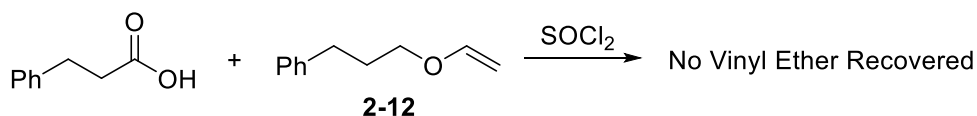
2.4 Intramolecular [2+2] Cyclization of Vinyl Ethers and Ketenes

Disappointed with the previous results, we turned our attention to the cyclization of ketenes. After successfully reproducing Matsuo's results (Scheme 2.8),⁷ we set about finding an alternate method of acid chloride formation, as thionyl chloride, the standard method, reacts with vinyl ethers (Scheme 2.9).

Scheme 2.8 Replication of Matsuo's Results

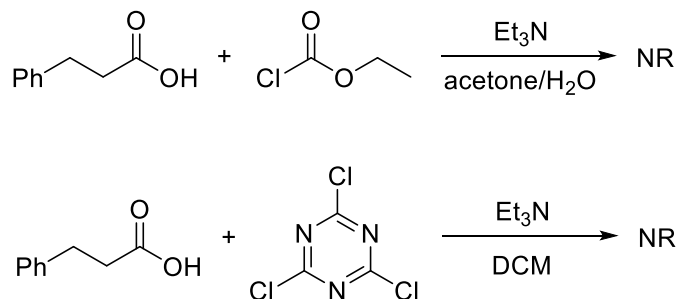


Scheme 2.9 Thionyl Chloride Decomposes Vinyl Ethers

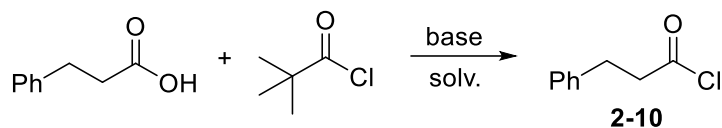


Ethyl chloroformate and trichlorotriazine have both been reported to convert carboxylic acids to acid chlorides, but neither worked in this case (Scheme 2.10).¹⁸ Hoveyda and co-workers reported that pivaloyl chloride can be used for this conversion via the mixed anhydride.¹⁹ However, variation of reaction time, temperature, solvent, equivalents of pivaloyl chloride and

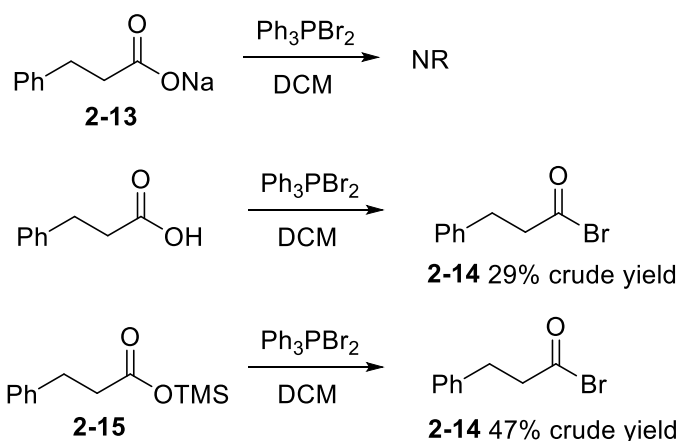
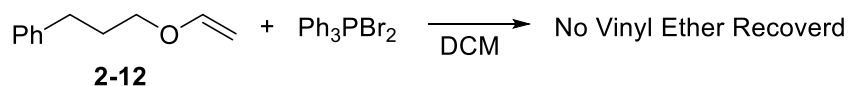
Scheme 2.10 Failed Alternative Access to Acid Chlorides



even adding base only gave a maximum conversion of 70% to the desired acid chloride (Table 2.5). The possibility of using triphenylphosphine dibromide was also examined.²⁰ Best results were achieved when using the TMS protected carboxylic acid **2-15**, rather than the free carboxylic acid or the carboxylate salt (Scheme 2.11). Before this reaction was optimized, however, it was found that triphenylphosphine dibromide decomposes vinyl ethers, and is therefore not up to the task (Scheme 2.12).

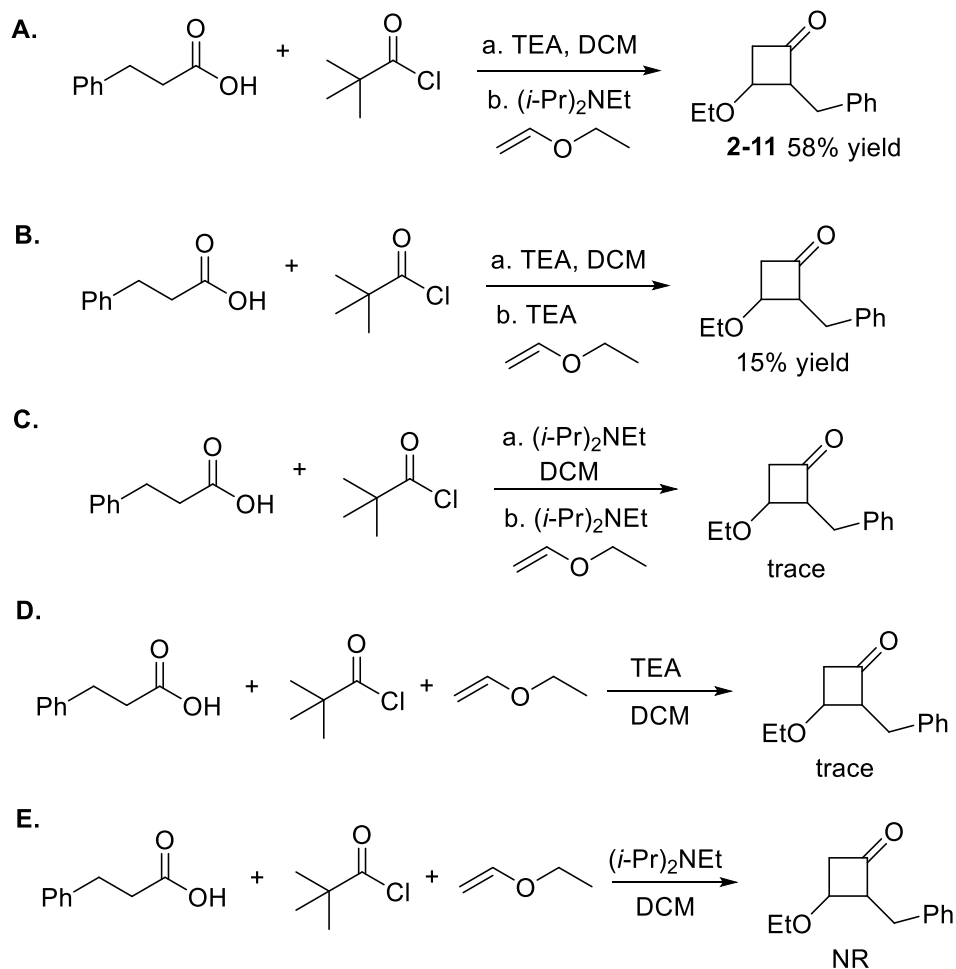
Table 2.5 Acid Chloride Synthesis using Pivaloyl Chloride

Entry	Equiv. Piv. Chloride	Time (hrs)	Temp. (°C)	Base	Solvent	Conversion (%)
1	1	2	20	-	DCM	25
2	1	24	20	-	DCM	33
3	10	24	20	-	DCM	70
4	40	24	20	-	DCM	52
5	10	24	50	-	CHCl ₃	55
6	10	24	50	-	DCM	68
7	10	24	20	(<i>i</i> -Pr) ₂ NEt	DCM	63

Scheme 2.11 Acid Bromide Synthesis**Scheme 2.12** Triphenylphosphine Dibromide Decomposes Vinyl Ether

Previous reports by the Romo and Wu groups have shown that mixed anhydrides can be used as precursors to ketenes for cyclization with ketones.²¹ Therefore, we decided to continue working with pivaloyl chloride, but make use of the mixed anhydride itself rather than converting to the acid chloride. After using conditions reported by Nishioka and co-workers²² for the synthesis of the mixed anhydride and changing the extraction solvent in Matsuo's workup from ethyl acetate to dichloromethane, the intermolecular [2+2] cycloaddition product **2-11** was

Scheme 2.13 Investigation of Intermolecular Model

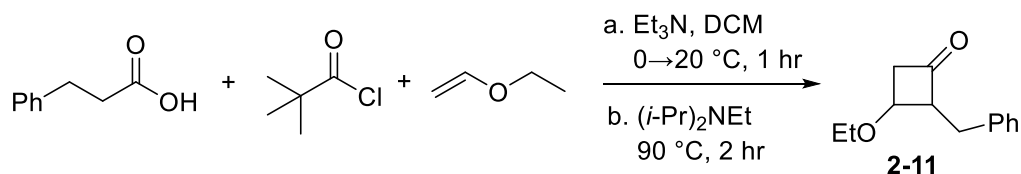


obtained in an isolated yield of 58% (Scheme 2.13A). Surprisingly, triethylamine and Hunig's base were required for each of their respective steps. Attempting to use only one or the other led to very poor results under otherwise identical conditions (Scheme 2.13B-C). Even worse results were obtained if the vinyl ether was added at the beginning of the reaction to better represent intramolecular conditions (Scheme 2.13D-E).

Table 2.6 shows alterations made to the reaction conditions in an attempt to optimize the intermolecular model reaction. Extending the reaction time of each step of the reaction had small positive effects on the yield of the reaction, but only to a point (entries 2, 5-6). Lowering the temperature of the mixed anhydride formation did not improve results (entries 3-4), and other

amine bases proved ineffective for formation of the mixed anhydride (entries 7-8). Despite the low yield of 28% for **2-11**, an intramolecular substrate was synthesized to test the viability of the conditions before undertaking the laborious task of further optimization. The isopropyl ester form of the substrate (**2-19**) was made with little difficulty using a combination of known chemistry and our groups' copper coupling protocol (Scheme 2.14). The isopropyl ester was found to work better in the hydroboration than methyl ester. Hydrolysis of the isopropyl ester required a small solvent screen to find viable conditions, with a 1:1 mixture of dioxane and water providing the product **2-20** in 69% yield (Table 2.7). When this compound was subjected to the cyclization conditions, no reaction occurred, ending our investigation of ketenes (Scheme 2.15).

Table 2.6 Optimization of Intermolecular Model



Entry	Change in Conditions	Result
1	none	10% yield
2	step (a) ran 4 hours	23% yield
3	step (a) ran 24 hours at -20 °C	19% yield
4	step (a) ran at 0 °C	17% yield
5	step (b) ran for 4 hours	28% yield
6	step (b) ran for 8 hours	13% yield
7	replaced Et ₃ N with pyridine	NR
8	replaced Et ₃ N with 4-dimethylaminopyridine	NR

Scheme 2.14 Synthesis of Intramolecular Substrate Ester

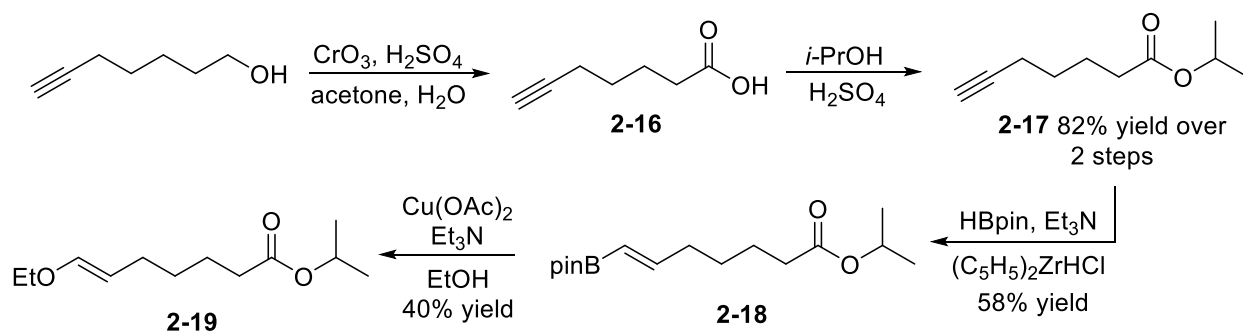
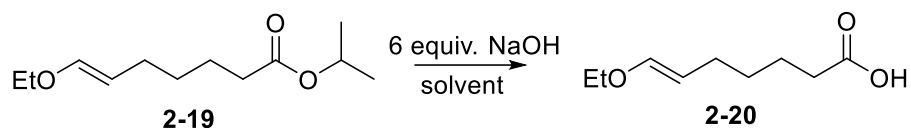
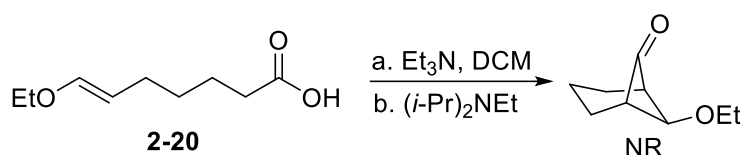


Table 2.7 Hydrolysis of Ester Solvent Screen



Entry	Solvent	Result
1	9:1 DCM/MeOH	NR
2	1:1 THF/H ₂ O	0% yield
3	1:1 dioxane/H ₂ O	69% yield

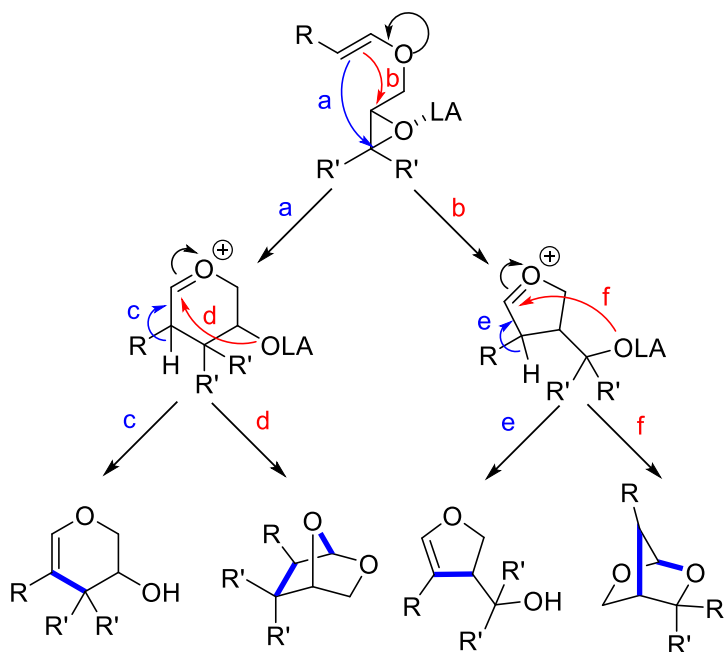
Scheme 2.15 Attempted Intramolecular Cyclization



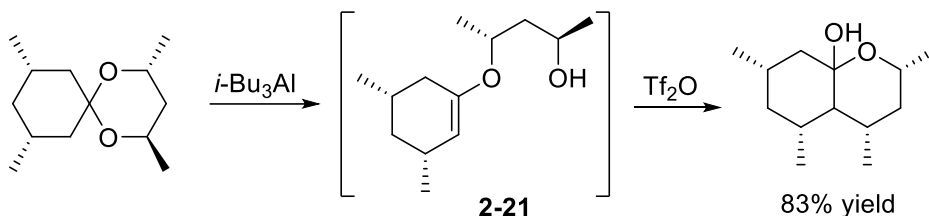
2.5 Lewis Acid Promoted Cyclization of Vinyl Ethers with Epoxides

A handful of examples exist in which a vinyl ether participates as a nucleophile in a cyclization reaction; the most notable of which is shown in Scheme 2.16.²³ Yamamoto and co-

Figure 2.3 Potential Reaction Pathways of Vinyl Ether Cyclization with Epoxides



Scheme 2.16 Precedent for Nucleophilic Vinyl Ether



workers utilized the alkyl vinyl ether in compound **2-21** to perform an intramolecular $\text{S}_{\text{N}}2$ reaction as part of a synthesis of (-)-Lardolure. Our proposal for a new cyclization reaction is that when an epoxide is activated by a Lewis acid, one of four cascading pathways could occur driven by the inherent nucleophilic reactivity of the vinyl ether (Figure 2.3).

Coupling partners for the synthesis of a model substrate were made using known reactions (Scheme 2.17). Table 2.8 shows the optimization of the copper coupling reaction used to synthesize a substrate for an intramolecular cyclization. Initial results were poor despite alteration of temperature, solvent, and equivalents of the alcohol coupling partner (entries 1-4), but switching to a substituted epoxide and benzyl ether substrates immediately yielded better results (entry 5). Switching to toluene as solvent gave the desired product in an acceptable yield of 49% (entry 6). Adding an allene ligand did not improve this reaction, although added ligand has worked for our group in the past.

Scheme 2.17 Synthesis of Coupling Partners for Intramolecular Substrate

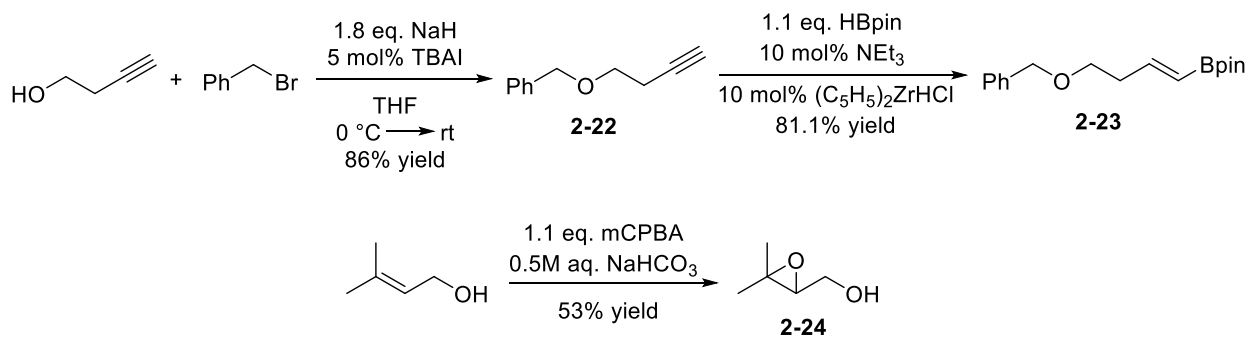
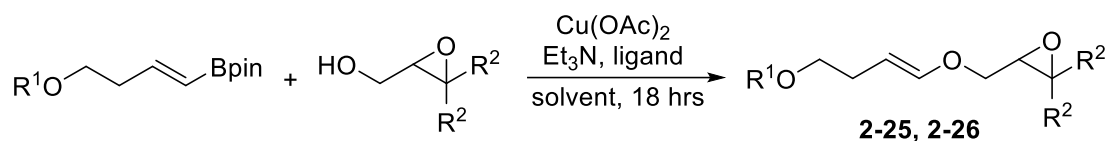
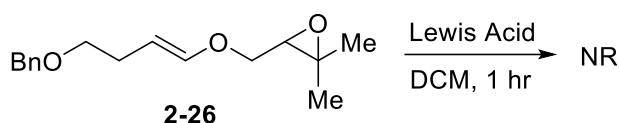


Table 2.8 Synthesis of Epoxide Cyclization Substrate

<i>Entry</i>	<i>R</i> ¹	<i>R</i> ²	<i>Ligand</i>	<i>Temp.</i> (°C)	<i>Solvent</i>	<i>Equiv. Epoxide</i>	<i>% Yield</i>
1	TBS	H	cyclononallene	55	toluene	4	NR
2	TBS	H	cyclononallene	20	none	60	trace
3	TBS	H	none	20	none	60	trace
4	TBS	H	none	55	CH ₃ CN	2	4
5	Bn	Me	none	20	benzene	6	40
6	Bn	Me	none	55	toluene	4	49
7	Bn	Me	cyclononallene	50	toluene	4	46

With a substrate in hand, a few different Lewis acids were examined as activators for the intramolecular cyclization (Table 2.9). Tin tetrachloride led to rapid opening of the epoxide forming a diol by trace water, despite the use of dry solvents and glassware (entry 1). Triisopropyl borate did not react at all (entry 6). Boron trifluoride etherate was examined more closely, varying the temperature of the reaction and the equivalents of the Lewis acid (entries 2-5). It was also unreactive however, save for higher equivalents at which point the substrate was decomposed.

Table 2.9 Attempted Cyclization with Epoxide

<i>Entry</i>	<i>Lewis Acid</i>	<i>Lewis Acid Equiv.</i>	<i>Temp.</i> (°C)	<i>Result</i>
1	SnCl ₄	1.1	-78	Epoxide opened to diol
2	BF ₃ •OEt ₂	0.5	-78	0% yield
3	BF ₃ •OEt ₂	0.1	-78	NR
4	BF ₃ •OEt ₂	0.1	-40	NR
5	BF ₃ •OEt ₂	0.1	0	NR
6	B(OiPr) ₃	0.1	0	NR

2.6 Conclusion

We had hoped that vinyl ethers would make good nucleophilic partners in a variety of intramolecular cyclization reactions. Unfortunately, in all cases some aspect of their reactivity proved incompatible with conditions. Vinyl ethers react rapidly with the triflic anhydride required to form ketaminium ions, precluding them as partners in a [2+2] cyclization. Ketenes are also very difficult to form in the presence of vinyl ethers, and although the intermolecular [2+2] was achieved, it could not be translated into an intramolecular system. Cyclization via nucleophilic attack on epoxides appears to have failed mainly due to the relative rates of competing side reactions, i.e. opening of the epoxide into a diol or breakdown of the vinyl ether into an alcohol and aldehyde. This is known to occur under acidic conditions. Of these three reactions, the epoxide system seems the most likely to remain achievable, as there are many more Lewis acids of varying reactivities which could be examined given enough time and resources.

2.7 Experimental Section

General Information

Unless otherwise specified, reactions were run open to air using dry solvents. DCM and Et₃N were distilled over CaH₂. All chemicals were used as purchased from commercial sources. NMR data was obtained using a Bruker ARX-400 instrument and calibrated to the solvent signal (CDCl₃ : $\delta = 7.26$ ppm for ¹H NMR, $\delta = 77.2$ ppm for ¹³C NMR). Data for ¹H NMR spectra are reported as follows: chemical shift (δ ppm), multiplicity, coupling constant (Hz), then integration. Data for ¹³C NMR spectra are reported in terms of chemical shift. The following abbreviations are used for the multiplicities: s = singlet, d = doublet, t = triplet, q = quartet, quin.

= quintet, sex. = sextet, hept. = heptet, dd = doublet of doublets, dt = doublet of triplets, td = triplet of doublets. Flash column chromatography was performed using 40-63 mesh silica gel.

Experimental Procedures

Synthesis of 2-1

An oven dried round bottom flask was charged with triethylamine (70 mL), γ -butyrolactone (9.14 mL), and pyrrolidine (19.7 mL). The reaction was placed under a nitrogen atmosphere and heated at reflux for 16 hours. After cooling to room temperature, the reaction was concentrated *in vacuo* to give **2-1** as a neon orange oil. The crude product was vacuum distilled at 180 °C and 3 mm Hg to give pure **2-1** (15.57 g, 82.5%). $^1\text{H NMR}$ (400 MHz, CDCl_3): δ 3.65 (m, 3 H), δ 3.42 (m, 4 H), δ 2.44 (q, $J = 6.2$, 2 H), δ 1.89 (m, 6 H).

Synthesis of 2-2

E-Styrylboronic acid (1.48 g), pinacol (1.42 g), MgSO_4 (1.44 g), and Et_2O (25 mL) were stirred in a round bottom flask for 1 hour. The reaction was then filtered through silica gel and concentrated *in vacuo* to give a pale-yellow oil. The crude product was purified by flash column chromatography (silica gel, 90:10 hexanes/ Et_2O), giving pure **2-2** (1.74 g, 76% yield). $^1\text{H NMR}$ (400 MHz, CDCl_3): δ 7.49 (d, $J = 8.3$, 2 H), δ 7.4 (d, $J = 18.4$, 1 H), δ 7.32 (m, 3 H), δ 6.17 (d, $J = 18.4$, 1 H), δ 1.32 (s, 12 H).

Synthesis of 2-3

An oven dried flask was charged with toluene (12 mL), **2-2** (0.46 g), **2-1** (1.26 g), triethylamine (1.12 mL), and cupric acetate (0.73 g), equipped with a reflux condenser and flushed with nitrogen atmosphere. The reaction was heated at 50 °C overnight. After cooling to room temperature, the reaction was diluted with aqueous NaHCO_3 and extracted 3x with Et_2O . The combined organic layer was washed with saturated NaHCO_3 and brine, dried over MgSO_4 ,

filtered, and concentrated *in vacuo* to a brown oil. The crude product was purified by flash column chromatography (silica gel, 35:64:1 hexanes/EtOAc/Et₃N) to give pure **2-3** (76 mg, 14% yield). ¹H NMR (400 MHz, C₆D₆): δ 7.08 (m, 4 H), δ 6.96 (m, 1 H), δ 6.92 (d, *J* = 13.0, 1 H), δ 5.85 (d, *J* = 13.0, 1 H), δ 3.67 (t, *J* = 5.8, 2 H), δ 3.29 (t, *J* = 6.3, 2 H), δ 2.63 (t, *J* = 6.8, 2 H), δ 2.01 (m, 4 H), δ 1.18 (m, 4 H).

Synthesis of **2-4**

Mercury (II) acetate (0.16 g) was added to a flask charged with **2-1** (0.79 g) and ethyl vinyl ether (15 mL), and stirred at room-temperature for 48 hours. The reaction was then quenched with saturated aqueous NaHCO₃ (15 mL) and extracted 3x with Et₂O. The combined organic layer was dried over MgSO₄, filtered, and concentrated *in vacuo* to a neon orange oil. The crude product was purified by flash column chromatography (silica gel, 59:40:1 EtOAc/hexanes/Et₃N) to give pure **2-4** (0.354 g, 39% yield). ¹H NMR (400 MHz, CDCl₃): δ 6.44 (dd, *J* = 14.4, 6.8, 1 H), δ 4.17 (dd, *J* = 14.4, 2.0, 1 H), δ 3.97 (dd, *J* = 6.8, 2.0, 1 H), δ 3.74 (t, *J* = 6.0, 2 H), δ 3.43 (m, 6 H), δ 2.36 (m, 3 H), δ 1.83 (m, 3 H). ¹³C NMR (100 MHz, CDCl₃): δ 170.8, 151.8, 86.6, 67.3, 46.5, 45.6, 30.9, 26.1, 24.4.

Synthesis of **2-5**²⁴

2-Hydroxyphenylacetic acid (1 g), toluene (14 mL) and p-toluenesulfonic acid in a round bottom flask were placed under Dean-Stark conditions and heated at reflux for 18 hours. After cooling to room temperature, the reaction was washed 3x with NaHCO₃ and brine. The aqueous layer was back extracted with EtOAc, and the combined organic layers were washed with H₂O, dried over MgSO₄, filtered, and concentrated *in vacuo* to give **2-5** as a red orange oil, which was used without further purification (1.02 g).

Synthesis of 2-6

An oven dried flask was charged with toluene (40 mL), **2-5** (0.75 g), and pyrrolidine (0.68 mL), and heated at 110 °C for 18 hours. After cooling to room temperature, the reaction was acidified to pH 1 using 1M aqueous HCl. The aqueous layer was extracted with EtOAc and the combined organic layers were washed with H₂O and brine, then dried over MgSO₄, filtered, and concentrated *in vacuo* to a pale yellow crystalline solid **2-6**, and used without further purification (1.01 g, 75% yield over 2 steps). ¹H NMR (400 MHz, DMSO-d₆): δ 9.89 (br s, 1 H), δ 7.20 (m, 2 H), δ 7.00 (d, *J* = 7.2, 1 H), δ 6.81 (t, *J* = 7.2, 1 H), δ 3.66 (m, 4 H), δ 3.46 (t, *J* = 6.8, 2 H), δ 1.99 (quin., *J* = 6.7, 2 H), δ 1.87 (quin., *J* = 6.7, 2 H).

Failed Procedure for cyclization of 2-3 and 2-4

An oven dried flask under nitrogen atmosphere containing the substrate (0.25 mmol) was charged with dry DCM (1.1 mL), then collidine (0.04 mL), the triflic anhydride (0.04 mL). The reaction was stirred at room temperature for 18 hours. Concentrated aqueous NaHCO₃ (1 mL) was added and stirred overnight. The aqueous layer was extracted with DCM 3x, and the combined organic layers were dried over MgSO₄, and concentrated *in vacuo* to an orange oil containing starting material and phenylacetaldehyde in the case of **2-3**.

Representative Procedure for Table 2.4

The amide and vinyl ether substrates (1 mmol) and THF (2 mL) were added to a flask under nitrogen atmosphere at -78 °C. LDA (0.14 mL) was prepared under standard conditions and added to the reaction via canula. After 1.5 hours triflic anhydride (0.17 mL) was added, turning the reaction orange, and the reaction was allowed to warm to room temperature. After 18 hours, aqueous saturated NaHCO₃ was added, and stirred for 24 hours. The reaction was diluted with DCM and H₂O, and the aqueous layer was extracted with DCM. The combined organic layers

were washed with brine, dried over MgSO₄, filtered, and concentrated *in vacuo* to give an orange oil, which primarily contained the amide substrate and no traces of **2-7** or **2-8** were detected by examination of spectra from authentic samples.

Synthesis of **2-7**

Ethyl vinyl ether (6.7 mL), Hunig's base (1.5 mL), and acetyl chloride (0.5 mL) were added to a glass pressure tube, which was sealed and heated at 90 °C overnight. After cooling to room temperature, the reaction was quenched with aqueous saturated NaHCO₃, and the aqueous layer was extracted with EtOAc. The combined organic layers were washed with brine, dried over MgSO₄, filtered, and concentrated *in vacuo* to a red oil. The crude product was purified by flash column chromatography (silica gel, 8:1 hexanes/Et₂O) to give **2-7** (186 mg, 23% yield). ¹H NMR (400 MHz, CDCl₃): δ 4.28 (m, 1 H), δ 3.50 (q, *J* = 7.0, 2 H), δ 3.22 (m, 2 H), δ 3.08 (m, 2 H), δ 0.88 (t, *J* = 6.7, 3 H).

Synthesis of **2-8**⁷

Butyl vinyl ether (5.1 mL), Hunig's base (0.84 mL), and acetyl chloride (0.27 mL) were added to a glass pressure tube, which was sealed and heated at 90 °C overnight. After cooling to room temperature, the reaction was quenched with aqueous saturated NaHCO₃, and the aqueous layer was extracted with EtOAc. The combined organic layers were washed with brine, dried over MgSO₄, filtered, and concentrated *in vacuo* to a red oil. The crude product was purified by flash column chromatography (silica gel, 8:1 hexanes/Et₂O) to give **2-8** (260 mg, 46% yield). ¹H NMR (400 MHz, CDCl₃): δ 4.26 (m, 1 H), δ 3.43 (t, *J* = 6.6, 2 H), δ 3.22 (m, 2 H), δ 3.07 (m, 2 H), δ 1.59 (quin., *J* = 6.7, 2 H), δ 0.9 (m, 5 H). ¹³C NMR (100 MHz, CDCl₃): δ 205.3, 69.4, 63.9, 54.2, 31.7, 19.4, 13.9.

Synthesis of **2-10** ⁷

An oven dried flask was charged with hydrocinnamic acid (1.24 g) and thionyl chloride (1.5 mL), and equipped with a reflux condenser and a drying tube containing CaCl₂. The reaction was heated at 80 °C for 3 hours. After cooling to room temperature concentration *in vacuo* gave **2-10** which was used without further purification (1.37 g, 99% yield). ¹H NMR (400 MHz, CDCl₃): δ 7.32 (m, 2 H), δ 7.21 (m, 3 H), δ 3.21 (t, *J* = 7.4, 2 H), δ 3.02 (t, *J* = 7.7, 2 H).

Synthesis of **2-11** ⁷

2-10 (0.67 g) was added to a pressure tube containing ethyl vinyl ether (3.8 mL) and Hunig's base (0.84 mL). The tube was sealed and heated at 90 °C for 2 hours. After cooling to room temperature, the reaction was quenched with aqueous saturated NaHCO₃. The aqueous layer was extracted with EtOAc, and the combined organic layers were washed with brine, dried over MgSO₄, filtered and concentrated *in vacuo* to give a red oil. The crude product was purified by flash column chromatography (silica gel, 88:12 hexanes/EtOAc) to give pure **2-11** as 2 diastereomers (424 mg, 69% yield). ¹H NMR (400 MHz, CDCl₃): δ 7.25 (m, 5 H), δ 4.13 (m, 1 H), δ 3.49 (m, 2 H), δ 3.08 (m, 5 H), δ 1.19 (t, *J* = 7.0, 3 H).

Synthesis of **2-12**

Hg(OAc)₂ (0.024 g) was added to a flask charged with hydrocinnamyl alcohol (0.41 g) and ethyl vinyl ether (4.8 mL). The reaction was stirred for 72 hours, and then quenched with aqueous saturated NaHCO₃. The aqueous layer was extracted 3x with Et₂O, and the combined organic layers were dried over MgSO₄, filtered, and concentrated *in vacuo* to a pale yellow oil. This oil was passed through a silica gel plug (80:20 hexanes/EtOAc) to give **2-12**, which was used without further purification (395 mg, 81% yield). ¹H NMR (400 MHz, CDCl₃): δ 7.28 (m, 2

H), δ 7.20 (m, 3 H), δ 6.49 (dd, $J = 14.3, 6.8, 1$ H), δ 4.17 (dd, $J = 14.3, 1.9, 1$ H), δ 3.99 (dd, $J = 6.8, 1.9, 1$ H), δ 3.69 (t, $J = 6.3, 2$ H), δ 2.73 (t, $J = 7.4, 2$ H), δ 1.98 (quin., $J = 6.4, 2$ H).

Representative Procedure for Table 2.5

Hydrocinnamic acid (0.15 g), solvent (2 mL), and pivaloyl chloride were added to a flask and stirred under a nitrogen atmosphere. After the designated time, the reaction was concentrated *in vacuo*, and the percent conversion was measured by ^1H NMR.

Synthesis of 2-15

Hexamethyldisilazane (1.05 mL) was added to an oven dried flask charged with pyridine (1 mL) and hydrocinnamic acid (0.15 g), and stirred at room temperature for 1 hour. The reaction was then concentrated *in vacuo* to give **2-15** as a pale yellow oil which was used without further purification (222 mg, 99% yield). ^1H NMR (400 MHz, CDCl_3): δ 7.28 (m, 2 H), δ 7.19 (m, 3 H), δ 2.93 (t, $J = 7.6, 2$ H), δ 2.63 (t, $J = 8.0, 2$ H), δ 0.26 (s, 9 H). ^{13}C NMR (100 MHz, CDCl_3): δ 173.5, 140.7, 128.4, 128.3, 126.2, 37.4, 31.1, -0.3.

Synthesis of 2-14

Bromine (0.05 mL) was added to an oven dried flask charged with triphenylphosphine (0.26 g) and DCM (2 mL) at 0 °C and stirred for 30 minutes. **2-15** (0.22 g) was then added as a solution in DCM (2 mL), and stirred at room temperature for 30 minutes. The reaction was then concentrated *in vacuo* to a thick red oil. This oil was extracted 4x with 4 mL of 1:1 hexanes/ Et_2O . The combined solution was concentrated *in vacuo* to give the crude product, a mixture of **2-14** and hydrocinnamic acid as a pale yellow oil. ^1H NMR (400 MHz, CDCl_3): δ 7.3 (m, 2 H), δ 7.21 (m, 3 H), δ 2.97 (t, $J = 8.0, 2$ H), δ 2.69 (t, $J = 6.9, 2$ H).

Representative Procedure for Scheme 2.13 and Table 2.6 (Scheme 2.13 A)

An oven dried glass pressure tube was charged with hydrocinnamic acid (0.15 g), cooled to 0 °C and flushed with a nitrogen atmosphere. Dry DCM (2 mL) and triethylamine (0.31 mL) were added and stirred for 1 hour. Ethyl vinyl ether (0.95 mL) and Hunig's base (0.21 mL) were added, and the tube was sealed and heated at 90 °C for 2 hours. After cooling to room temperature, the reaction was quenched with aqueous saturated NaHCO₃. The aqueous layer was extracted 3x with DCM, and the combined organic layers were then washed with brine, dried over MgSO₄, filtered, and concentrated *in vacuo* to an orange oil. The crude product was purified by flash column chromatography (silica gel, 88:12 hexanes/EtOAc) to give pure **2-11** (119 mg, 58% yield).

Synthesis of 2-17

Jones reagent was created by adding 6 mL of H₂SO₄ to a 12 mL solution of chromium trioxide (6.22 g) in H₂O. The Jones solution was added dropwise to a flask charged with acetone (50 mL) and 6-heptynol (3.36 mL). Addition was stopped once an orange color persisted in solution. The reaction was quenched with isopropanol, then extracted 2x with CHCl₃. The combined CHCl₃ layers were washed with brine, dried over MgSO₄, filtered, and concentrated *in vacuo* to give **2-16**, which was used without further purification. Sulfuric acid (0.1 mL) was added to a flask charged with **2-16** () and isopropanol (325 mL). The reaction was heated at reflux for 18 hours, then concentrated *in vacuo* to give **2-17**, which was used without further purification (3.67 g, 82% yield over 2 steps). ¹H NMR (400 MHz, CDCl₃): δ 5.00 (hept., *J* = 6.3, 1 H), δ 2.29 (t, *J* = 7.3, 2 H), δ 2.21 (td, *J* = 7.1, 2.7, 2 H), δ 1.94 (t, *J* = 2.6, 1 H), δ 1.73 (quin., *J* = 7.4, 2 H), δ 1.56 (quin., *J* = 7.1, 2 H), δ 1.22 (d, *J* = 6.2, 6 H).

Synthesis of 2-18

A flame dried flask under a nitrogen atmosphere was charged with **2-17** (3.67 g), pinacolborane (3.5 mL), Et₃N (0.31 mL), and zirconocene hydrochloride (0.57 g). The reaction was heated at 60 °C for 18 hours. The reaction was concentrated *in vacuo*, then purified by flash column chromatography (silica gel, 90:10 hexanes/EtOAc) to give **2-18** as a colorless oil (2.13 g, 58% yield). ¹H NMR (400 MHz, CDCl₃): δ 6.60 (dt, *J* = 17.1, 5.5, 1 H), δ 5.42 (d, *J* = 17.9, 1 H), δ 4.99 (hept., *J* = 6.2, 1 H), δ 2.25 (t, *J* = 7.7, 2 H), δ 2.16 (q, *J* = 6.8, 2 H), δ 1.61 (m, 2 H), δ 1.44 (m, 2 H), δ 1.26 (s, 12 H), δ 1.22 (d, *J* = 6.3, 6 H).

Synthesis of 2-19

An oven dried flask under a nitrogen atmosphere was charged with **2-18** (1.66 g), EtOH (18 mL), Et₃N (3.12 mL), and anhydrous cupric acetate (2.03 g). The reaction was stirred for 18 hours at room temperature. The reaction was then diluted with aqueous NaHCO₃ and extracted 3x with Et₂O. The combined organic layer was washed with saturated NaHCO₃ and brine, dried over MgSO₄, filtered, and concentrated *in vacuo* to an oil. The crude product was purified by flash column chromatography (silica gel, 97:2:1 hexanes/EtOAc/Et₃N) to give pure **2-19** (483 mg, 40% yield). ¹H NMR (400 MHz, CDCl₃): δ 6.21 (d, *J* = 12.6, 1 H), δ 4.99 (hept., *J* = 6.3, 1 H), δ 4.74 (dt, *J* = 12.6, 7.4, 1 H), δ 3.69 (q, *J* = 7.0, 2 H), δ 2.25 (t, *J* = 7.4, 2 H), δ 1.92 (q, *J* = 7.4, 2 H), δ 1.61 (quin., *J* = 7.5, 2 H), δ 1.35 (quin., *J* = 7.6, 2 H), δ 1.25 (t, *J* = 7.0, 3 H), δ 1.22 (d, *J* = 6.3, 6 H). ¹³C NMR (100 MHz, CDCl₃): δ 173.3, 146.2, 103.7, 67.4, 64.6, 34.6, 30.2, 27.4, 24.4, 21.9, 14.8.

Synthesis of 2-20

2-19 (0.11 g) was added to a flask charged with dioxane (2.5 mL), H₂O (2.5 mL), and NaOH (0.15 g). The reaction was heated at reflux for 2 hours, and then after cooling to room

temperature, was acidified to pH 4 using 1M aqueous HCl. The reaction was extracted with DCM, and the combined organic layers were washed with brine, dried over MgSO₄, filtered, and concentrated to give **2-20** as a pale yellow oil which was used without further purification (119 mg, 69% yield). ¹H NMR (400 MHz, CDCl₃): δ 9.77 (s, 1 H), δ 6.22 (d, *J* = 12.6, 1 H), δ 4.74 (dt, *J* = 12.6, 7.4, 1 H), δ 3.69 (q, *J* = 7.0, 2 H), δ 2.35 (t, *J* = 7.4, 2 H), δ 1.93 (q, *J* = 7.3, 2 H), δ 1.64 (quin., *J* = 7.5, 2 H), δ 1.39 (quin., *J* = 7.4, 2 H), δ 1.25 (t, *J* = 7.0, 3 H). ¹³C NMR (100 MHz, CDCl₃): δ 146.31, 103.5, 64.7, 33.6, 30.1, 27.4, 24.0, 14.8. (A likely peak around 170 is indiscernible from noise.)

Synthesis of 2-22

3-Butynol (10.9 mL) was added to a dried flask under nitrogen atmosphere at 0 °C containing dry THF (110 mL) and NaH (4.3 g). After 30 minutes tetrabutylammonium iodide (4.84 mmol) was added, and benzyl bromide (11.9 mL) was added dropwise. The reaction was allowed to slowly warm to room temperature. After 18 hours the reaction was cooled to 0 °C and quenched with NH₄Cl until the solution was clear orange. The aqueous layer was extracted 4x with Et₂O, and the combined organic layers were washed with H₂O and brine, dried over MgSO₄, filtered, and concentrated to a clear orange oil. The crude product was vacuum distilled (3 mmHg, 100 °C) to give **2-22** as a pale yellow oil (12.55 g, 86% yield). ¹H NMR (400 MHz, CDCl₃): δ 7.35 (d, *J* = 4.5, 4 H), δ 7.30 (m, 1 H), δ 4.57 (s, 2 H), δ 3.61 (t, *J* = 7.0, 2 H), δ 2.51 (td, *J* = 6.9, 2.7, 2 H), δ 1.99 (t, *J* = 2.7, 1 H).

Synthesis of 2-23

A flame dried flask under a nitrogen atmosphere was charged with **2-22** (3.2 g), pinacolborane (3.2 mL), Et₃N (0.28 mL), and zirconocene hydrochloride (0.52 g). The reaction was stirred at room temperature for 18 hours. The reaction was concentrated *in vacuo*, then

purified by flash column chromatography (silica gel, 90:10 hexanes/EtOAc) to give **2-23** as a colorless oil (4.68 g, 81% yield). ^1H NMR (400 MHz, CDCl_3): δ 7.33 (m, 4 H), 7.27 (m, 1 H), δ 6.63 (dt, $J = 18.0, 6.4$, 1 H), δ 5.52 (dt, $J = 18, 1.6$, 1 H), δ 4.51 (s, 2 H), 3.56 (t, $J = 6.9$, 2 H), δ 2.49 (qd, $J = 6.8, 1.6$, 2 H), 1.26 (s, 12 H).

Synthesis of **2-24**²⁵

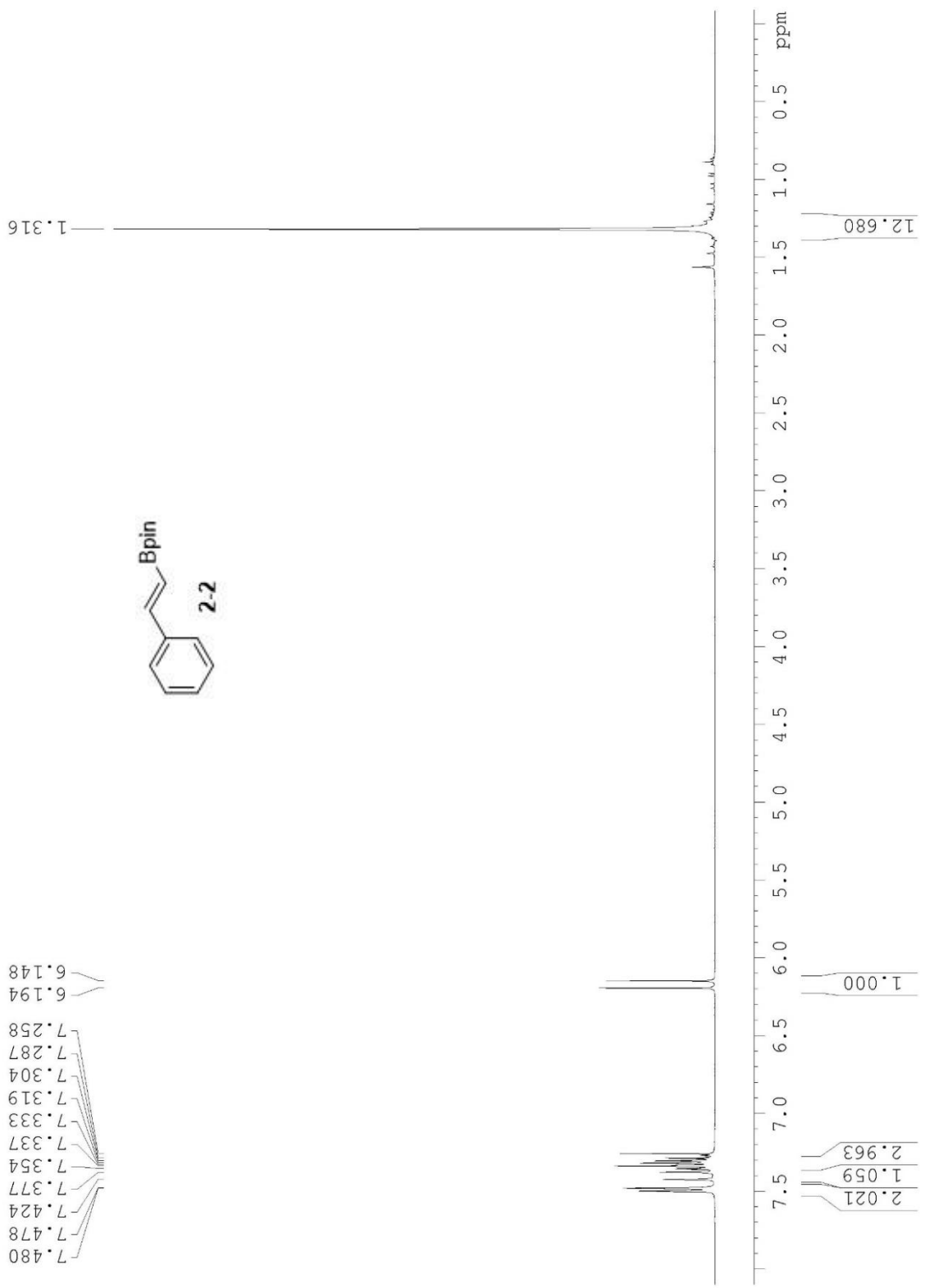
Prenol (6.1 mL) was added at 0 °C to a flask containing 0.5M NaHCO_3 in H_2O . MCPBA (11.4 g) was added slowly, then after 15 minutes the reaction was allowed to warm up to room temperature, and stirred for 18 hours. The reaction was then saturated with NaCl, then extracted 5x with DCM. The combined organic layers were dried over MgSO_4 , filtered, and concentrated *in vacuo* to a colorless oil. The crude product was purified by flash column chromatography (silica gel, 70:30 hexanes/EtOAc) to give **2-24** (3.27 g, 53% yield). ^1H NMR (400 MHz, CDCl_3): δ 3.84 (dd, $J = 12.0, 4.2$, 1 H), δ 3.68 (dd, $J = 12.0, 6.6$, 1 H), δ 2.97 (dd, $J = 6.6, 4.4$, 1 H), δ 1.33 (s, 3 H), δ 1.32 (s, 1 H).

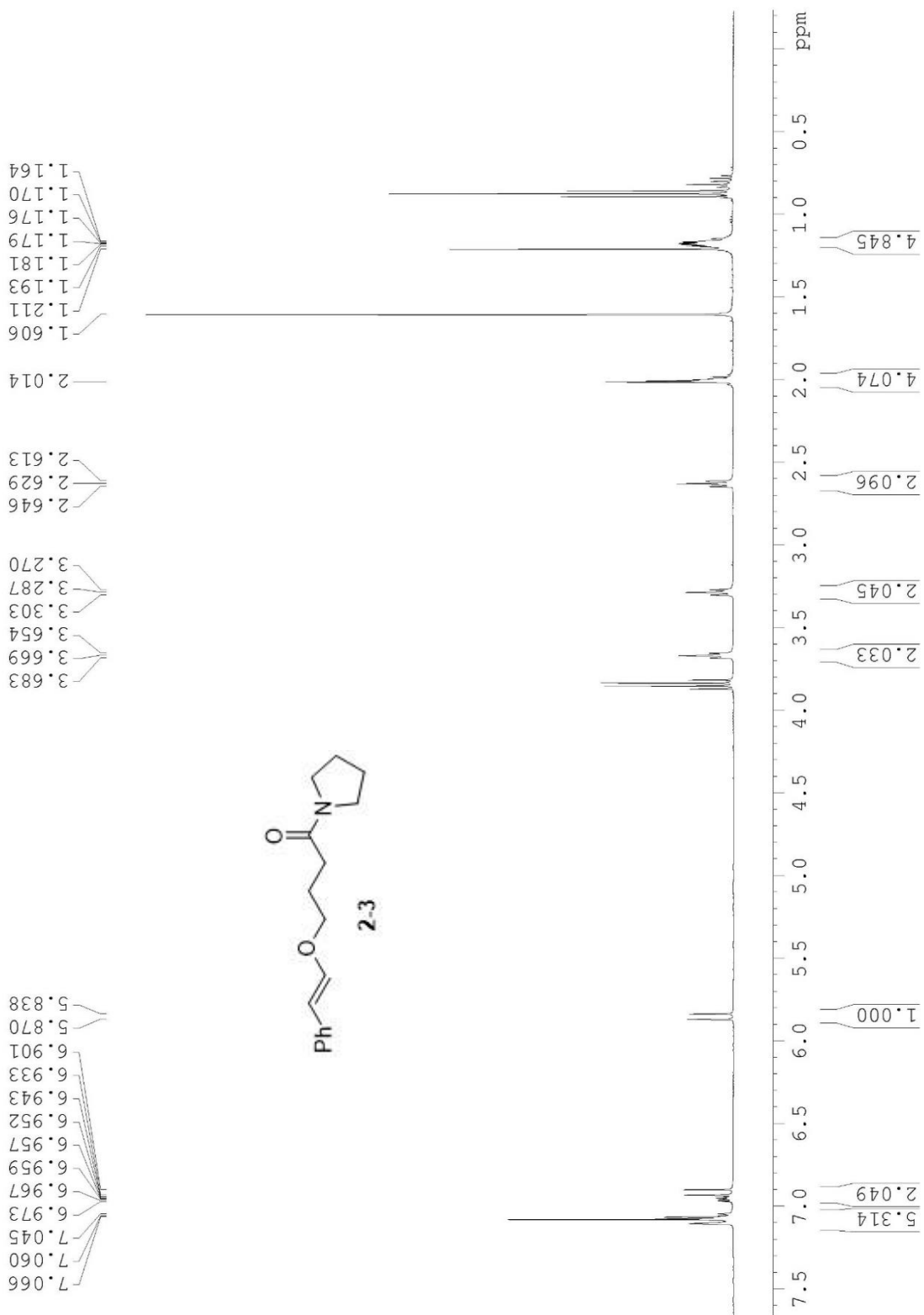
Synthesis of **2-26**

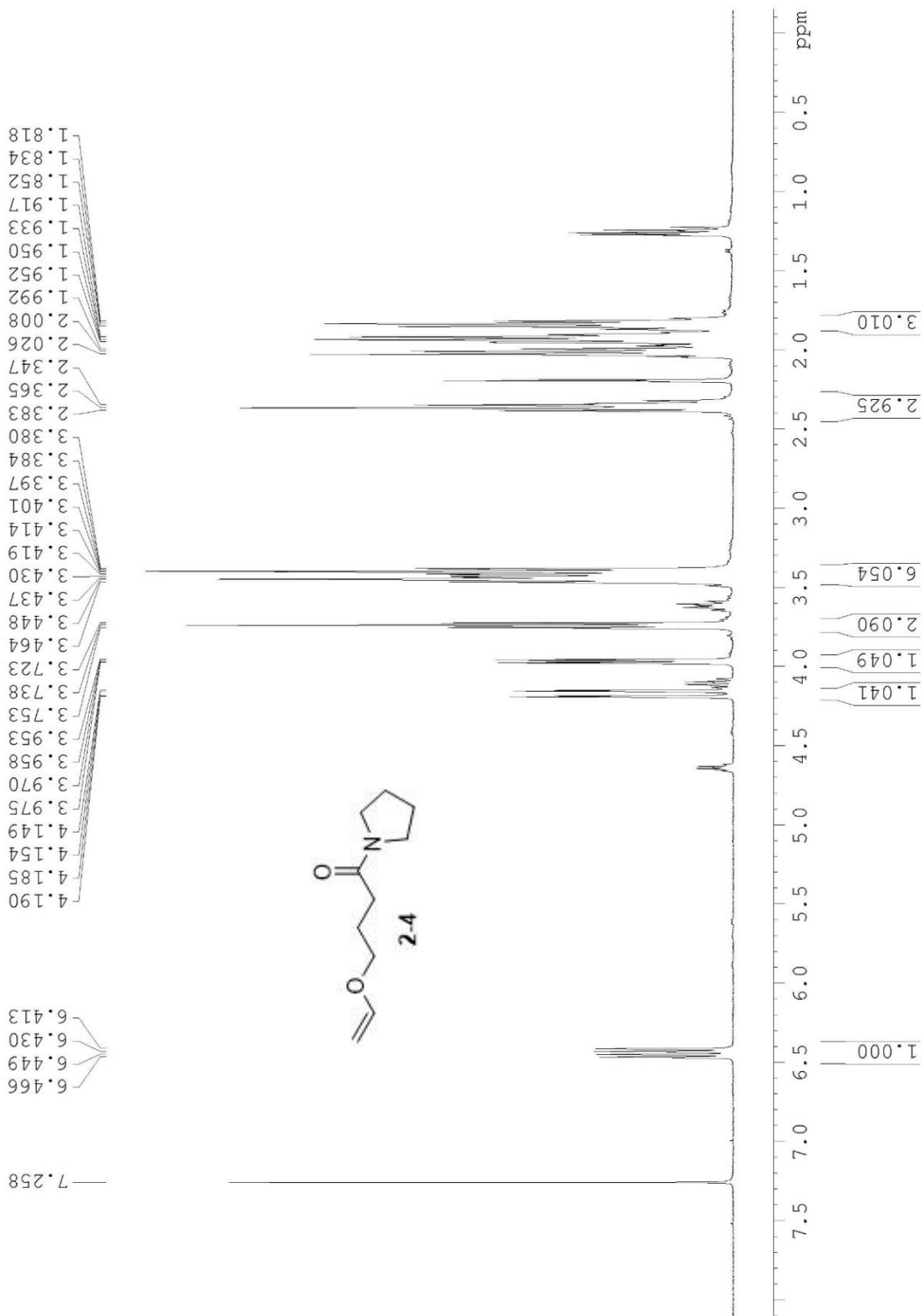
Cupric acetate (0.18 g) was added to a dry flask charged with **2-23** (0.144 g), **2-24** (0.2 g), Et_3N (0.28 mL), and toluene (3 mL) under nitrogen atmosphere. The reaction was heated at 55 °C for 24 hours, then cooled to room temperature and filtered through a silica plug. The crude product was then purified via flash column chromatography (silica gel, 93:7 hexanes/EtOAc) to give **2-26** (65 mg, 49.5% yield). ^1H NMR (400 MHz, CDCl_3): δ 7.34 (m, 4 H), δ 7.27 (m, 1 H), δ 6.35 (d, $J = 12.6$, 1 H), δ 4.83 (dt, $J = 12.6, 7.4$, 1 H), δ 4.51 (s, 2 H), δ 3.81 (dd, $J = 11.2, 4.8$, 1 H), δ 3.73 (dd, $J = 11.2, 5.9$, 1 H), δ 3.45 (t, $J = 6.8$, 2 H), δ 2.99 (t, $J = 5.0$, 1 H), δ 2.24 (q, $J = 6.9$, 2 H), δ 1.35 (s, 3 H), δ 1.30 (s, 3 H).

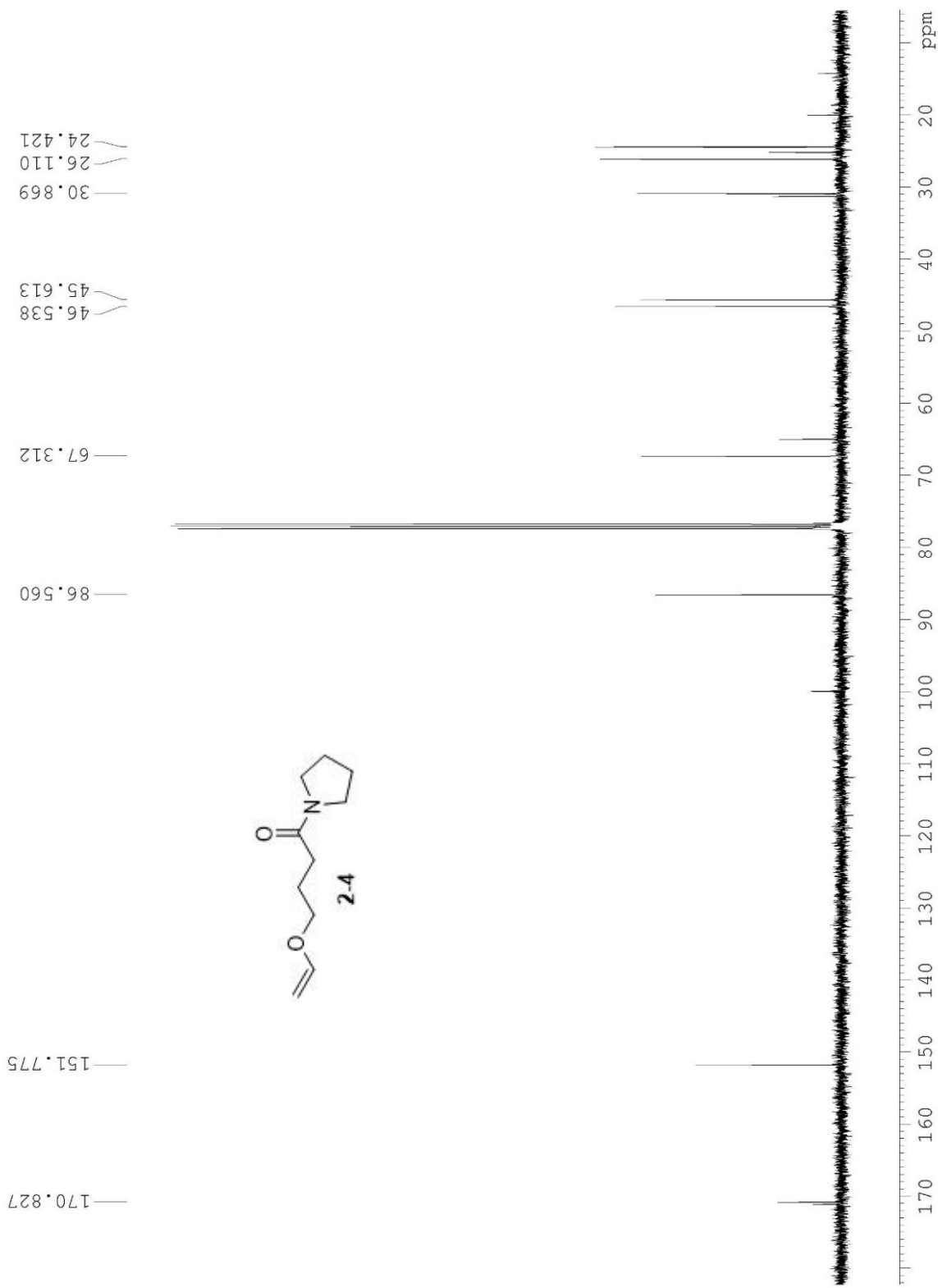
2.8 ^1H and ^{13}C NMR Data

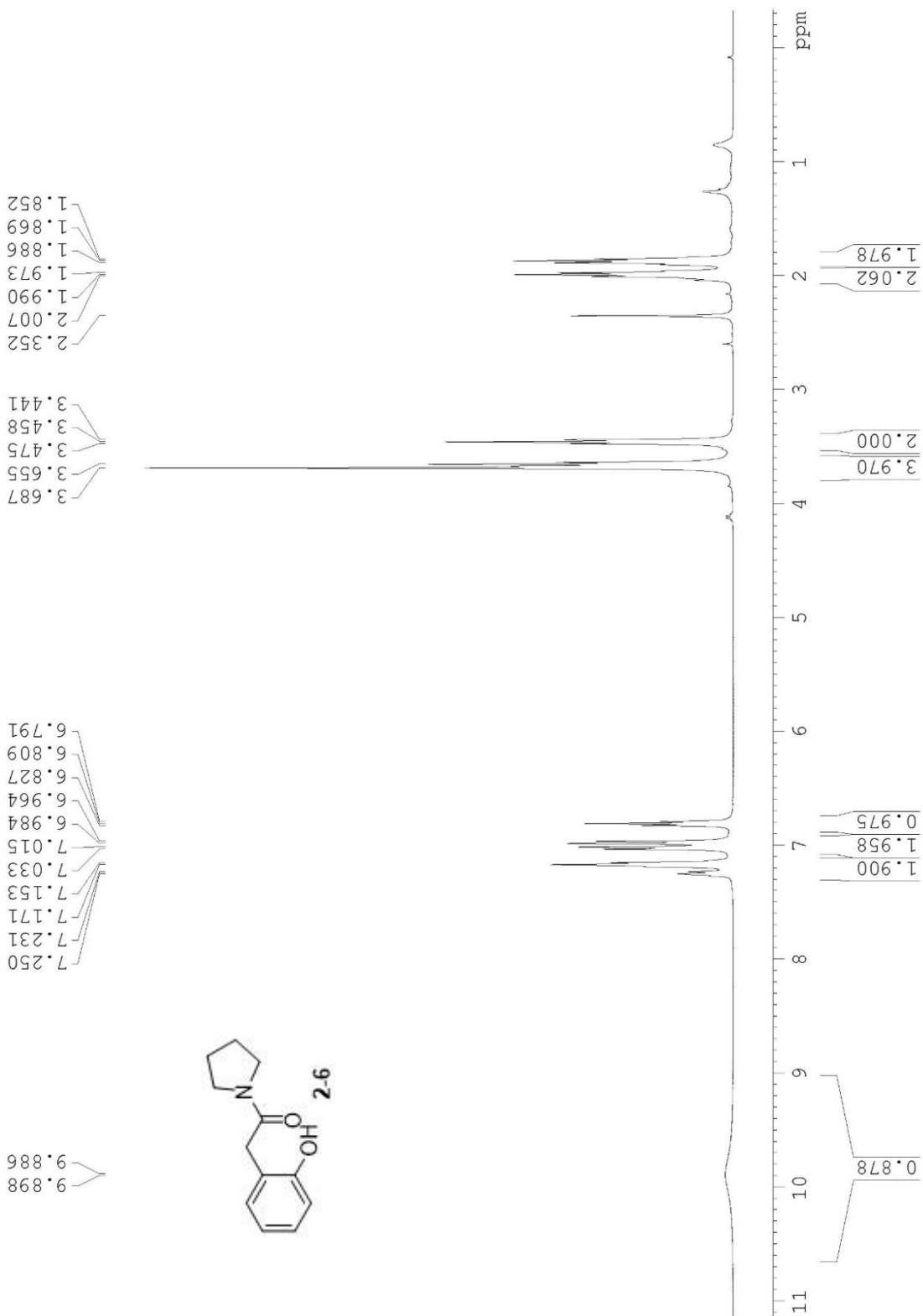


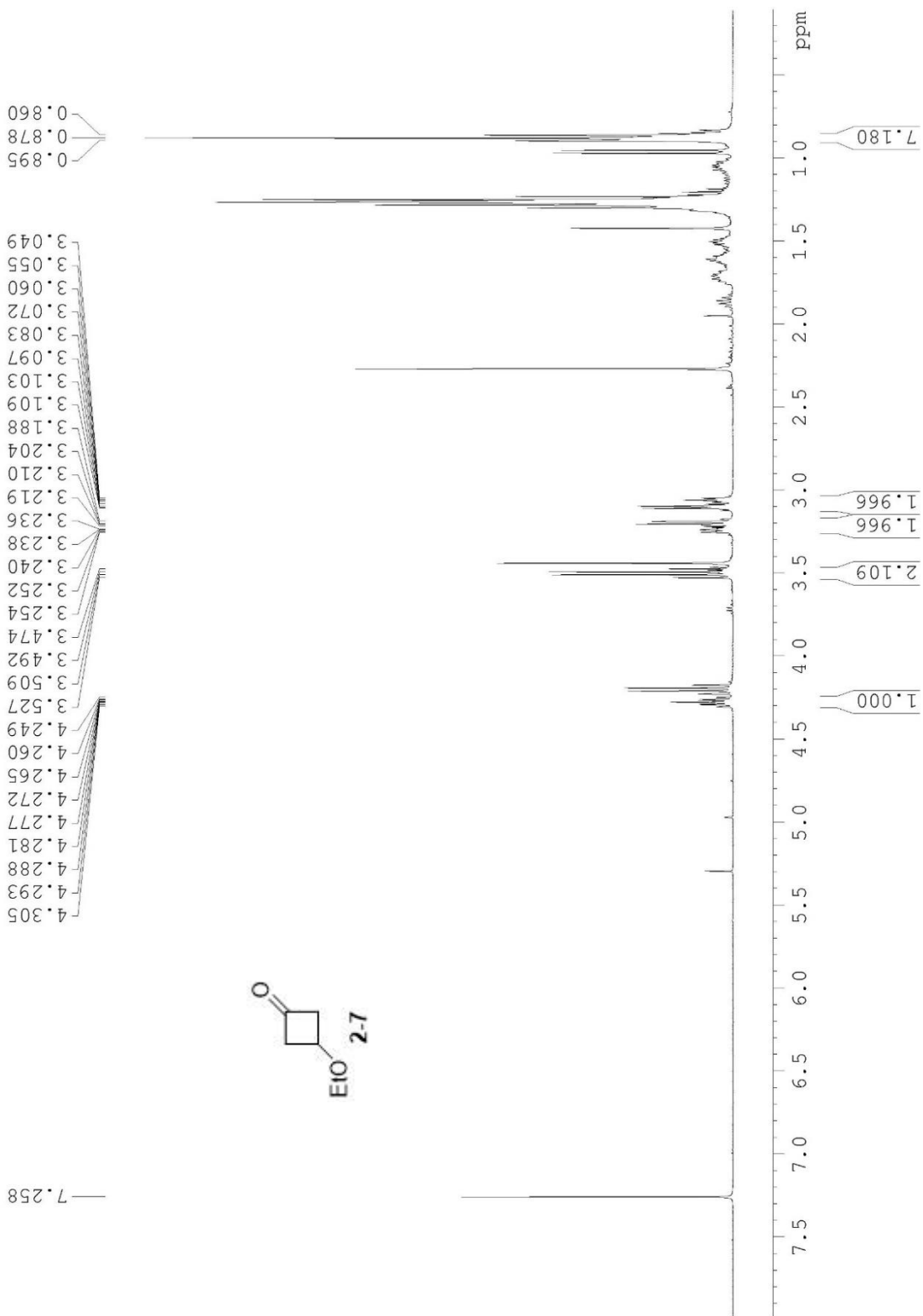


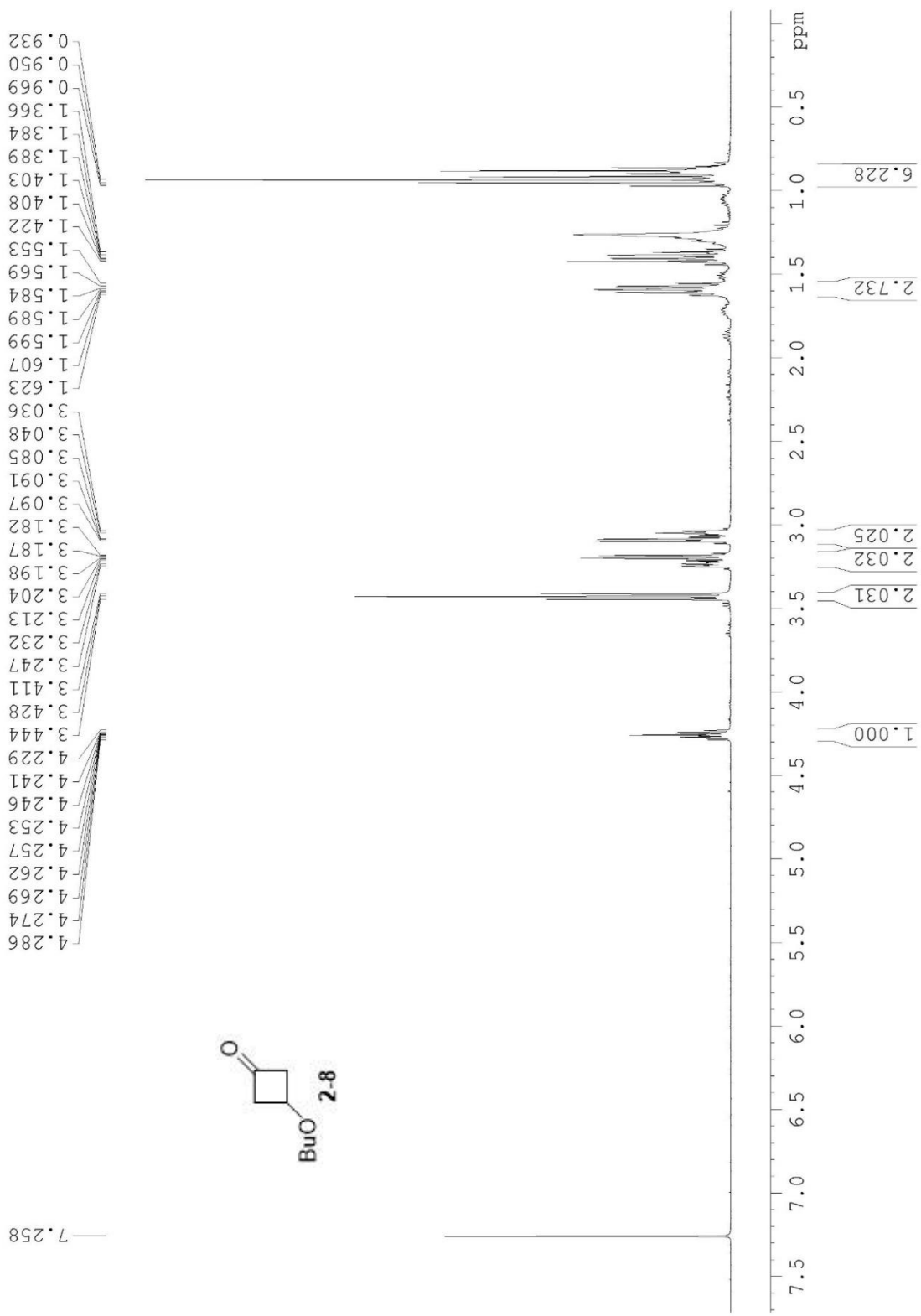


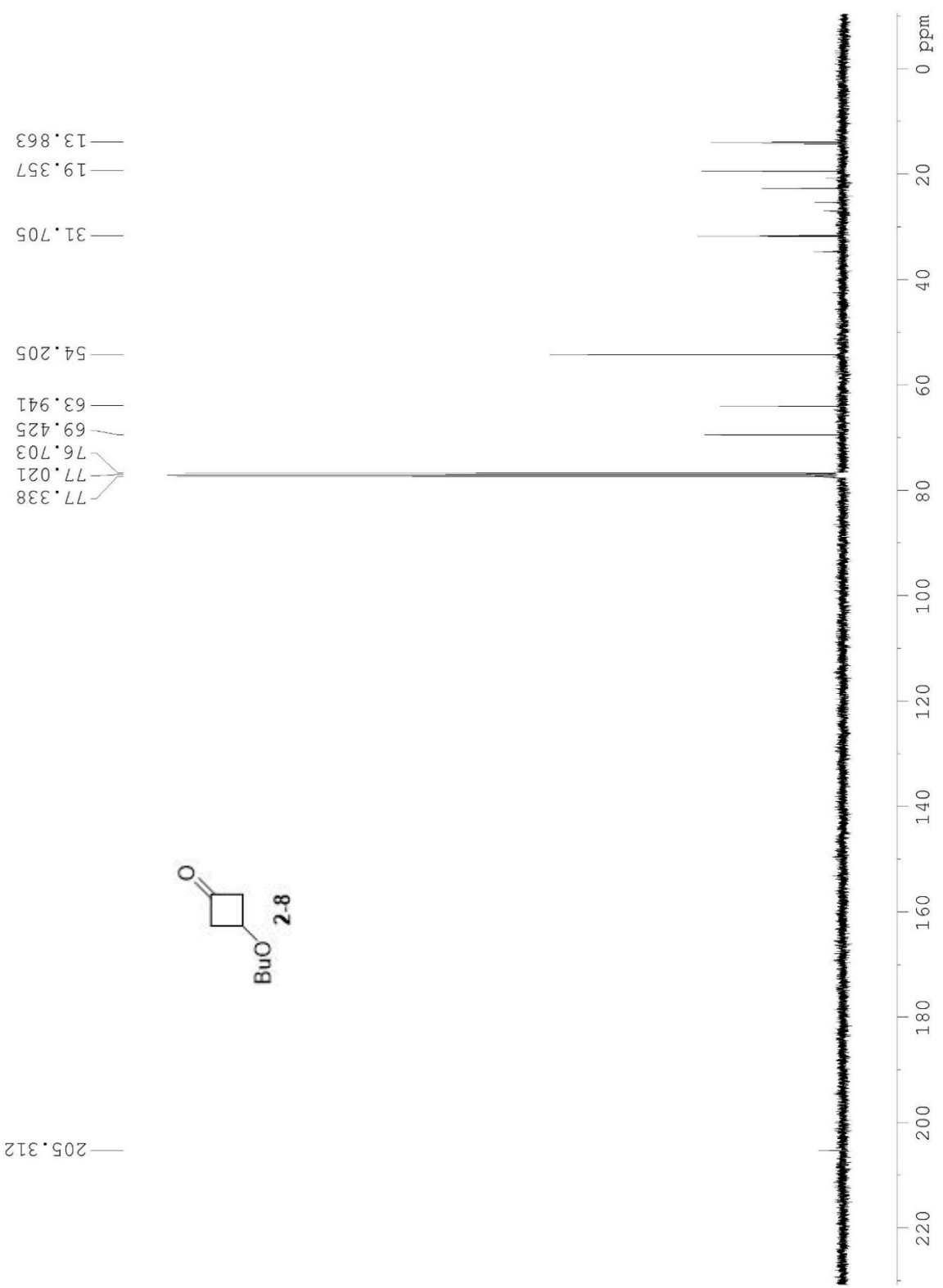


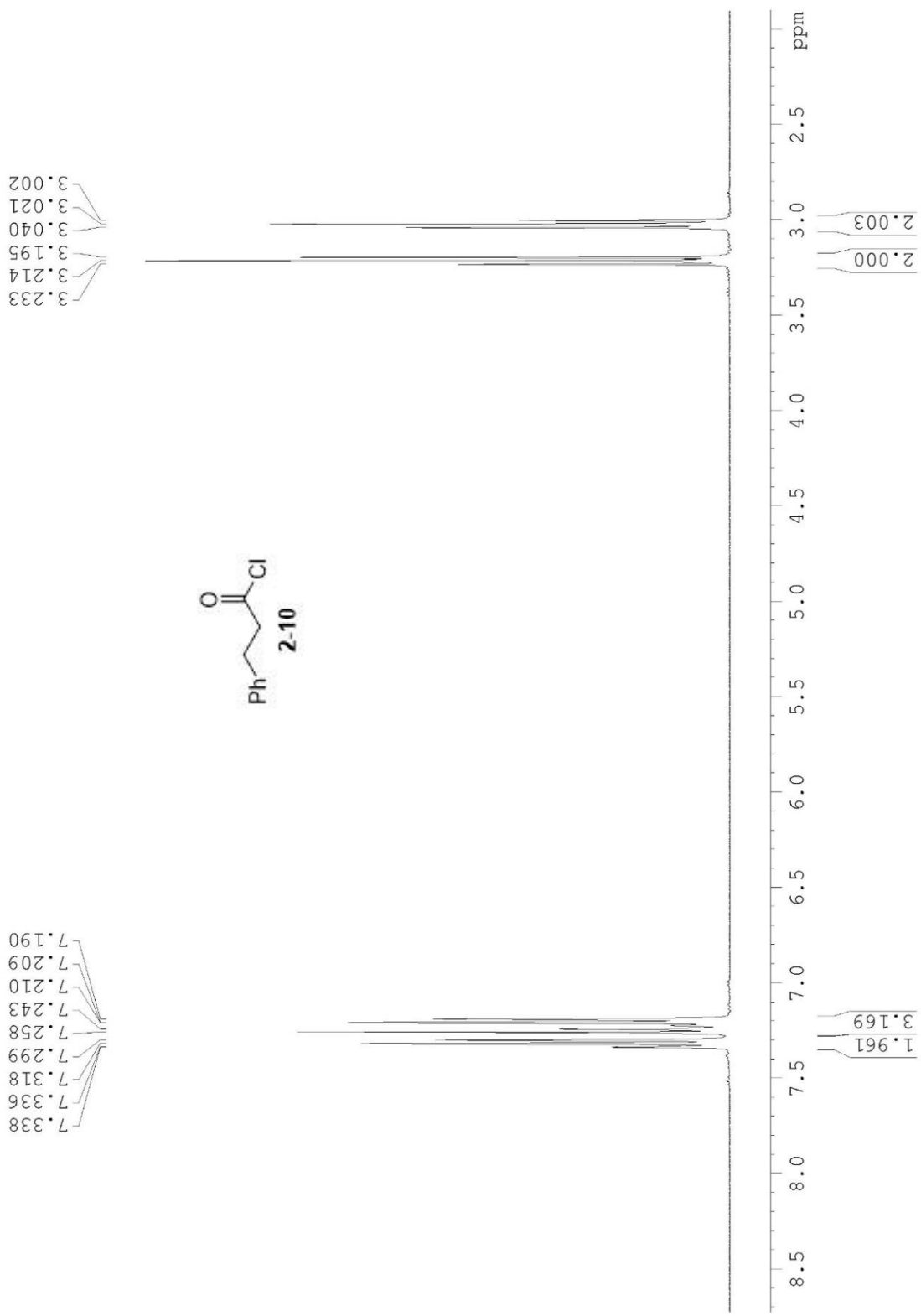


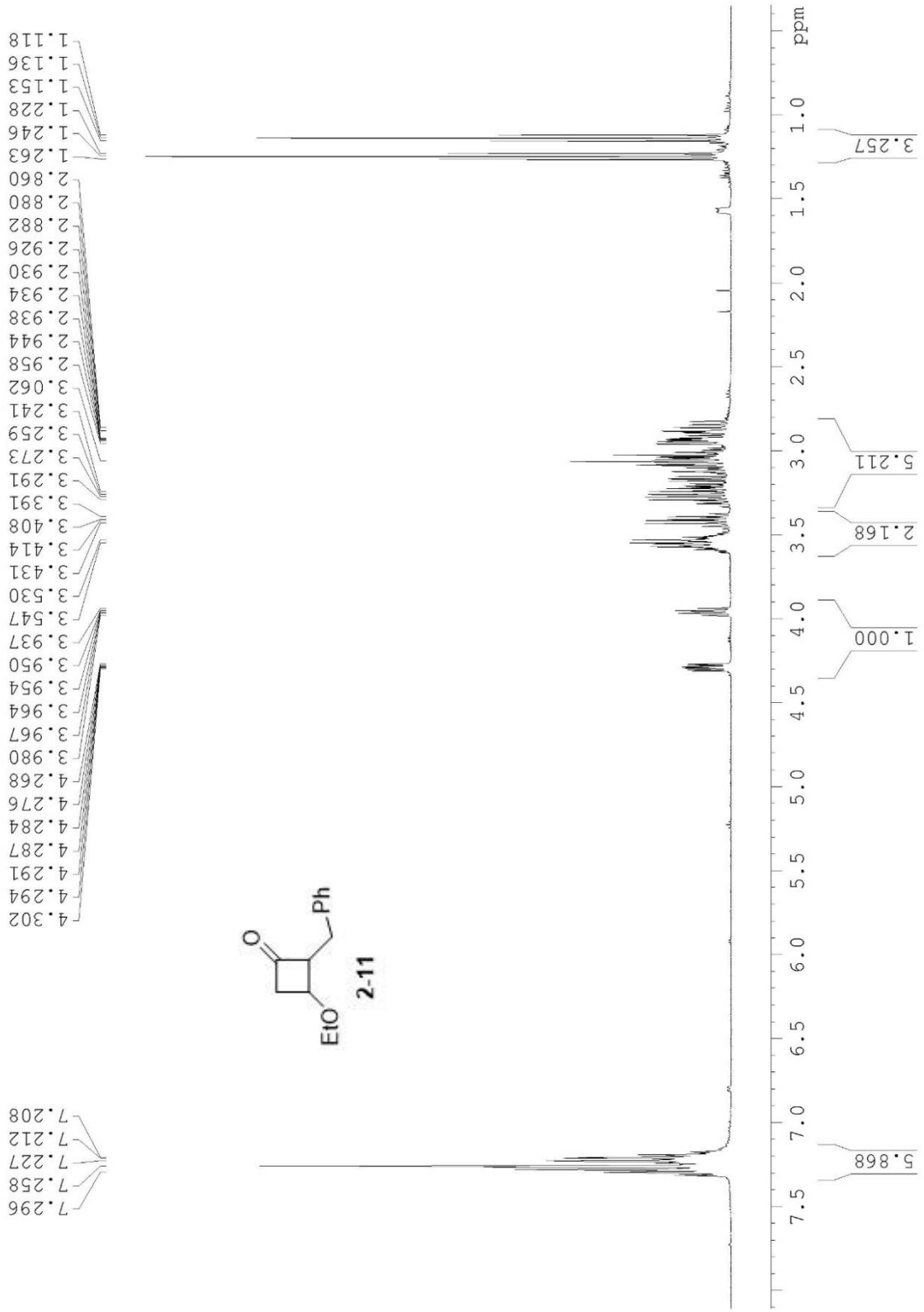


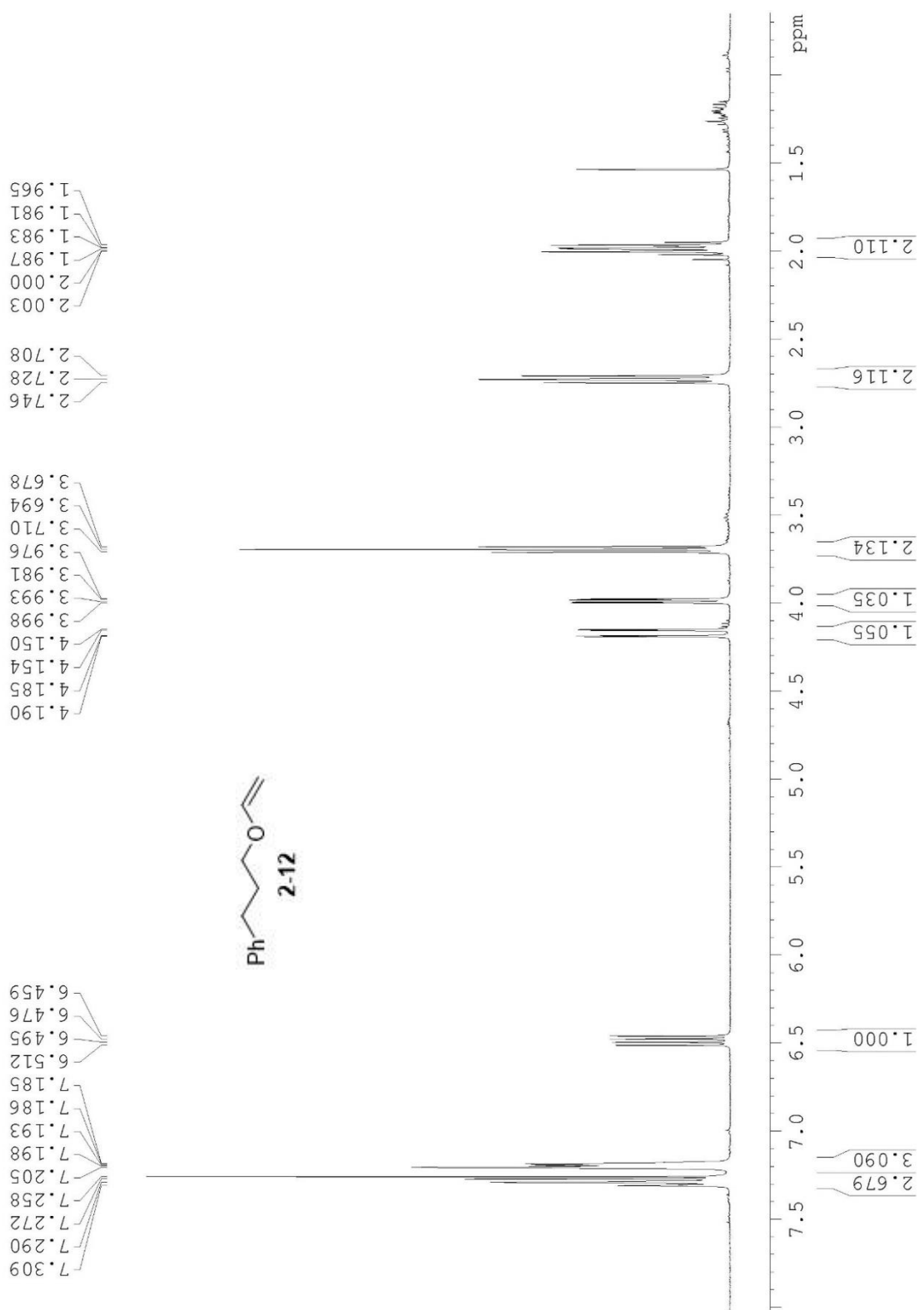


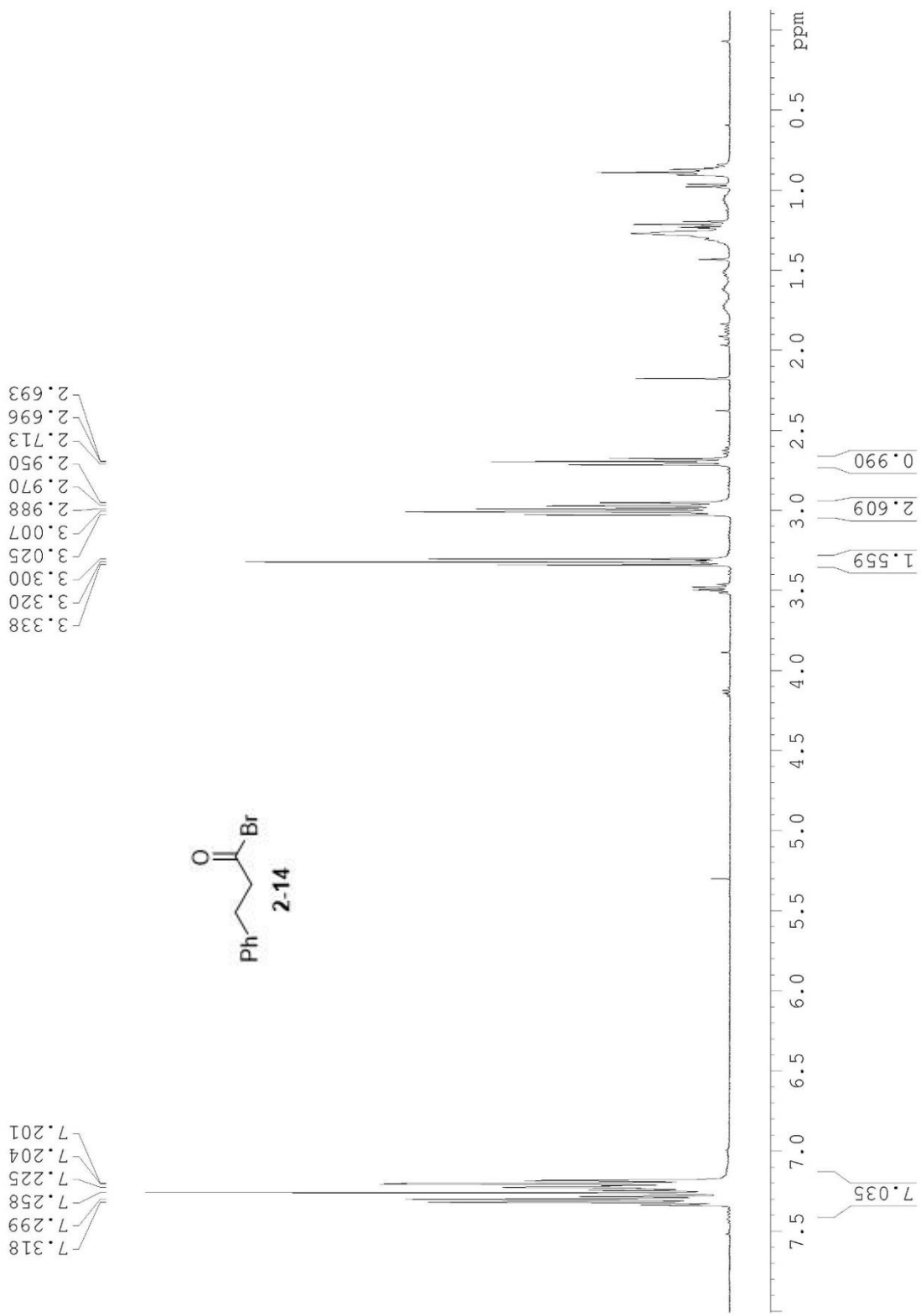


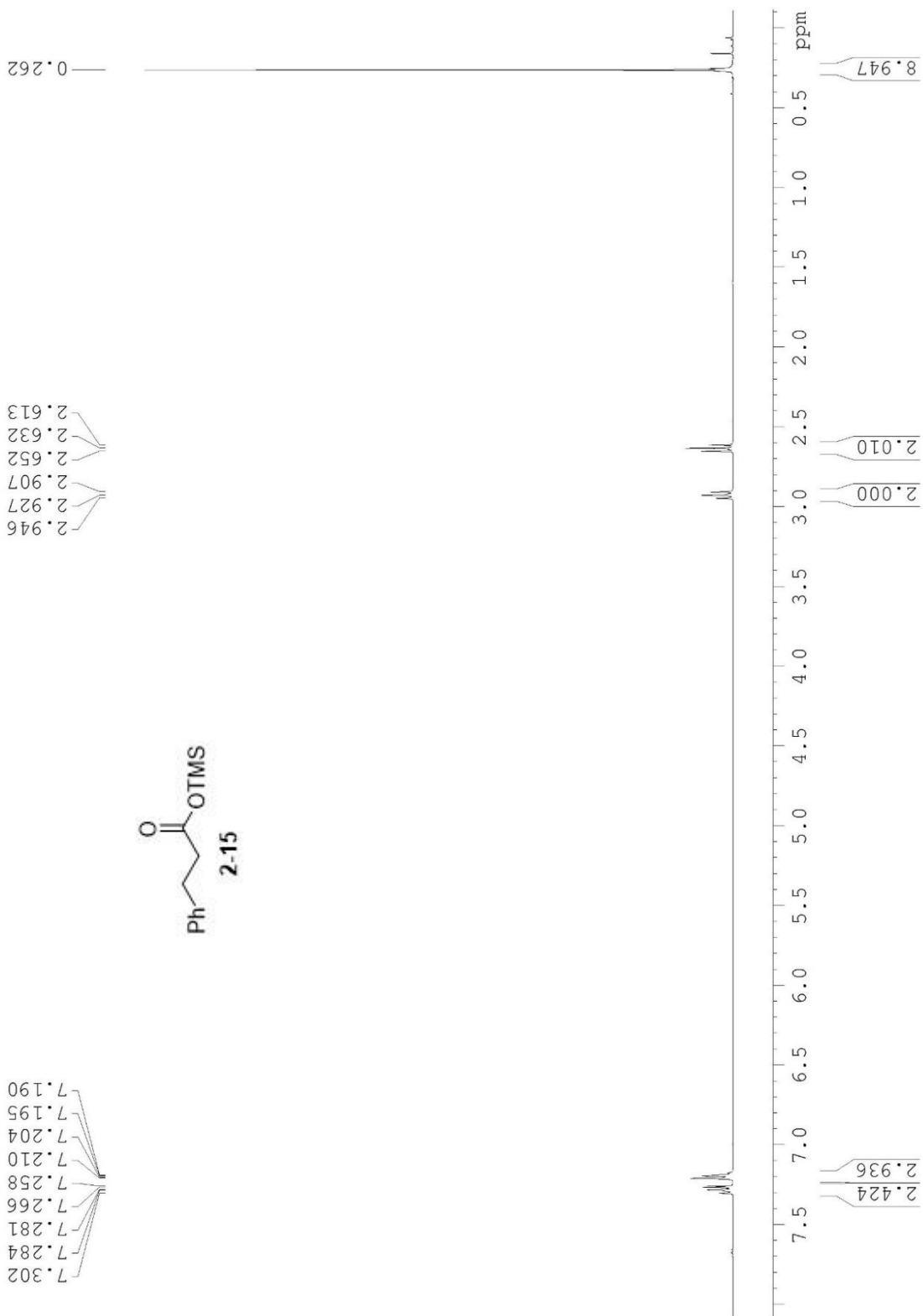


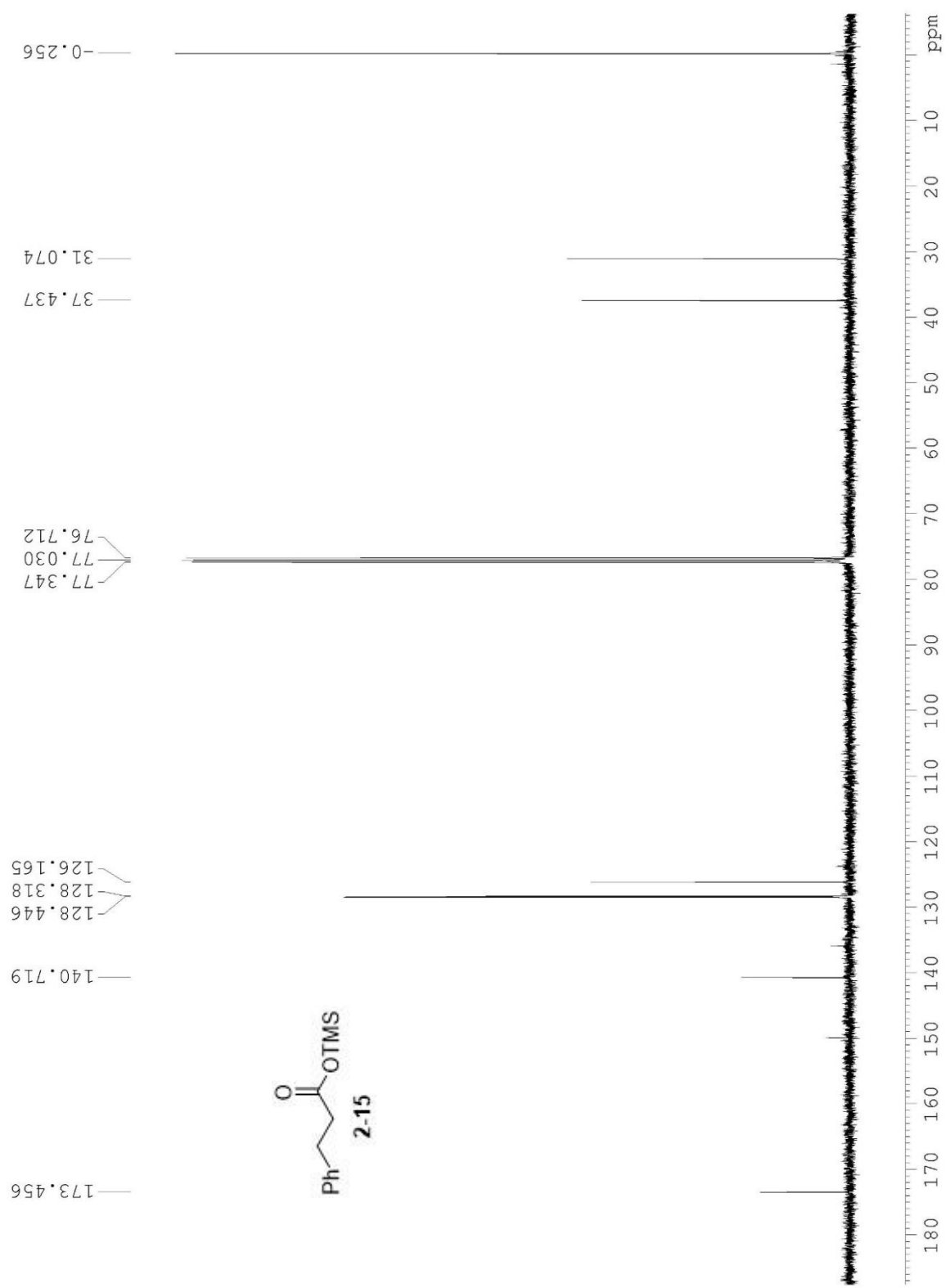


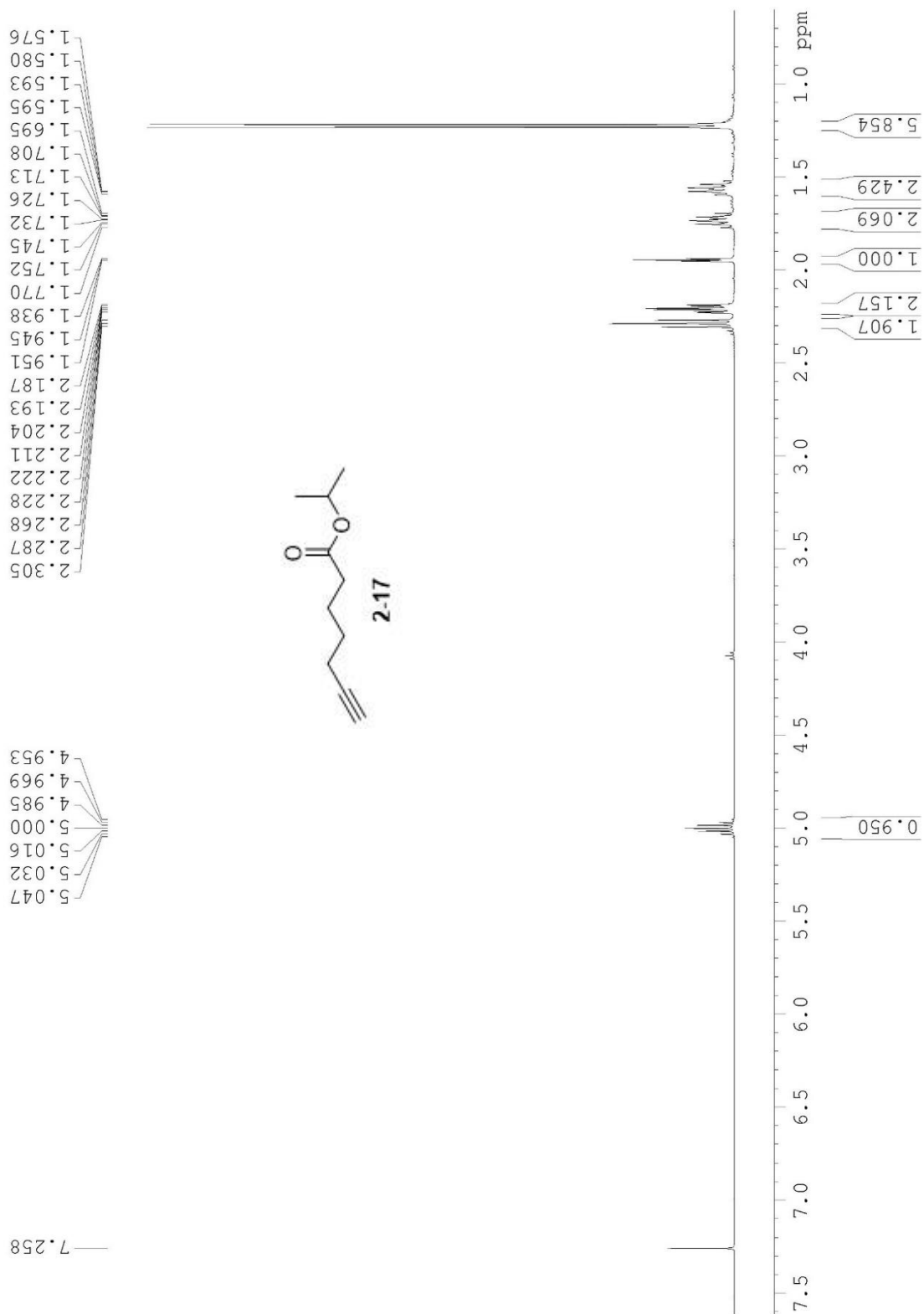


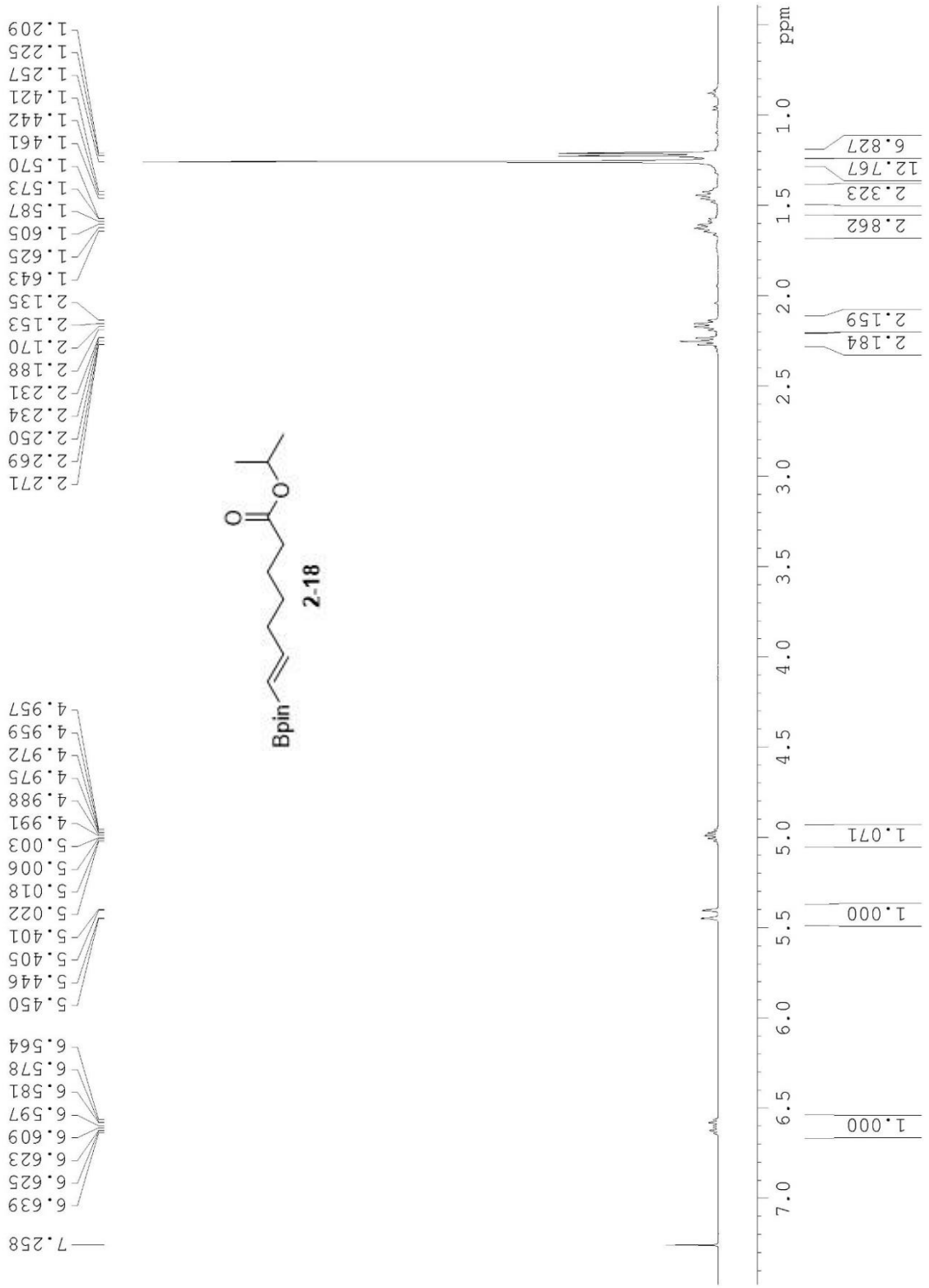


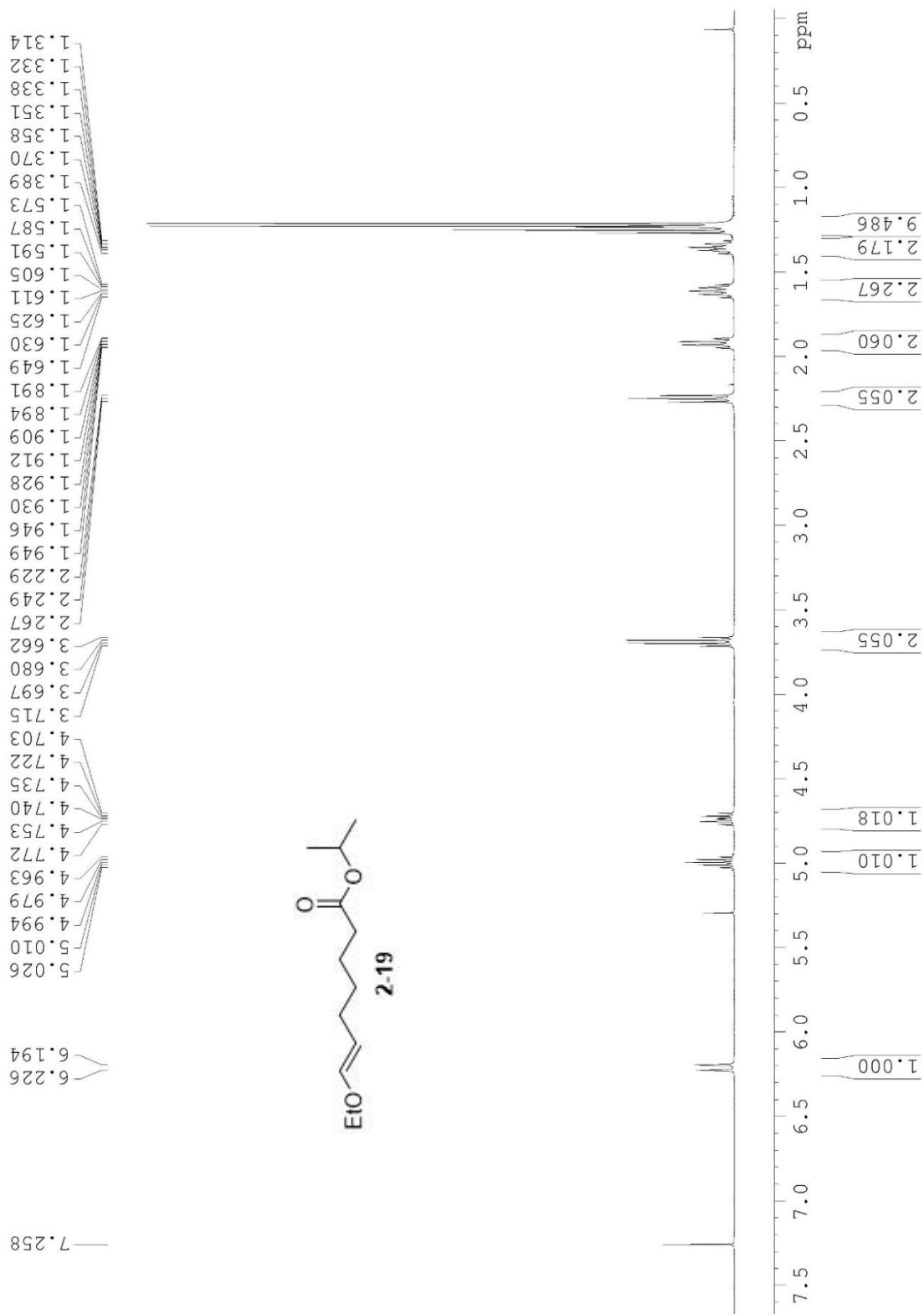


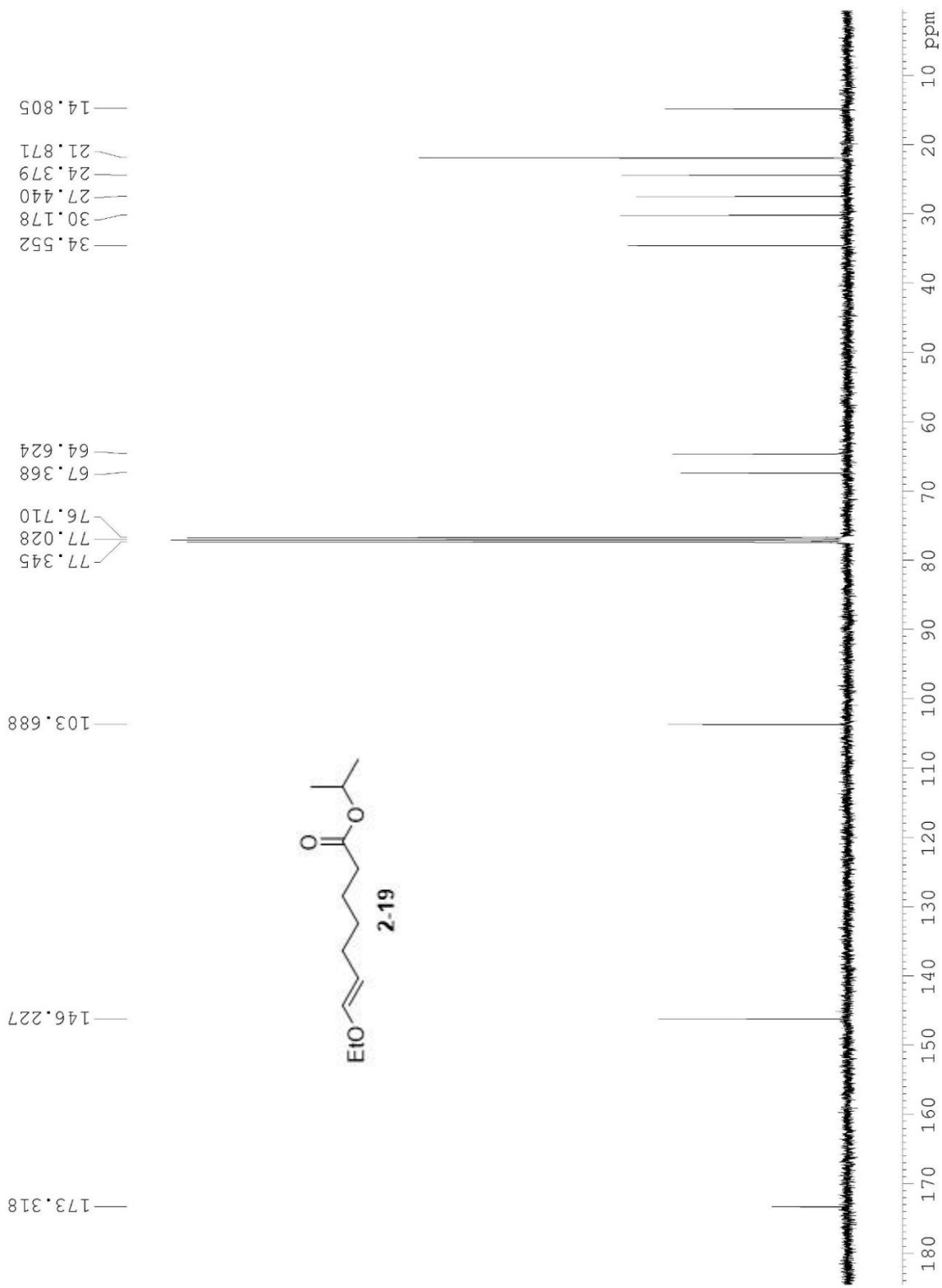


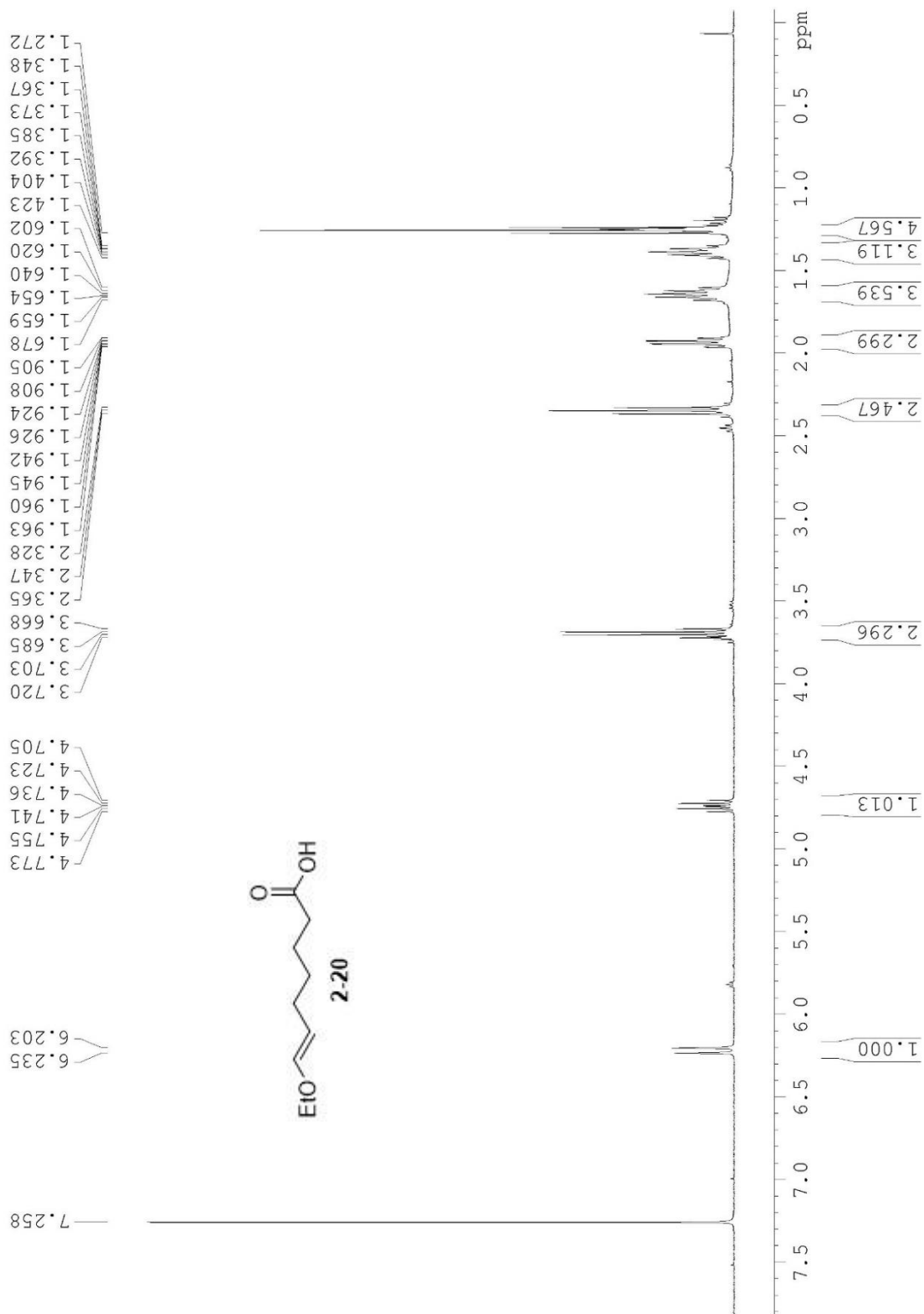


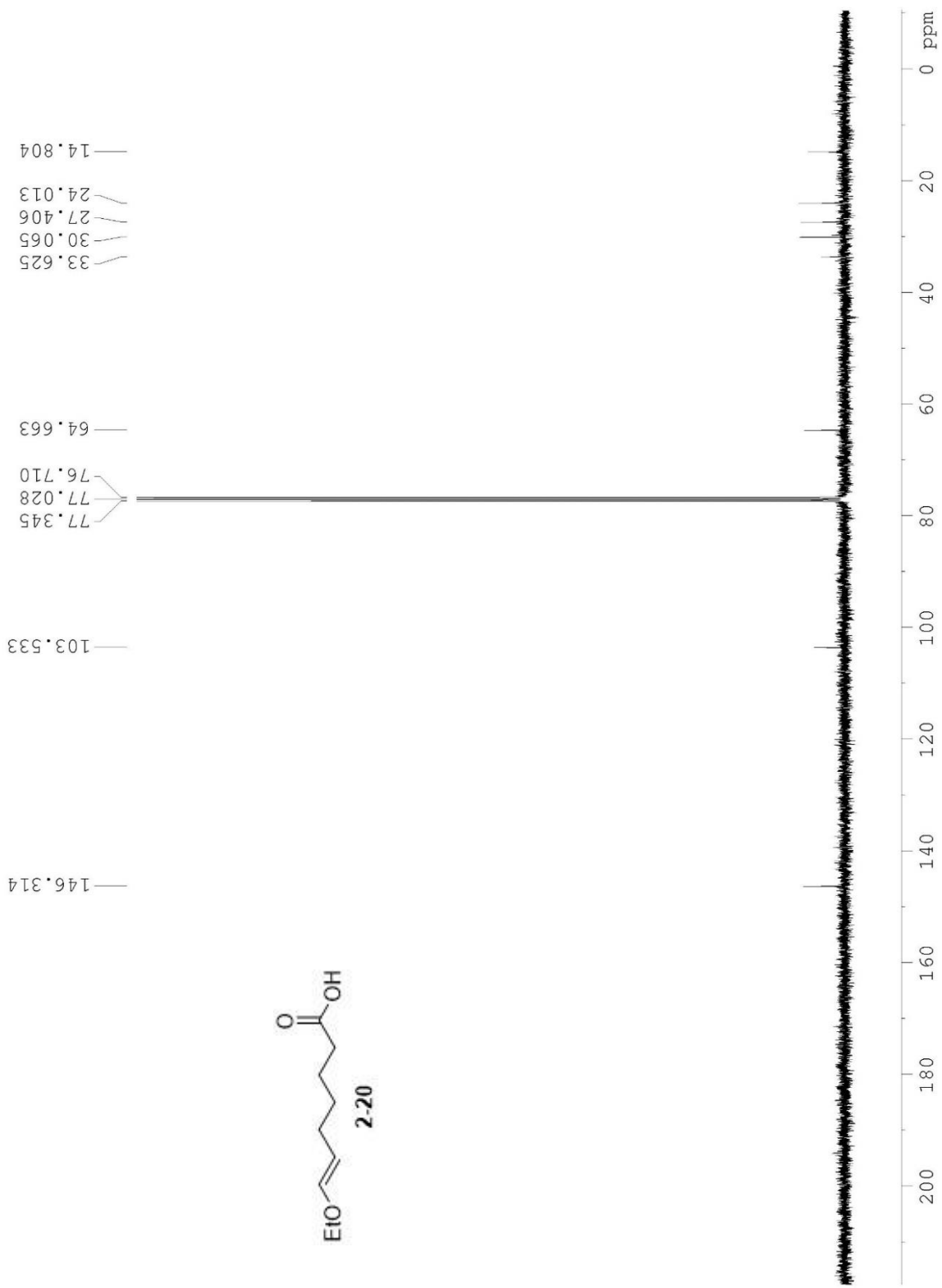


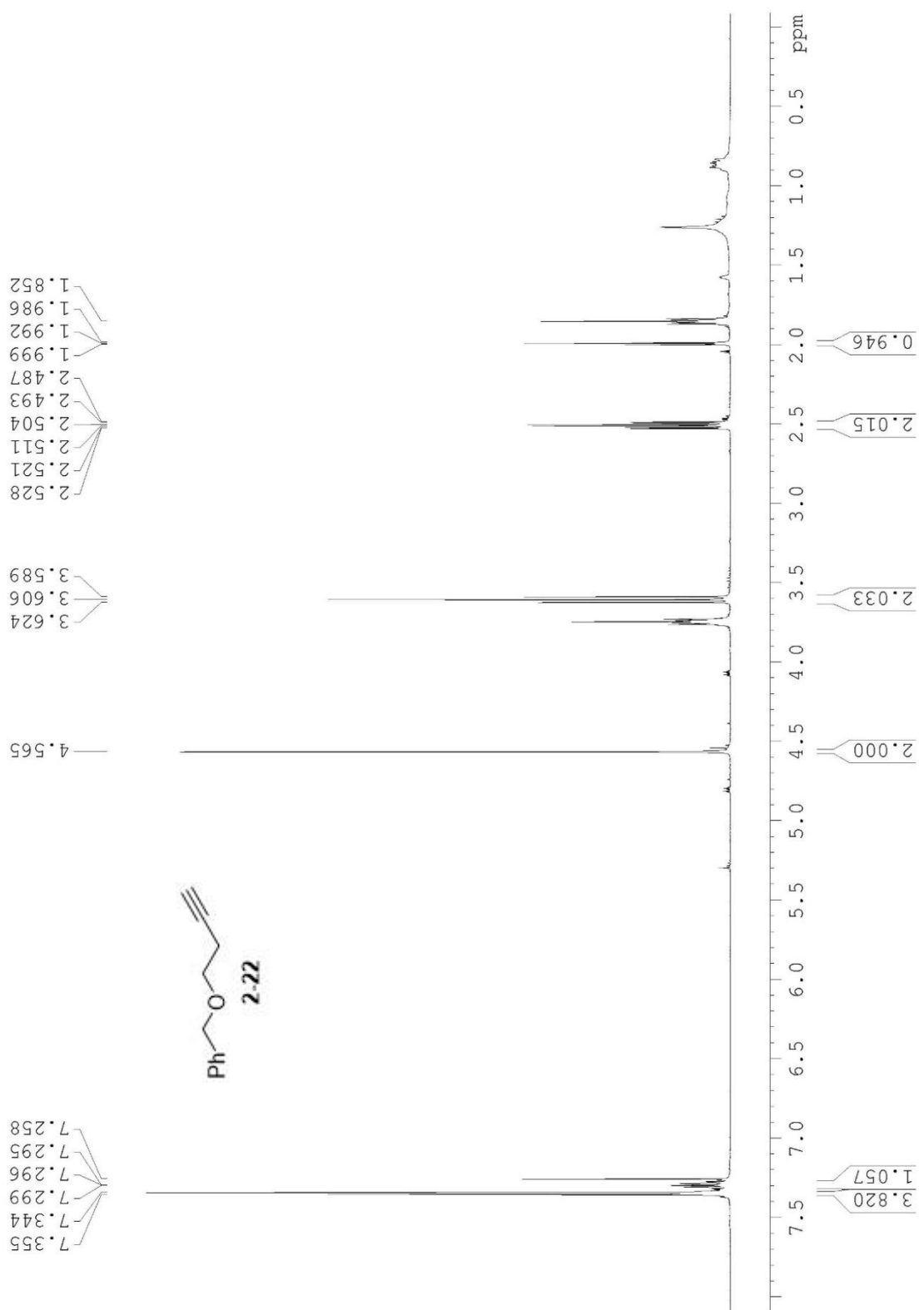


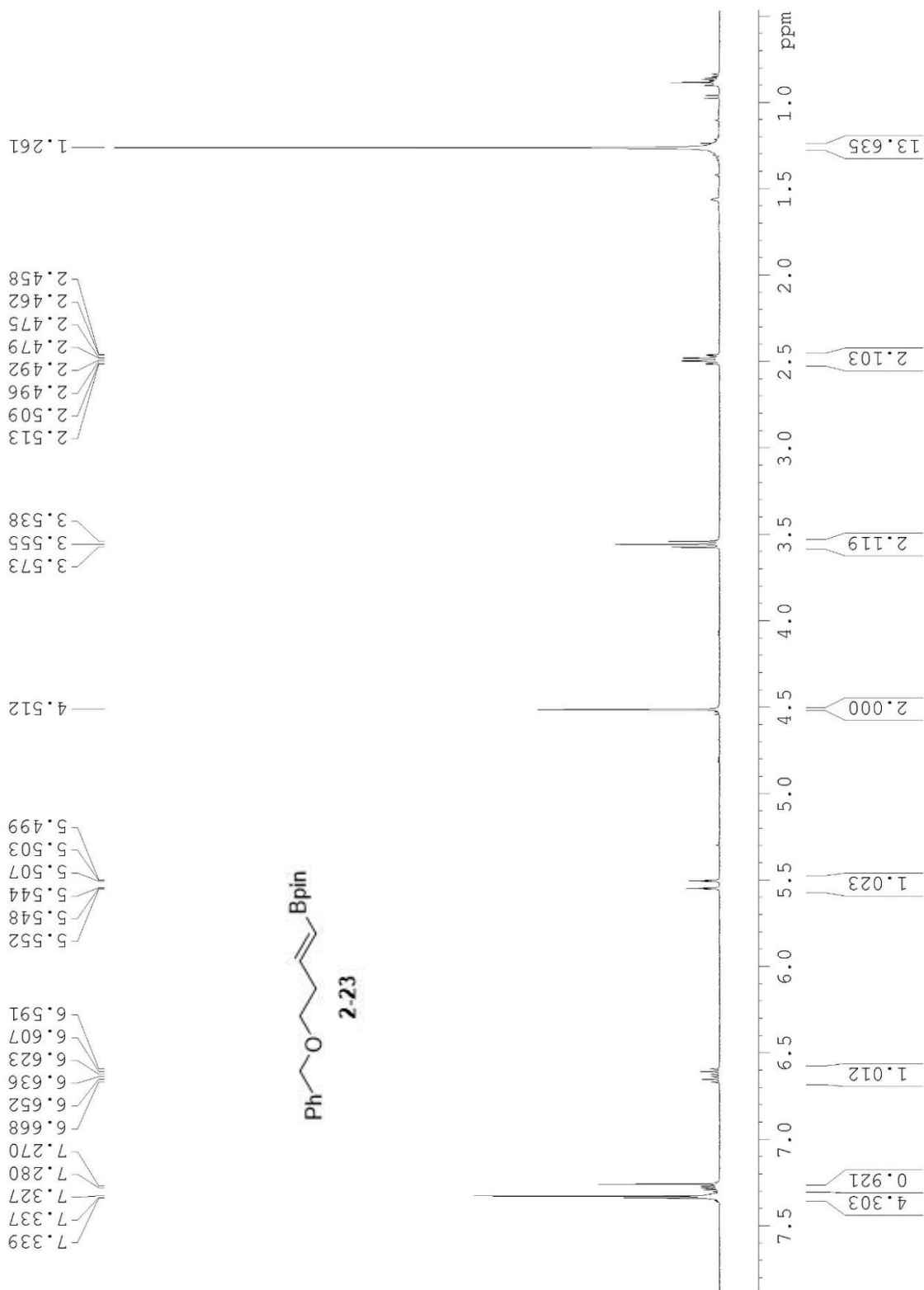


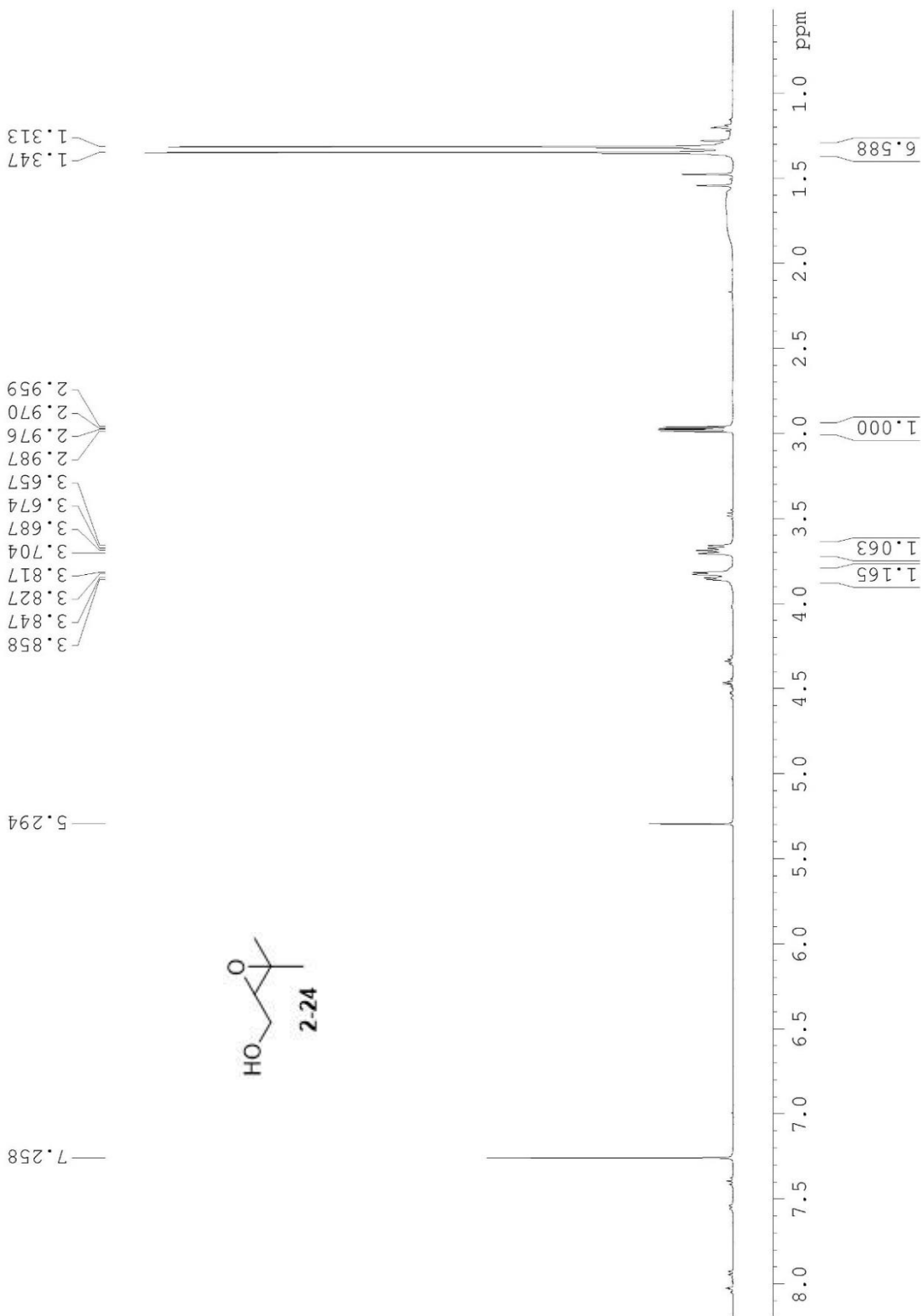












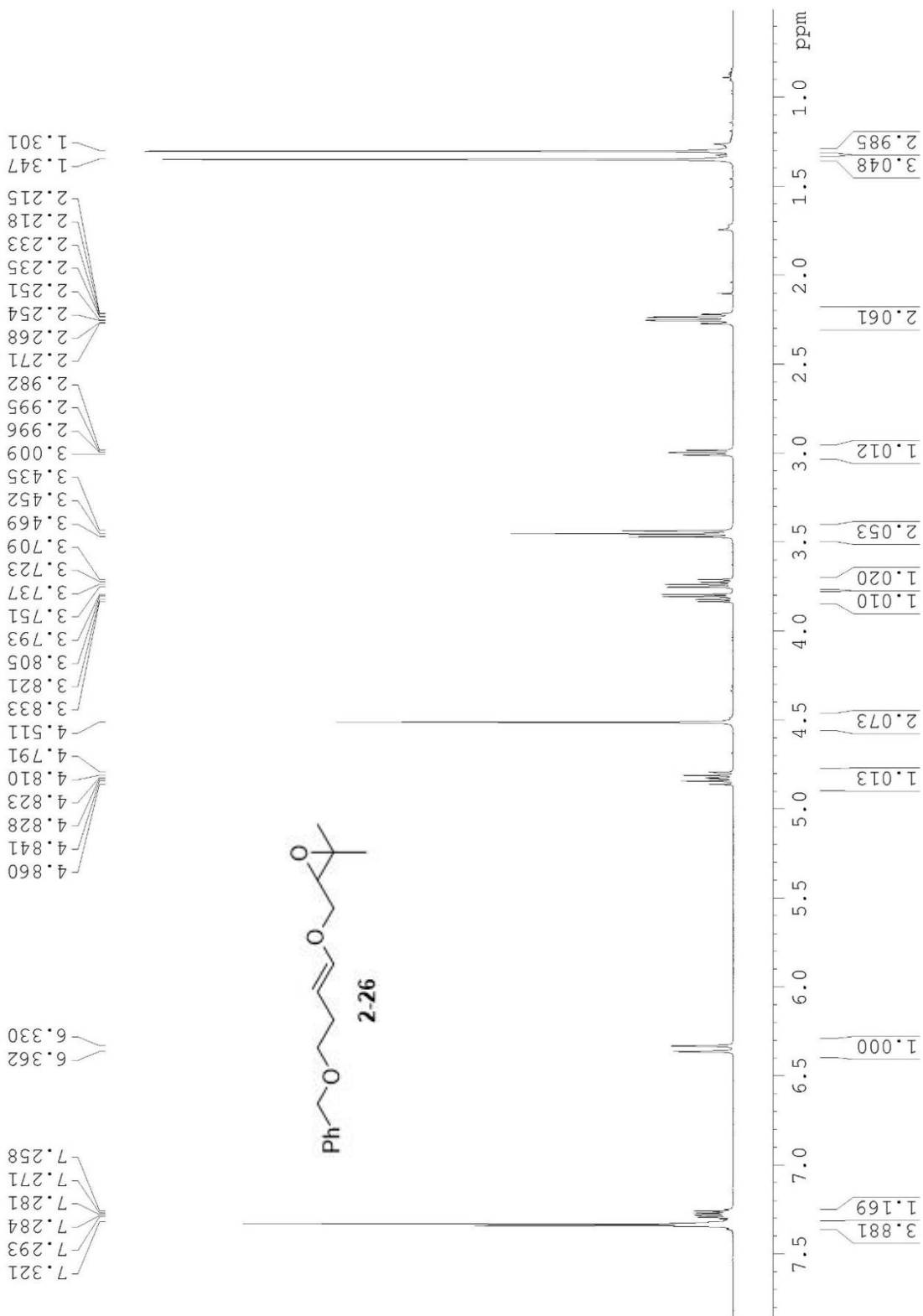


Table 2.4 Entry 1

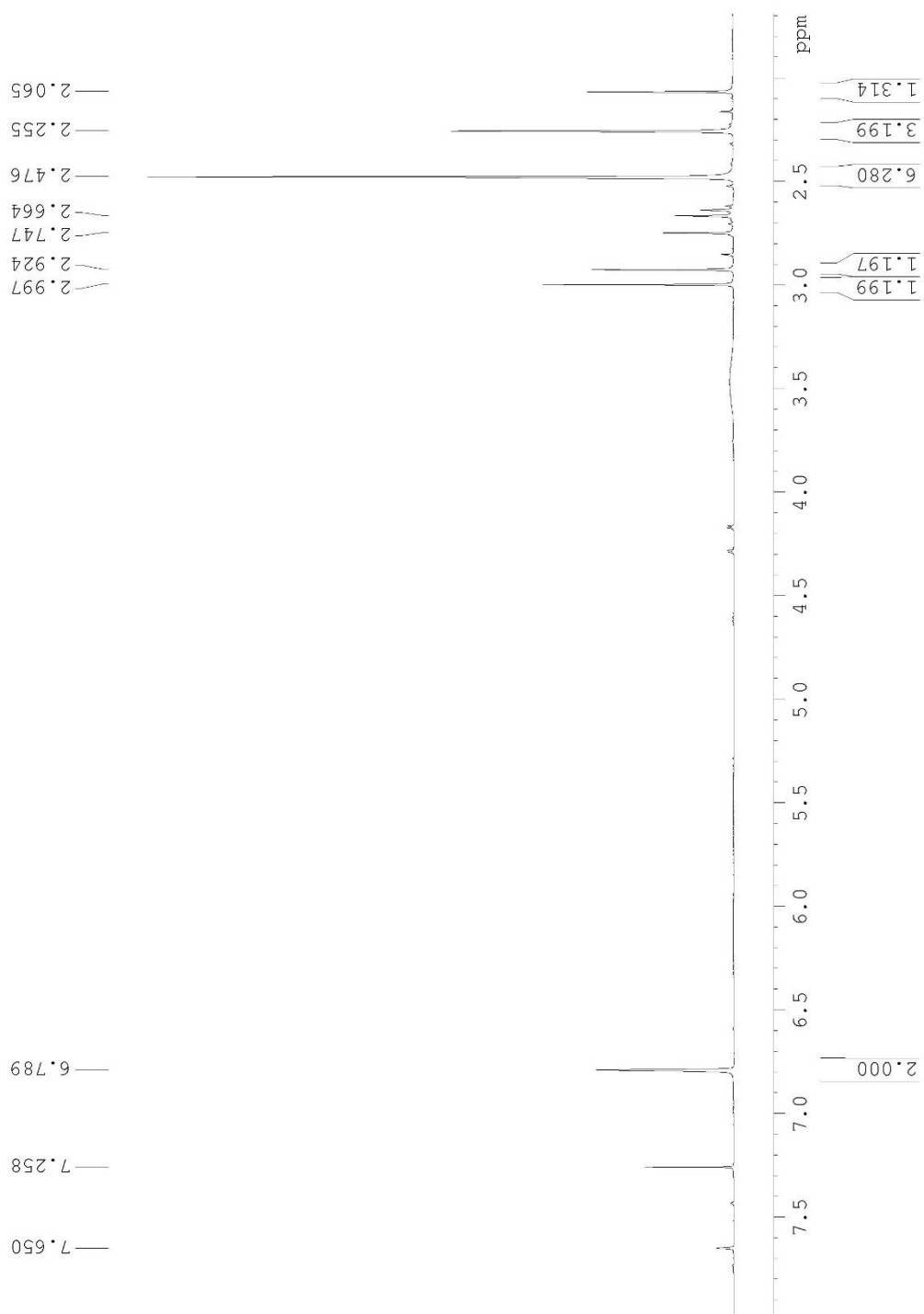


Table 2.4 Entry 2

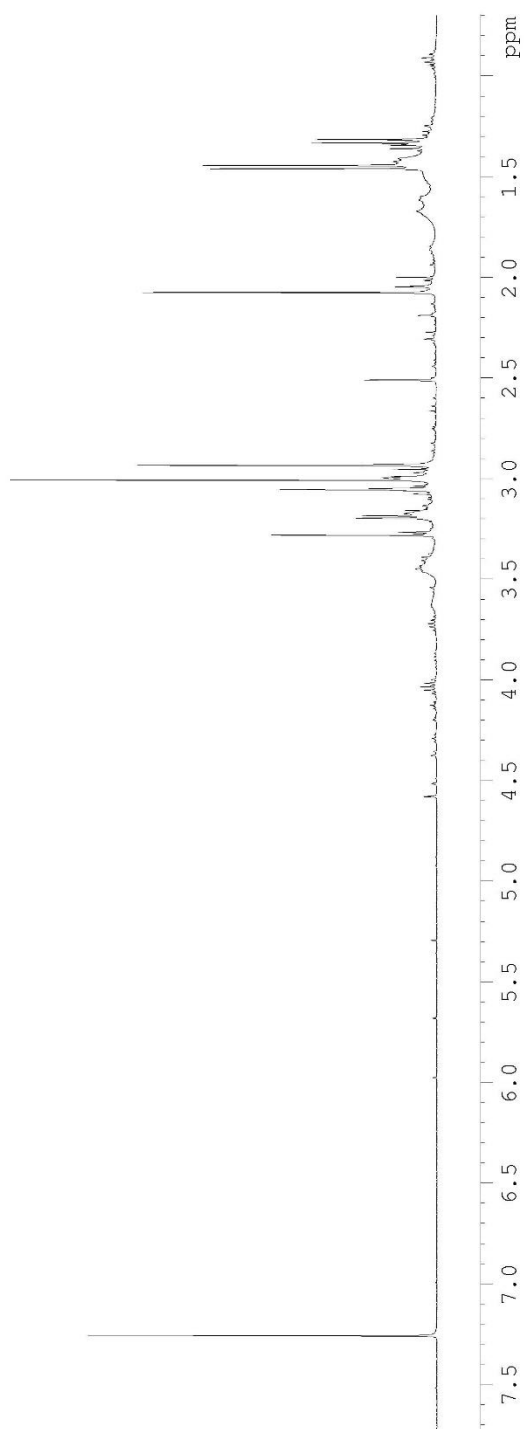


Table 2.4 Entry 3

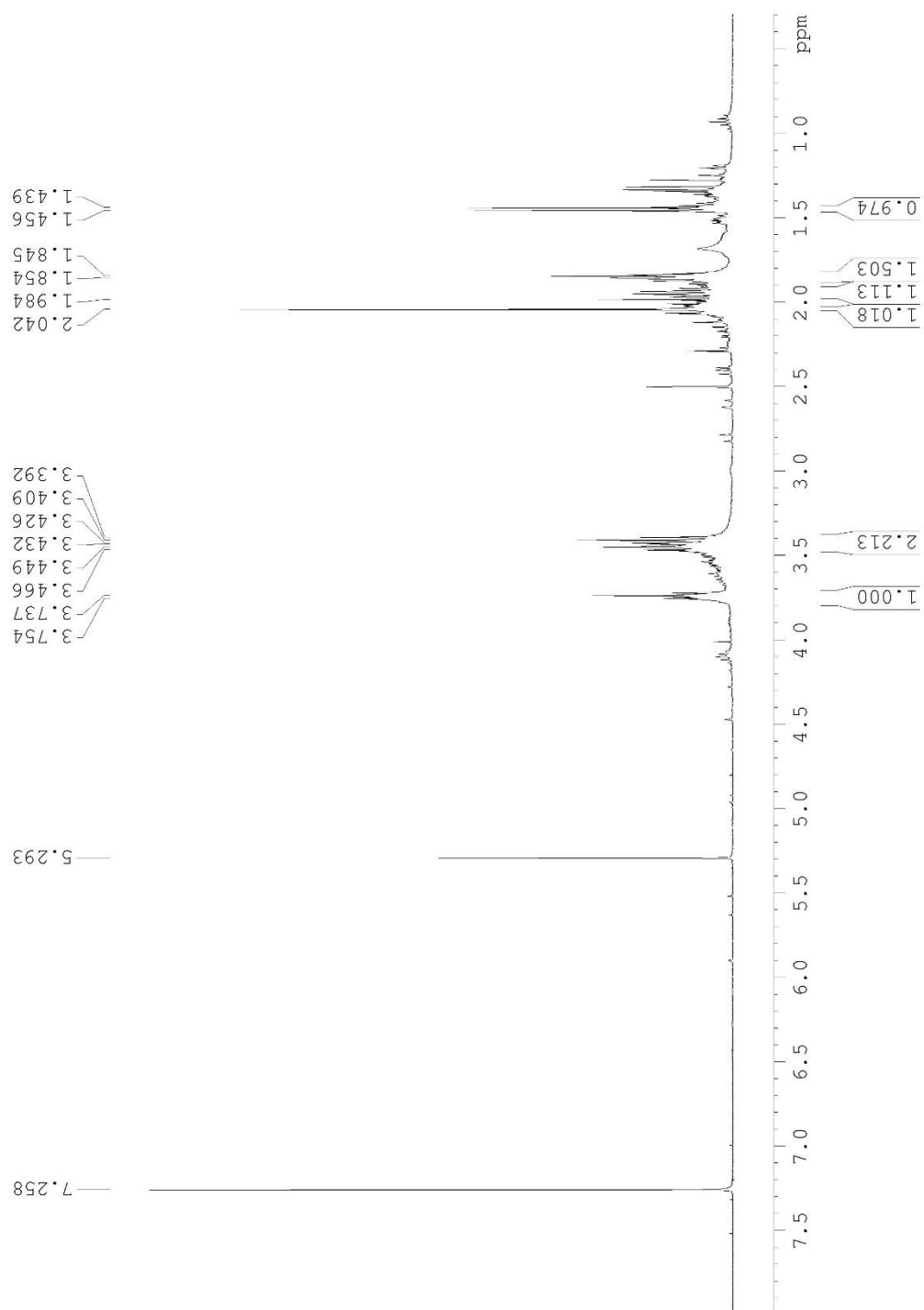


Table 2.4 Entry 4

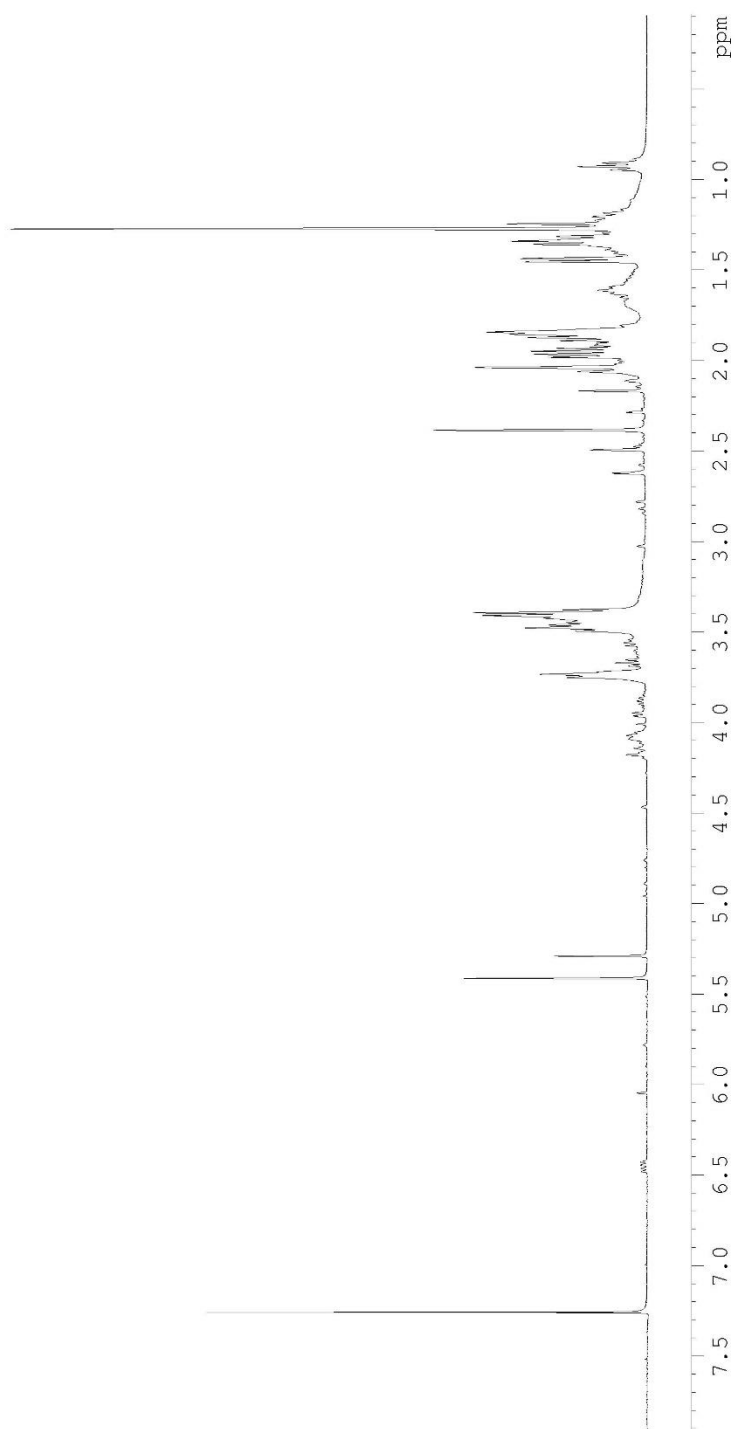


Table 2.4 Entry 5

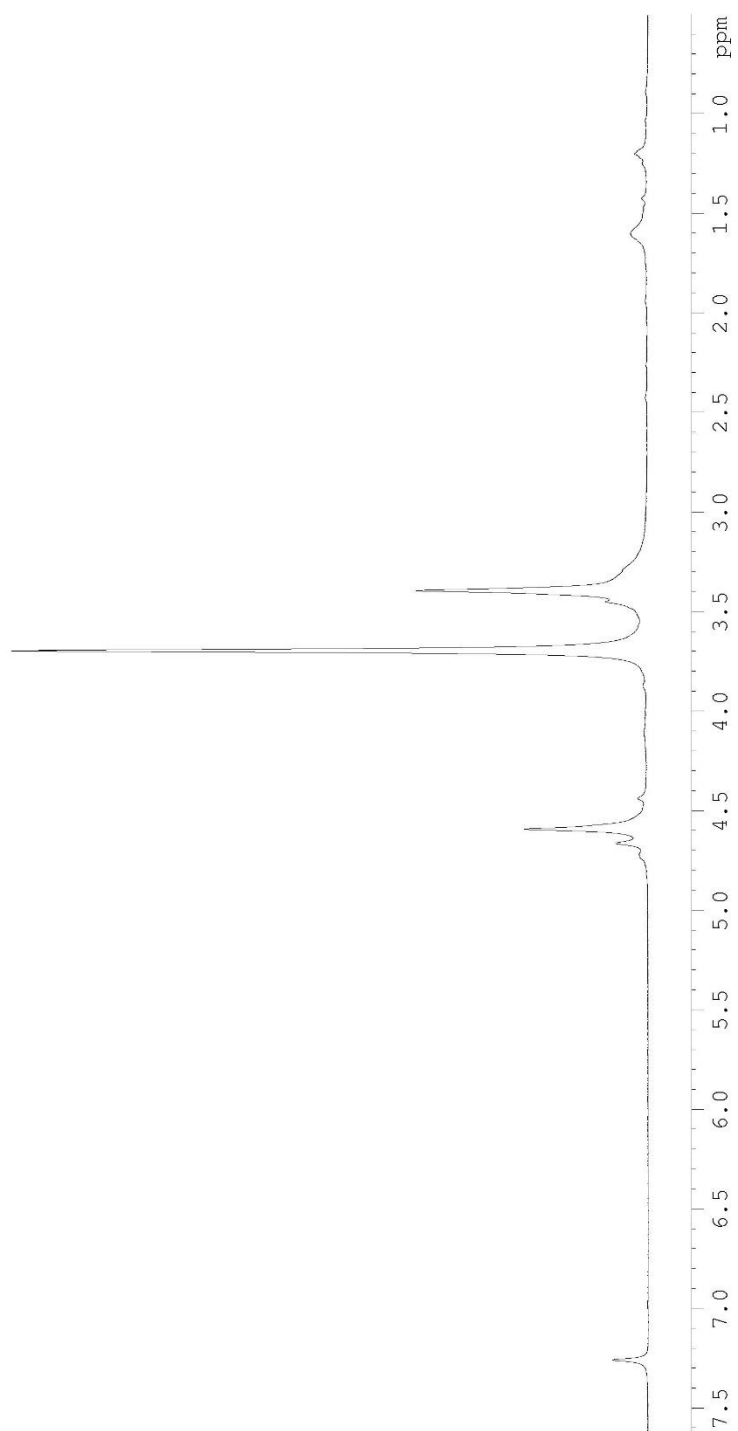
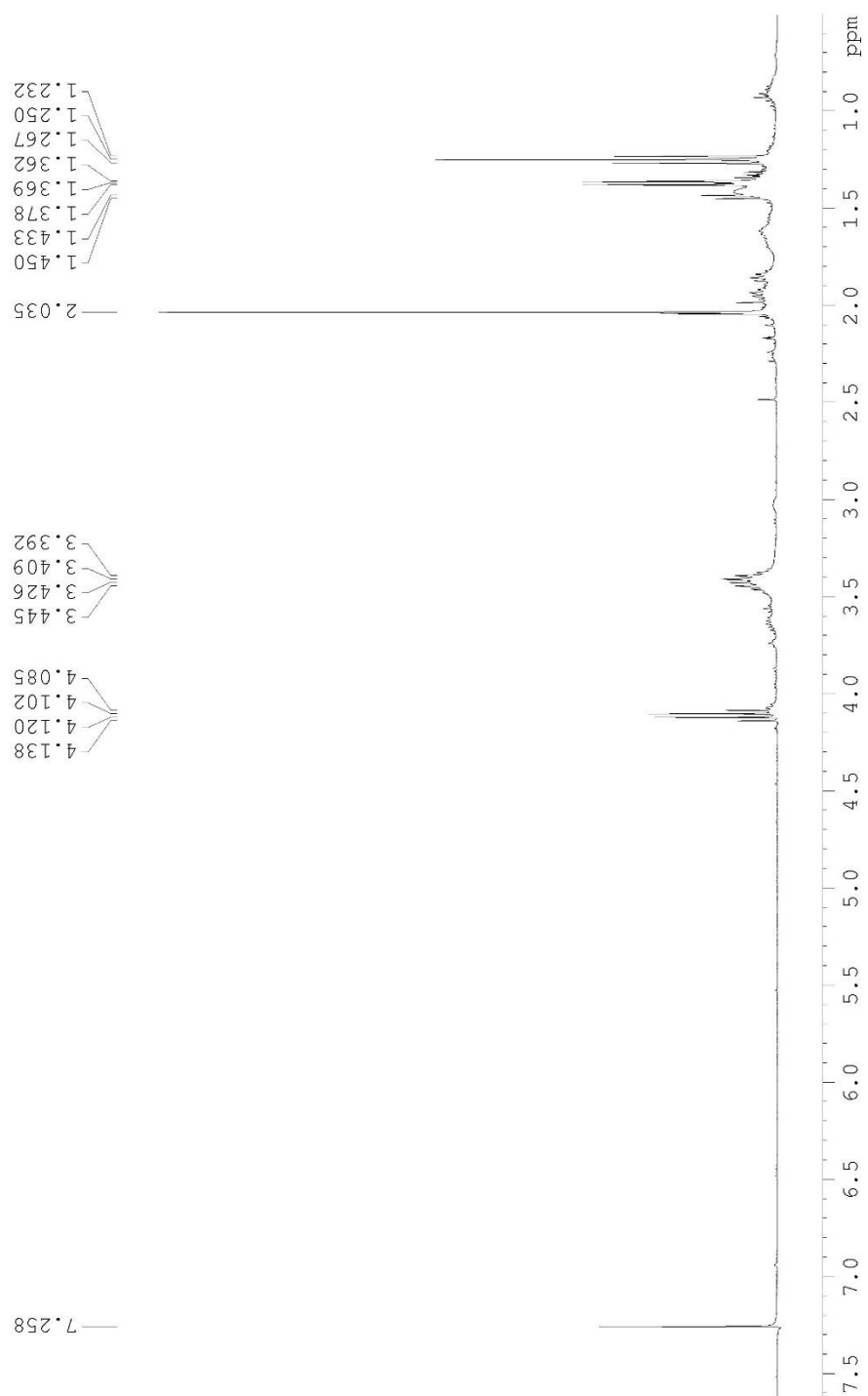


Table 2.4 Entry 6



Scheme 2.9

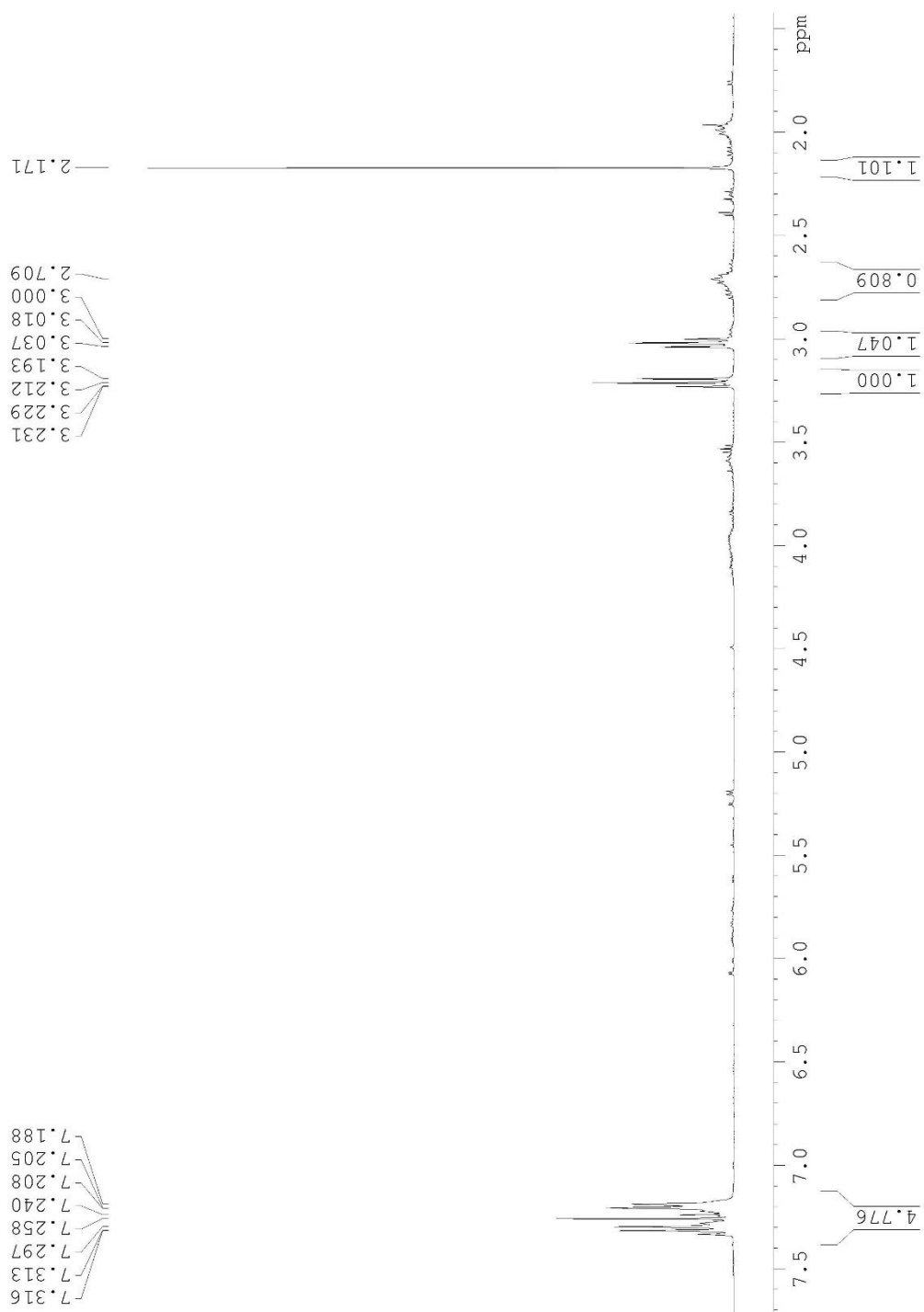


Table 2.5 Entry 1

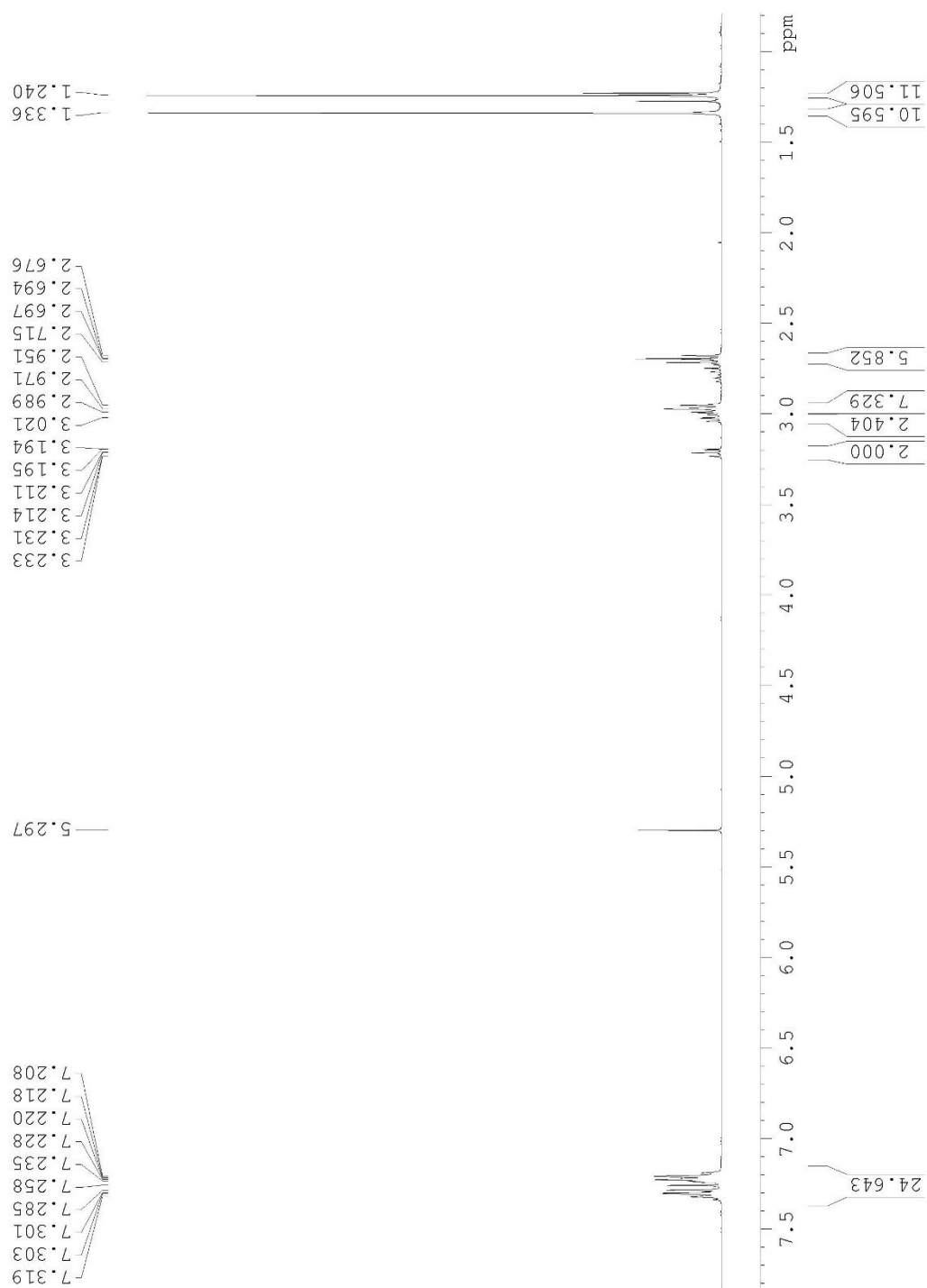


Table 2.5 Entry 2



Table 2.5 Entry 3

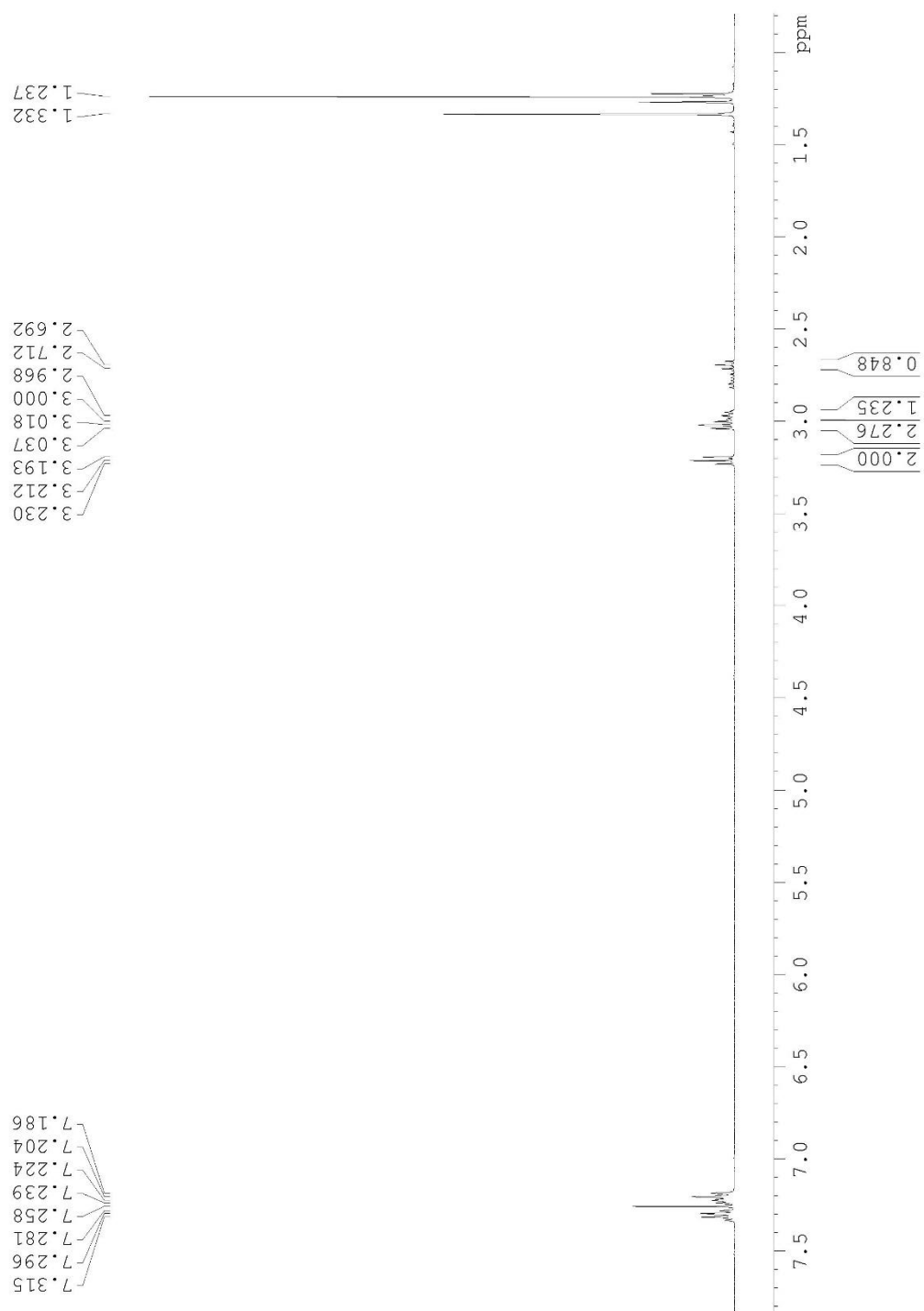


Table 2.5 Entry 4

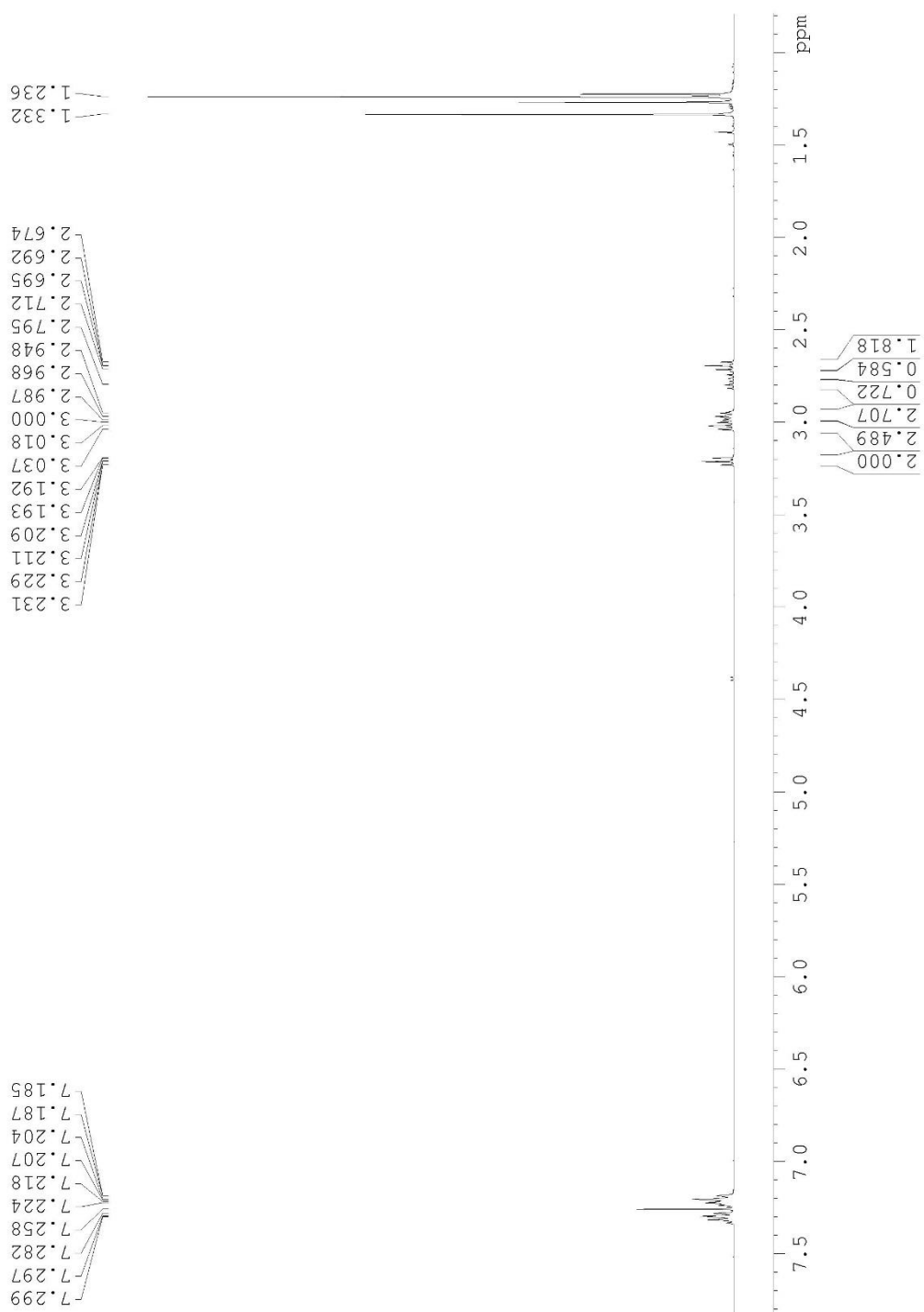


Table 2.5 Entry 5

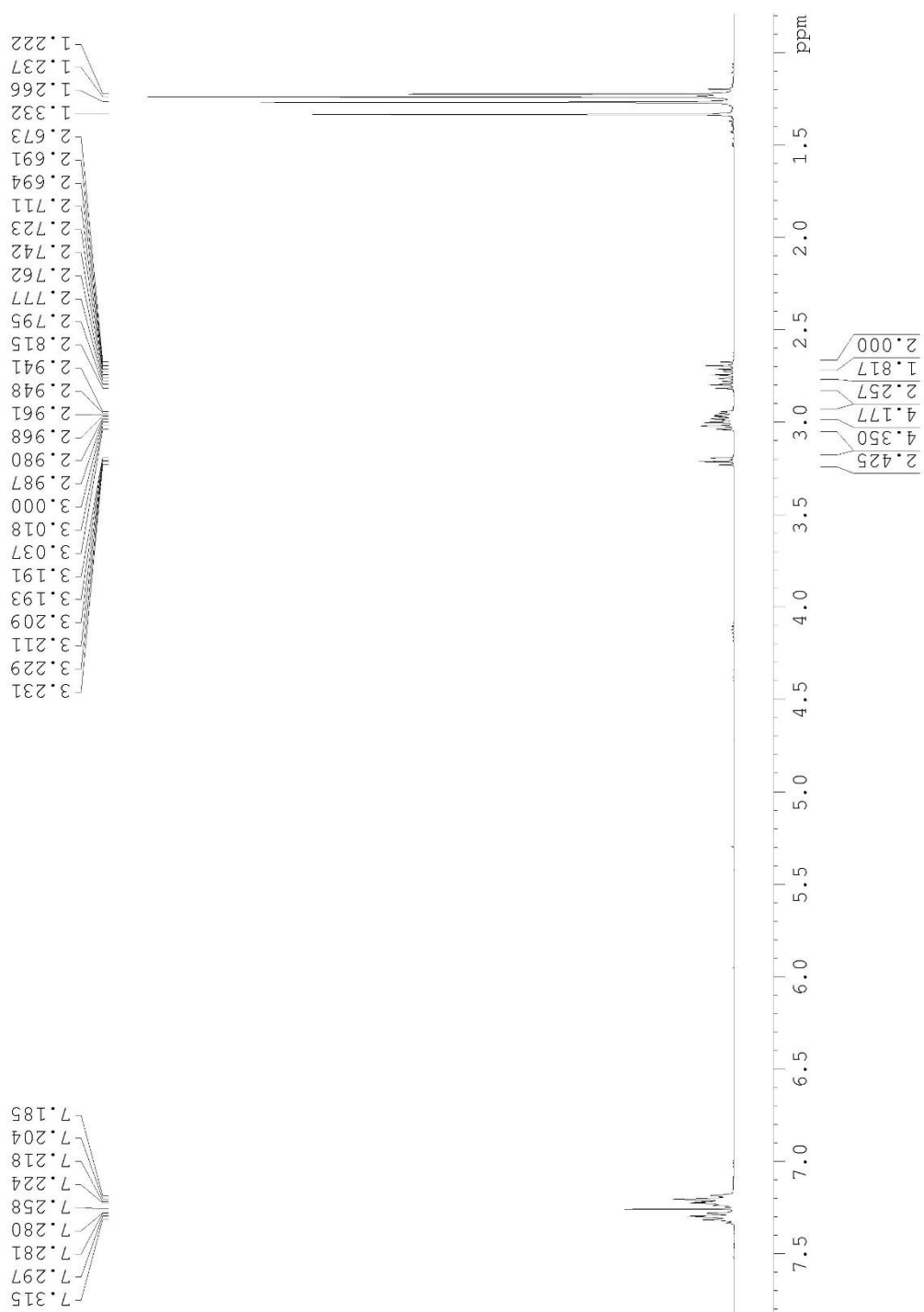


Table 2.5 Entry 6

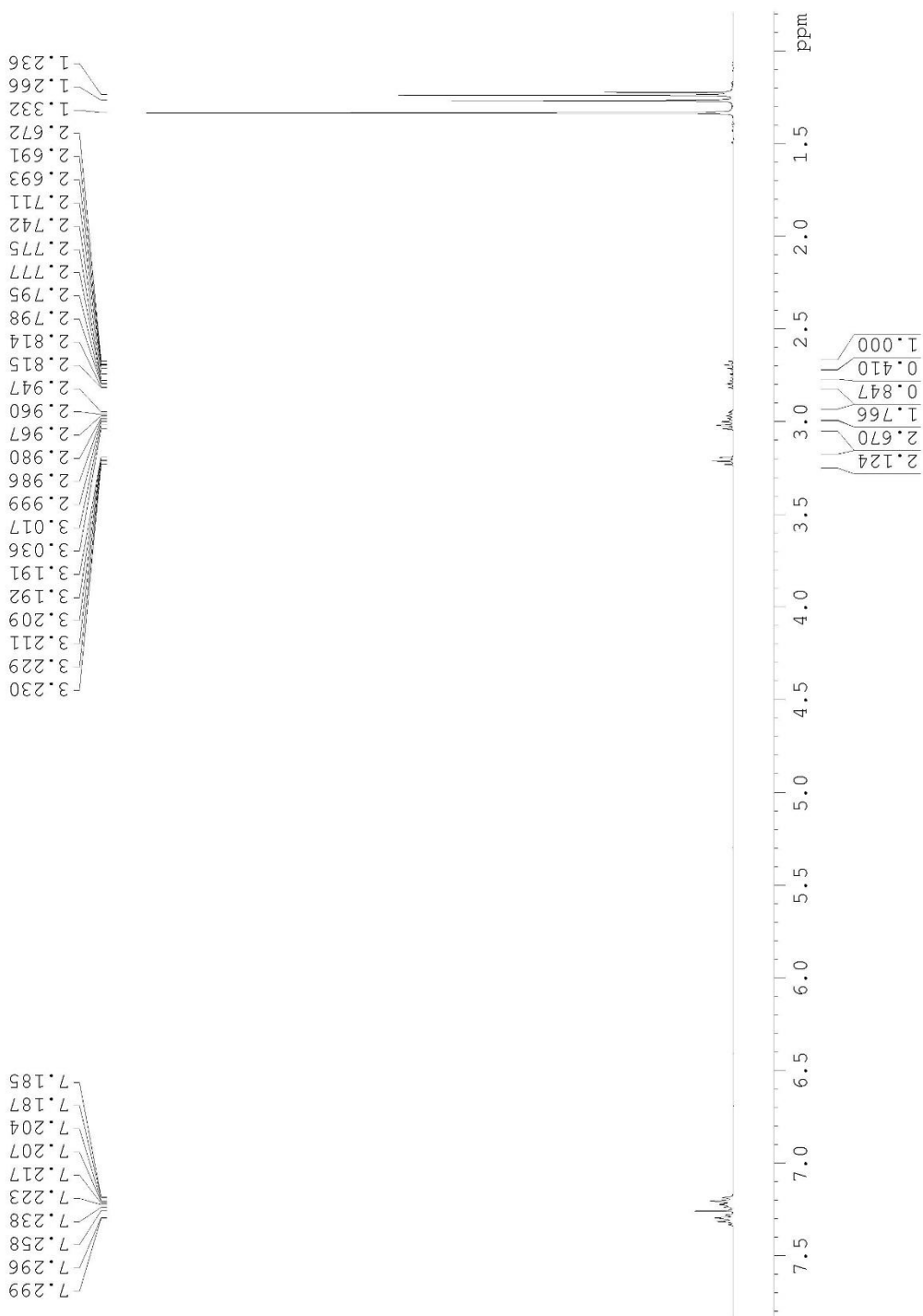
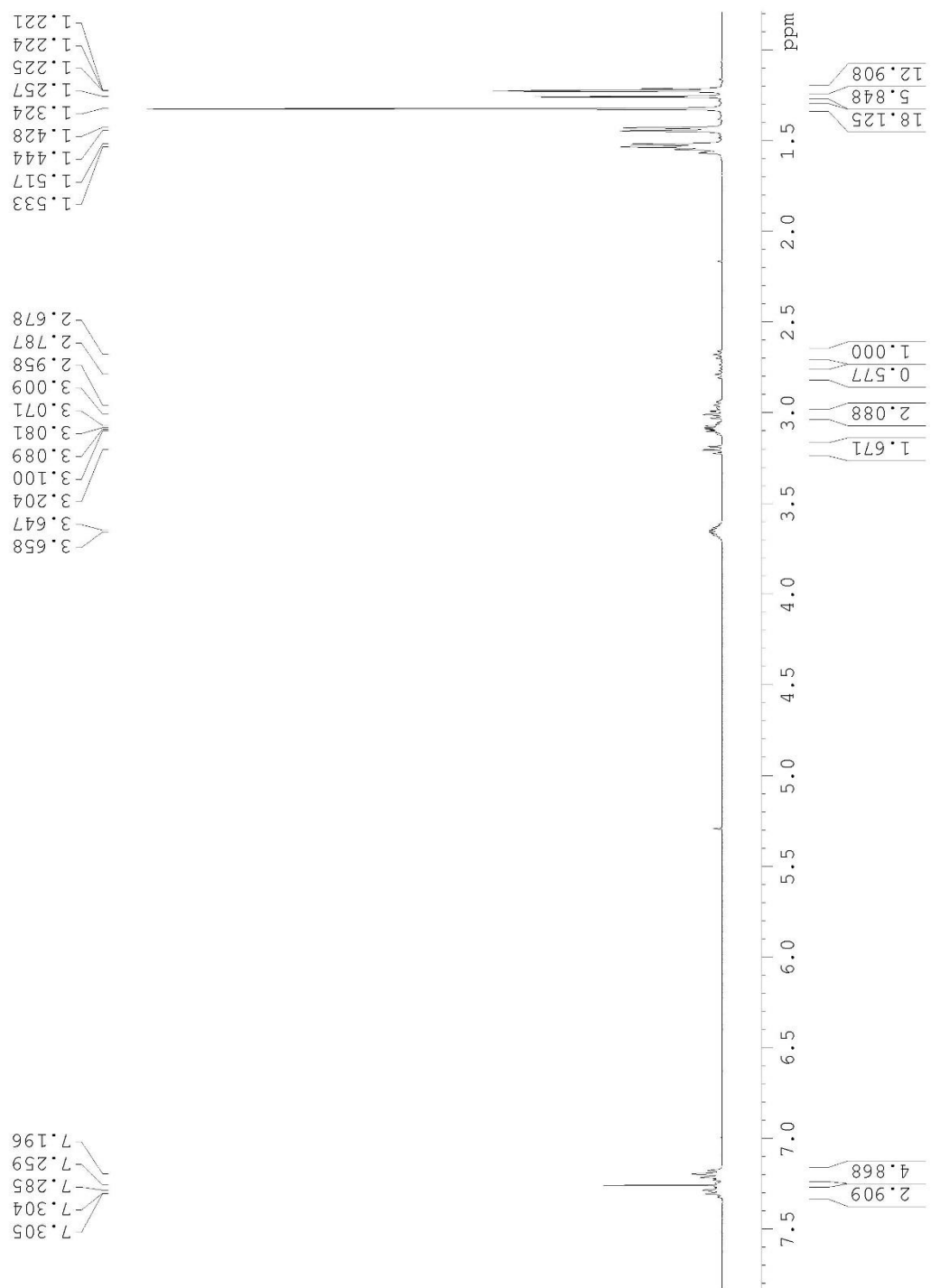
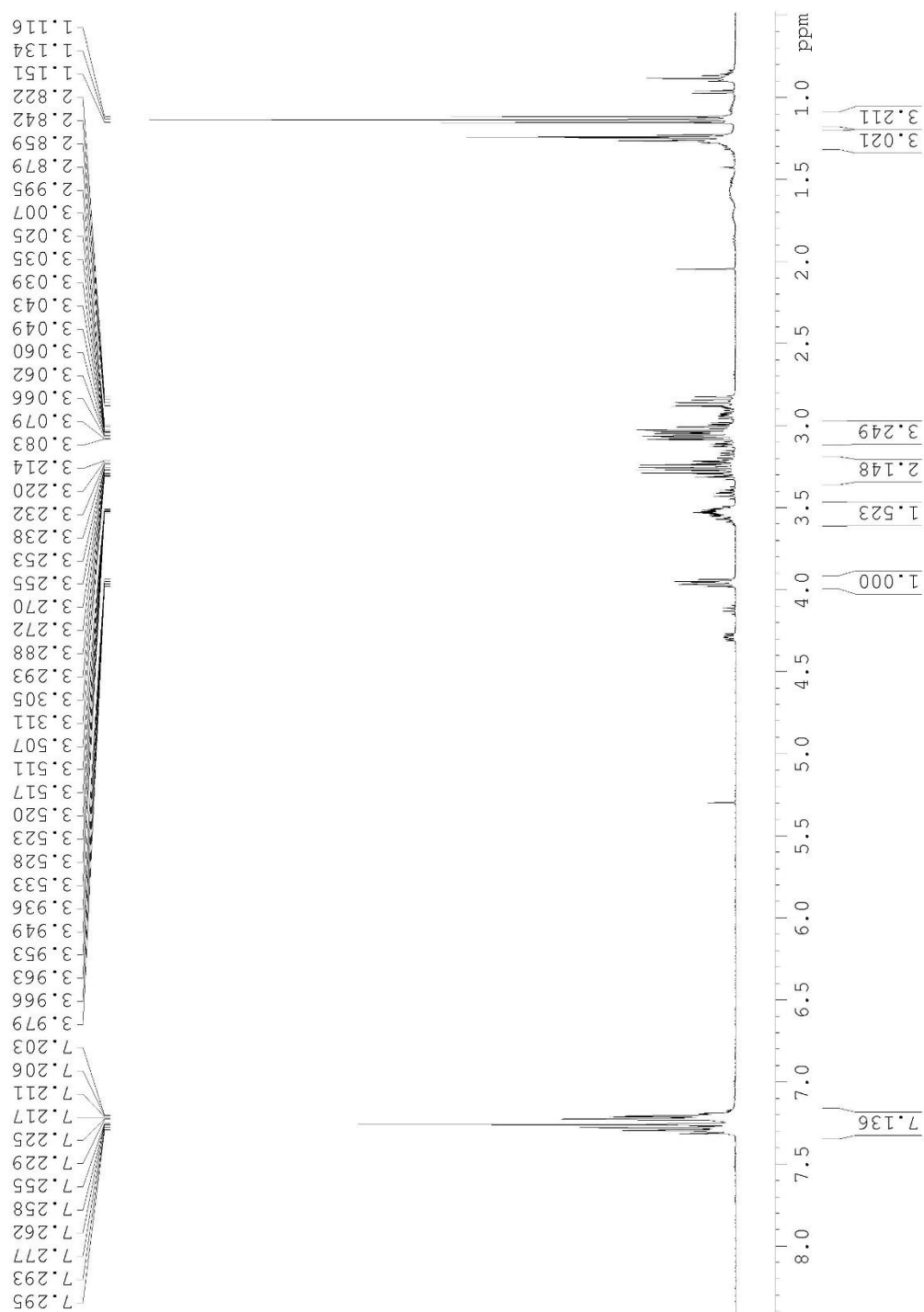


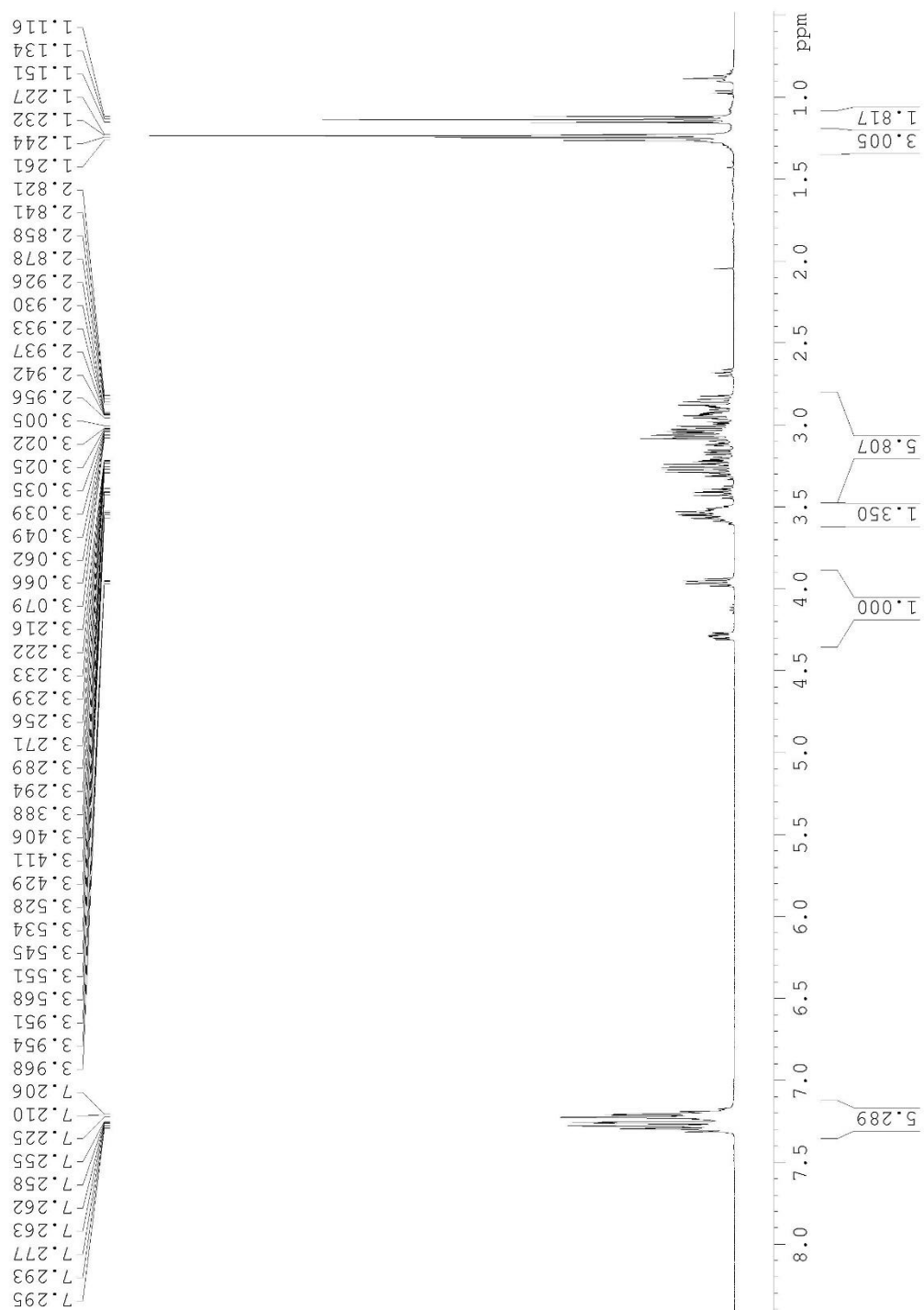
Table 2.5 Entry 7



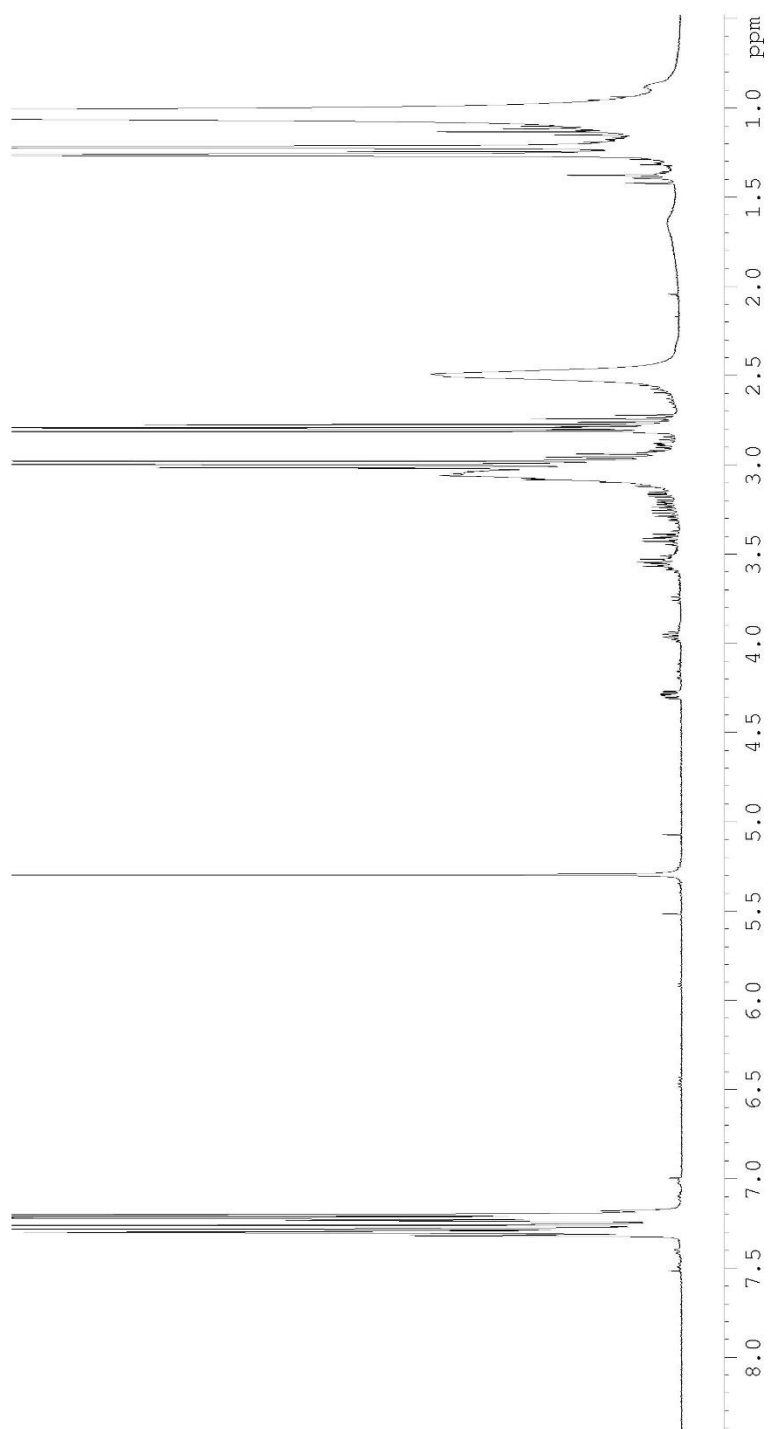
Scheme 2.13 Entry A



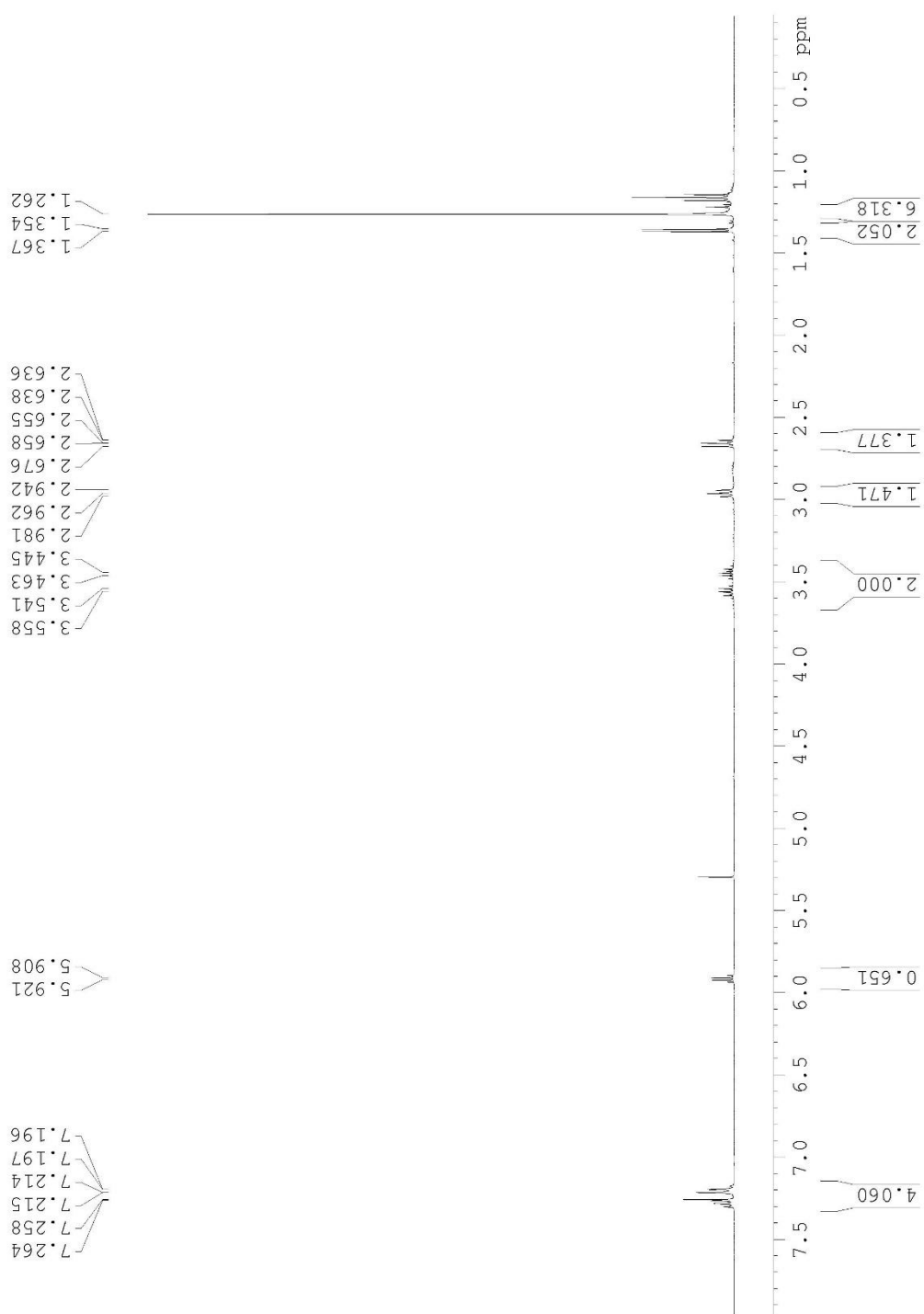
Scheme 2.13 Entry B



Scheme 2.13 Entry C



Scheme 2.13 Entry D



Scheme 2.13 Entry E

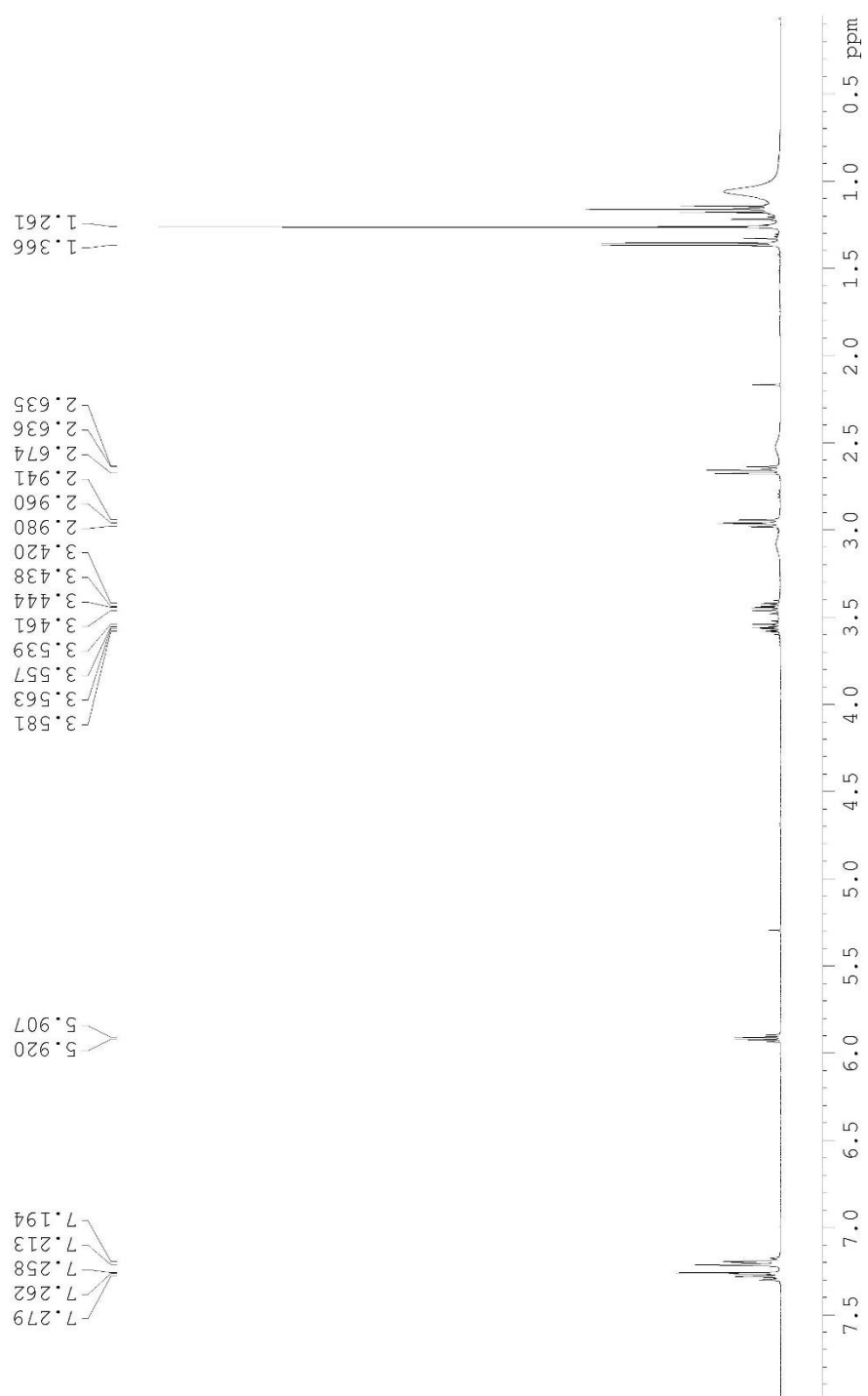


Table 2.6 Entry 1

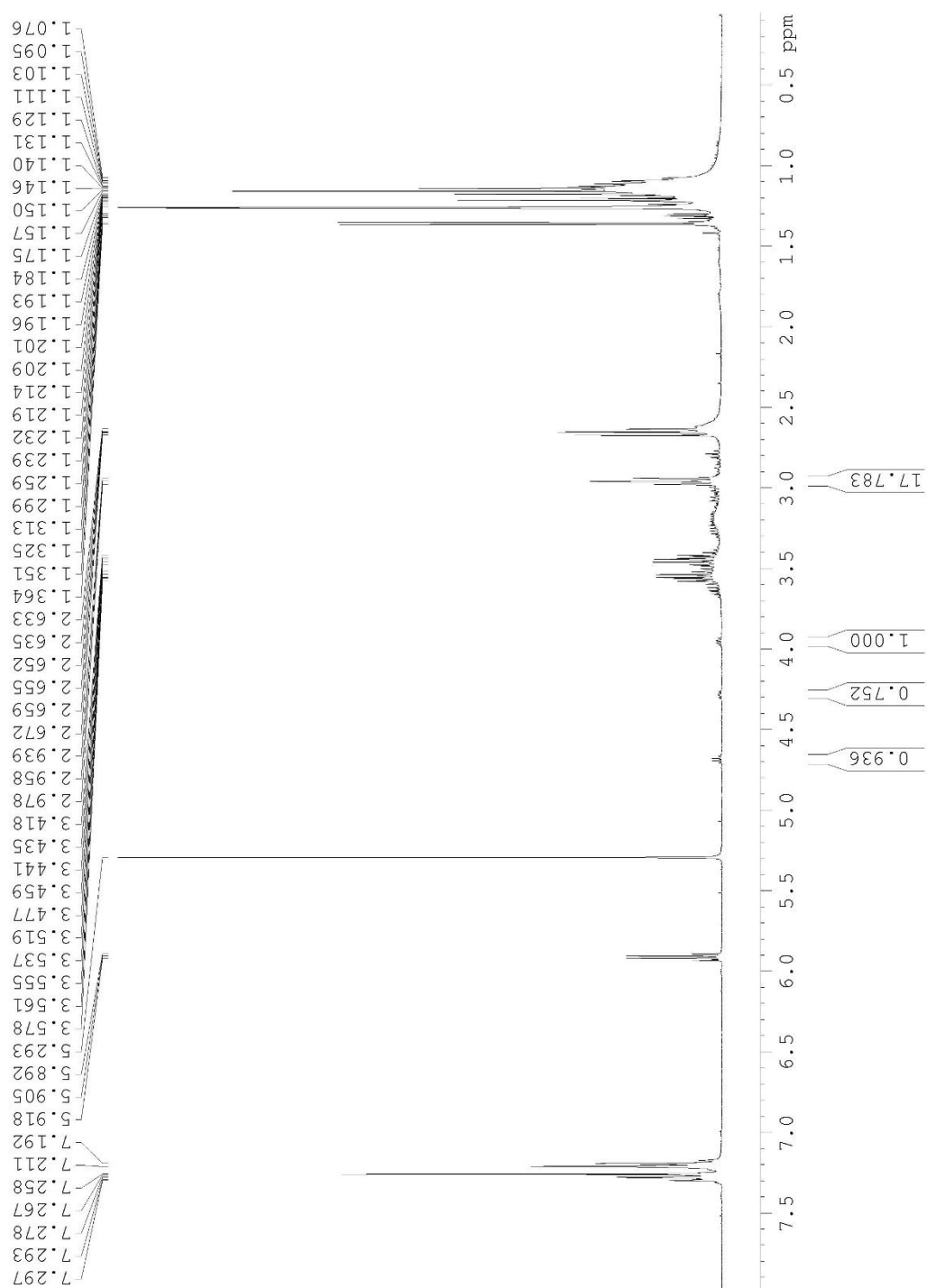


Table 2.6 Entry 2

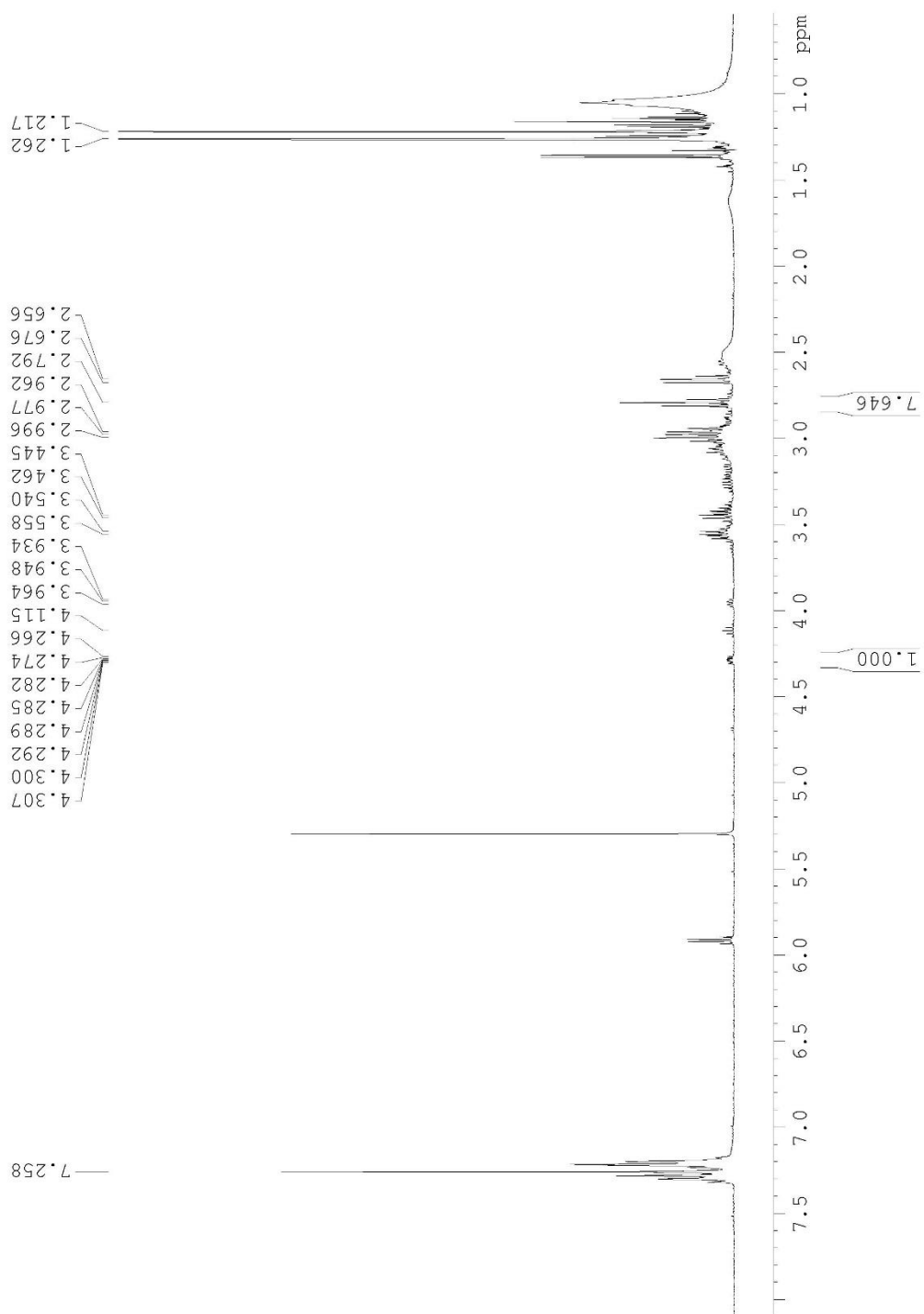


Table 2.6 Entry 3

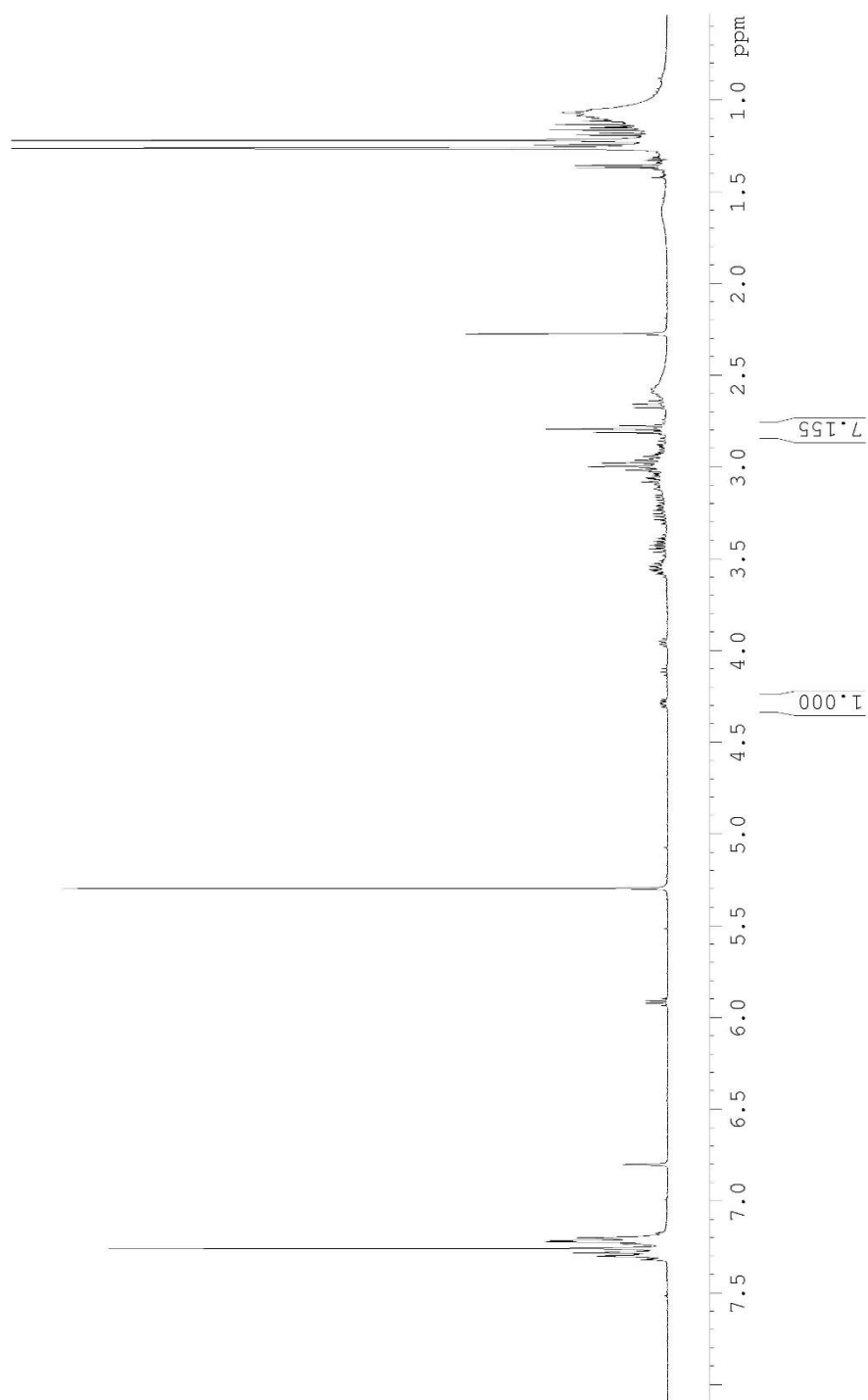


Table 2.6 Entry 4

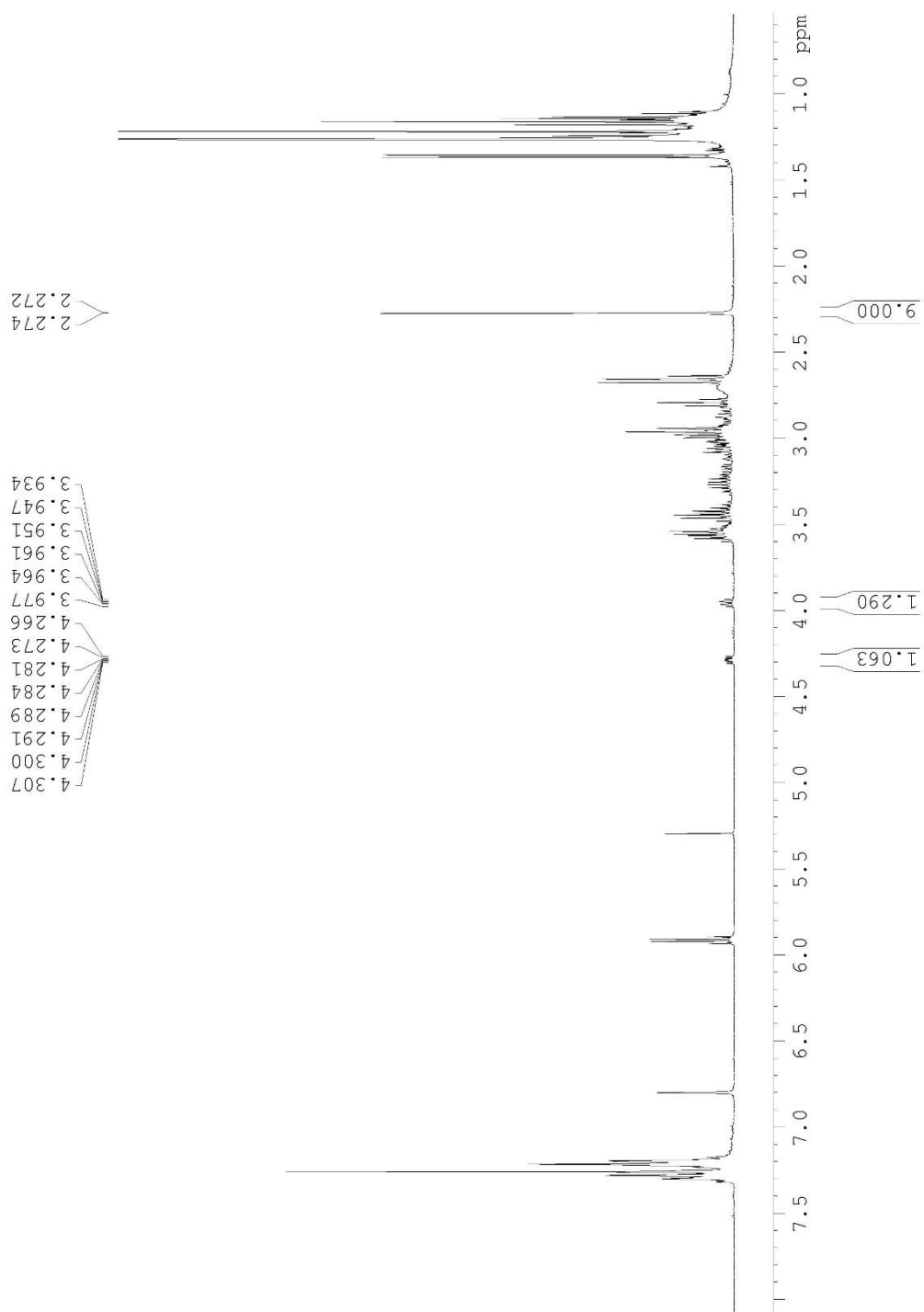


Table 2.6 Entry 5

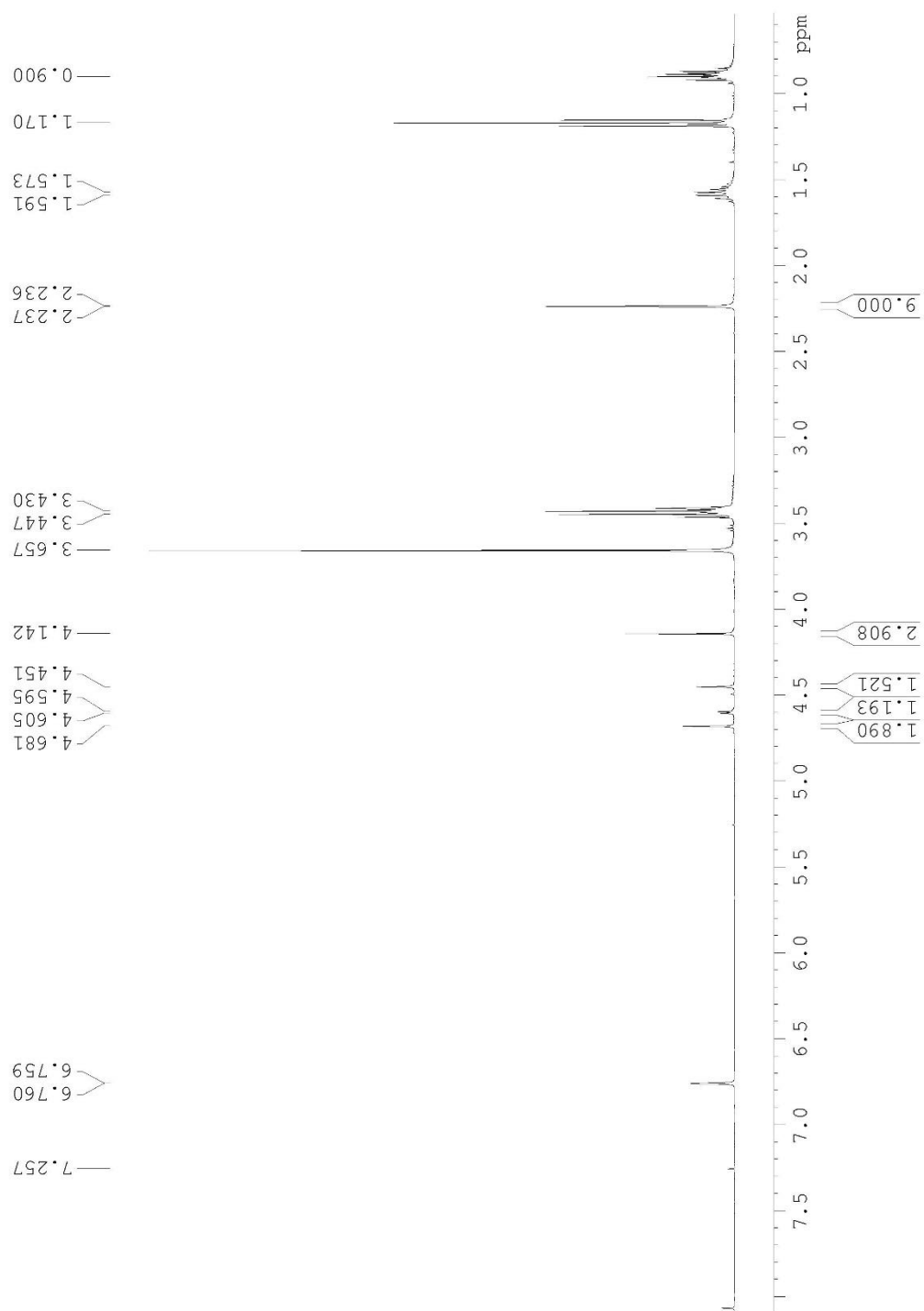


Table 2.6 Entry 6

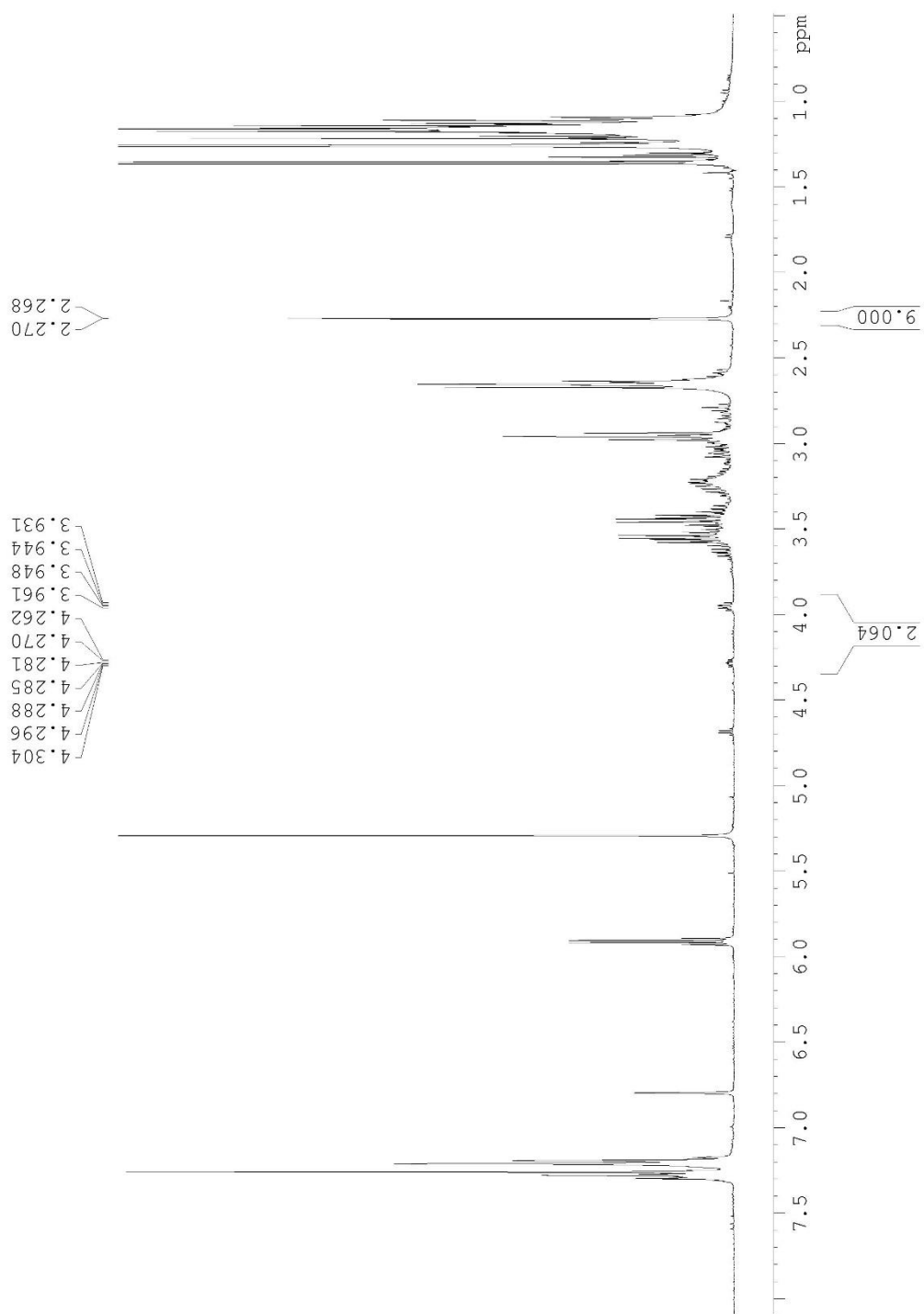


Table 2.6 Entry 7

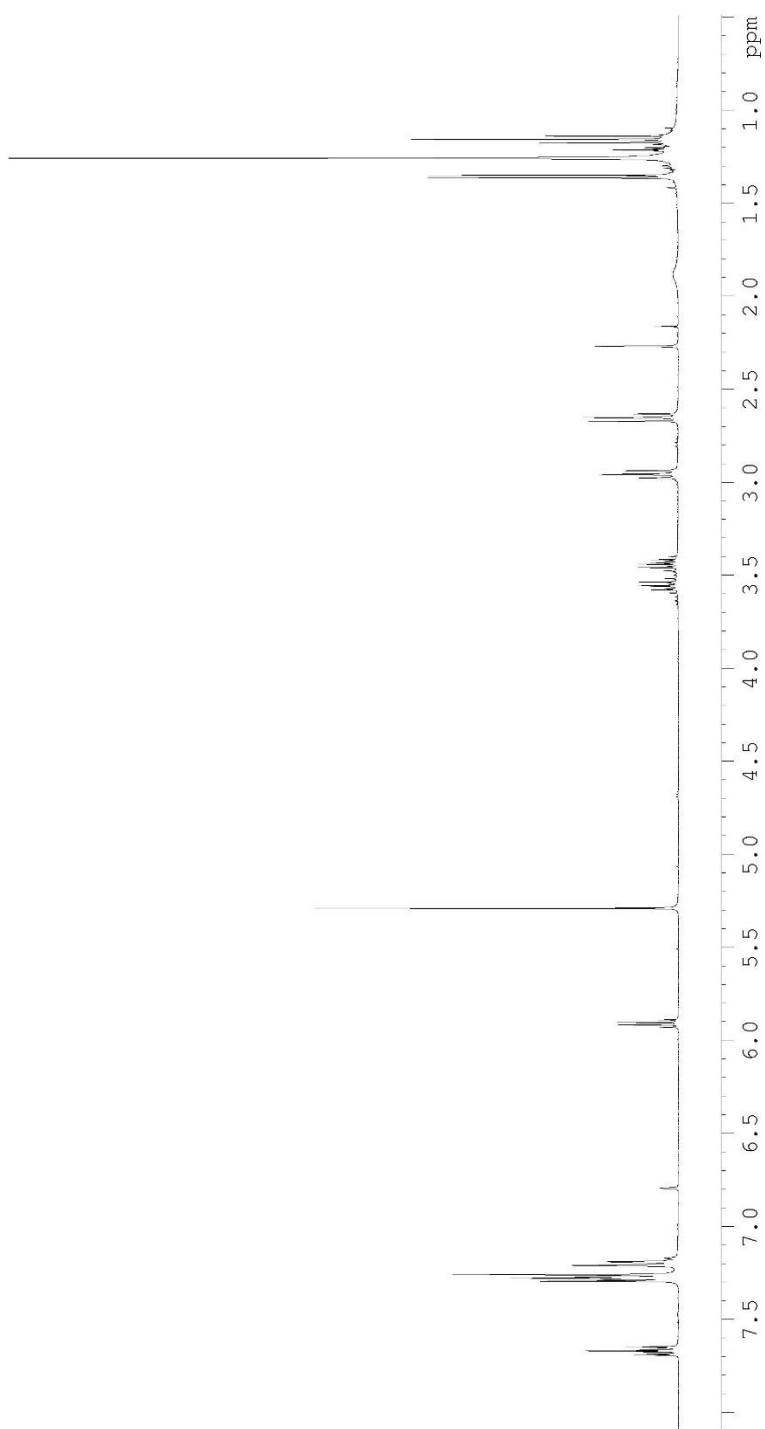


Table 2.6 Entry 8

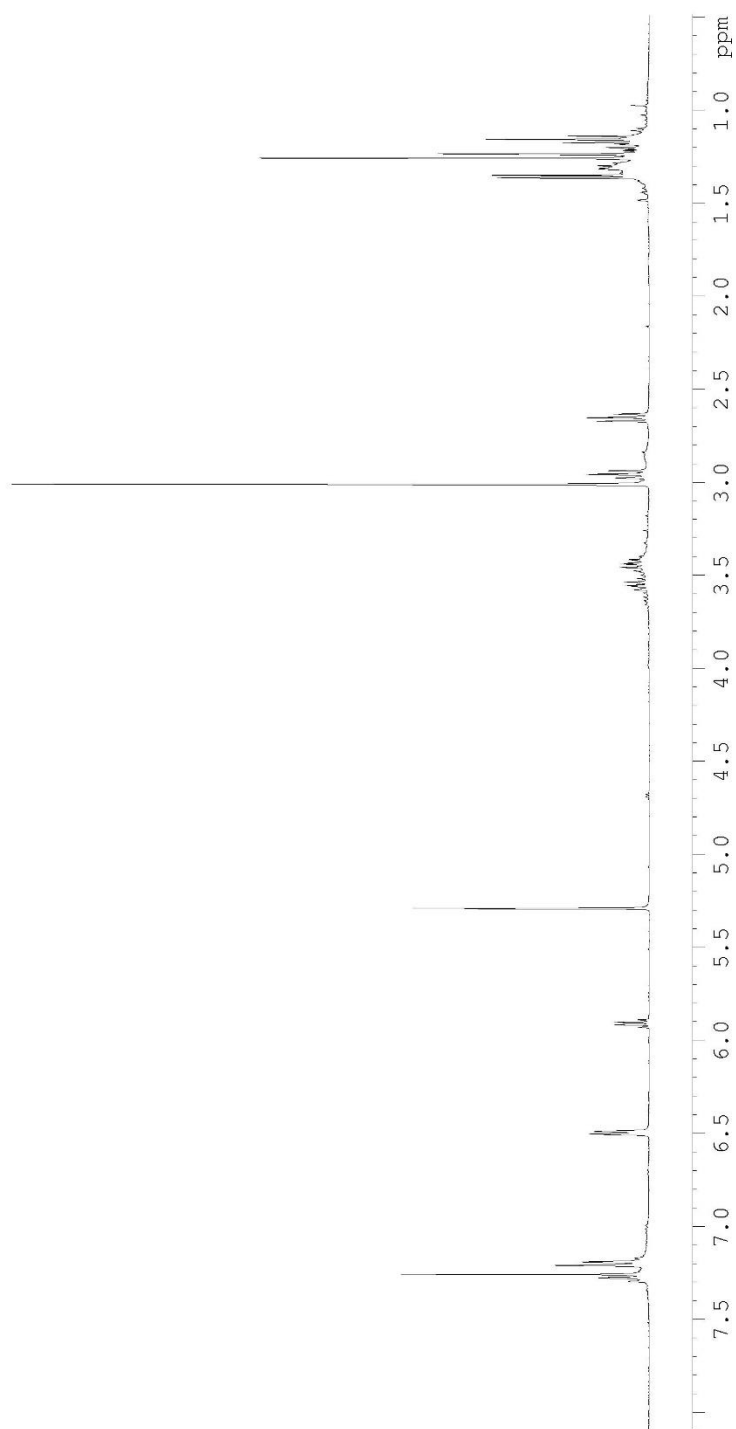


Table 2.9 Entry 1

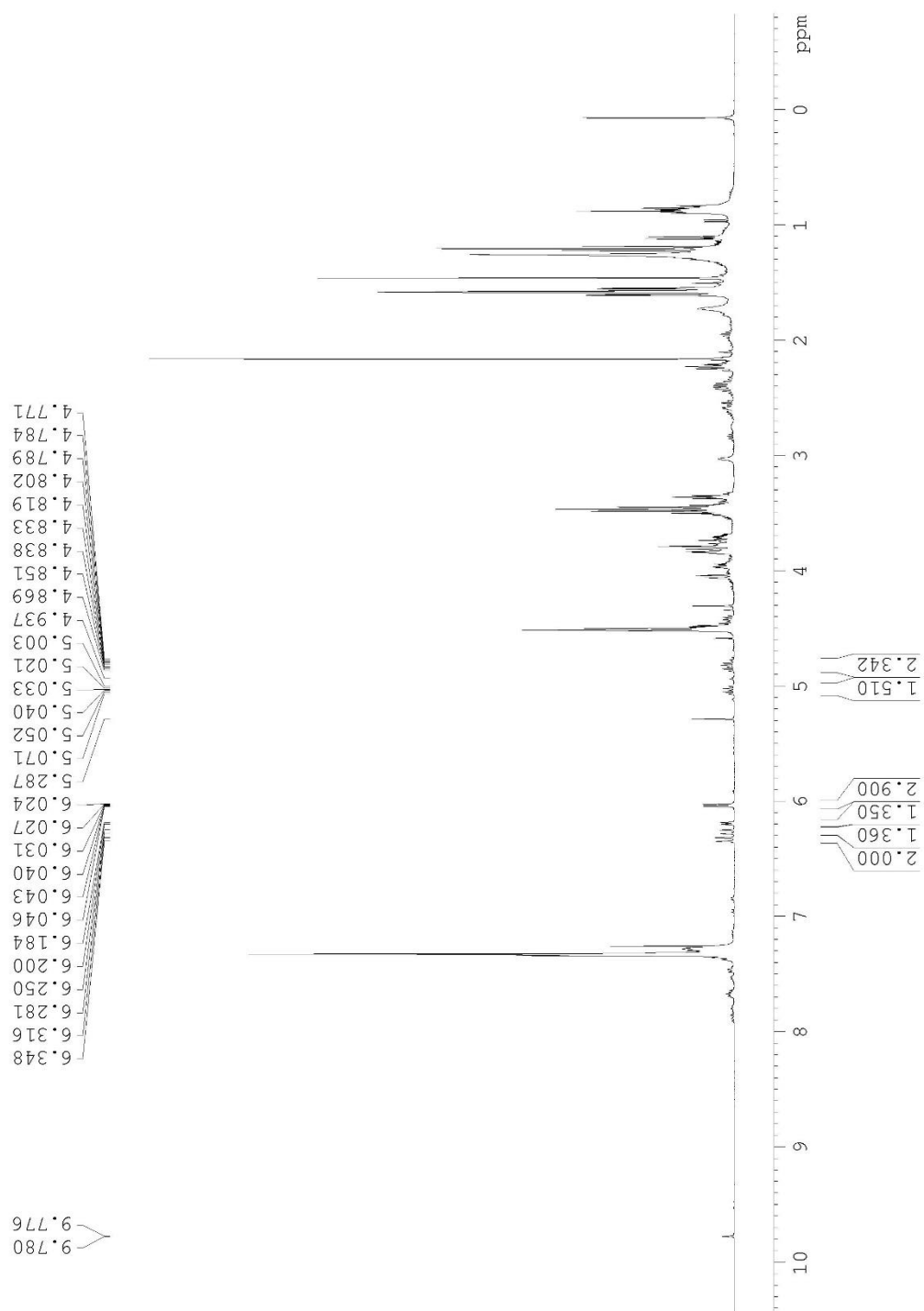


Table 2.9 Entry 2

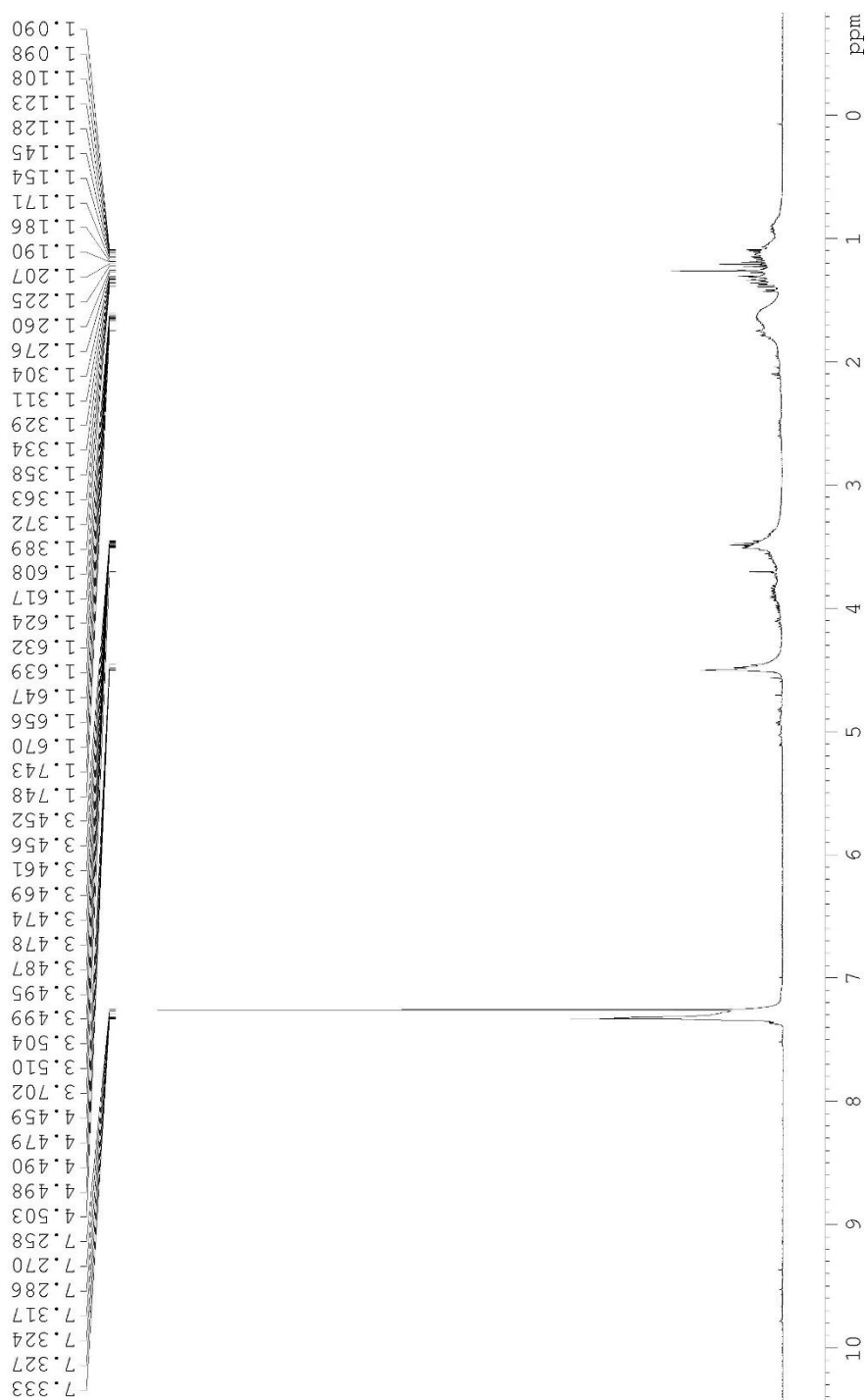


Table 2.9 Entry 3

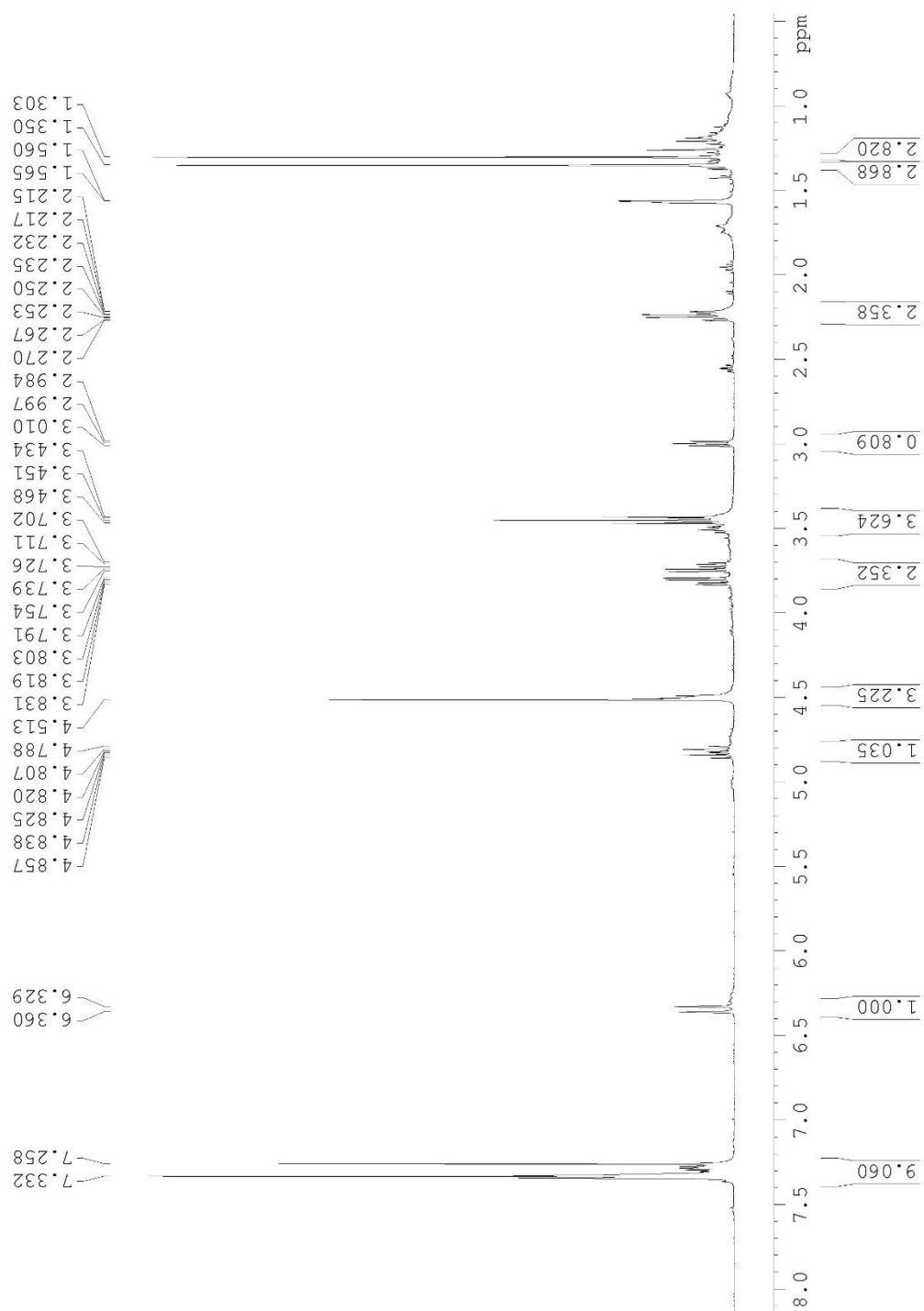


Table 2.9 Entry 4

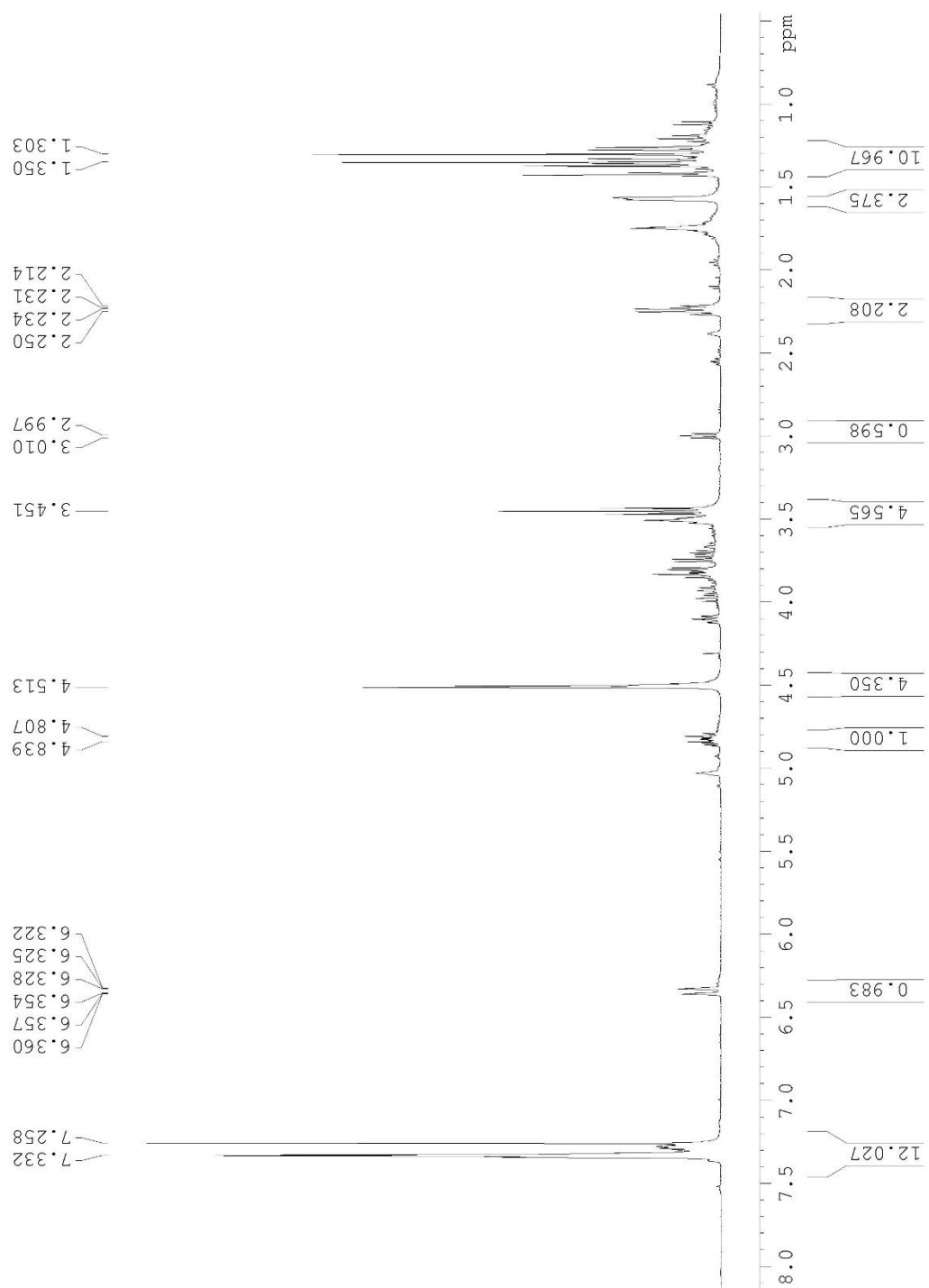


Table 2.9 Entry 5

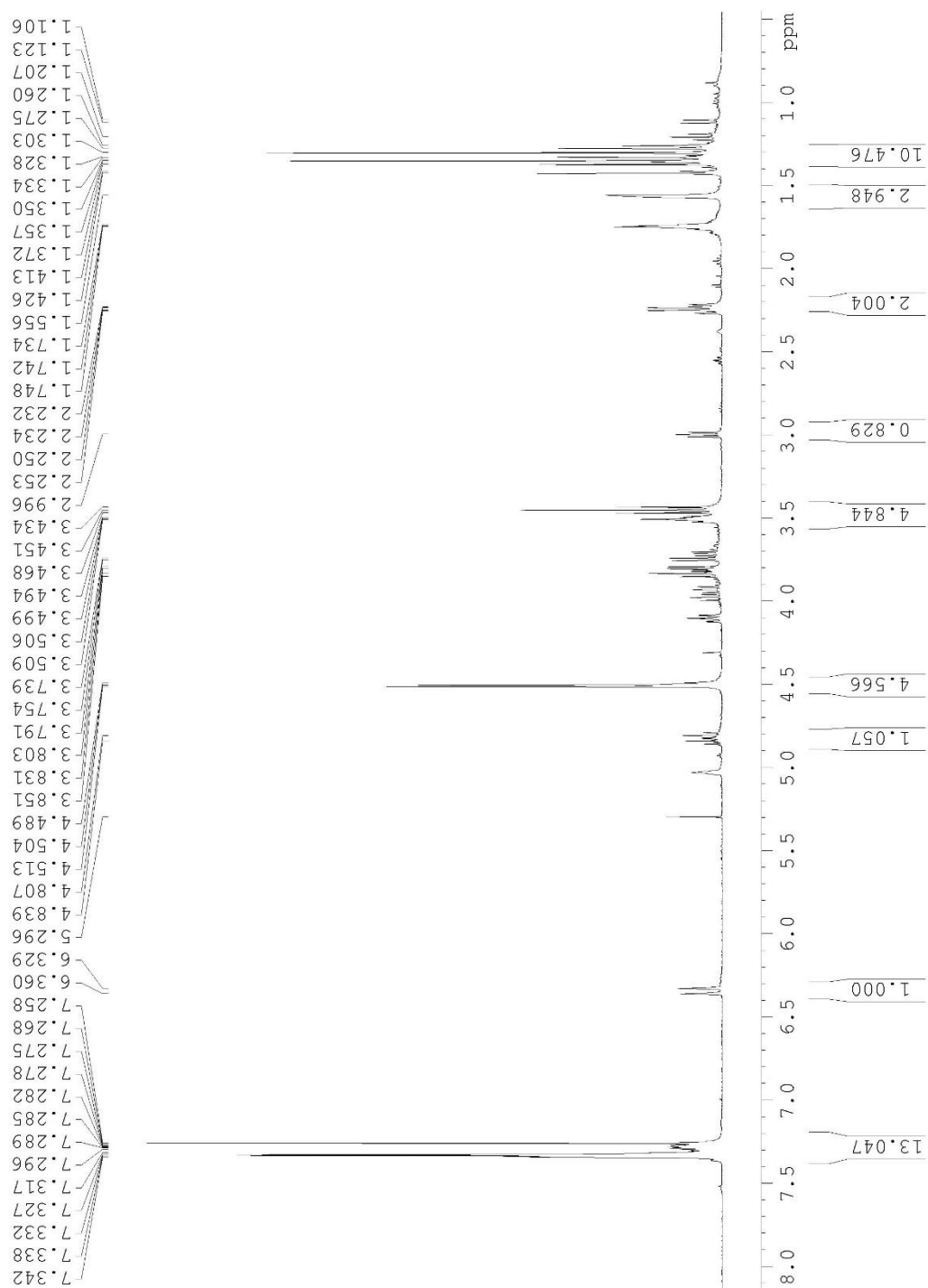
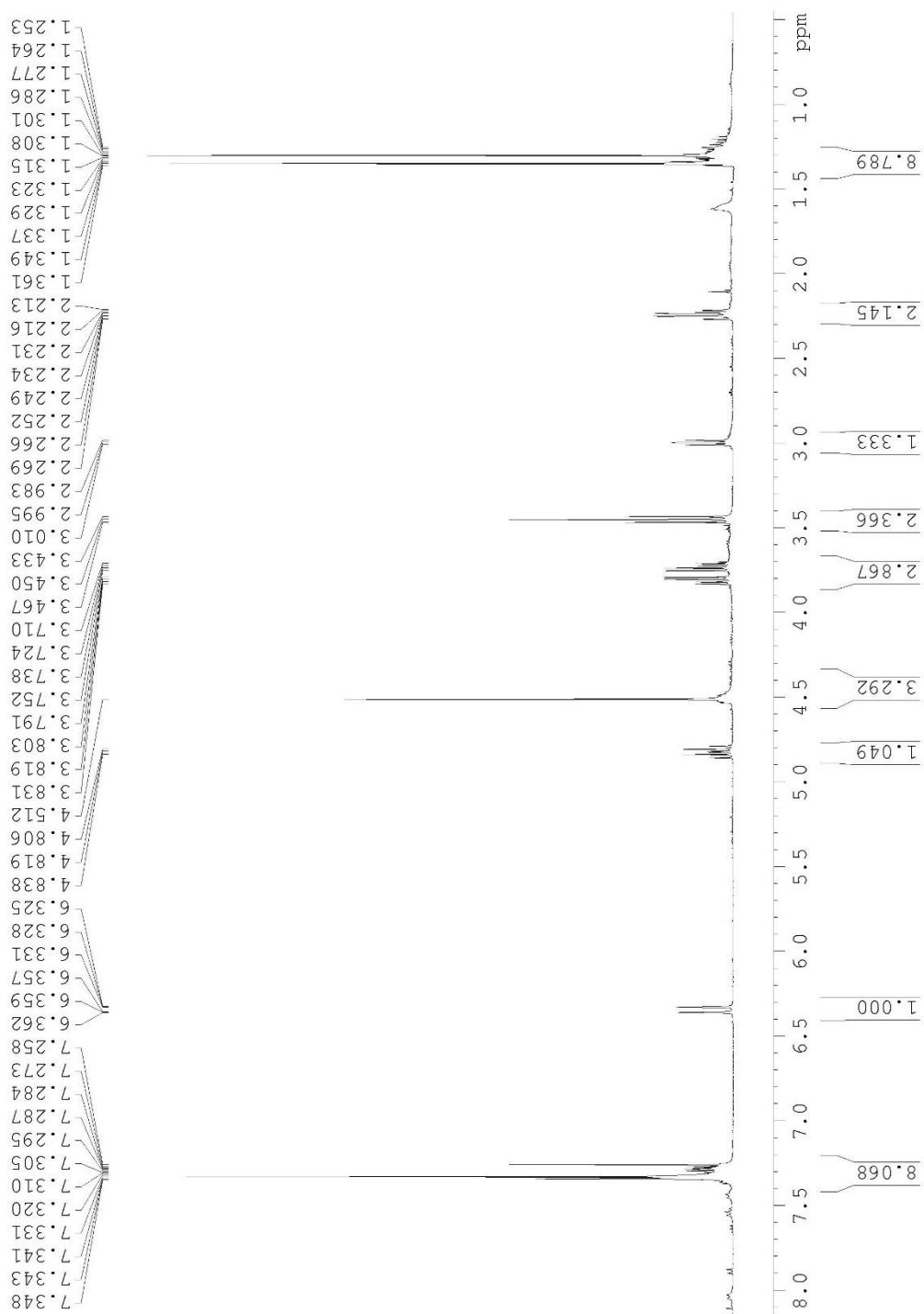


Table 2.9 Entry 6



2.9 References

1. Staudinger and Suter, *Ber.*, **1920**, *53*, 1092.6
2. (a) Lewis, J. R.; Ramage, G. R.; Simonsen, J. L.; Wainwright, W. G. *J. Chem. Soc.* **1937**, *59*, 1837-1841. (b) Smith, L. I.; Agre, C. L.; Leekley, R. M.; Prichard, W. W. *J. Am. Chem. Soc.* **1939**, *61*, 7-11.
3. (a) Brady, W. T. *Tetrahedron* **1981**, *37*, 2949-2966. (b) Snider, B. B. *Chem. Rev.* **1988**, *88*, 793-811. (c) Hyatt, J. A.; Reynolds, P. W. *Organic Reactions* **1994**, *45*, 159-237.
4. Huisgen, R.; Feiler, L.; Binsch, G. *Angew. Chem. Int. Ed.* **1964**, *3*, 753-754.
5. (a) Isaacs, N. S.; Stanbury, P. *J. Chem. Soc., Perkin Trans. 2* **1973**, 166-169. (b) Brady, W. T.; O'Neal, H. R. *J. Org. Chem.* **1967**, *32*, 2704-2707. (c) DoMinh, T.; Strausz, O. P. *J. Am. Chem. Soc.* **1970**, *92*, 1766-1768. (d) Frey, H. M.; Isaacs, N. S. *J. Chem. Soc. (B)* **1970**, 830-832.
6. Aben, R. W.; Scheeren, H. W. *J. Chem. Soc., Perkin Trans. 1*, **1979**, 3132-3138.
7. Matsuo, J.; Okuno, R.; Takeuchi, K.; Kawano, M.; Ishibashi, H. *Tet. Lett.* **2010**, *51*, 3736-3737.
8. (a) Marchand-Brynaert, J.; Ghosez, L. *J. Am. Chem. Soc.* **1972**, *94*, 2870-2872. (b) Falmagne, J.-B.; Escudero, J.; Taleb-Sahraoui, S.; Ghosez, L. *Angew. Chem. Int. Ed.* **1981**, *20*, 879-880.
9. Ding, W.-J.; Fang, D.-C. *J. Org. Chem.* **2001**, *66*, 6673-6678.
10. Beereboom, J. J. *J. Org. Chem.* **1965**, *30*, 4230-4234.
11. Baldwin, S. W. *J. Chem. Soc., Chem. Commun.*, **1972**, 1337-1338.
12. (a) Marko, I.; Ronsmans, B.; Hesbain-Frisque, A.-M.; Dumas, S.; Ghosez, L. *J. Am. Chem. Soc.* **1985**, *107*, 2192-2194. (b) Snider, B. B.; Hui, R. A. H. F.; Kulkarni, Y. S. *J. Am. Chem. Soc.* **1985**, *107*, 2194-2196.
13. Snider, B. B.; Walner, M. *Tetrahedron* **1989**, *45*, 3171-3182.

14. (a) Brady, W. T.; Marchand, A. P.; Giang, Y. F.; Wu, A.-H. *Synthesis* **1987**, 395-396. (b) Madelaine, C.; Valerio, V.; Maulide, N. *Angew. Chem. Int. Ed.* **2010**, *49*, 1583-1586. (c) Lachia, M.; Jung, P. M.; De Mesmaeker, A. *Tet. Lett.* **2012**, *53*, 4514-4517. (d) Ryabukhin, S. V.; Fominova, K. I.; Sibgatulin, D. A.; Grygorenko, O. O. *Tet. Lett.* **2014**, *55*, 7240-7242.
15. (a) Shade, R. E.; Hyde, A. M.; Olsen, J.-C.; Merlic, C. A. *J. Am. Chem. Soc.* **2010**, *132*, 1202-1203. (b) Chen, D. G.; Winterheimer, D. J.; Merlic, C. A. *Org. Lett.* **2011**, *13*, 2778-2781.
16. Chio, F. K.; Warne, J.; Gough, D.; Penny, M.; Green, S.; Coles, S. J.; Hursthouse, M. B.; Jones, P.; Hassall, L.; McGuire, T. M.; Dobbs, A. P. *Tetrahedron*, **2011**, *67*, 5107-5124.
17. (a) Winterheimer, D. J.; Merlic, C. A. *Org. Lett.* **2010**, *12*, 2508-2510. (b) Cory, B. H. Ligand Effect on Copper-Promoted Coupling Reactions: Analysis of Allenes as Pi-Bond Ligands; Synthesis and Applications of Substituted 1,3-Dienes and [n]Dendralenes. PhD Dissertation, University of California, Los Angeles, Los Angeles, CA, **2019**.
<https://escholarship.org/uc/item/1st97912>
18. Novartis AG. Novartis Pharma GMBH. WO2004/87142, **2004**.
19. Zhang, H.; Yu, E. C.; Torker, S.; Schrock, R. R.; Hoveyda, A. H. *J. Am. Chem. Soc.* **2014**, *136*, 16493-16496.
20. Aizpurua, J.M.; Palomo, C. *Synthesis* **1982**, 684-687.
21. (a) Henry-Riyad, H.; Lee, C.; Purohit, V. C.; Romo, D. *Org. Lett.* **2006**, *8*, 4363-4366. (b) Brady, W. T.; Marchand, A. P.; Giang, Y. F.; Wu, A.-H. *Synthesis*, **1987**, 395-396.
22. Arai, H.; Nishioka, H.; Niwa, S.; Yamanaka, T.; Tanaka, Y.; Yoshinaga, K.; Kobayashi, N.; Miura, N.; Ikeda, Y. *Chem. Pharm. Bull.* **1993**, *41*, 1583-1588.

23. (a) Hashimoto, S.; Itoh, A.; Kitagawa, Y.; Yamamoto, H.; Nozaki, H. *J. Am. Chem. Soc.* **1977**, *99*, 4192-4194. (b) Kaino, M.; Naruse, Y.; Ishihara, K.; Yamamoto, H. *J. Org. Chem.* **1990**, *55*, 5814-5815.
24. Ameen, D.; Snape, T. *Eur. J. Org. Chem.* **2014**, 1925-1934.
25. Fringuelli, F.; Germani, R.; Pizzo, F.; Santinelli F.; Savelli, G. *J. Org. Chem.* **1992**, *57*, 1198-1202.

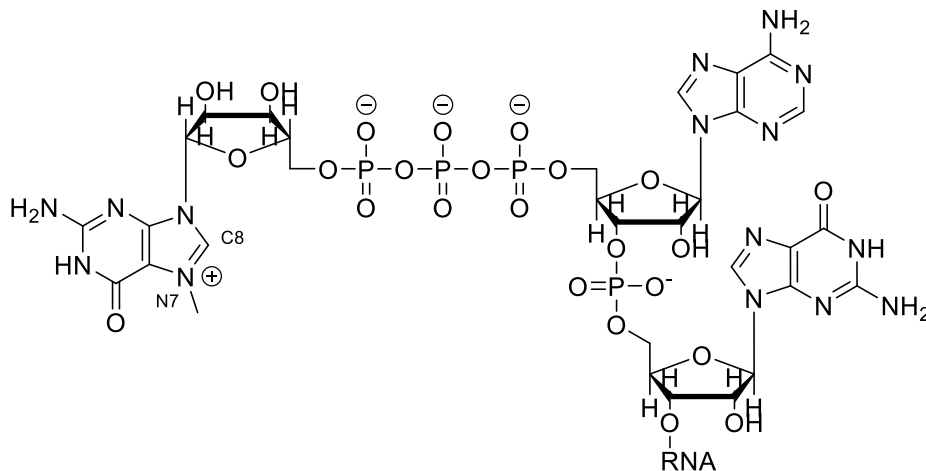
Chapter 3

Synthesis of a Gold-Carbene Complex with a mRNA 5'-Cap Analog

3.1 Introduction

The 5'-Cap, discovered by Rottman, Shatkin, and Perry, is a conserved structural motif in messenger RNA (mRNA) found in all eukaryotic life.¹ The structure of the 5'-Cap is shown in Figure 3.1. It consists of a single guanosine nucleoside, which has been methylated at the N7

Figure 3.1 Structure of the 5'-Cap



position, bound 5' to 5' with the strand of mRNA via a triphosphate linkage. The 5'-Cap is crucial to the central dogma of biology, hence its ubiquity across the eukaryotic domain. The cap acts as a recognition site for a wide variety of proteins which interact with mRNA, participating in splicing, intracellular transportation, and translation into proteins; it identifies mRNA as mRNA (Figure 3.2).

Thanks to its crucial role in cellular function, the interactions between the 5'-Cap and proteins make for a tantalizing drug target. Figure 3.3 shows a crystal structure of 7-methyl guanosine triphosphate (m⁷Gppp) bound to eIF4E, the protein subunit which recognizes mRNA for loading onto the ribozyme for translation. Both the anionic phosphates and the cationic imidazolium ring are required for effective binding. Overexpression of eIF4E is common in a variety of cancers, so analogs of the 5'-Cap have been examined as competitive inhibitors.^{1h} To the best of our

Figure 3.2 Role of the 5'-Cap

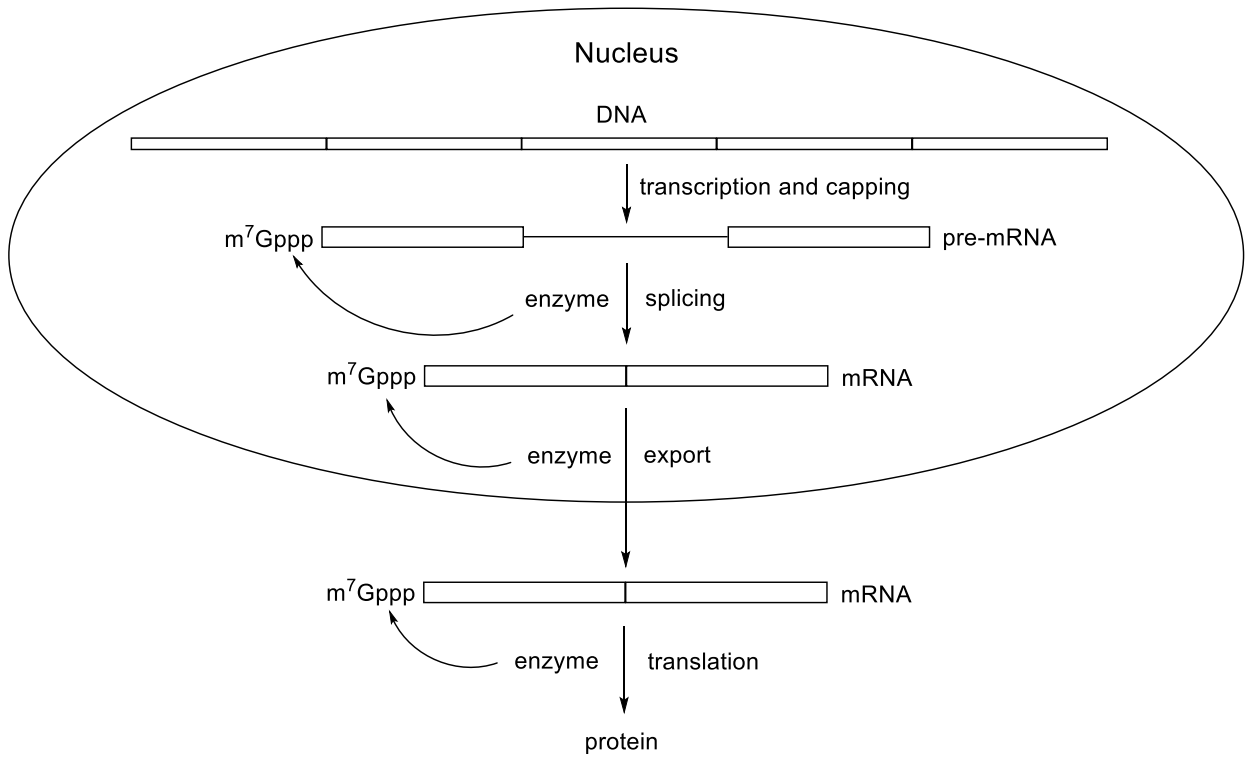
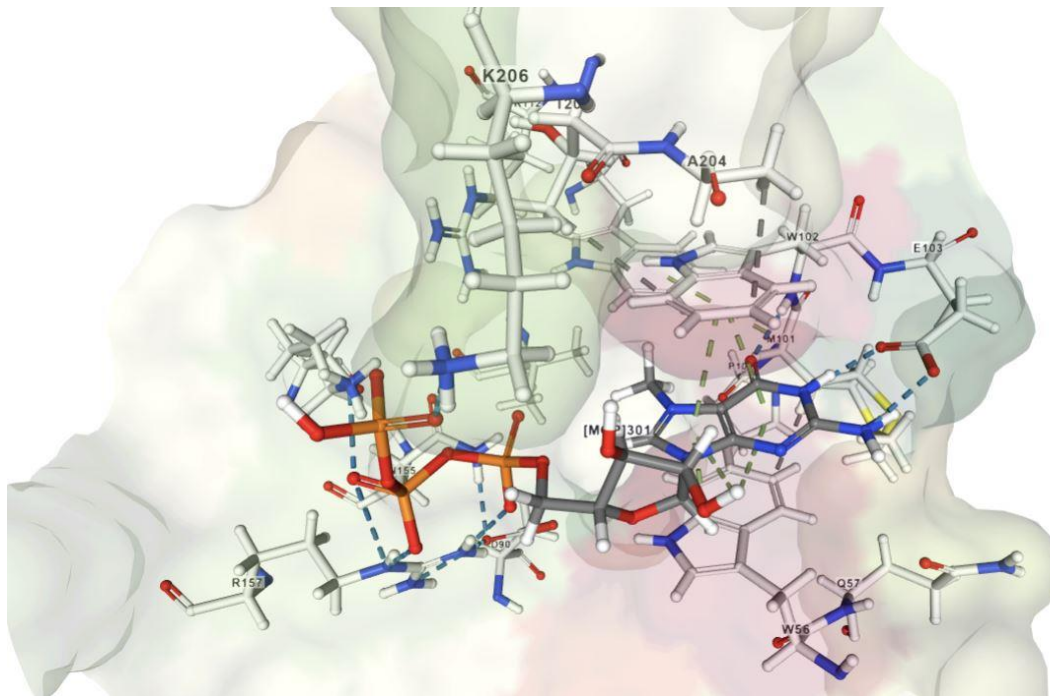


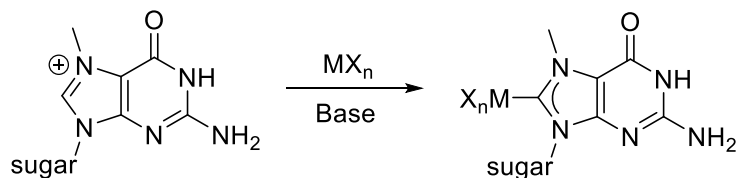
Figure 3.3 5'-Cap Bound to eLF4E



knowledge, however, none have made it into pharmaceutical trials. Altering the 5'-Cap itself could provide an alternate route to blocking translation.

From the perspective of organometallic chemistry, the imidazolium ring in the structure of the 5'-Cap appears to be primed to act as the precursor to an N-heterocyclic carbene (NHC) ligand for a transition metal. This chapter will discuss the first example of complexation of a free 7-methyl guanosine (7-MeG) NHC, generated in situ, to a transition metal (Scheme 3.1). Considering the ultimate goal of performing such a reaction under biologically relevant conditions, a few major challenges must be overcome. Water must be used as the solvent, or at least as a co-solvent if the reaction is to be performed on an RNA oligomer. The temperature must be kept at or below 40 °C and the pH between 7 and 9 to avoid denaturing RNA and to best represent biological conditions.^{2,3}

Scheme 3.1 Proposed General Scheme



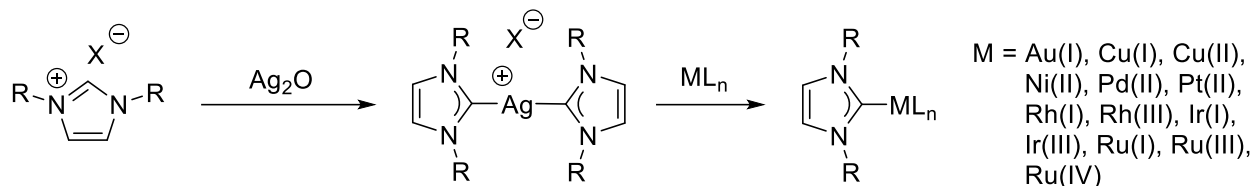
3.2 Background

Recently there have been many advances in the direct complexation of NHC ligands to transition metals. Within the last ten years bulky imidazolium derivatives, under basic conditions, have been complexed to iridium, rhodium, palladium, and platinum.⁴ For this project, however, we chose to focus on silver and gold, as these two metals have much more historic precedence for binding directly to NHCs.

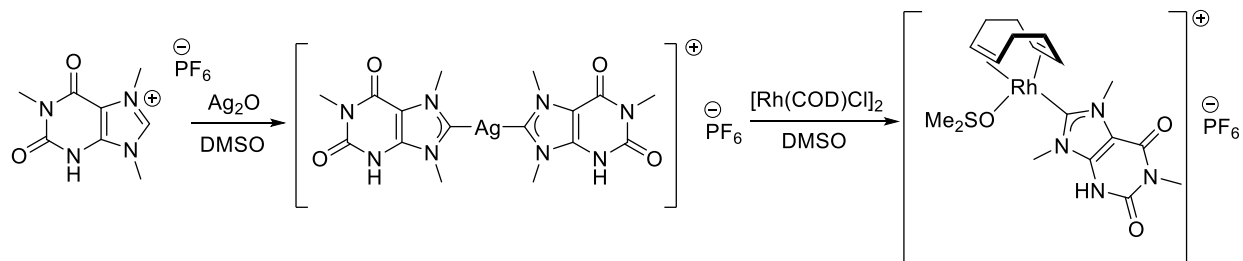
Since the introduction of NHCs as organometallic catalyst ligands in the 1990's, and their huge rise in popularity thanks to the inclusion of the IMes ligand in Grubb's second-generation catalyst, the primary method of incorporating NHCs onto transition metal complexes has been via transmetalation from silver (Scheme 3.2).⁵ This method has been successfully applied to a wide variety of transition metals. Non-ligated NHCs high reactivity makes them unstable, but

they are also particularly labile when ligated to silver. This means that silver complexes are formed easily, but will also readily undergo transmetalation to other transition metals which don't react fast enough with a free NHC. Therefore, silver is an obvious first choice when working with a challenging precursor such as 7MeG.

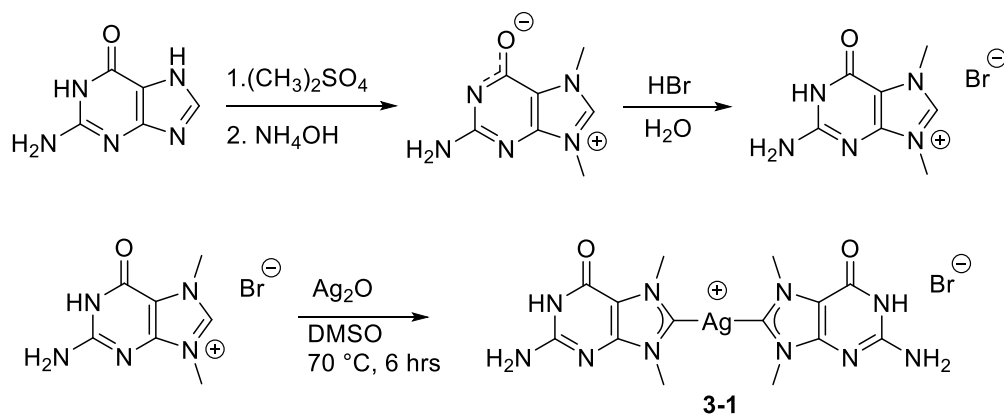
Scheme 3.2 Transmetalation of Silver NHC Complexes



Scheme 3.3 NHC-Metal Complexes with Methylated Caffeine



Scheme 3.4 Purported Silver Complex with 7,9-Dimethylguanine



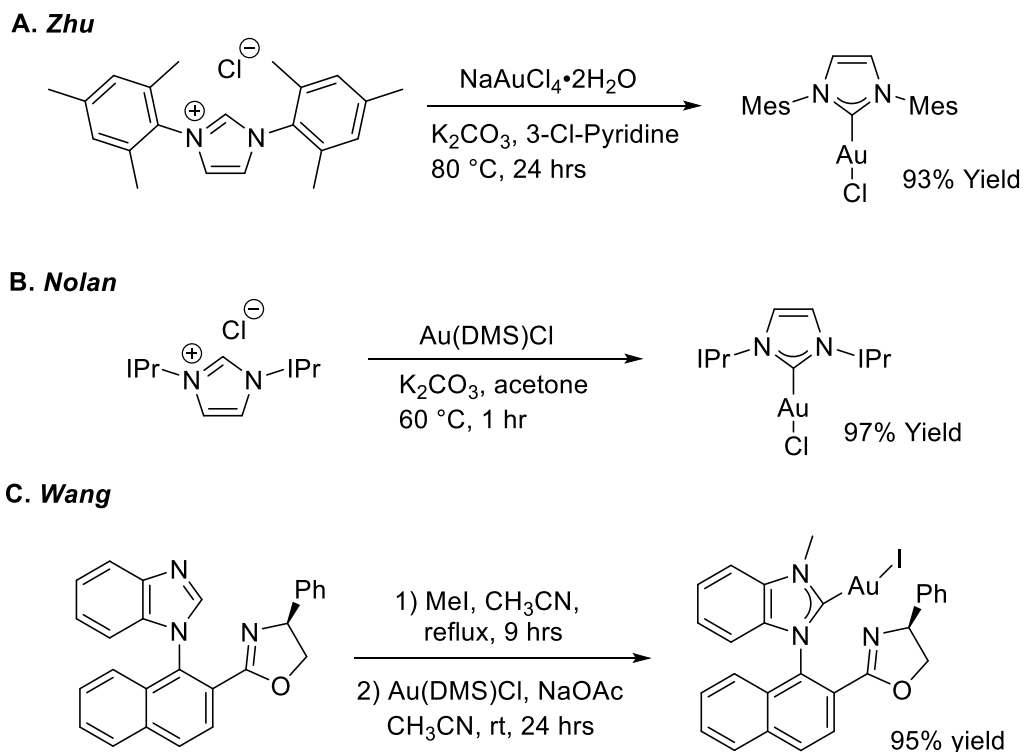
There are limited reports of xanthine derivatives forming NHC complexes with silver, most notably methylated caffeine (Scheme 3.3).⁶ Caffeine, while structurally similar to guanine, has much better solubility, and is therefore often used as a guanine analog in pharmaceuticals.

Youngs and coworkers, in a patent awarded in 2005, present the chemistry shown in Scheme 3.4,

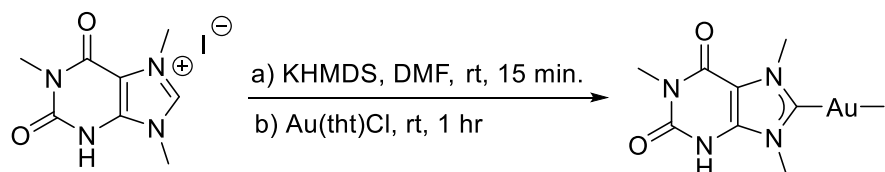
but provide no characterization data for the final silver complex **3-1**.⁷ This particular reaction will be elaborated on later in this chapter.

Perhaps unsurprisingly due to its chemical similarities to silver, gold has more recently proven to readily form bonds with bulky free NHCs. There has been a particular interest in these gold complexes thanks to their anti-cancer and anti-bacterial activities.⁸ The groups of Nolan, Wang, and Zhu reported a variety of conditions for the direct formation of gold complexes with imidazolium derivatives (Scheme 3.5).⁹ Of particular interest to our work, however, is a report by Casini and co-workers in which they demonstrate the reaction of gold with the free NHC of methylated caffeine (Scheme 3.6).¹⁰ Although none of these reactions quite meet the

Scheme 3.5 Direct Formation of Gold-NHC Complexes



Scheme 3.6 Direct Formation of Gold-NHC Complex with Methylated Caffeine

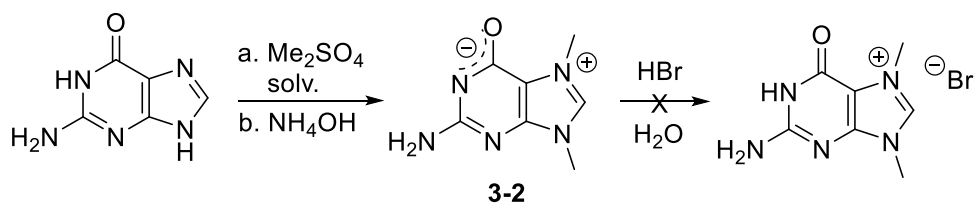


experimental requirements set out for our project, they do instill confidence that a metal NHC complex can be formed under biologically relevant conditions.

3.3 Synthesis of 5'-Cap Analogs and Silver NHC Complexes

We began our investigation by attempting to repeat the experiment reported by Youngs⁷ which is shown in Scheme 3.4. However, many details of the procedure were left out, and so some trial and error was required (Table 3.1). Varying temperature, solvent, and concentration of the reaction led to the isolation of what we believe to be the intermediate **3-2**, but its total insolubility in any solvents made characterization challenging (Entry 5). Repeated inability to perform the ion exchange reported by Youngs led us to pursue alternative paths of inquiry.

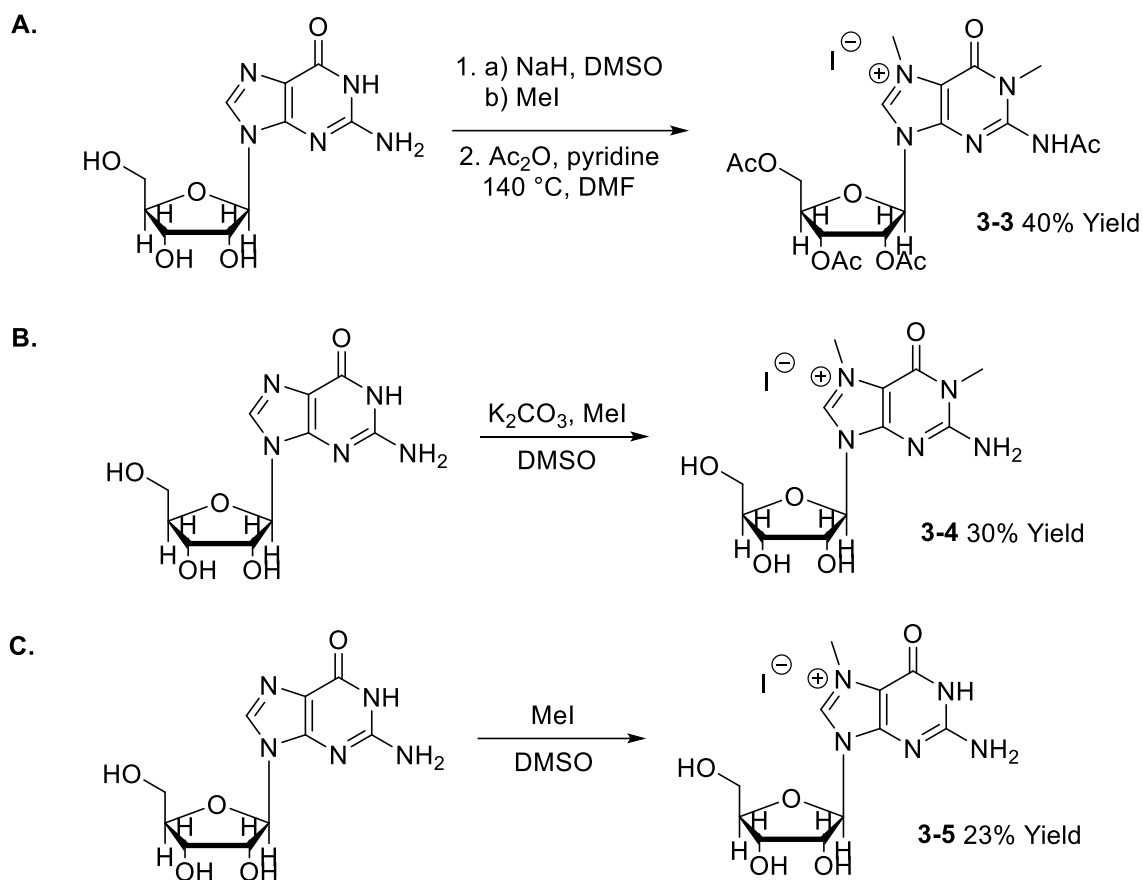
Table 3.1 Attempted Replication of Youngs Patent



Entry	Equiv. Me_2SO_4	Temp. ($^{\circ}C$)	Solvent	Concentration (M)
1	1	20	H ₂ O	0.1
2	2	35	H ₂ O	1.0
3	2	40	EtOH	0.1
4	2	20	Et ₂ O	0.1
5	2.5	90	DMSO	0.66

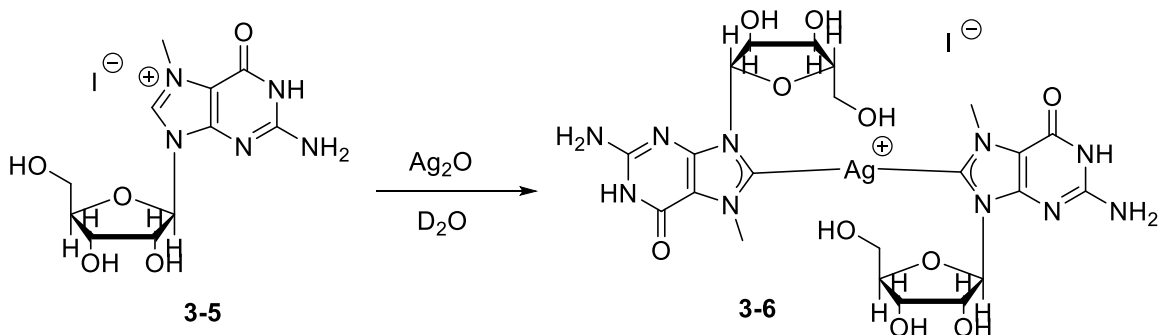
Initially, we were concerned about the numerous potentially reactive positions on guanosine, particularly the sugar alcohols, and therefore began with methylation of the N-1 position followed by polyacetylation of the sugar fragment (Scheme 3.7A).¹¹ However, it turns out that simply by using a milder base, dimethylation at the N-1 and N-7 positions without protection of the sugar is possible, albeit in low yield (Scheme 3.7B).¹² Reaction of **3-4** with silver oxide (Ag₂O) yielded an unknown undesired product based on NMR data. Guanosine has been

Scheme 3.7 Modification of Guanosine



reported in the past to ring open the imidazole ring under basic aqueous conditions.¹³ This was concerning to us, but **3-4** proved to be stable to 30% NaOD in D₂O even after 36 hours by NMR analysis. In a move which seemed obvious in hindsight, by removing base from the methylation conditions we were able to isolate 7-methylguanosine using an exceptionally specific solvent mixture developed by Jones and Robins to crash out the product (Scheme 3.7C).¹⁴ When **3-5** was reacted with Ag₂O in D₂O, after one hour no organic compounds were detected in solution by NMR (Scheme 3.8). We believe the desired silver complex was created and immediately crashed out of solution. Unfortunately, the large excess of Ag₂O stirs in water as a suspension, making isolating the crashed-out product extremely challenging.

Scheme 3.8 Reaction of 7-Methylguanosine with Ag₂O



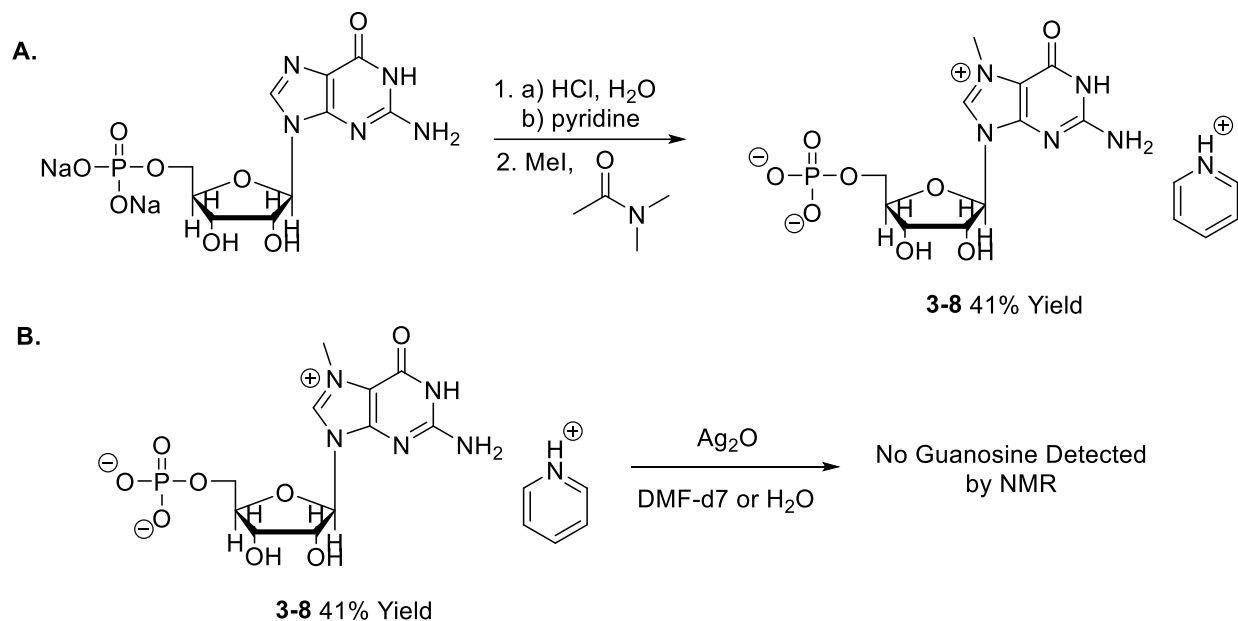
In hopes of making the silver complex more water soluble, we turned our attention to guanosine monophosphate. Solubility of guanosine monophosphate proved to be an obstacle to methylation of the N-7 position. Several solvents were examined and the temperature of the reaction adjusted, but in all cases inability to solvate the substrate led to no reaction occurring (Table 3.2). Ion exchange with tetrabutylammonium iodide was also unsuccessful.

Table 3.2 Failed Methylation of Guanosine Monophosphate

<i>Entry</i>	<i>Equiv. MeI</i>	<i>Solvent</i>
1	2	Dimethyl Acetamide
2	4	Dimethyl Acetamide
3	4	1-Methyl-2-piperidone
4	4	DMSO

Finally, using a modified version of a protocol developed by Paul Gershon, we were able to isolate the pyridinium salt of 7-methyl guanosine monophosphate (Scheme 3.9A).¹⁵ Attempts to

Scheme 3.9 Methylation of Guanosine Monophosphate and Reaction with Ag₂O



convert back to a sodium salt were unsuccessful, so we moved forward with the pyridinium salt.

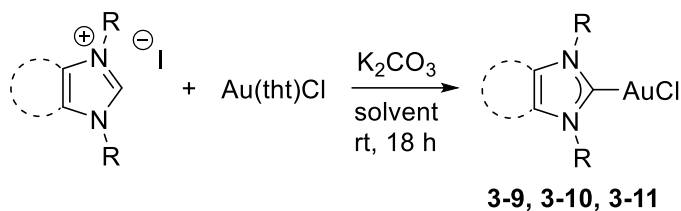
Unfortunately, with either DMF-d₇ or H₂O as solvent, reaction with Ag₂O yielded the same results as before: no detection of guanosine by NMR, likely due to insolubility of the silver-NHC complex (Scheme 3.9B).

3.4 Synthesis of a Gold-NHC Complex with a 5-Cap Analog

We used the conditions reported by Nolan^{9a-b} (Scheme 3.5B) as a jumping off point for gold complex synthesis which would be compatible with actual RNA (Table 3.3). The reaction was kept at room temperature to accommodate RNA and the time extended to 18 hours to compensate for the change in temperature. The gold source we had on hand, Au(tht)Cl, turned out to not be soluble in acetone (Entry 1), but a switch in solvent to DMF proved these conditions to be equally as effective as those of Nolan with the common NHC ligand 1,3-Dimesitylimidazol-2-ylidene (IMes) (Entry 2). While use of water as a cosolvent greatly reduced the effectiveness of the reaction, the desired product was still obtained (Entry 3). This is excellent precedent for the formation of a RNA NHC complex under biological conditions, since

it is aqueous and the base is very mild.

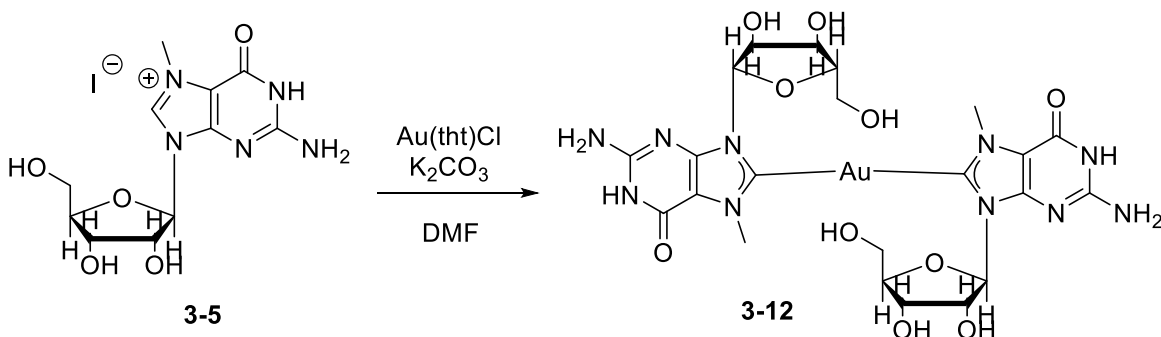
Table 3.3 Conditions for Gold Complex Formation



Entry	Substrate	Solvent	Product	Yield
1	IMes	Acetone	3-9	NR
2	IMes	DMF	3-9	97 %
3	IMes	1:1 DMF/H ₂ O	3-9	30 %
4	Dimethyl Imidazolium	DMF	3-10	0 %
5	Dimethyl Benzimidazolium	DMF	3-11	33 %

Unsurprisingly, the much less bulky N,N-dimethylimidazolium did not react, which follows known NHC reactivity trends (Entry 4). However, we were pleasantly surprised to find that N,N-dimethylbenzimidazolium does in fact form a complex with gold (Entry 5). This particular result, along with the reaction reported by Wang^{9d} (Scheme 3.5C), gave us much more confidence that the electronic effects of guanosine and the steric bulk of the sugar would make up for the lack of steric bulk provided by the N7 Methyl group on the 5'-Cap.

Scheme 3.10 Synthesis of Gold-NHC Complex with Guanosine



Following these results, we moved forward and applied the conditions from Table 3.3, entry 2 to compounds **3-5** and **3-8**. In both experiments we observed the products were not soluble in any solvents, and so **3-5** was studied for easier characterization (Scheme 3.10). Based on the data

so far, we believe we have successfully synthesized the guanosine gold NHC-complex **3-12**. The calculated exact mass of **3-12** is 791.181, and using MALDI-mass spectrometry to directly analyze the solid crude product mixture, the main mass peak found was 791.268, an excellent match. Analysis by solid state ^{13}C NMR also supports this conclusion. The C8 carbon in **3-5** is present in solid state NMR at 139.2 ppm as a very strong peak. In the spectrum recorded of the material recovered after removal of all volatiles *in vacuo*, presumed to be a mixture of **3-12** and K_2CO_3 , all the other peaks from **3-5** are present, but the peak at 139.2 ppm is clearly missing. There is, however, a new peak at 171.9, which is in a range consistent with carbons in an NHC bond with gold. In our own observations of compounds **3-9**, **3-10**, and **3-11**, as well as similar compounds described in other reports,⁹ carbon atoms in carbene bonds to gold consistently appear between 170-175 ppm in ^{13}C NMR. For example, the NHC carbon in compound **3-9** appears in ^{13}C NMR as a peak at 173.4 ppm. Interestingly, when water is added to the crude product mixture in order to remove the inorganic salts, the color of the solid changes from white to red-brown, a color shift consistent with oxidation from Gold (I) to Gold (III), and a new primary peak is detected by MALDI at 805.449. This result is quite puzzling, and we are currently working with a collaborator to obtain crystal structures of both of these structures using MicroED x-ray crystallography to definitively confirm our results.

3.5 Conclusion and Future Studies

We would be remiss not to mention that during the course of these investigations, a report was published by Ana Petronilho and co-workers, in which they reported the successful synthesis of a platinum-NHC complex with guanosine.¹⁶ There are, however, some key differences with our work. The guanosine used for the synthesis of Petronilho's compound contained a polyacetylated sugar, and rather than deprotonation to form the carbene, the metal carbon bond

was formed by heating to 100 °C to affect an oxidative addition. Once the structure of **3-12** is confirmed by MicroED, we intend to use our mild conditions to form a similar complex with an oligomer of RNA, which would be impossible at high temperatures, as the RNA would decompose. We also hope to perform *in vitro* studies to determine whether or not formation of a metal complex such as **3-12** forming with the 5'-cap of mRNA could inhibit translation. In conclusion, we have presented evidence for the first N-heterocyclic carbene bond between a transition metal and the C8 carbon of a fully unprotected 7-methylguanosine. This complex was formed under exceedingly mild conditions, pointing to the potential for such a complex to form with the 5'-cap of mRNA within a eukaryotic cell.

3.6 Experimental Section

General Information

Unless otherwise specified, reactions were run open to air using dry solvents. DCM and Et₃N were distilled over CaH₂. All chemicals were used as purchased from commercial sources. NMR data was obtained using a Bruker ARX-400 instrument and calibrated to the solvent signal (CDCl₃ : $\delta = 7.26$ ppm for ¹H NMR, $\delta = 77.2$ ppm for ¹³C NMR). Data for ¹H NMR spectra are reported as follows: chemical shift (δ ppm), multiplicity, coupling constant (Hz), then integration. Data for ¹³C NMR spectra are reported in terms of chemical shift. The following abbreviations are used for the multiplicities: s = singlet, d = doublet, t = triplet, q = quartet, quin. = quintet, sex. = sextet, hept. = heptet, dd = doublet of doublets, dt = doublet of triplets, td = triplet of doublets. Solid State ¹³C NMR was obtained using Bruker AV-600 with natural abundance powdered samples spun at a rate of 10 kHz. Flash column chromatography was performed using 40-63 mesh micron silica gel.

Experimental Procedures

Synthesis of 3-2 (Table 3.1, Entry 4)

Guanine (0.76 g) and DMSO (7.5 mL) were added to a flask and heated to 90 °C. Dimethyl sulfate (1.19 mL) was added and the temperature was increased to 140 °C, changing the solution from opaque white to clear yellow orange in color over time. After 2 hours the reaction was cooled to room temperature and MeOH (13 mL) was added. Aqueous NH₄OH (3 mL) was added and a white precipitate immediately crashed out of solution. The white precipitate, presumed to be **3-2**, was filtered out and dried overnight. **3-2** was insoluble in all solvents preventing characterization, and was used as-is.

Synthesis of 3-3

Guanosine (0.28 g), sodium hydride (0.024 g) and DMSO (3 mL) were stirred under a nitrogen atmosphere for 1.5 hours. MeI (0.06 mL) was added and stirred for 4 hours, after which the reaction was heated to 70 °C and placed under vacuum at 3 mmHg. After 60 hours DMF (5 mL), pyridine (5 mL), and acetic anhydride (5 mL) were added and the reaction was heated to 140 °C for 36 hours. The reaction was then evaporated *in vacuo* at 80 °C for 48 hours to give the crude product. The product was then purified by flash column chromatography (silica gel, 25:1 DCM/MeOH) to give **3-3** (185 mg, 40% yield). ¹H NMR (400 MHz, CDCl₃): δ 9.73 (br s, 1 H), δ 7.81 (s, 1 H), δ 5.97 (d, *J* = 5.0 Hz, 1 H), δ 5.82 (t, *J* = 5.2 Hz, 1 H), δ 5.59 (m, 1 H), δ 5.26 (s, 2 H), δ 4.37 (s, 3 H), δ 3.56 (s, 3 H), δ 2.27 (s, 3 H), δ 2.07 (s, 3 H), δ 2.02 (s, 6 H).

Synthesis of 3-4

Guanosine (0.28 g), MeI (0.09 mL), K₂CO₃ (0.17 g), and DMSO (3 mL) were stirred together overnight. More MeI (0.03 mL) and K₂CO₃ (0.06 g) were added and once again stirred overnight. DCM (30 mL) was added, and the solid product crashed out of solution. The solvent

was decanted off and **3-4** was allowed to dry in open air overnight (132 mg, 30% yield). ^1H NMR (400 MHz, DMSO- d_6): δ 9.33 (s, 1 H), δ 7.83 (br s, 2 H), δ 5.80 (d, $J = 4.1$ Hz, 1 H), δ 5.60 (d, $J = 5.3$, 1 H), δ 5.30 (d, $J = 5.4$ Hz, 1 H), δ 5.06 (t, $J = 5.3$ Hz, 1 H), δ 4.34 (m, 1 H), δ 4.11 (m, 1 H), δ 3.99 (s, 3 H), δ 3.95 (m, 1 H), δ 3.62 (m, 2 H), δ 2.50 (s, 3 H).

Synthesis of **3-5**

Guanosine (5 g), MeI (2.2 mL), and dimethyl acetamide (50 mL) were stirred at room temperature for 48 hours. Celite (2 g) was added and stirred, then filtered out of the reaction. Ethanol (250 mL) and hexanes (600 mL) were added, and then decanted off, leaving behind an oily residue. Acetone (300 mL) was added and stirred for 10 minutes, crashing out the product. **3-5** was isolated by filtration and washed with acetone, then Et_2O , and used without further purification (1.74 g, 23.1% yield). ^1H NMR (400 MHz, D_2O): δ 8.89 (s, 1 H), δ 5.92 (d, $J = 3.8$, 1 H), δ 4.55 (t, $J = 4.8$, 1 H), δ 4.25 (t, $J = 5.4$, 1 H), δ 4.15 (m, 1 H), δ 3.98 (s, 3 H), δ 3.84 (dd, $J = 12.9, 2.8$, 1 H), δ 3.72 (dd, $J = 12.8, 4$, 1 H). ^{13}C NMR (100 MHz, D_2O): δ 155.6, 155.2, 149.5, 136.7, 108.7, 89.9, 85.3, 74.2, 69.3, 60.5, 35.8.

Attempted Synthesis of **3-6**

3-5 (35 mg), D_2O (2 mL), and Ag_2O (49 mg) were stirred together for 1 hour. Excess solid was filtered out to leave colorless solution which was analyzed by NMR, showing only a solvent peak.

Representative Procedure for Table 3.2 (Entry 2)

Disodium guanosine monophosphate (0.2 g), MeI (0.12 mL), and dimethyl acetamide (10 mL) were stirred at room temperature under a nitrogen atmosphere overnight. The solvent was removed *in vacuo* and the remaining solid analyzed by ^1H NMR, showing only starting material.

Synthesis of 3-8

Disodium guanosine monophosphate (0.41 g), H₂O (4 mL), and concentrated HCl (0.06 mL) were stirred together. Pyridine (0.16 mL) was added and a semitransparent solid immediately crashed out. H₂O was removed *in vacuo*. Dimethyl acetamide (6 mL) was added under a nitrogen atmosphere, followed by MeI (0.62 mL), turning the solution yellow, and the reaction was stirred overnight. The solvent was removed *in vacuo*, then acetone was added and stirred, crashing out the product. The acetone was decanted off and **3-8** was dried *in vacuo* and used without further purification. (193 mg, 41% yield). ¹H NMR (400 MHz, D₂O): δ 9.12 (s, 1 H), δ 8.58 (tt, *J* = 12.6, 2.1, 1 H), δ 8.48 (t, *J* = 10.0, 1 H), δ 5.99 (d, *J* = 4.8, 1 H), δ 5.89 (d, *J* = 4.8, 1 H), δ 4.58 (m, 1 H), δ 4.39 (m, 1 H), δ 4.35 (s, 3 H), δ 4.31 (m, 1 H), δ 4.26 (m, 1 H), δ 4.18 (m, 1 H).

Synthesis of 3-9

1,3-Bis(mesityl)imidazolium chloride (0.07 g), Au(tht)Cl (0.054 g), K₂CO₃ (0.03 g), and DMF (2 mL) were stirred together overnight. The solvent was then removed *in vacuo* and DCM (2 mL) was added. The reaction was filtered through silica then concentrated to a white solid. The solid was then stirred in hexanes, which was decanted off and **3-9** was dried *in vacuo* (88.5 mg, 97% yield). ¹H NMR (400 MHz, CDCl₃): δ 7.09 (s, 2 H), δ 6.99 (s, 4 H), δ 2.34 (s, 6 H), δ 2.10 (s, 12 H). ¹³C NMR (100 MHz, CDCl₃): δ 173.4, 139.8, 134.7, 130.0, 129.5, 122.1, 21.2, 17.8. HRMS (DART-TOF) *m/z*: Calculated for C₂₃H₂₇AuN₃ [M - Cl + Acetonitrile]: 542.1871, found 542.1854.

Synthesis of 3-11

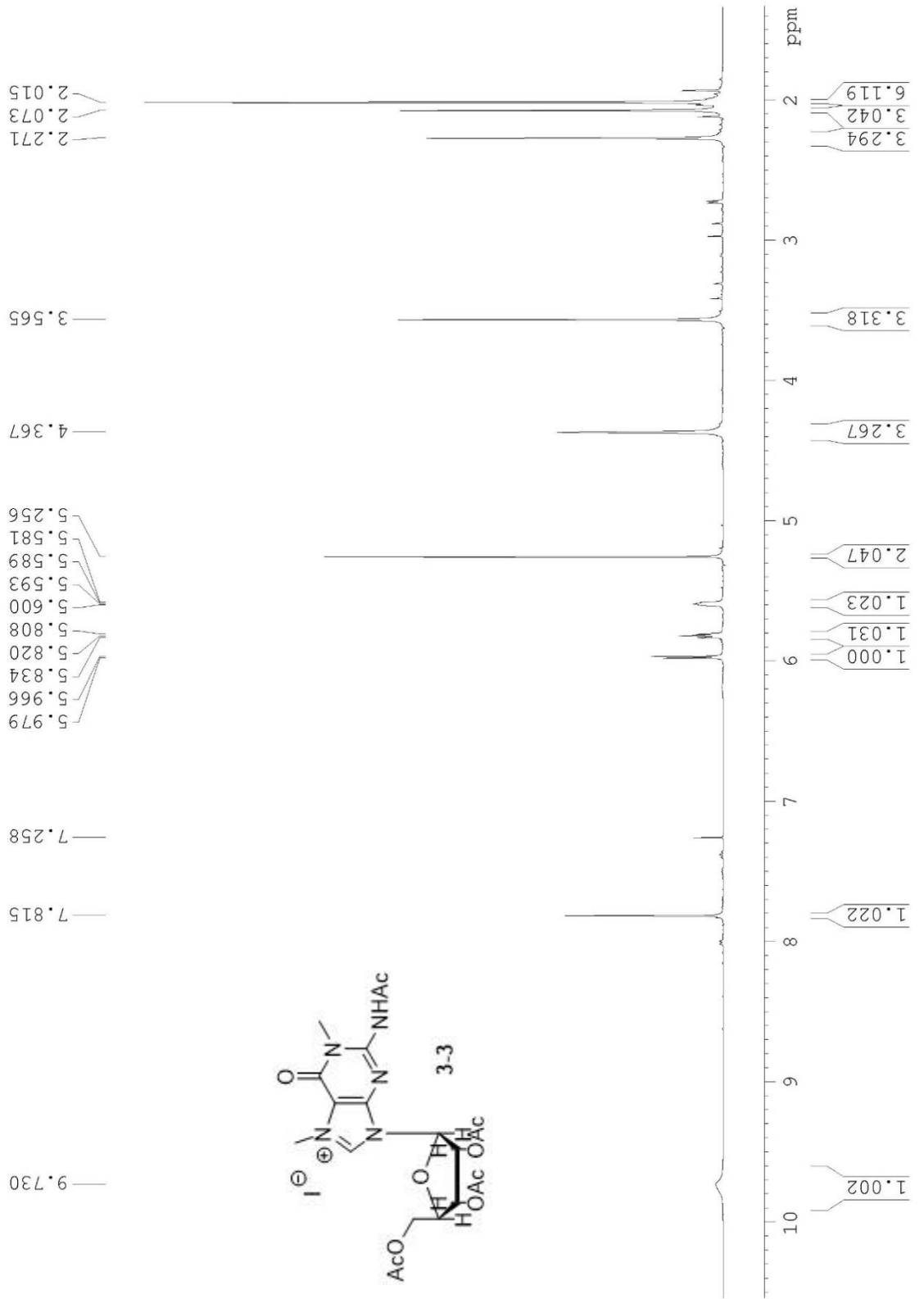
1,3-Dimethylbenzimidazolium iodide (0.02 g), Au(tht)Cl (0.02 g), K₂CO₃ (0.01 g), and DMF (1 mL) were stirred together overnight. The solvent was then removed *in vacuo* and DCM (1 mL) was added. The reaction was filtered through silica then concentrated to give **3-11** as a

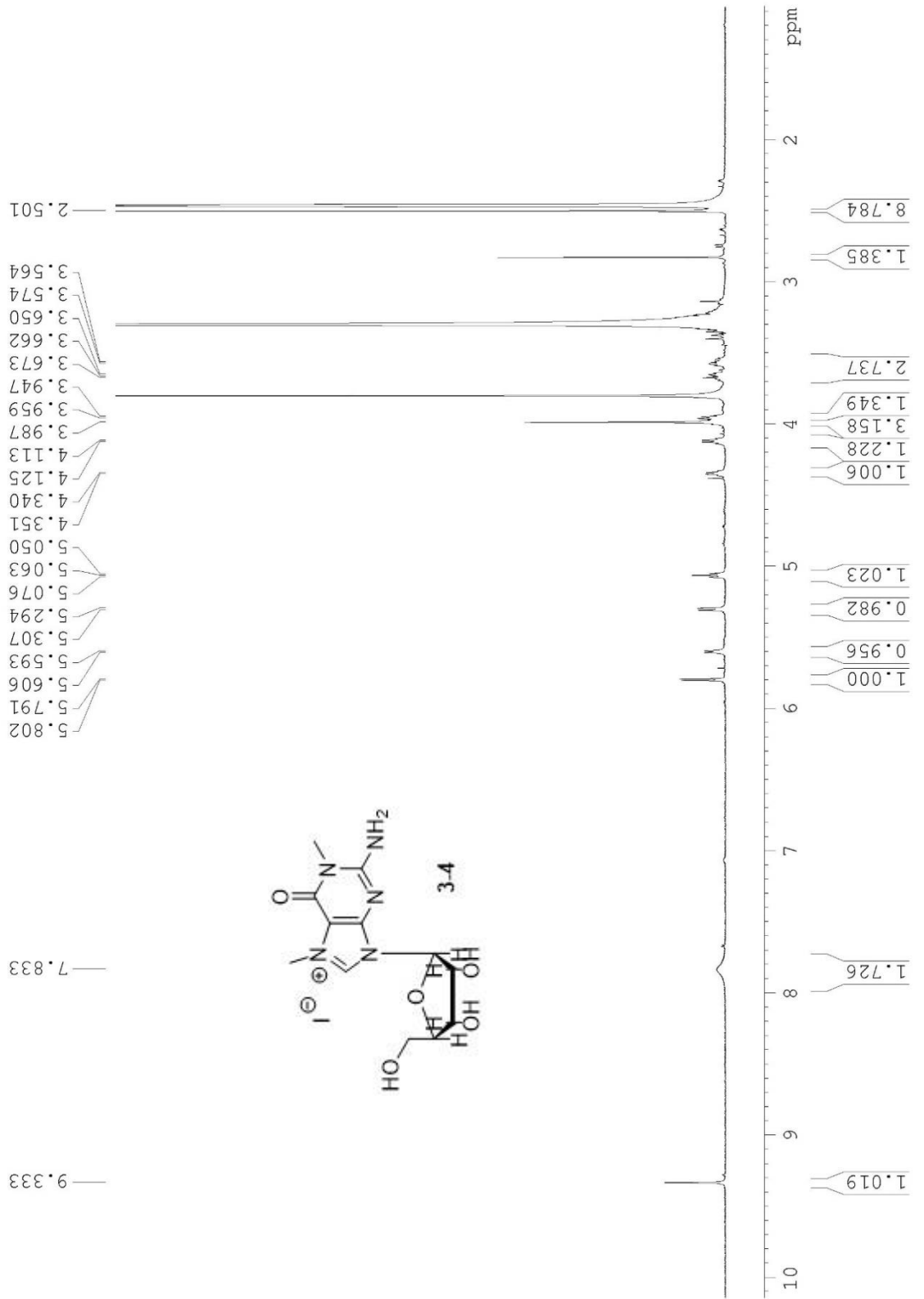
white solid (7 mg, 33% yield). ^1H NMR (400 MHz, CDCl_3): δ 7.48 (m, 4 H), δ 4.06 (s, 6 H). ^{13}C NMR (100 MHz, CDCl_3): δ 133.6, 124.7, 111.2, 34.7.

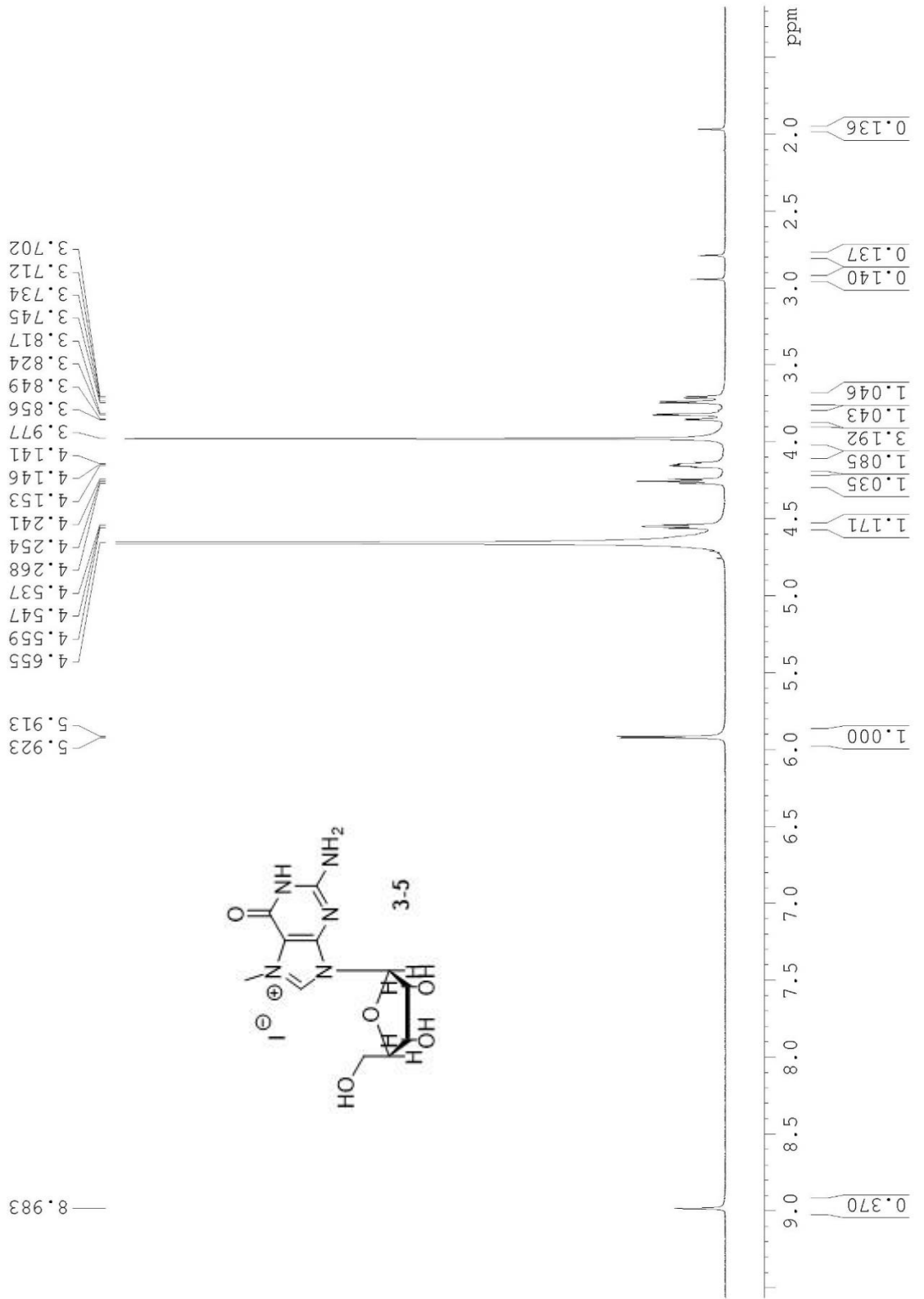
Synthesis of **3-12**

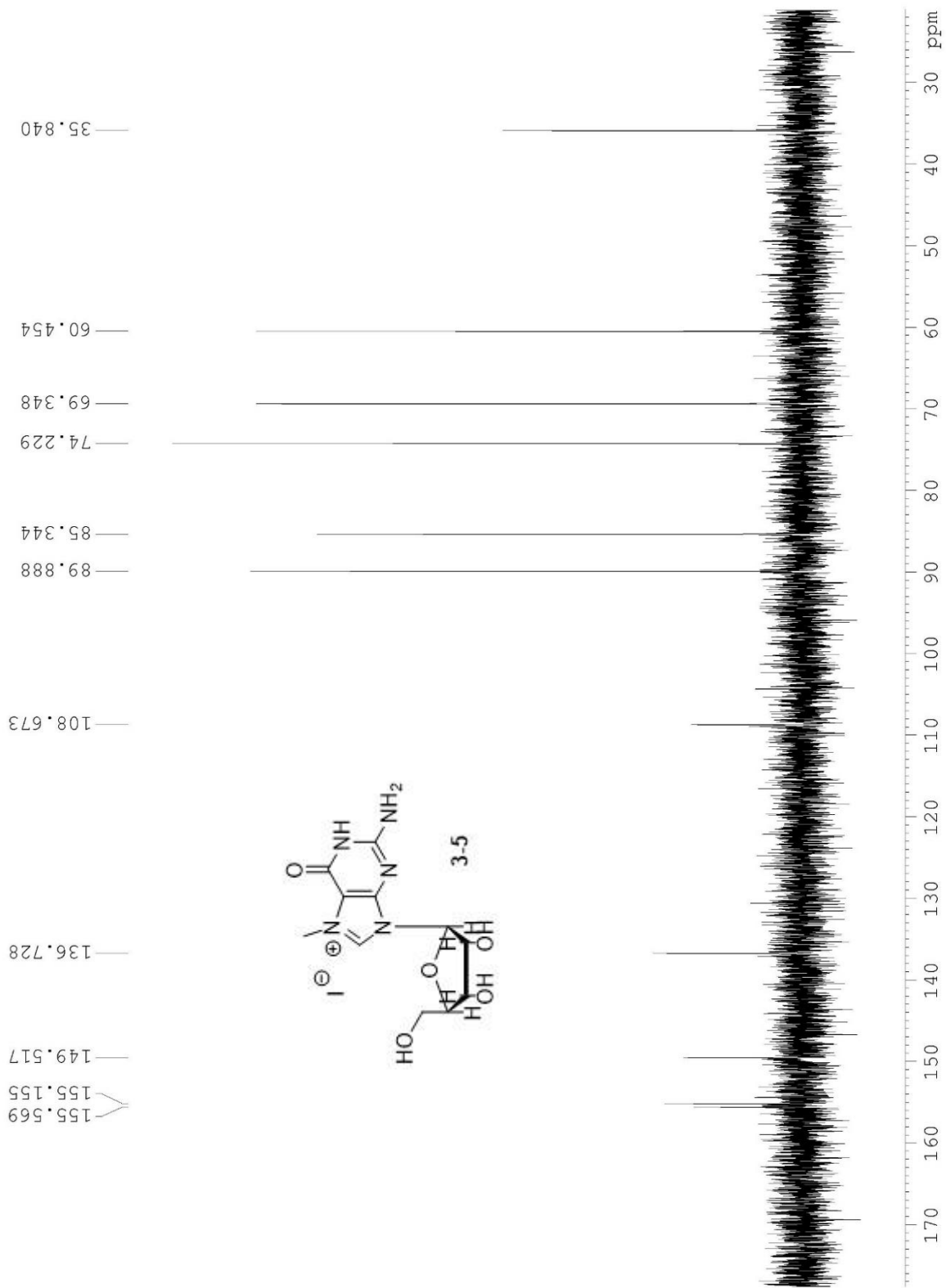
3-5 (0.09 g), $\text{Au}(\text{tht})\text{Cl}$ (0.05 g), K_2CO_3 (0.03 g), and DMF (2 mL) were stirred together overnight under a nitrogen gas atmosphere. The solvent was removed *in vacuo*, and the crude white powder product was analyzed as a mixture of **3-12** and inorganic salts. ^{13}C NMR (600 MHz, solid state): δ 171.7, 164.1, 157.8, 148.3, 109.5, 95.2, 85.2, 71.5, 62.2, 37.3. MS (MALDI) m/z : Calculated for $\text{C}_{22}\text{H}_{30}\text{AuN}_{10}\text{O}_{10}$: 791.181, found 791.268.

3.7 ^1H and ^{13}C NMR Data









Attempted synthesis of 3-6 shows no guanosine

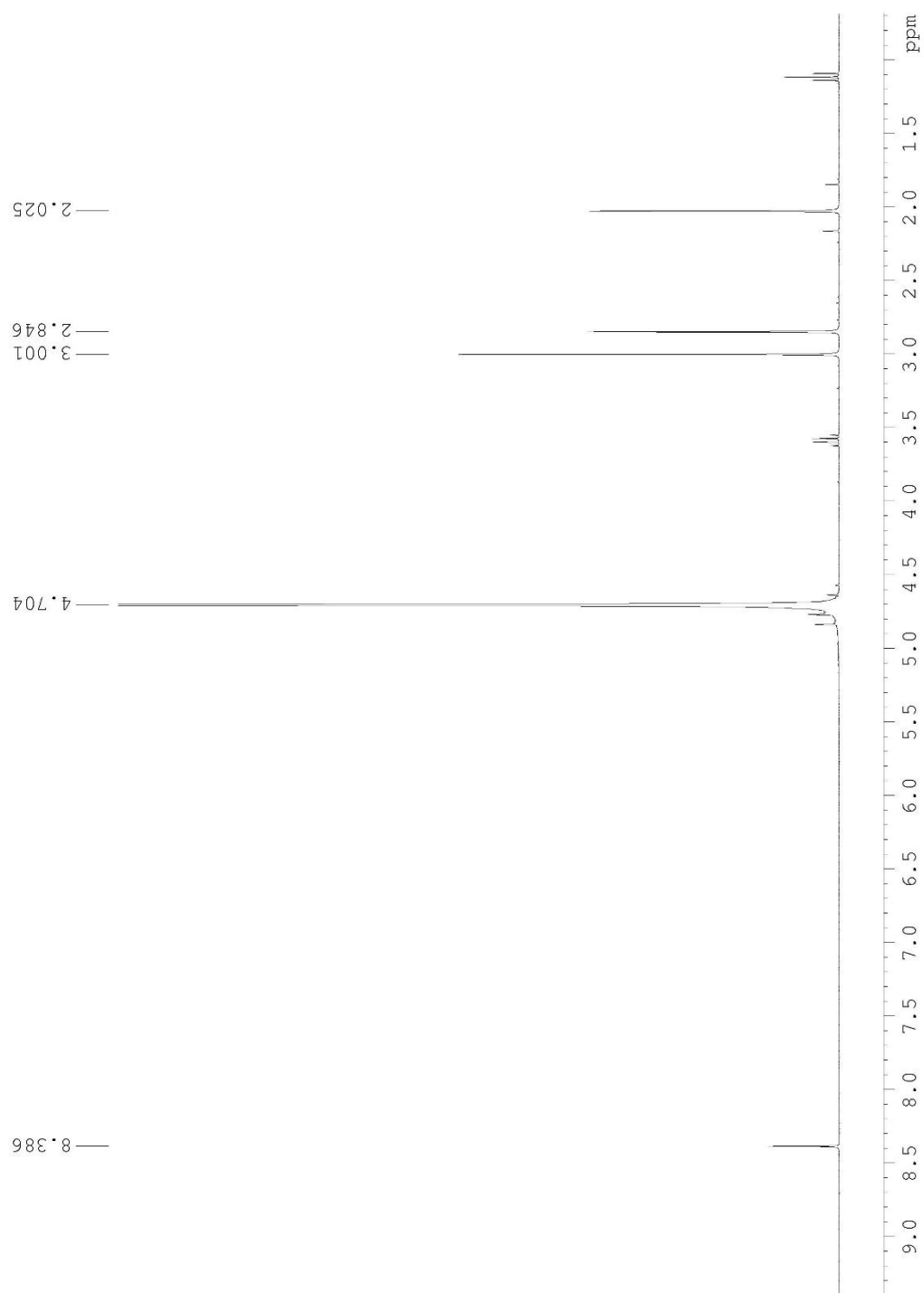
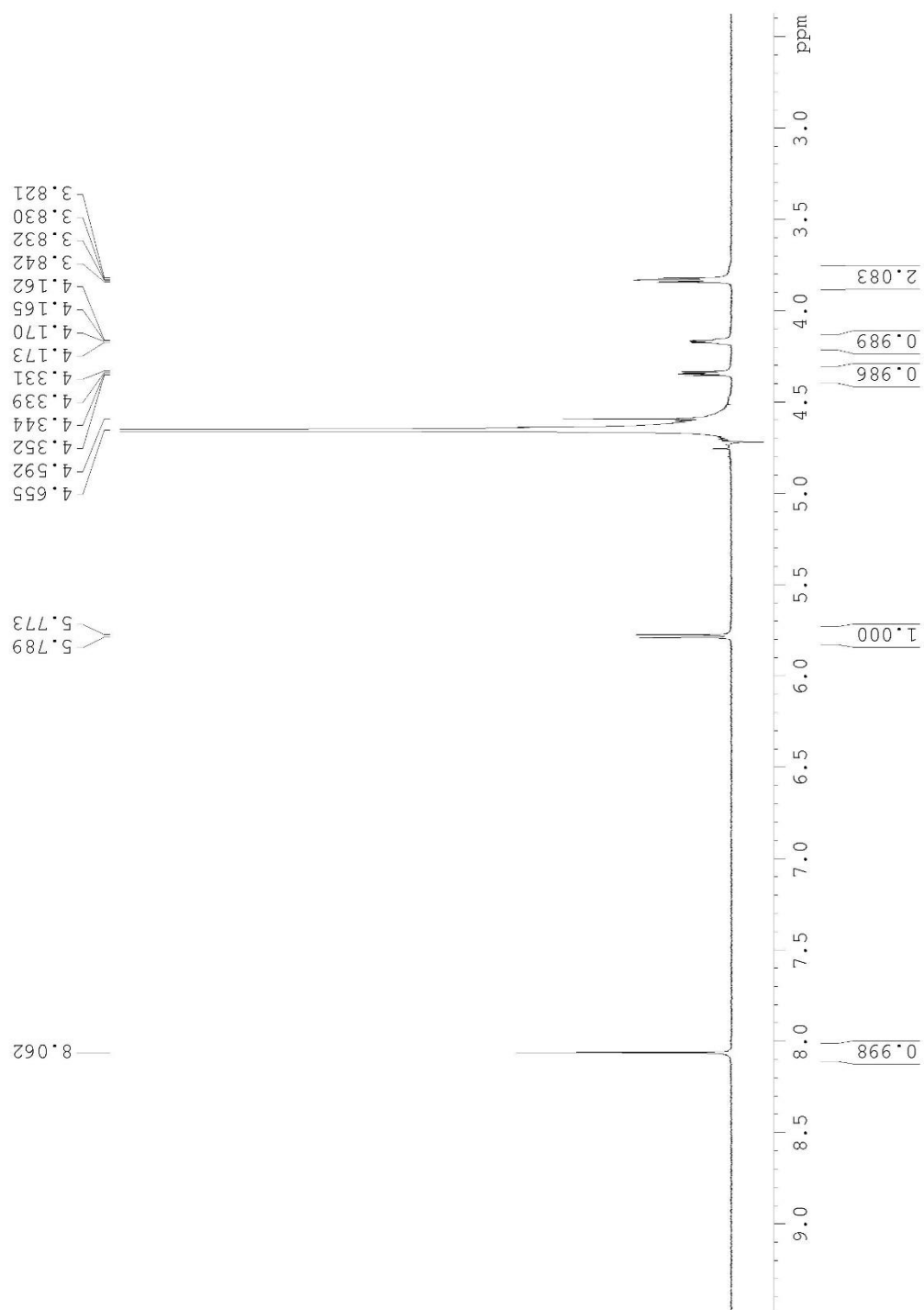
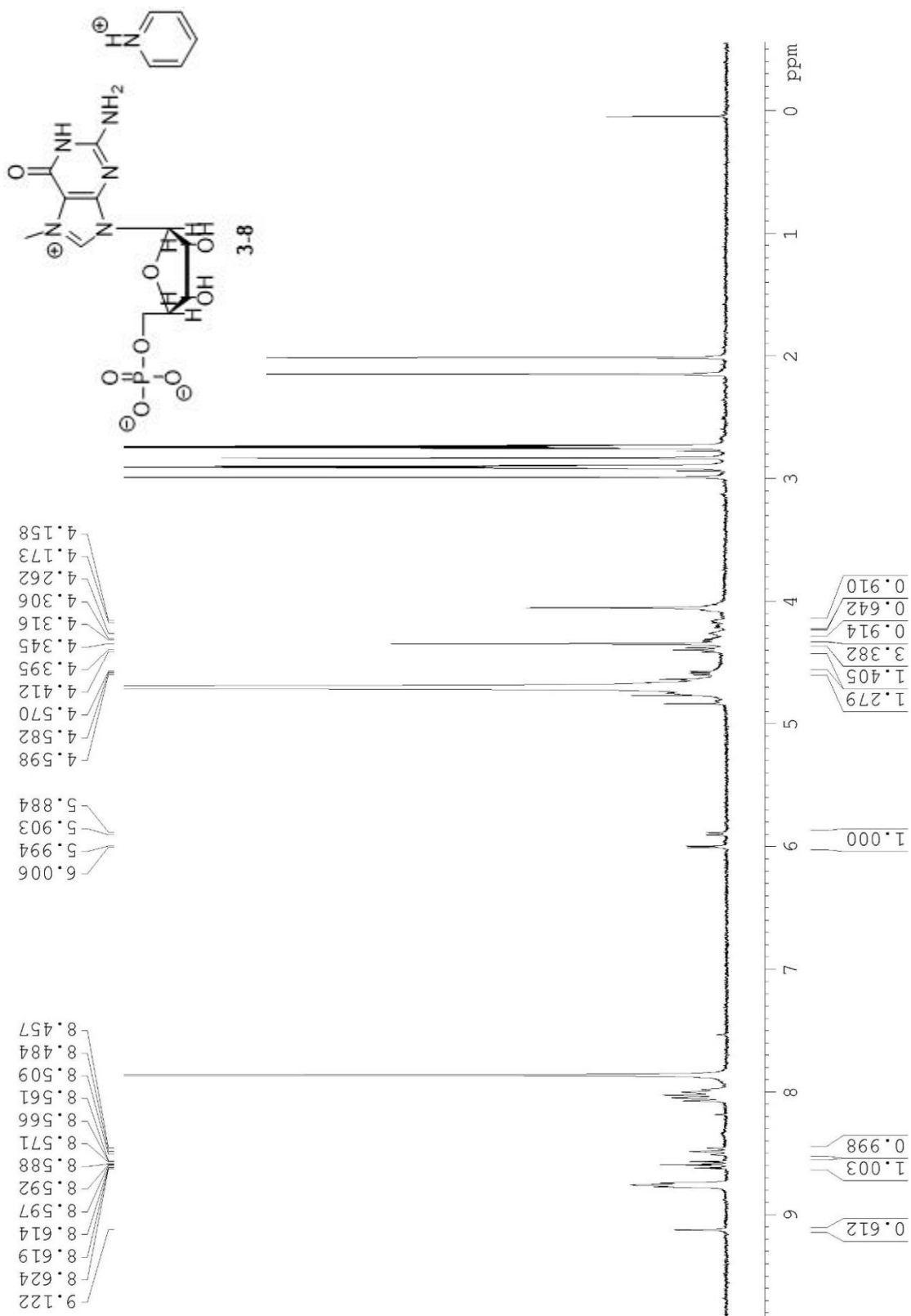
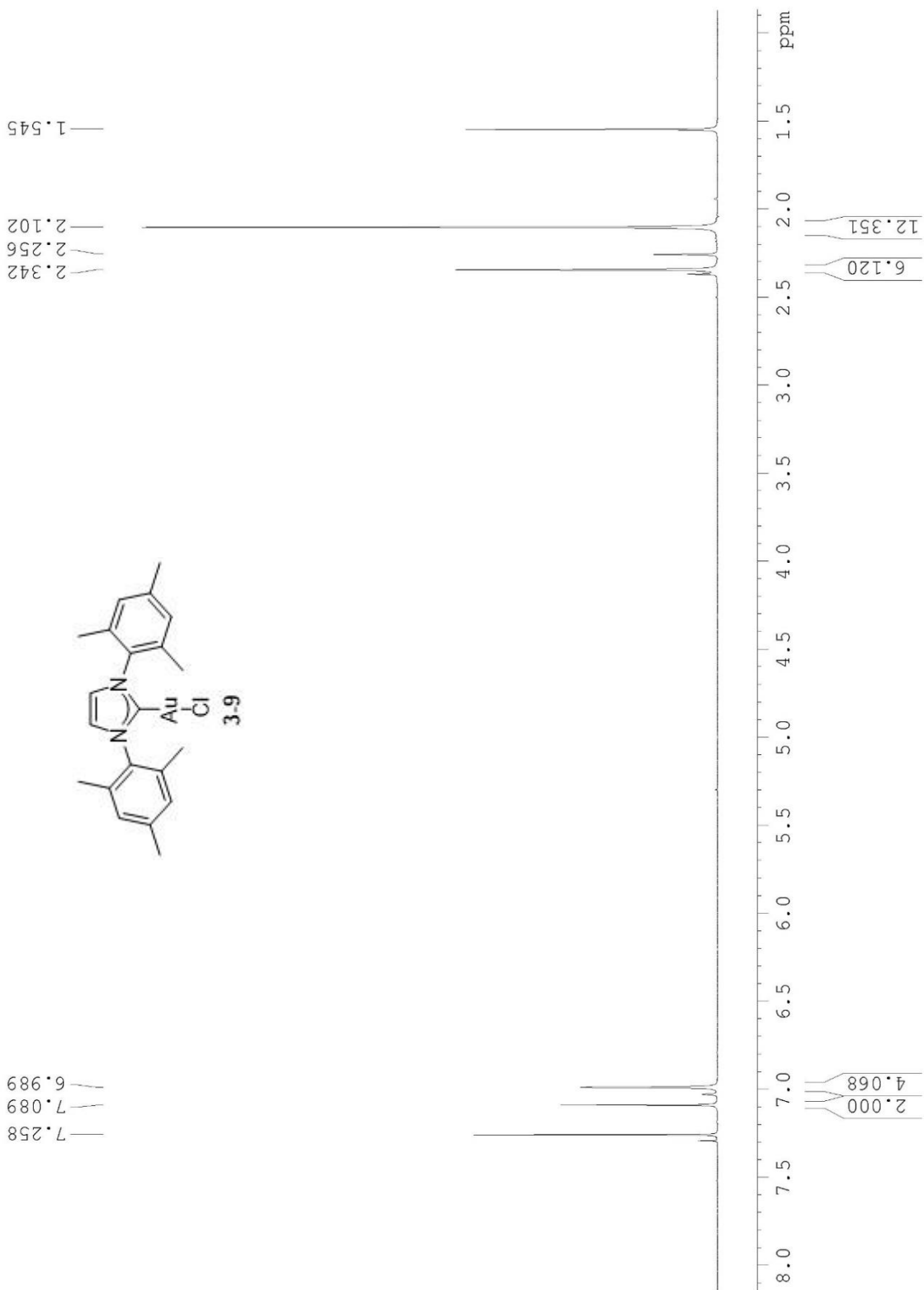
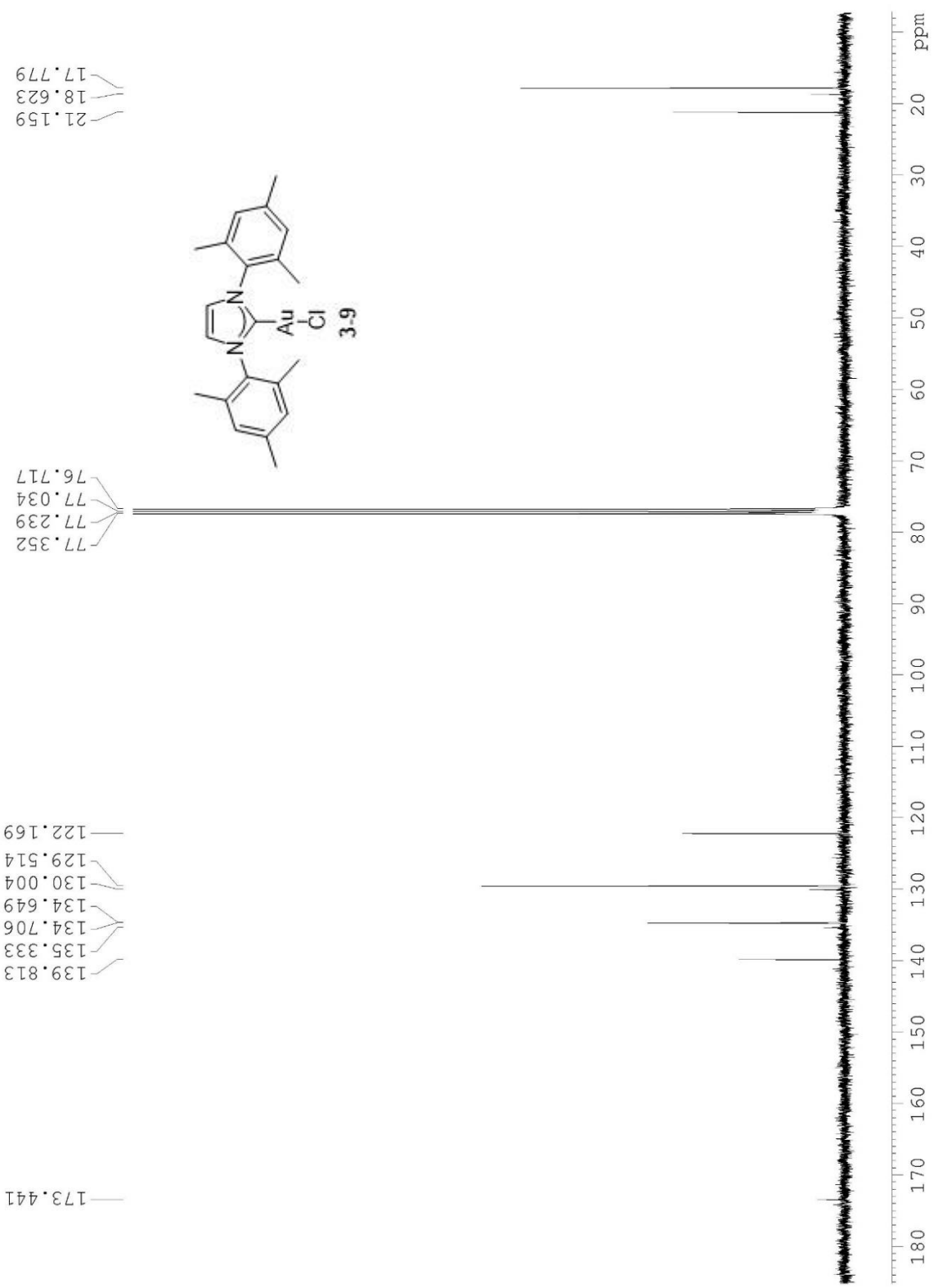


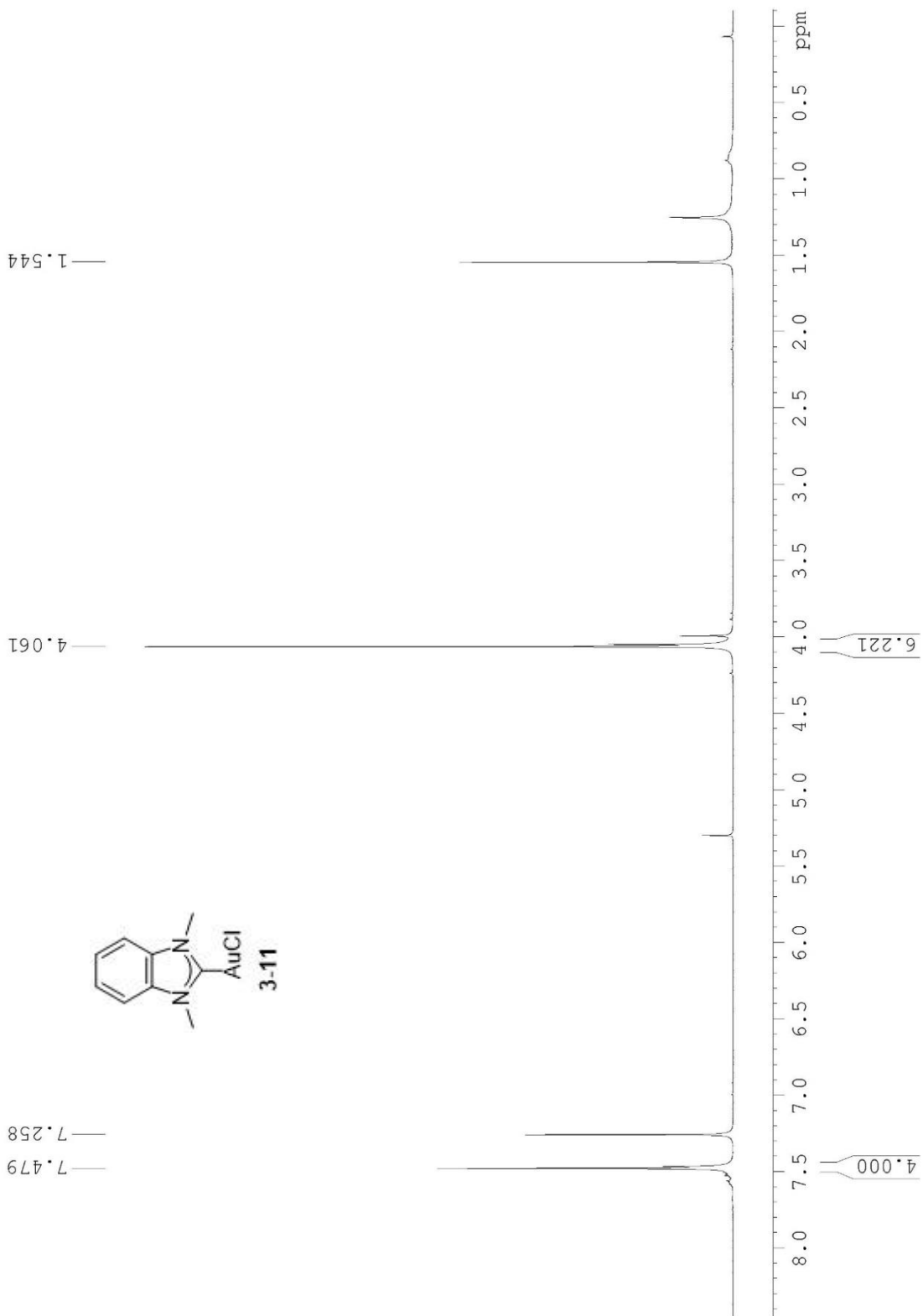
Table 3.2, Entry 2

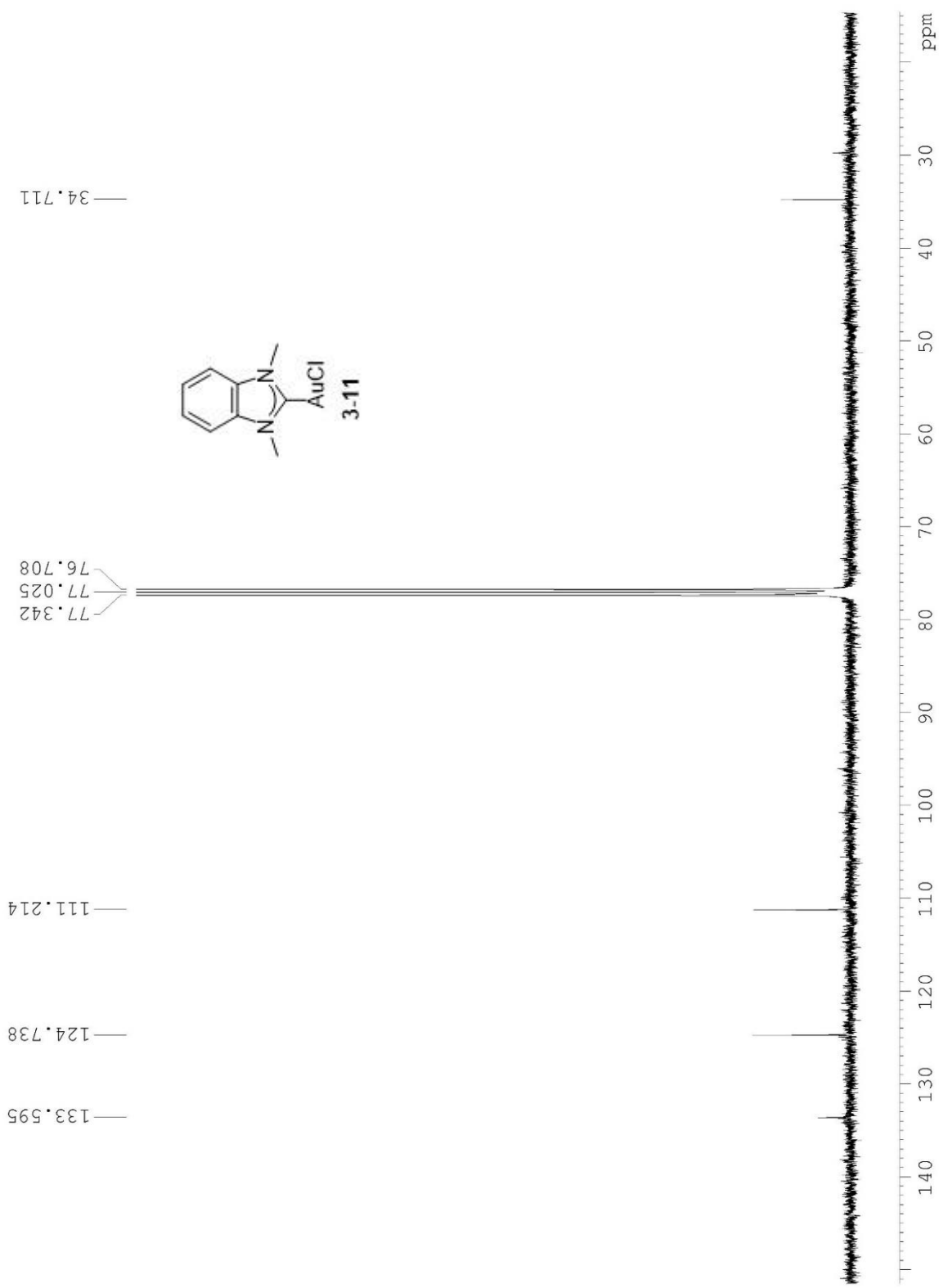


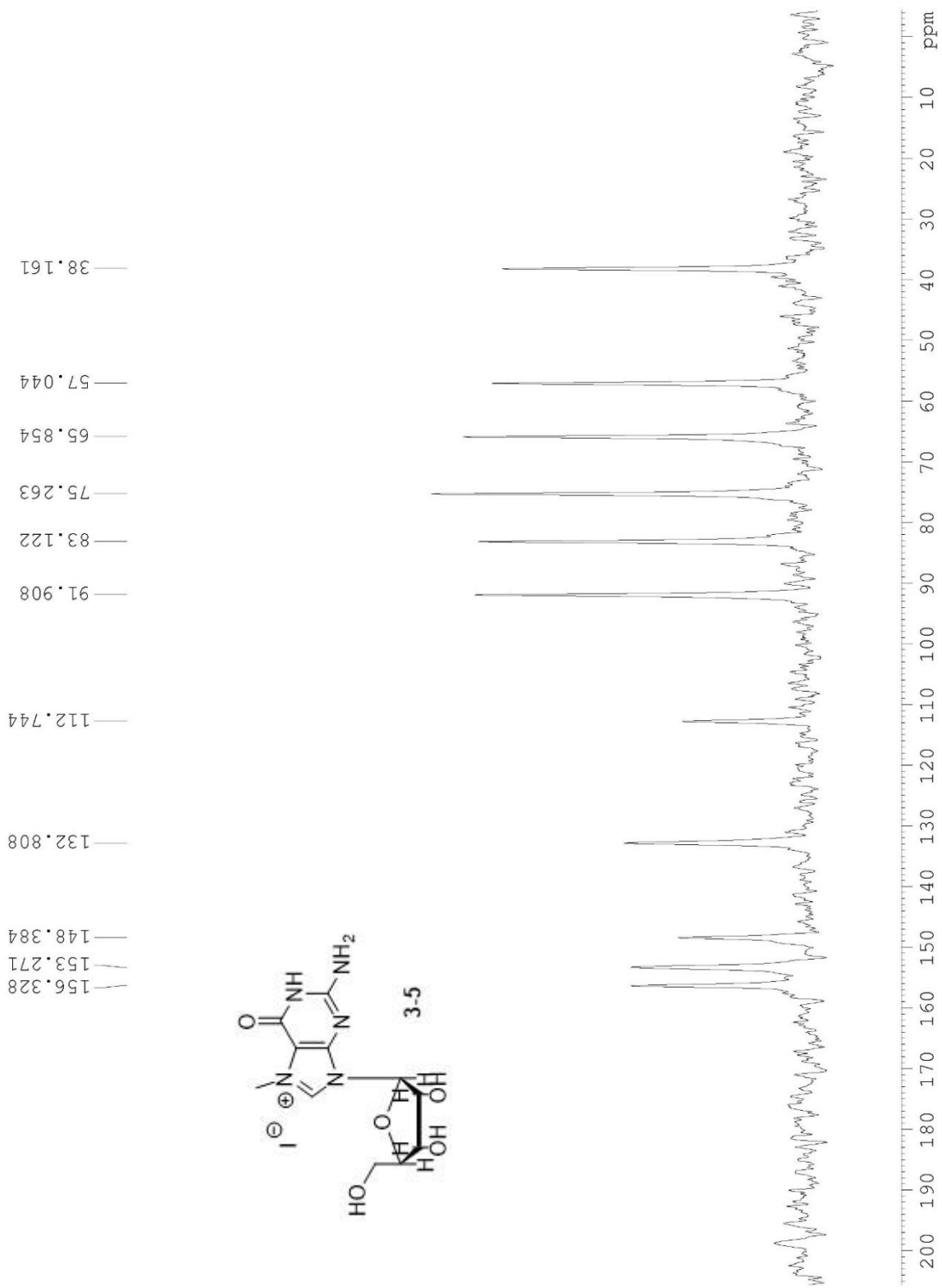


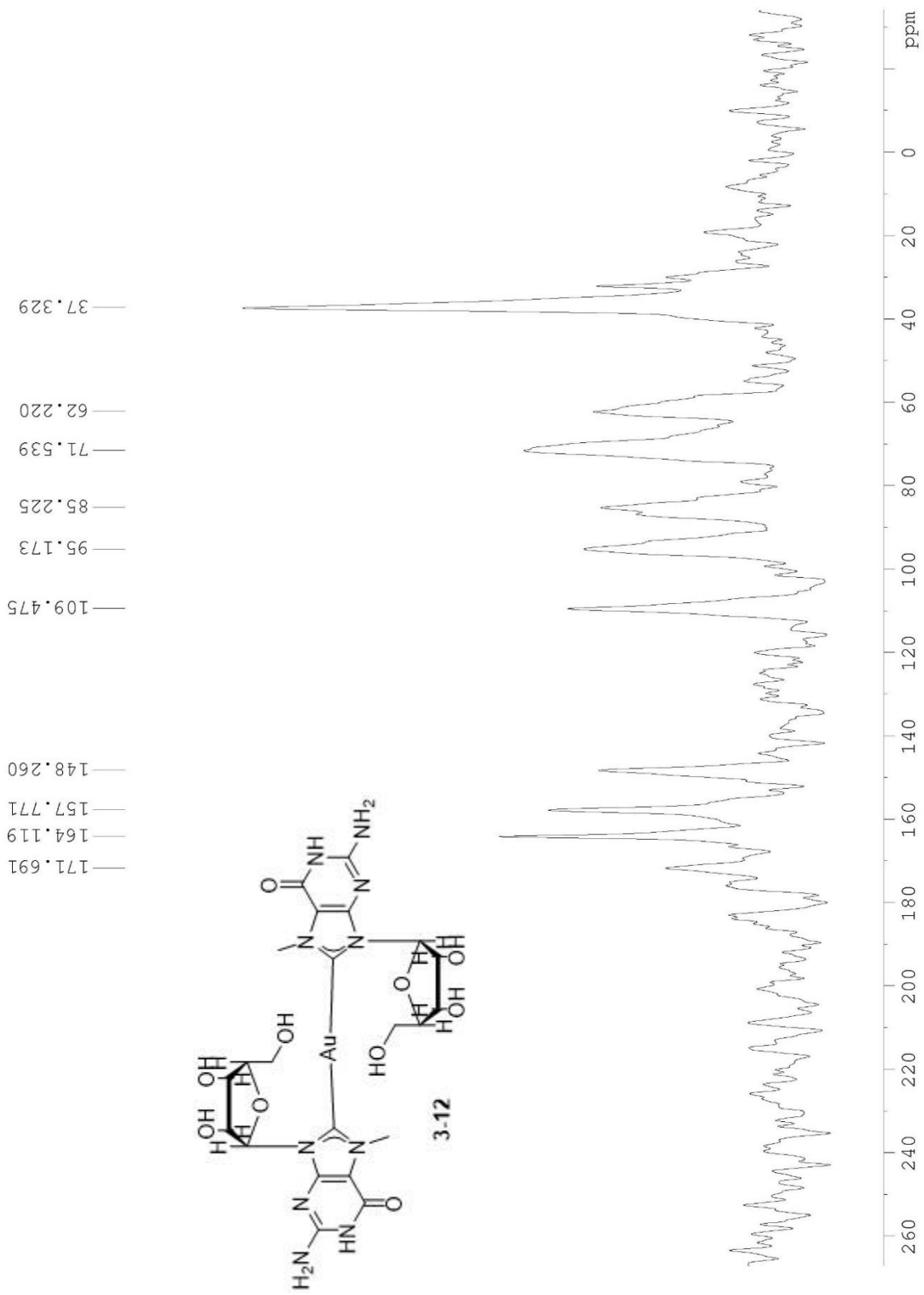












3.8 References

1. (a) Rottman F.; Shatkin, A. J.; Perry, R. P. *Cell* **1974**, *3*, 197-199. (b) Muthukrishnan, S.; Both, G. W.; Furuichi, Y.; Shatkin, A. J. *Nature* **1975**, *255*, 33-37. (c) Shatkin, A. J. *Cell* **1976**, *9*, 645-653. (d) Banerjee, A. K. *Microbiological Reviews* **1980**, *44*, 175-205. (e) Konarska, M. M.; Padgett, R. A.; Sharp, P. A. *Cell* **1984**, *38*, 731-736. (f) Lewis, J. D.; Gunderson, S. I.; Mattaj, I. W. *Journal of Cell Science, Supplement 19* **1995**, 13-19. (g) Sonenberg, N.; Gingras, A.-C. *Current Opinion in Cell Biology* **1998**, *10*, 268-275. (h) Brown, C. J.; Mcnae, I.; Fischer, P. M.; Walkinshaw, M. D. *J. Mol. Biol.* **2007**, *372*, 7-15. (i) Yap, L. J.; Luo, D.; Chung, K. Y.; Lim, S. P.; Bodenreider, C.; Noble, C.; Shi, P.-Y.; Lescar, J. *PLoS ONE* **2010**, *5*, e12836. (j) Ramanathan, A.; Robb, G. B.; Chan, S.-H. *Nucleic Acids, Research* **2016**, *44*, 7511-7526.
2. Freier, S. M.; Kierzek, R.; Jaeger, J. A.; Sugimoto, N.; Caruthers, M. H.; Neilson, T.; Turner, D. H. *Proc. Natl. Acad. Sci. USA* **1986**, *83*, 9373-9377.
3. Jarvinen, P.; Oivanen, M.; Lonnberg, H. *J. Org. Chem.* **1991**, *56*, 5396-5401.
4. (a) Savka, R.; Plenio, H. *Dalton, Trans.* **2015**, *44*, 891-893. (b) Zinser, C. M.; Naha, F.; Brill, M.; Meadows, R. E.; Cordes, D. B.; Slawin, A. M. Z.; Nolan S. P.; Cazin, C. S. J. *Chem. Commun.* **2017**, *53*, 7990-7993. (c) Zinser, C. M.; Warren, K. G.; Meadows, R. E.; Naha, F.; Al-Majid, A. M.; Barakat, A.; Islam, M. S.; Nolan, S. P.; Cazin, C. S. J. *Green Chem.* **2018**, *20*, 3246-3252. (d) Bolbat, E.; Suarez-Alcantara, K.; Canton, S. E.; Wendt, O. F. *Inorganica Chimica Acta* **2016**, *445*, 129-133.
5. (a) Garrison, J. C.; Youngs, W. J. *Chem. Rev.* **2005**, *105*, 3978-4008. (b) Doddi, A.; Peters, M.; Tamm, M. *Chem. Rev.* **2019**, 6994-7112. (c) Appelhans, L. N.; Incarvito, C. D.; Crabtree, R. H. *J. Organomet. Chem.* **2008**, *693*, 2761-2766. (d) Wanniarachchi Y. A.; Khan, M. A.; Slaughter, L. M. *Organometallics* **2004**, *23*, 5881-5884.

6. (a) Kascatan-Nebioglu, A.; Panzner, M. J.; Garrison, J. C.; Tessier, C. A.; Youngs, W. J. *Organometallics* **2004**, *23*, 1928-1931. (b) Scattolin, T.; Giust, S.; Bergamini, P.; Caligiuri, I.; Canovese, L.; Demitri, N.; Gambari, R.; Lampronti, I.; Rizzolio, F.; Visentin, F. *Appl. Organometal. Chem.* **2019**, *33*, e4902.
7. Youngs, W. J.; Tessier, C. A.; Garrison, J.; Quezada, C.; Melaiye, A.; Panzner, M.; Durmas, S. WO 2005/023760 A2, **2005**.
8. (a) Zou, T.; Lok, C.-N.; Wan, P.-K.; Zhang, Z.-F.; Fung, S.-K.; Che, C.-M. *Current Opinion in Chemical Biology* **2018**, *43*, 30-36. (b) Al-Majid, A. M.; Yousuf, S.; Choudhary, M. I.; Nahra, F.; Nolan, S. P. *ChemistrySelect* **2016**, *1*, 76-80.
9. (a) Collado, A.; Gomez-Suarez, A.; Martin, A. R.; Slawin, A. M. Z.; Nolan, S. P. *Chem. Commun.* **2013**, *49*, 5541-5543. (b) Nahra, F.; Tzouras, N. V.; Collado, A.; Nolan, S. P. *Nature Protocols* **2021**, *16*, 1476-1493. (c) Zhu, S.; Liang, R.; Jiang, H. *Tetrahedron* **2012**, *68*, 7949-7955. (d) Wang, F.; Li, S.; Qu, M.; Zhao, M.-X.; Liu, L.-J.; Shi, M. *Beilstein J. Org. Chem.* **2012**, *8*, 726-731.
10. Bertrand, B.; Stefan, L.; Pirrotta, M.; Monchaud, D.; Bodio, E.; Richard, P.; Le Gendre, P.; Warmerdam, E.; de Jager, M. H.; Groothuis, G. M. M.; Picquet, M.; Casini, A. *Inorg. Chem.* **2014**, *53*, 2296-2303.
11. Hobartner, C.; Kreutz, C.; Flecker, E.; Ottenschlager E.; Pils, W.; Grubmayr, K.; Micura, R. *Monatshefte fur Chemie*, **2003**, *134*, 851-873.
12. Zoltewicz, J. A.; Clark, D. F.; Sharpless, T. W.; Grahe, G. *J. Am. Chem. Soc.* **1970**, *92*, 1741-1750.

13. (a) Chetsanga, C. J.; Makaroff, C. *Chem.-Biol. Interactions* **1982**, *41*, 235-249. (b) Darzynkiewicz E.; Labadi, I.; Haber, D.; Burger, K.; Lonnerberg, H. *Acta Chemica Scandinavica B* **42** **1988**, 86-92.
14. Jones, J.W.; Robins R. K. *J. Am. Chem. Soc.* **1962**, *85*, 193-201.
15. Peng, Z.-H.; Sharma, V.; Singleton, S. F.; Gershon, P. D. *Org. Lett.* **2002**, *4*, 161-164.
16. Leitao, M. I. P. S.; Gonzalez, C.; Francescato, G.; Filipiak, Z.; Petronilho, A. *Chem. Commun.*, **2020**, *56*, 13365.